A Study of Symmetries and Phases in Gravity with Application to Holography and Cosmology

A thesis submitted to

Tata Institute of Fundamental Research, Mumbai, India

for the degree of

Doctor of Philosophy in Physics

By

Nilay Kundu

Department of Theoretical Physics

Tata Institute of Fundamental Research

Mumbai - 400 005, India

September, 2014

(Final Version Submitted in May, 2015)

Declaration

This thesis is a presentation of my original research work. Wherever contributions of others are involved, every effort is made to indicate this clearly, with due reference to the literature, and acknowledgement of collaborative research and discussions.

The work was done under the guidance of Professor Sandip P Trivedi, at the Tata Institute of Fundamental Research, Mumbai.

(Nilay Kundu)

In my capacity as the supervisor of the candidate's thesis, I certify that the above statements are true to the best of my knowledge.

(Sandip P Trivedi)

Acknowledgments

Firstly, I am deeply grateful to my thesis supervisor Sandip P Trivedi for his constant support and encouragement. His insights and intuition for Physics has been a great source of learning for me. The lengthy discussion sessions with him, as I believe, were the most enjoyable part of my days as a research scholar at TIFR. His enormous enthusiasm and excitement for research as well as simple but insightful ways of explaining things to students as a teacher has been immensely influential and motivating.

I would also like to thank Shiraz Minwalla, Gautam Mandal for many stimulating discussions and also for the wonderful courses they taught. I would also like to thank all the other faculty members of string group for many stimulating discussions and comments. I am grateful to the other faculty members of our department, specifically to Sunil Mukhi, Deepak Dhar, Saumen Datta, Kedar Damle for teaching great courses during my course work at TIFR. I would also like to thank my childhood teachers Mr. Abdul Halim and Pranati Di for all their support and inspirations.

I am grateful to Prithvi Narayan, Nilanjan Sircar, Sachin Jain, Rickmoy Samanta and Ashish Shukla for wonderful collaboration and working together. Specifically, I would like to acknowledge the support and advice received from Prithvi Narayan which were very influential to have a smooth start of my research at TIFR. I was also fortunate to have seniors like Jyotirmoy, Satyabrata and Sayantan for their kind help in many ways. Over the years I have stayed at TIFR through all the ups and downs, the theory students room with all its inmates has been the most comfortable place to stay. I would like to thank all the other students in DTP, who were present during the course of my stay, for maintaining such an excellent and lively environment. It was great to come across Debjyoti, Geet, Kusum, Mangesh, Nikhil, Padmanath, Rahul, Ritam, Sambuddha, Tarun, Umesh, Yogesh and also the other friends of mine at TIFR, especially Amaresh, Chandradoy, Kinjalk, Naveen, Pankaj, Sanmay, Sumanta and Vivek. It was great fortune to have them in all the fun during the weekend football, food outside or be it the monsoon treks in Sahyadri. I am also grateful to my friends Manik, Devagnik and Pinaki from my university days at Jadavpur for their support. It would be otherwise incomplete if I don't admit that I owe a lot to Sudeshna for this and that and mostly for being there all along as a friend.

Finally and above all, this thesis owes a lot for its existence to the unconditional support I got from my parents and sister. Undoubtedly, it is my parents, all their sacrifices and compromises in their own lives, along with their encouragement and belief in me, which have driven me to pursue my research.

Collaborators

This thesis is based on work done in collaboration with several people.

- The work presented in chapter 2 was done in collaboration with Norihiro Iizuka, Shamit Kachru, Prithvi Narayan, Nilanjan Sircar and Sandip P. Trivedi and is based on the publication that appeared in print as JHEP 1207 (2012) 193.
- The work presented in chapter 3 was done in collaboration with Prithvi Narayan, Nilanjan Sircar and Sandip P. Trivedi and is based on the publication that appeared in print as JHEP 1303 (2013) 155
- The work presented in chapter 4 was done in collaboration with Archisman Ghosh, Suvrat Raju, and Sandip P. Trivedi and is based on the publication that appeared in print as JHEP 1407 (2014) 011.

To

My Baba and Ma

Synopsis

Introduction

One of the most challenging and conceptually deep problems in theoretical physics, in recent years, has been to understand the quantum nature of gravity. String theory, besides being a consistent and mathematically elegant framework in itself, is considered to be the leading candidate to demystify quantum gravity. It contains a plethora of low energy ground states, usually referred to as the landscape. Each one of these vacua has widely different symmetry properties from others and the low energy excitations around each one of them constitute different phases of the theory. These different phases emerging out of String theory are able to explain the familiar symmetries that play a role in nature. It contains, within its framework, the ingredients to realize, for example, the symmetries of the Standard Model of particle physics. In addition, String theory embodies new and strange symmetries beyond the Standard model, *e.g.* supersymmetry, which is ubiquitous in it's construction but is yet to be realized in experiments. Therefore it is of immense importance to study and understand symmetries and phases in general within the framework of String theory.

In this thesis we explore various aspects of symmetries and study different phases in a gravity theory to understand some interesting features prevalent in nature around us. In particular, guided by the lessons from such studies in gravity we find their applications to two considerably different areas of physics: strongly coupled field theories and early Universe cosmology. To establish this connection, the main computational technique that we use, follows from the AdS/CFT[1] correspondence in String theory, also known as holography.

The AdS/CFT correspondence, also frequently referred to as gauge-gravity duality, is one of the most significant results that String theory has produced. It relates two considerably different theories, a gauge theory without gravity to a quantum theory of gravity living in one higher dimension, see [1] for a review and the references therein. Most importantly, being a strong-weak duality it provides us a powerful computational tool to explore strongly coupled field theories, which are otherwise beyond the scope of perturbative calculation, via tractable Einstein gravity. As a consequence, research in String theory has now found its widespread application in other branches of physics as well, for example, condensed matter

[1]The abbreviation AdS/CFT stands for anti de-Sitter/conformal field theory.

physics, QCD etc.; see the reviews [2, 3, 4, 5] for connections to condensed matter physics and [6] for QCD related applications.

On the other hand, both theoretically and observationally, the physics of our Universe shortly after its birth is by itself a fascinating subject of modern day research. The approximate homogeneity and isotropy at large enough length scales leads us to believe that our Universe at that early stage went through a tiny phase of rapid expansion. In cosmology, theoretical calculations on various toy models come up with predictions that are tested against observations. In view of the abundance of models and lack of any compelling one it is more natural to try to understand model independent features of the early Universe based on symmetry considerations alone. Interestingly, as we will see in this thesis, in some contexts for the study of early Universe the holographic principle happens to be an useful computational tool.

In the first part of the thesis, based on [7], we address the question: what kind of phases found in nature can be realized in gravity description. With the help of a symmetry classification for the generalized translational symmetries, named the Bianchi classification, we find possible near horizon gravity solutions, which are homogeneous but not necessarily isotropic, falling into each class. These gravity solutions extend the existing set of a very few solutions known so far on the gravity side and correspond to similar homogeneous but possibly anisotropic phases abundantly observed in condensed matter systems.

In the next part of the thesis, based on [8], we run our investigation the other way round and try to understand if phases in gravity are of interest in condensed matter physics. We consider a specific solution in a system of gravity coupled to scalar and gauge fields with a negative cosmological constant. It corresponds to a compressible phase on the field theory side with an unbroken global symmetry at finite chemical potential, *e.g.* Fermi liquids. We further investigate the existence of a Fermi surface in those phases by looking at its response to turning on a small magnetic field. For that we study an interesting property of the system called entanglement entropy and compute it using holography in the gravity side.

In the third and concluding part of this thesis, in [9], we study conformal invariance during inflation, a proposed theoretical mechanism to describe the phase of rapid expansion of our Universe at a very early epoch. The approximate de-Sitter (dS_4) spacetime during inflation has symmetries which are same as that of a 3 dimensional Euclidean conformal field theory (CFT) and that imposes non-trivial constraints on the correlation functions of the cosmological perturbations produced at that time. These correlation functions are measured directly in the sky by looking at the anisotropies in the cosmic microwave background (CMB) radiation. In slow-roll inflation we compute the four point correlator[2] of the temperature perturbations in the CMB using techniques borrowed from AdS/CFT correspondence and further investigate the non-trivial constraints on it imposed by the

[2] In cosmology literature it is also known as the trispectrum.

approximate conformal symmetry of the spacetime during inflation. The clarification of a subtle issue regarding gauge fixing leads us to the understanding of the conformal invariance of this correlator.

Finally we conclude with some discussions and further comments on future prospects.

Bianchi Attractors: A Classification of Extremal Black Branes

The huge landscape of vacua in string theory and the varied phases in nature indicate that perhaps some of the vacua in string theory can help in describing some of these phases in nature. This hope has initiated an interesting dialogue between AdS gravity and condensed matter systems, particularly strongly correlated aspects of the latter. The quantum effects in strongly correlated systems are particularly important at zero temperature leading to novel physical phenomena like quantum criticality. On the gravity side the different kinds of behavior at zero temperature maps to different kinds of extremal black hole/black brane solutions. It is then natural to ask about the kind of phases found in nature, that can be realized in a gravity description. To our surprise, at a first glance, it appears that there exists many such phases in condensed matter systems compared to a very few extremal black brane solutions. This also suggests that on the gravity side we are only looking at the "tip of the iceberg", and that there is a much bigger zoo of solutions waiting to be discovered in theories of gravity with reasonable matter. A particular example of that is the finding of holographic superconductor, [10, 11, 12, 13].

With this motivation, in [7], we find many new extremal black brane solutions in (4+1) dimensions and classify all of them which preserve homogeneity along the spatial directions in which the extremal brane extends. These solutions belong to the general class of solutions in gravity known as attractors, in the sense that the near horizon solution is determined only by the charges carried by the black hole and is insensitive to the differences away from the horizon. From the dual field theory perspective it is a statement of universality *i.e.* differences in the ultraviolet (UV) often become irrelevant in the infrared (IR).

The Generalized Translations and Bianchi Classification:

The black brane solutions known so far, *e.g.* AdS_5, $AdS_2 \times R^3$, Lifshitz etc. preserve translational invariance along the spatial directions in which the brane extends. The new solutions we find are homogeneous along these directions but not translationally invariant. To be more specific, any two points can be connected by a symmetry transformation but the symmetry transformations do not necessarily commute. For example, consider we are in three dimensional space described by coordinates x^1, x^2, x^3 and suppose the system of interest has the usual translational symmetries along the x^2, x^3 directions. It also has an additional symmetry but instead of being the usual translation in the x^1 direction it is now a translation accompanied by a rotation in the $x^2 - x^3$ plane. The symmetry generators with their commutation relations are

$$\begin{aligned} \xi_1 = \partial_2, \quad \xi_2 = \partial_3, \quad \xi_3 = \partial_1 + x^2\partial_3 - x^3\partial_2, \\ [\xi_1, \xi_2] = 0; \quad [\xi_1, \xi_3] = \xi_2; \quad [\xi_2, \xi_3] = -\xi_1. \end{aligned} \tag{1}$$

It is worth noting that there couldn't be any scalar order parameter respecting the symmetries in eq.(1), but we need a vector order parameter for that.

All such symmetry groups preserving homogeneity in three dimensions have been classified and have been used in the study of homogeneous solutions in cosmology, see [14, 15]. Homogeneous 3 dimensional spaces are classified by the Bianchi classification with each different class corresponding to inequivalent 3 dimensional real algebras. In the mathematics literature there are 9 such classes of real 3 dimensional algebras.

The Gravity Solutions: General Considerations

We consider a spacetime metric incorporating the generalized translational symmetries described above and look for it as a solution to Einstein equations of gravity coupled with matter. We work in 5 dimensions with the homogeneity along the spatial directions along with time translational invariance and stationary situations,

$$ds^2 = dr^2 - a(r)^2 dt^2 + g_{ij} dx^i dx^j, \tag{2}$$

with the indices i, j taking values $1, 2, 3$. For any fixed value of r and t, we get a three dimensional homogeneous subspace spanned by x^i's corresponding to one of the 9 types in the Bianchi classification.

As discussed in [15], for each of the 9 cases there are three invariant one forms, $\omega^{(i)}, i = 1, 2, 3$, which are invariant under all 3 isometries. A metric expressed in terms of these one-forms with x^i independent coefficients will be automatically invariant under the isometries. In addition, the further assumption of an additional isometry, the scale invariance under $r \to r + \epsilon$ and $t \to t\, e^{-\beta_t \epsilon}$ along with $\omega^{(i)} \to e^{-\beta_i \epsilon}\, \omega^{(i)}$, fixes the metric to be of the form

$$ds^2 = R^2 \left[dr^2 - e^{2\,\beta_t\, r}\, dt^2 + \eta_{ij}\, e^{(\beta_i + \beta_j)\, r}\, \omega^{(i)} \times \omega^{(j)} \right], \tag{3}$$

with η_{ij} being a constant matrix which is independent of all coordinates.

The system we consider is consisted of massive gauge fields coupled to gravity with an action[3]

$$S = \int d^5x \sqrt{-g} \left\{ R + \Lambda - \frac{1}{4} F^2 - \frac{1}{4} m^2 A^2 \right\} \tag{4}$$

and has two parameters, m^2, Λ.

[3] Note that in our conventions $\Lambda > 0$ corresponds to AdS space.

An Explicit Example: Type-VII

To construct a simple and explicit example we show that a metric of type-VII symmetry can arise as a solution to Einstein equations. The invariant one-forms are

$$\omega^{(1)} = dx^1; \qquad \omega^{(2)} = \cos(x^1)\, dx^2 + \sin(x^1)\, dx^3; \qquad \omega^{(3)} = -\sin(x^1)\, dx^2 + \cos(x^1)\, dx^3. \quad (5)$$

In fact situations with this type of a vector order parameter are well known to arise in condensed matter physics, *e.g.* in spin systems, where the order parameter is the magnetization. In the presence of parity violation in such a system a helical spin density wave of appropriate wavelength can be set up [16], [17]. The gauge field and the metric can be written as,

$$\begin{aligned} A =& \tilde{A}_2\, e^{\beta\, r} \omega^{(2)} \qquad \text{and} \\ ds^2 =& R^2 \left[dr^2 - e^{2\,\beta_t\, r} dt^2 + (dx^1)^2 + e^{2\,\beta\, r} \left((\omega^{(2)})^2 + \lambda^2 (\omega^{(3)})^2 \right) \right]. \end{aligned} \quad (6)$$

Note that when $\lambda = 1$ the symmetries in the (x^1, x^2, x^3) directions are enhanced to the usual translations and rotations. From eq.(5) we see that the coordinate distance in x^1 direction needed to complete one full rotation in the $x^2 - x^3$ plane is 2π and from eq.(6) it follows that the physical distance along the x^1 direction that is needed is $2\pi R$. Thus R determines the pitch of the helix.

The Einstein equations and the equation of motion for the gauge field gives an explicit solution where the unknown parameters R, β_t, β, λ, entering in the metric and $\tilde{A}_2$, denoting the gauge field, are determined in terms of the parameter Λ, m^2, which appear in the action.

Working with the same system eq.(4), we obtain solutions of other Bianchi types as well.

The solution we described above is only the near horizon part of a full solution that asymptotes to AdS_5 at large radial distance. We couldn't obtain a full analytical solution of that kind but for type-VII we construct a numerical solution that asymptotes to AdS_5. Start from the near horizon region with a particular perturbation turned on which grows in the UV we numerically integrate out to asymptotic infinity. This, using the prescription of holography, allows us to consider a field theory living in flat space but subjected to a helically varying external current. The gravity solution teaches us that the field theory flows to a fixed point in the infra-red with an emergent non-trivial metric of the type-VII kind.

Summary and Comments

In summary, in this work we extend the known solutions of black brane geometries and find new solutions with reduced symmetry relaxing the requirement of isotropy. We show that extremal black branes need not be translationally symmetric, instead, they can be homogeneous. In (4+1) dimensions such extremal branes are classified by the Bianchi classification and fall into 9 classes. The near horizon geometry for several classes can be constructed in relatively simple gravitational systems. In the follow up works, [18], [19] we extended our study of these Bianchi attractors to situations with further reduced symmetries and also to constructing full interpolating solutions for other types as well. Embedding some of these solutions in String/Supergravity theories has also been studied in [20]. The stability of these solutions along with thermodynamic and transport properties are worth exploring.

A Compressible Phase From Gravity: Fermi Surface and Entanglement

In the previous part of this thesis we have already seen that insights from condensed matter physics appear to be useful in the understanding of various phases arising in gravity. In this work we try to investigate this connection the other way round, exploring the possible relevance of a study of interesting brane solutions in gravity to condensed matter systems.

The Einstein-Maxwell-Dilaton (EMD) system in (3+1) spacetime dimensions consisting of gravity and a Maxwell gauge field coupled to a neutral scalar (the dilaton) allows promising new phases in gravity to arise corresponding to compressible states of matter[4], see [21, 22]. On the field theory side this enables one to study fermions at finite density with strong correlations, in particular with an unbroken global $U(1)$ symmetry. The gauge field in the bulk corresponds to having the fermions in the boundary theory carrying a conserved charge - fermion number, corresponding to the unbroken global $U(1)$ symmetry. The thermodynamics and transport properties of these systems do not fit those of a Landau Fermi liquid. For example, the specific heat at small temperatures is typically not linear in the temperature (T) and the electric resistivity also does not have the required T^2 dependence.

In an exciting independent development it was proposed that one can compute entanglement entropy, a measure of the degree of correlation within any system, using holographic techniques. Holographic calculation of Entanglement Entropy, S_{EE}, for EMD system yields

$$S_{EE} \sim A \log(A), \tag{7}$$

where A is the area of the boundary of the region in the field theory, of which entanglement entropy is calculated.[5] The log enhancement is believed to be the tell-tale signature of a Fermi surface, [23]. Taken together, these developments suggest that EMD system, perhaps,

[4] A compressible phase is one in which the density of particles can be varied smoothly by an external chemical potential, without changing the basic characteristics of the phase. More specifically, the criteria of a phase being compressible is $\frac{\partial n}{\partial \mu} \neq 0$, where n is the charge density and μ being the chemical potential.

[5] It is important to remember that this logarithmic behavior is the leading contribution in entanglement entropy when the UV cut off energy scale is of the same order as the Fermi energy, which is quite common

describes phases with Fermi surface but of non-Fermi liquid type. While this is a promising possibility it is far from being definitely established. In fact, at large N (classical gravity) the system does not exhibit some of the standard characteristics expected of a system with a Fermi surface, for example, neither any de Haas-van Alphen effect nor Friedel oscillations.

We, in [8], investigate this EMD system from the gravity side by subjecting it to a small magnetic field and look at the response. More specifically we study the fate of the gravity solution, thermodynamics and existence of a Fermi surface through entanglement entropy.

The Dilaton Gravity System with Hyperscaling Violating Solutions

We work with an action,

$$S = \int d^4x \sqrt{-g} \left[R - 2(\nabla\phi)^2 - e^{2\,\alpha\,\phi} F_{\mu\nu}F^{\mu\nu} + |V_0|\, e^{2\,\delta\,\phi} \right]. \tag{8}$$

The two parameters, α, δ, govern the behavior of the system. We obtain an electrically charged black brane solution of the form,

$$ds^2 = -C_a^2\, r^{2\gamma}\, dt^2 + \frac{dr^2}{C_a^2\, r^{2\gamma}} + r^{2\beta}(dx^2 + dy^2) \qquad \text{and} \qquad \phi = k \log r, \tag{9}$$

with the parameters C_a, γ, β, k and the electric charge Q_e are solved in terms of α, δ.

The solution is not scale invariant, rather under a scaling of the form

$$r = \lambda\, \tilde{r}, \qquad t = \lambda^{1-2\gamma}\, \tilde{t}, \qquad \{x,\, y\} = \lambda^{1-\gamma-\beta}\, \{\tilde{x},\, \tilde{y}\} \tag{10}$$

it remains invariant up to an overall conformal factor[6]. From the dual field theory point of view this means that the free energy does not scale with its naive dimensions, which is referred to as hyperscaling violation, see [22].

It is important to note that in our two dimensional phase space (*i.e.* α, δ -plane) of the solutions, the holographic entanglement entropy shows a logarithmic enhancement, given in eq.(7), for $\alpha + 3\delta = 0$ indicating existence of a Fermi surface.

Effect of Small Magnetic Field

Describing the solution obtained with only electric charge, we further study the effects of turning on a small magnetic field[7] specified by Q_m. Depending on which region of the

in condensed matter physics. On the other hand for analysis in high energy physics the UV cut off scale is generally considered as much higher than the Fermi energy and we get the area law in entanglement entropy as the leading divergent contribution. Besides this divergent term, there is however a finite term which gives a logarithmic contribution as in eq.(7).

[6] The scale transformation in eq.(10) is a conformal Killing vector for the metric in eq.(9).

[7] The magnetic field is small compared to the only scale available in the electric solution, *i.e.* chemical potential (μ), such that $|Q_m| < \mu^2$.

parameter space (α, δ -plane) we are considering, the effect of magnetic field either becomes relevant or irrelevant in the IR. For the cases when it is relevant towards IR, in particular for $|\alpha| > \delta$, we find that the near horizon solution changes from being purely electric hyperscaling violating type to a completely different $AdS_2 \times R^2$ type[8]. The effects of the magnetic field according to particular parametric regions in α, δ-plane along with the new IR solutions are summarized in table 1.

Region in α, δ-plane	Effect of magnetic field	Nature of the new IR solution
$0 > \alpha > -\delta$	Irrelevant in IR	Remains purely Electric
$\|\alpha\| > \delta$	Relevant in IR	A new $AdS_2 \times R^2$ solution
$0 < \alpha < \delta$	Relevant in IR	Purely magnetic solution (?)

Table 1: Effect of turning on a small magnetic field in the purely electric solution.

We further demonstrate that, for the case $|\alpha| > \delta$, starting from the purely electric hyperscaling violating solution and studying linearized perturbations around it growing towards the IR, one can numerically integrate inwards to IR and obtain the $AdS_2 \times R^2$ solution. Besides this we also obtain perturbations of the electric solution growing towards UV and connecting it to asymptotic AdS_4 spacetime. We couldn't carry out the same numerical study for the case $0 < \alpha < \delta$, nevertheless we guess the near horizon solution and show that such a solution is allowed.

For $|\alpha| > \delta$, where the near horizon solution becomes of the form $AdS_2 \times R^2$, the thermodynamics also changes considerably in the presence of the magnetic field. For example, the specific heat scales linearly with temperature while the state still remains to be compressible. Most importantly, the entropy density now becomes non-zero even at extremality, for $\alpha + 3\delta = 0$, it scales with Q_m as

$$s \sim (Q_m)^{1/3}, \tag{11}$$

with a non-trivial and universal exponent, suggesting that the ground state is more interesting and strange.

Study of Holographic Entanglement Entropy

The entanglement entropy for the hyperscaling violating metrics we are considering, has already been worked out, using holography, in [24], see also [22]. Consider a circular region, **R**, in the dual field theory such that it's boundary, ∂**R**, is a circle of radius L. To compute the entanglement entropy of **R** we work on a fixed constant time slice and find the surface in the bulk which has minimum area subject to the condition that it terminates in ∂**R** at the boundary of AdS. The entanglement entropy is then computed as given in [25, 26], as

$$S_{EE} = \frac{A_{min}}{4G_N}, \tag{12}$$

[8]It is important to note that $\alpha + 3\delta = 0$, indicating the existence of Fermi surface, is contained here.

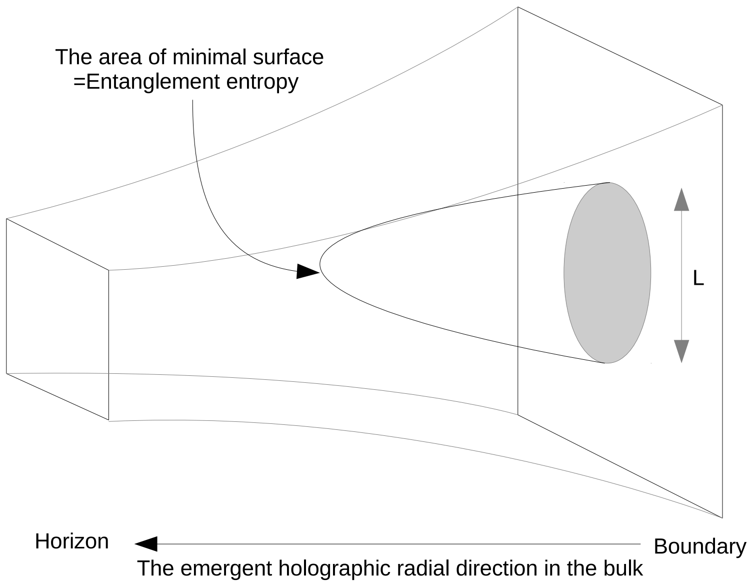

Figure 1: Holographic entanglement entropy.

where A_{min} is the area of this surface in the bulk and G_N is the Newton's constant.

Following this proposal we consider the situation with the small magnetic field turned on and $|\alpha| > \delta$, where the near horizon solution is of the form $AdS_2 \times R^2$. As we start with a boundary circle of very small radius ($L \ll 1$) and slowly increase its size the bulk surface penetrates deeper and for sufficiently large L, it starts seeing the near horizon $AdS_2 \times R^2$ region. Consequently the entanglement entropy starts getting contribution from $AdS_2 \times R^2$ region and scales like L^2. This shows that the entanglement entropy starts scaling extensively with the "volume"[9] of the region **R** under consideration.

Summary and Outlook

In summary, our study of the EMD system showed that for parameters where the electric theory has an entanglement of the form eq.(7) the magnetic field is a relevant perturbation in the IR. As a result even a small magnetic field has a dramatic effect on the state of the system, more generally we learn that the compressible state described by the purely electric solution "anti-screens" the effects of the magnetic field.

[9] In our case with (2+1) dimensional boundary, this is the "area" of the boundary circular region.

The behavior mentioned above is roughly analogous to what happens in a weakly coupled system with a Fermi surface. While in this case the introduction of a small magnetic field leads to the formation of Landau levels, at intermediate energies still low compared to the Fermi energy but big compared to the spacing of the Landau levels (correspondingly at intermediate length scales smaller than the magnetic length) the behavior continues to be essentially that of a system with a Fermi surface. In particular the thermodynamics is essentially unchanged by the small magnetic field and the entanglement entropy is also expected to have the $A\,log(A)$, eq.(7), behavior at these length scales. Though going to much lower energies of order the spacing between the Landau level (correspondingly to distance scales of order or longer than the magnetic length) the behavior of the system can change. For example in the free fermion theory, depending on the fermion density, a Landau level can be fully or partially filled, and partial filling would result in an extensive ground state entropy.

The near extremal hyperscaling violating attractors in EMD theories are not IR-complete since the possible IR end point $AdS_2 \times R^2$ has extensive ground state entropy along with spatially modulated instabilities. Thus the issue of the IR completion and the true ground state of the hyperscaling violating geometries is yet to be understood properly, see [27, 28, 29]. It would also be worth understanding these constructions better and also gaining a better understanding of their dual field theory descriptions.

Conformal Invariance During Inflation: Four Point Correlator of Temperature Perturbations in CMB

In this final part of the thesis, based on [9], we turn our attention to a study of cosmological perturbations during inflation and the constraints put on them by approximate conformal symmetry of the spacetime. Inflation is an elegant formalism that not only explains the approximate homogeneity and isotropy of our Universe at large length scales but also provides a mechanism for producing perturbations to break them. The Universe during inflation was approximately de-Sitter, with a symmetry group $SO(4,1)$ which is same as that of a 3 dimensional Euclidean CFT. It is then natural and useful to ask how this symmetry group can be used to learn about the correlations of cosmological perturbations, if possible in a model independent way.

Cosmic Microwave Background (CMB) radiation is the oldest light in our Universe that reaches us. It is a snapshot of the moment when the neutral atoms were first formed and the photons started free streaming ever after, also referred to as the last scattering surface. The cosmological perturbations produced during inflation are imprinted in the CMB as the tiny anisotropies (1 part in 10^5) of it's temperature and polarization.

It has already been learnt that symmetry considerations alone can put non-trivial constraints on correlation functions of cosmological perturbations, see [30]. To be more specific, these symmetries are realized as Ward identities on their correlation functions. In a CFT, the symmetries fix all the three point correlators in terms of their functional form and also the normalizations, see [31, 32]. In this work we extend this study to the higher point correlator, namely the four point correlator of the temperature perturbations in CMB. This correlator is not fixed, as expected from CFT arguments. In canonical slow-roll model of inflation it has been already computed, [33], using "in-in" formalism. But the answer was not invariant under conformal symmetry. This puzzling feature motivated us to embark on a two stage analysis: calculating the correlator using a different technique borrowed from AdS/CFT correspondence and studying its invariance under conformal symmetry. We calculate the correlator at late enough time when the modes crosses horizon. In the process we discover a subtlety in the way the symmetries are at play for the four point correlator owing to the fact that gravity is a gauge theory. We also learn to ask the correct question regarding how the invariance under conformal symmetries are implemented in the correlators.

Basic Set Up

The de-Sitter spacetime has a metric of the form

$$ds^2 = -dt^2 + e^{2\,H\,t} \sum_{i=1}^{3} dx^{i^2}, \tag{13}$$

where the constant H is the de-Sitter scale or the Hubble parameter. The isometry group of dS_4, $SO(4,1)$, has 10 Killing generators: 3 translations, 3 rotations, 1 scaling and 3 special conformal transformations. It is interesting to recall that Euclidean AdS_4 ($EAdS_4$) also has the same symmetry group as dS_4 and upon analytic continuation they can be transformed to each other. Without assuming anything in particular about the as yet speculative dS/CFT correspondence these symmetry considerations help us to translate the questions regarding dS_4 to those in a 3 dimensional CFT and also use techniques from AdS/CFT correspondence for calculating correlation functions of cosmological perturbations .

Inflation is explained through a model of scalar field (inflaton) with a slowly varying potential coupled to Einstein gravity. As a result the $SO(4,1)$ symmetry of dS_4 is slightly broken due the slow rolling of the inflaton. We consider a single inflaton with the action of the form

$$S = \int d^4x\,\sqrt{-g}\,\frac{1}{8\pi G_N}\left[\frac{1}{2}R - \frac{1}{2}(\nabla\phi)^2 - V(\phi)\right]. \tag{14}$$

The slow-roll conditions introduces two additional parameters apart from the Hubble scale H, characterizing the slow variation of H or equivalently that of the scalar potential,

$$\epsilon = \left(\frac{V'}{2V}\right)^2 = -\frac{\dot{H}}{H^2} = \frac{1}{2}\frac{\dot{\phi}^2}{H^2} \ll 1, \qquad \text{and} \qquad \eta = \frac{V''}{V} = \epsilon - \frac{\ddot{H}}{2H\dot{H}} \ll 1. \tag{15}$$

Since we are interested in situations at a given time instant it is useful to consider the ADM formalism which is well suited for hamiltonian construction of general relativity and write the metric in terms of the shift and lapse functions, N_i and N respectively, as

$$ds^2 = -N^2\,dt^2 + h_{ij}\,(dx^i + N^i\,dt)\,(dx^j + N^j\,dt). \tag{16}$$

The cosmological perturbations are of two types, scalars ($\delta\phi$, ζ) and tensors (γ_{ij}). They are defined as follows,

$$h_{ij} = e^{2Ht}(\delta_{ij}(1+2\zeta) + \gamma_{ij}) \qquad \text{and} \qquad \phi = \bar{\phi} + \delta\phi, \tag{17}$$

where $\bar{\phi}$ is the background value of the inflaton. These cosmological perturbations are related to the anisotropies in the CMB radiation and provided seeds for the structure formation in this Universe. More specifically the scalar perturbations ($\delta\phi$, ζ) are related to temperature anisotropies and the tensor one (γ_{ij}) is related to the polarization of the CMB radiation.

We make a choice to work in coordinates such that $N = 1$, $N_i = 0$ and also use the remaining gauge redundancy of time and spatial parametrization at late enough times to consider transverse-traceless gauge for the graviton, *i.e.* $\partial_i\gamma_{ij} = \gamma^i_i = 0$, and the scalar perturbations can also be chosen such that either $\delta\phi = 0$ and $\zeta \neq 0$ or $\delta\phi \neq 0$ and $\zeta = 0$.

It is important to note that we will work in momentum space and though position space analysis of the correlation functions are known in a CFT, it is not straight forward to convert them to momentum space due to presence of contact terms.

The Wave Function of The Universe From The AdS Partition Function

Symmetry considerations are useful when studied in terms of wave function of the universe, well known in the context of quantum cosmology. Invariance under symmetry translates to the invariance of this wave function. It is defined as a functional of the late time values of the perturbations $\delta\phi$, γ_{ij} through the path integral

$$\psi[\delta\phi,\,\gamma_{ij}] = \int^{\delta\phi,\,\gamma_{ij}} D\chi\; e^{i\,S[\chi]}, \tag{18}$$

where χ on the RHS represent collectively $\delta\phi$, γ_{ij} and the boundary conditions at far past is the standard Bunch-Davies one[10]. With the knowledge of the perturbations being nearly

[10] The Bunch-Davies boundary condition basically means that the modes at far past had wavelength much smaller than the Hubble scale, hence they were insensitive to the curvature of the de-Sitter space and essentially propagated as if in Minkowski space.

Gaussian, we can write the wave function as

$$\psi[\delta\phi,\gamma_{ij}] = \exp\Bigg[\Bigg(-\frac{1}{2}\int d^3x\,d^3y\,\delta\phi(x)\,\delta\phi(y)\,\langle O(x)O(y)\rangle - \frac{1}{2}\int d^3x\,d^3y\,\gamma_{ij}(x)\,\gamma_{kl}(y)\,\langle T^{ij}(x)T^{kl}(y)\rangle$$
$$- \frac{1}{4}\int d^3x\,d^3y\,d^3z\,\delta\phi(x)\,\delta\phi(y)\,\gamma_{ij}(z)\,\langle O(x)O(y)T^{ij}(z)\rangle \tag{19}$$
$$+ \frac{1}{4!}\int d^3x\,d^3y\,d^3z\,d^3w\,\delta\phi(x)\,\delta\phi(y)\,\delta\phi(z)\,\delta\phi(w)\,\langle O(x)O(y)O(z)O(w)\rangle + \cdots \Bigg)\Bigg].$$

where the third, fourth terms and the ellipses in the exponent on RHS denote non-Gaussian corrections. Invariance of the wave function under conformal invariance will fix the transformations of the coefficient functions $\langle O(x)\,O(y)\rangle$, $\langle O(x)\,O(y)\,T^{ij}(z)\rangle$ confirming $O(x)$, $T^{ij}(x)$ as operators in a 3 dimensional CFT. This way we recast our study of symmetries for cosmological perturbations to that of correlation functions in a CFT. Furthermore invariance under the full conformal group translates to Ward identities involving these correlators.

The symmetries of dS_4 and $EAdS_4$ being same relates the wave function in dS_4, as a functional of the late time values of the perturbations, to the partition function in $EAdS_4$, which is a functional of the boundary values of the fields. Alternatively in terms of the on-shell action, working in the leading semi-classical saddle point approximation, we write for the wave function

$$\psi = e^{i\,S^{dS}_{\text{on-shell}}} = e^{S^{EAdS}_{\text{on-shell}}}. \tag{20}$$

In the leading slow-roll approximation we compute the on-shell action in $EAdS_4$ space using the techniques of holography, namely Feynman-Witten diagrams, as a functional of boundary values of the fields. A further analytic continuation gives us the wave function of the Universe as a functional of the late time values of the perturbations.

The Four Point Correlator and Conformal Invariance

Once we know the wave function as a functional of the late time values of the perturbations, $\delta\phi$, γ_{ij}, the four point correlator can be obtained through the functional integration,

$$\langle\delta\phi(\mathbf{k}_1)\delta\phi(\mathbf{k}_2)\delta\phi(\mathbf{k}_3)\delta\phi(\mathbf{k}_4)\rangle = \mathcal{N}\int\mathcal{D}[\delta\phi]\,\mathcal{D}[\gamma_{ij}]\,\prod_{i=1}^{4}\delta\phi(\mathbf{k}_i)\;|\psi[\delta\phi,\,\gamma_{ij}]|^2$$
$$\text{with}\quad \mathcal{N}^{-1} = \int\mathcal{D}[\delta\phi]\,\mathcal{D}[\gamma_{ij}]\;|\psi[\delta\phi,\,\gamma_{ij}]|^2. \tag{21}$$

The final answer for the four point correlator has three contributions: (a) from graviton exchange in the boundary, (b) from the transverse component of the graviton exchange in the bulk, and (c) from the longitudinal component of the graviton exchange in the bulk. This answer matches with the already existing answer in the literature, [33, 34]. This is very surprising because the already existing answer was not invariant under the Ward identities of conformal symmetry and it was this feature that at the first place we set out to calculate the correlator using a different technique.

The wave function that we calculated satisfies the Ward identity of conformal invariance. The puzzling feature of the correlator not being invariant under the conformal Ward identities unfolds a subtlety related to how the symmetries are at play for correlators as opposed to the wave function. This is because, to compute the correlator we need to do the functional integration over the tensorial perturbations in eq.(21). But to make sense of this integration in a gauge theory we had already fixed the gauge of the tensor perturbations to be transverse and traceless, as mentioned earlier. Interestingly the conformal transformation takes the graviton out of that gauge and we need to do a compensating coordinate reparametrization to bring it back to the transverse gauge. Thus the Ward identity for the correlator should be correctly modified and correspond to the combined change: the conformal transformation and the compensating coordinate reparametrization. The four point scalar correlator is indeed invariant under this refined Ward identity.

Summary and Comments

To summarize, we calculated the scalar four point correlator in slow-roll inflation agreeing with the existing result. In different relevant limits, as we checked, the result agrees with expectations from general considerations in a CFT.

We also clarified a subtle issue regarding the implementation of conformal invariance for the correlators as opposed to the wave function. This subtlety of conformal invariance for de-Sitter space correlators doesn't exist in AdS space. One needs to proceed differently in calculating a correlation function from a wave function in de-Sitter as opposed to from the partition function (in the presence of sources) in AdS. In AdS space the boundary value of the metric is a non-dynamical source and further taking derivatives of the partition function with respect to the source produces the correlation function. On the other hand in de-Sitter case, the metric at late times is a genuine degree of freedom and hence to calculate correlation functions from the wave function one must fix gauge completely.

Though there is no immediate hope of observational significance owing to small magnitude of the four point correlator, our study clarifies an important conceptual point regarding symmetries in general. Despite this, using the symmetry considerations we can consider other correlators which are observationally significant and try to make some predictions. Another interesting extension of our analysis would be to understand the breaking of conformal symmetry systematically within this framework.

Discussion

In this thesis we studied various aspects of symmetries and different phases in gravity. The AdS/CFT correspondence played an important role in our analysis since the main computational technique we used followed from it. It enabled us to find an useful application of our analysis to a different branch of physics, namely condensed matter physics. In the first two parts of this thesis we explored this relatively new connection between gravity theory and strongly coupled field theories. In the final part of the thesis we turned to a significantly different area of theoretical physics which is early universe cosmology. In all the three sections, the importance of symmetry principles and the existence of various phases in the study of gravity was highlighted. Apart from this the holographic principle also proved to be a common feature in all of them.

In the first part, in section , insights from the phases in dual field theory inspired our gravity analysis. Using the classification of real 3 dimensional algebras studied in Mathematics, and previously used in cosmology, *i.e.* the Bianchi classification, we found solutions corresponding to homogeneous but not necessarily isotropic geometries. The type-VII geometry is indeed realized in condensed matter systems with a helical symmetry, *e.g.* in spin density waves.

In the next part, in section , we used the gauge-gravity duality in the reversed way, exploring the possibility of some gravity solutions in specific systems can provide insights for condensed matter physics. The hyperscaling violating solutions in dilatonic gravity models indeed serve the purpose, as they provide a set up for studying strongly correlated aspects of field theories like non-Fermi liquid behavior etc. Though there are promising hopes a lot has to be understood in order to put this connection between phases in gravity and condensed matter systems on a firm footing.

Finally, in section , in the last part of this thesis, we analyzed the symmetries of a CFT and constraints put by them on correlation functions of operators. The general lessons obtained were then applied to learn about the correlations between the cosmological perturbations encoded in CMB radiation. We believe that our analysis would thus serve as an important conceptual advancement in the understanding of the physics of early Universe based on symmetry considerations alone. On the other hand, study of conformal field theories in itself is also fascinating and it will be interesting to see if our analysis can be extended to that field of research.

Bibliography

[1] O. Aharony, S. S. Gubser, J. M. Maldacena, H. Ooguri, and Y. Oz, *Large N field theories, string theory and gravity*, *Phys.Rept.* **323** (2000) 183–386, [hep-th/9905111]. ix

[2] S. A. Hartnoll, *Lectures on holographic methods for condensed matter physics*, *Class.Quant.Grav.* **26** (2009) 224002, [arXiv:0903.3246]. x

[3] C. P. Herzog, *Lectures on Holographic Superfluidity and Superconductivity*, *J.Phys.* **A42** (2009) 343001, [arXiv:0904.1975]. x

[4] J. McGreevy, *Holographic duality with a view toward many-body physics*, *Adv.High Energy Phys.* **2010** (2010) 723105, [arXiv:0909.0518]. x

[5] S. Sachdev, *What can gauge-gravity duality teach us about condensed matter physics?*, *Ann.Rev.Condensed Matter Phys.* **3** (2012) 9–33, [arXiv:1108.1197]. x

[6] J. Casalderrey-Solana, H. Liu, D. Mateos, K. Rajagopal, and U. A. Wiedemann, *Gauge/String Duality, Hot QCD and Heavy Ion Collisions*, arXiv:1101.0618. x

[7] N. Iizuka, S. Kachru, N. Kundu, P. Narayan, N. Sircar, et al., *Bianchi Attractors: A Classification of Extremal Black Brane Geometries*, *JHEP* **1207** (2012) 193, [arXiv:1201.4861]. x, xi

[8] N. Kundu, P. Narayan, N. Sircar, and S. P. Trivedi, *Entangled Dilaton Dyons*, *JHEP* **JHEP03** (2013) 155, [arXiv:1208.2008]. x, xv

[9] A. Ghosh, N. Kundu, S. Raju, and S. P. Trivedi, *Conformal Invariance and the Four Point Scalar Correlator in Slow-Roll Inflation*, arXiv:1401.1426. x, xviii

[10] S. S. Gubser, *Breaking an Abelian gauge symmetry near a black hole horizon*, *Phys.Rev.* **D78** (2008) 065034, [arXiv:0801.2977]. xi

[11] S. A. Hartnoll, C. P. Herzog, and G. T. Horowitz, *Building a Holographic Superconductor*, *Phys.Rev.Lett.* **101** (2008) 031601, [arXiv:0803.3295]. xi

[12] S. A. Hartnoll, C. P. Herzog, and G. T. Horowitz, *Holographic Superconductors*, *JHEP* **0812** (2008) 015, [arXiv:0810.1563]. xi

[13] G. T. Horowitz, *Introduction to Holographic Superconductors*, *Lect.Notes Phys.* **828** (2011) 313–347, [arXiv:1002.1722]. xi

[14] L. D. Landau and E. M. Lifshitz, *The Classical Theory of Fields*. Butterworth-Heinemann, 4 ed., Jan., 1980. xii

[15] M. P. Ryan and .-j. a. Shepley, Lawrence C., *Homogeneous relativistic cosmologies / by Michael P. Ryan, Jr., and Lawrence C. Shepley*. Princeton, N.J. : Princeton University Press, 1975. xii

[16] M. Kataoka and O. Nakanishi, *Helical spin density wave due to antisymmetric exchange interaction*, *Journal of the Physical Society of Japan* **50** (1981), no. 12 3888–3896, [http://dx.doi.org/10.1143/JPSJ.50.3888]. xiii

[17] M. L. Plumer and M. B. Walker, *Wavevector and spin reorientation in mnsi*, *Journal of Physics C: Solid State Physics* **14** (1981), no. 31 4689. xiii

[18] N. Iizuka, S. Kachru, N. Kundu, P. Narayan, N. Sircar, et al., *Extremal Horizons with Reduced Symmetry: Hyperscaling Violation, Stripes, and a Classification for the Homogeneous Case*, *JHEP* **1303** (2013) 126, [arXiv:1212.1948]. xiv

[19] S. Kachru, N. Kundu, A. Saha, R. Samanta, and S. P. Trivedi, *Interpolating from Bianchi Attractors to Lifshitz and AdS Spacetimes*, *JHEP* **1403** (2014) 074, [arXiv:1310.5740]. xiv

[20] K. Inbasekar and P. K. Tripathy, *Stability of Bianchi attractors in Gauged Supergravity*, *JHEP* **1310** (2013) 163, [arXiv:1307.1314]. xiv

[21] N. Iizuka, N. Kundu, P. Narayan, and S. P. Trivedi, *Holographic Fermi and Non-Fermi Liquids with Transitions in Dilaton Gravity*, *JHEP* **1201** (2012) 094, [arXiv:1105.1162]. xiv

[22] L. Huijse, S. Sachdev, and B. Swingle, *Hidden Fermi surfaces in compressible states of gauge-gravity duality*, *Phys.Rev.* **B85** (2012) 035121, [arXiv:1112.0573]. xiv, xv, xvi

[23] Y. Zhang, T. Grover, and A. Vishwanath, *Entanglement Entropy of Critical Spin Liquids*, *Physical Review Letters* **107** (Aug., 2011) 067202, [arXiv:1102.0350]. xiv

[24] N. Ogawa, T. Takayanagi, and T. Ugajin, *Holographic Fermi Surfaces and Entanglement Entropy*, *JHEP* **1201** (2012) 125, [arXiv:1111.1023]. xvi

[25] S. Ryu and T. Takayanagi, *Holographic derivation of entanglement entropy from AdS/CFT*, *Phys.Rev.Lett.* **96** (2006) 181602, [hep-th/0603001]. xvi

[26] S. Ryu and T. Takayanagi, *Aspects of Holographic Entanglement Entropy*, *JHEP* **0608** (2006) 045, [hep-th/0605073]. xvi

[27] A. Donos, J. P. Gauntlett, and C. Pantelidou, *Spatially modulated instabilities of magnetic black branes*, *JHEP* **1201** (2012) 061, [arXiv:1109.0471]. xviii

[28] A. Donos and J. P. Gauntlett, *Holographic helical superconductors*, *JHEP* **1112** (2011) 091, [arXiv:1109.3866]. xviii

[29] J. Bhattacharya, S. Cremonini, and A. Sinkovics, *On the IR completion of geometries with hyperscaling violation*, *JHEP* **1302** (2013) 147, [arXiv:1208.1752]. xviii

[30] J. M. Maldacena, *Non-Gaussian features of primordial fluctuations in single field inflationary models*, *JHEP* **0305** (2003) 013, [astro-ph/0210603]. xviii

[31] J. M. Maldacena and G. L. Pimentel, *On graviton non-Gaussianities during inflation*, *JHEP* **1109** (2011) 045, [arXiv:1104.2846]. xix

[32] I. Mata, S. Raju, and S. Trivedi, *CMB from CFT*, *JHEP* **1307** (2013) 015, [arXiv:1211.5482]. xix

[33] D. Seery, M. S. Sloth, and F. Vernizzi, *Inflationary trispectrum from graviton exchange*, *JCAP* **0903** (2009) 018, [arXiv:0811.3934]. xix, xxi

[34] D. Seery, J. E. Lidsey, and M. S. Sloth, *The inflationary trispectrum*, *JCAP* **0701** (2007) 027, [astro-ph/0610210].

xxi

List of Publications

Papers relevant to the thesis work:

- *" Bianchi Attractors: A Classification of Extremal Black Brane Geometries "*;
  Norihiro Iizuka, Shamit Kachru, Nilay Kundu, Prithvi Narayan, Nilanjan Sircar, Sandip P. Trivedi;
  JHEP 1207 (2012) 193; arXiv:1201.4861 [hep-th]

- *"Entangled Dilaton Dyons"*;
  Nilay Kundu, Prithvi Narayan, Nilanjan Sircar, Sandip P. Trivedi;
  JHEP 1303 (2013) 155; arXiv:1208.2008 [hep-th].

- *"The Four Point Scalar Correlator in Slow-Roll Inflation"*;
  Archisman Ghosh, Nilay Kundu, Suvrat Raju, and Sandip P. Trivedi;
  JHEP 1407 (2014) 011; arXiv:1401.1426 [hep-th]

Other papers:

- *"Holographic Fermi and Non-Fermi Liquids with Transitions in Dilaton Gravity "* ;
  Norihiro Iizuka, Nilay Kundu, Prithvi Narayan, Sandip P. Trivedi;
  JHEP 1201 (2012) 094; arXiv:1105.1162 [hep-th].

- *"Extremal Horizons with Reduced Symmetry: Hyperscaling Violation, Stripes, and a Classification for the Homogeneous Case"*;
  Norihiro Iizuka, Shamit Kachru, Nilay Kundu, Prithvi Narayan, Nilanjan Sircar, Sandip P. Trivedi, Huajia Wang;
  JHEP 1303 (2013) 126; arXiv:1212.1948 [hep-th].

- *"Interpolating from Bianchi Attractors to Lifshitz and AdS Spacetimes"*;
  Shamit Kachru, Nilay Kundu, Arpan Saha, Rickmoy Samanta, Sandip P. Trivedi;
  JHEP 1403 (2014) 074; arXiv:1310.5740 [hep-th];

- *"A Strongly Coupled Anisotropic Fluid From Dilaton Driven Holography"*;
  Sachin Jain, Nilay Kundu, Kallol Sen, Aninda Sinha, Sandip P. Trivedi;
  JHEP 1501 (2015) 005; arXiv:1406.4874 [hep-th];

- *"Constraints from Conformal Symmetry on the Three Point Scalar Correlator in Inflation"*;
  Nilay Kundu, Ashish Shukla, Sandip P. Trivedi;
  JHEP 1504 (2015) 061; arXiv:1410.2606 [hep-th];

Contents

Appendices

Chapter 1

Introduction

A general Motivation:

Research in theoretical physics aims at providing a conceptual framework for wide variety of natural phenomena, so that not only are we able to come up with predictions that can be experimentally verified, but the underlying mathematical structures governing the world around us can also be well understood. In the past century two of the greatest achievements in theoretical physics have been general relativity and quantum physics. Each, besides revolutionizing our understanding of the physical world, has been successful in describing the same in its own domain to a surprising degree of accuracy. Most interestingly, the region of applicability of each one of them are strikingly different. Indeed, it is quite astonishing to notice that, despite so deep a conflict in the way quantum mechanics and general relativity work, progress in theoretical physics kept going blissfully. The reason being accidental in the sense that the fundamental constants in our universe conspire to attribute a very high value to the Planck energy, where quantum mechanics and general relativity unavoidably come together, compared to laboratory scales. Precisely because of this, we can happily take an appropriate and practical stand to visualize the real universe using general relativity while dealing with cosmological and astrophysical phenomena, whereas borrow ideas from quantum mechanics to understand the physics of atoms and subatomic particles. But it is highly unsatisfactory from a conceptual viewpoint. Driven by this, a large portion of research in theoretical physics has been directed in pursuit of an unified theory that embodies all the four fundamental forces experienced in nature. Specifically these four basic forces are: gravitation, electromagnetism, strong and weak interaction.

Historically, electromagnetism, described by Maxwell's equations, was the first example of a theory that successfully encompasses two previously separate theories, i.e. electricity and magnetism. Subsequent research in the past century has revealed that all the other three forces except gravity can be embodied in a unified formalism known as the Standard model of particle physics. Attempts to combine gravity with strong and electroweak interactions run into inconsistencies which in technical terms is described as the non-renormalizability of the resulting theory. The incompatibility of quantum mechanics and general relativity stands out as one of the most challenging and conceptually deep problems in theoretical physics. A unified theory, which will be a quantum theory of gravity, therefore not only should correctly describe all physical phenomena happening at laboratory scale, but it should also be able to explain physics at Planck regime, for example the physics of big bang or the final states of black holes, where the worlds of general relativity and quantum mechanics must unavoidably meet.

String theory, besides being a consistent and mathematically elegant framework in itself, is considered to be the leading candidate, amongst others, to demystify quantum gravity. It is postulated that in string theory the fundamental objects are one dimensional strings rather than point like particles. The distinct vibrating modes of these strings are conceived as the elementary particles of our universe. Since every consistent quantum theory of strings necessarily contain a massless spin two particle with the same kinematical and dynamical properties of a graviton, it automatically includes gravity. The basic mathematical structure formulating string theory is tightly constrained by consistency of the theory and this leads to only one unique string theory as opposed to the situation in particle physics where there are several possible consistent models. Although in perturbative formulation of string theory there are five different possible string theories [1], at the non-perturbative level there are several dualities between all these different theories that relates one to another and it is expected that all of them are different effective descriptions in different regimes of a unique underlying theory called M-theory. Despite being an unique theory, the field content of string theory includes various scalar fields, gauge fields, spin 2 gravitons as well as higher rank tensor fields which can take several different consistent background values and thus give rise to a plethora of low energy ground states for the theory. The allowed number of these ground states can be estimated to be as large as 10^{120}, see [2]. This huge set of low energy states is usually referred to as the landscape. Each one of these vacua has widely different symmetry properties from others. The low energy excitations around each one of these vacua and their spectrum constitute different phases of the theory. Self-consistency of string theory also fixes the space-time dimensions of our universe to be ten. The extra six dimensions are microscopic and expected to be too small to have yet been detected. The shape and size of these extra microscopic dimensions determine the laws of physics that we experience in our four-dimensional macroscopic world by defining what kind of particles and forces they have along with their masses and interaction strengths. Which one of this huge set of vacua precisely describes the world we live in is yet not fully understood and active research is in progress to gain a better understanding of these various different ground states and corresponding phases of string theory.

The role of symmetry in theoretical physics has also evolved greatly in the past century. Rather than being considered as the consequence of dynamical laws of nature, the symmetry principles were explicitly used to dictate the dynamical laws. Through Einstein's general relativity, the invariance of the physical laws under the local change in space-time coordinates dictated the dynamics of gravity itself, and thus leading to geometrization of symmetry. The basic principle of unifying all four fundamental interaction in String theory is inspired from an idea first studied by Kaluza and Klein in early part of 20th century. It was shown that from a theory of gravity alone in five spacetime dimensions with one spatial dimension being curled up in a small circle, one can obtain a theory of both gravity and electromagnetism in four spacetime dimensions. This indicates that the symmetries of general relativity contains within it the symmetries of both gauge theories and gravity in lower dimensions. Further research extending this novel idea helped us uncover that the different phases emerging out of String theory are able to explain the familiar symmetries that play a role in nature. It contains, within its framework, the ingredients to realize, for example, the symmetries of the Standard Model of particle physics. In addition, String theory embodies new and strange symmetries beyond the Standard model, *e.g.* supersymmetry, which is ubiquitous in it's construction but is yet to be realized in experiments. Therefore it is of immense importance to study and understand symmetries and phases in general within the framework of String theory.

With this general motivation, in this thesis we aim at exploring various aspects of symmetries and studying different phases in a gravity theory to understand some interesting features prevalent in nature around us. In particular, guided by the lessons from such studies in gravity we find their applications to two considerably different areas of physics: strongly coupled field theories and early Universe cosmology. To establish this connection, the main computational technique that we use, follows from the AdS/CFT[1] correspondence in String theory, also known as holography.

A brief review of AdS/CFT correspondence relevant to the thesis:

The AdS/CFT correspondence is one of the most significant results that String theory has produced. It relates two considerably different theories, a gauge theory without gravity to a quantum theory of gravity living in one higher dimension and hence is frequently referred to as the gauge/gravity duality, see [3] for a review and the references therein. The gauge/gravity duality in its present state is a conjectured duality between two different theories and is best understood for example in situations where the gravity theory is a $d+1$-dimensional AdS space in the bulk whereas the gauge theory is a conformal field theory living at the d-dimensional boundary of the gravity theory. Despite the fact that a first principle proof of this conjecture is yet to be devised, there are overwhelming non-trivial evidences for several examples such that there is very little doubt regarding its correctness. The fact that the entire information of a bulk theory is encoded in a theory living in its boundary is reminiscent of the optical hologram and hence the study of AdS/CFT correspondence is also commonly referred to as Holography.

[1]The abbreviation AdS/CFT stands for anti de-Sitter/conformal field theory.

In view of the fact that the central theme of this thesis largely makes use of this gauge/gravity duality it will be useful to take a short detour and discuss in short about the AdS/CFT correspondence, highlighting its important consequences relevant for the material presented in this thesis. As already mentioned it is a conjectured duality between a theory with dynamical gravity and a gauge theory in one lower spacetime dimensions without gravity. In most applications of AdS/CFT correspondence the metric of AdS space in $(4+1)$-dimensions is written in a coordinate system as

$$ds^2 = \frac{R_{Ads}^2}{r^2}dr^2 + \frac{r^2}{R_{Ads}^2}[-dt^2 + dx^2 + dy^2 + dz^2]. \tag{1.1}$$

More specifically, this coordinate system describes a patch of the full AdS space. It comes as solution to a system of Einstein gravity in the presence of a negative cosmological constant with an action

$$S = \frac{1}{16\pi G_N}\int d^5x\sqrt{-g}\{\mathcal{R} + \Lambda\} \tag{1.2}$$

where $\mathcal{R}$ is the Ricci scalar and Λ the cosmological constant. The statement of the correspondence is best considered in terms of symmetries. The isometry group of AdS_5 space, a set of coordinate transformation that leaves the metric of AdS invariant, is $SO(4,2)$, Which is same as the conformal group in 4 dimensions. Thus it is quite plausible that the dynamics in AdS_5 space is captured by a CFT living in the $(3+1)$-dimensional boundary of AdS_5, situated at $r \to \infty$ and spanned by the coordinates t, x, y, z. It is also important to note that the correspondence is a statement of matching at the level of degrees of freedom for both of them. To illustrate this let us consider a CFT on $(3+1)$-dimensional flat space at temperature T. The entropy density, s, of the CFT can be understood based on dimensional analysis keeping in mind that the only scale in the problem is the temperature, T,

$$s \sim c\,T^3, \tag{1.3}$$

where c is a characteristic constant of the CFT, called the C-function. This C-function is a measure of the degrees of freedom of the CFT. In the dual AdS_5 spacetime this finite temperature state of the CFT is represented by a black brane geometry with temperature T. The metric of the black brane solution, obtained as a unique solution to the action given in eq.(1.2), can be written as,

$$ds^2 = R_{AdS}^2\left[-\left(r^2 - \frac{2\,g\,m}{r^2}\right)dt^2 + \frac{dr^2}{\left(r^2 - \frac{2\,g\,m}{r^2}\right)} + r^2(dx^2 + dy^2 + dz^2)\right], \tag{1.4}$$

where g is the dimensionless Newton's constant in $(4+1)$-dimensions and measures the effective gravitational coupling at AdS scale. It is defined in units of AdS radiaus as follows

$$g \sim \frac{G_N}{R_{AdS}^3}. \tag{1.5}$$

The important fact to notice is that we are considering "black brane" solutions compared to more familiar "black holes". The asymptotic boundary of these brane solutions admit additional translational invariance along the spatial directions. This asymptotic spatial planarity translates into the statement that the dual boundary field theory propagates on a flat Minkowskian spacetime. On the other hand the spherical foliation in the black hole solutions will in the same spirit correspond to a boundary quantum field theory living on a spatial sphere which is clearly not of significant interest in condensed matter systems.

The entropy density for the black brane solution in $(4+1)$-dimensions given in eq.(1.4) goes as

$$s \sim \frac{T^3}{g} \sim \frac{R_{AdS}^3}{G_N} T^3. \tag{1.6}$$

In deriving eq.1.6 one needs to use the relation between the temperature and the Schwarzschild radius, r_s, *i.e.* $T \sim r_s$, and also the fact that $r_s^4 \sim g\, m$, following from eq.(1.4). Comparing eq.(1.3) and eq.(1.6) we find,

$$c \sim \frac{1}{g} \sim \frac{R_{AdS}^3}{G_N}. \tag{1.7}$$

This relation makes it obvious that the central charge of the CFT scales as inverse of the Newton's constant. Therefore if we are interested in a weakly coupled gravity theory, *i.e.* $g \to 0$, the number of degrees of freedom in the CFT should be very large, a large number of fields in the boundary theory. It is therefore suggestive that we consider large N gauge theories in the boundary, where N indicates the rank of the gauge group in the boundary theory. In the large N limit a gauge theory admits to a classical limit (in some sense). All the Feynman diagrams for any scattering amplitude reorganize themselves in a way that only a finite set of them survive, namely the set of planar diagrams; the other non-planar diagrams get suppressed in $1/N^2$. Interestingly this resembles the perturbative expansion of string scattering amplitudes, where the higher genus diagrams are suppressed by the string coupling constant g_s, which scales like $g_s \sim 1/N^2$ and only the tree level diagrams contribute[2]. Thus large N limit of the dual gauge theory makes the string theory in the bulk non-interacting. Though the spectrum of the non-interacting oscillating string will in general have massive higher spin states. In order to obtain a simpler theory of gravity with the highest spin object being graviton, a spin 2 particle, one considers a further limit

$$R_{AdS} \gg l_s, \tag{1.8}$$

where l_s is the string length, the fundamental length scale in string theory. In this limit all the higher spin particles are truncated. As a result one is left with Einstein's theory of gravity, a tractable and simple two derivative theory of classical gravity. In the gauge theory side this limit corresponds to having strong coupling and thus beyond any other analytic computation. The most well understood examples of this correspondence is a

[2]It is important to note that the planar diagrams that survive in the large N limit do have non-trivial loops in them, hence the gauge theory is classical in the sense that only a set of diagrams, namely the planar diagrams, contribute.

duality between type-IIB superstring theory in $AdS_5 \times S^5$ and $\mathcal{N} = 4$ super-Yang-Mills (SYM) theory in $(3+1)$-dimensions with a gauge group $SU(N)$. The $\mathcal{N} = 4$ SYM theory with gauge group $SU(N)$ has two parameters - N itself and λ, the 't Hooft coupling[3], which are related to the parameters: R_{AdS}, the AdS_5 radius and the string coupling constant g_s in the following way,

$$g_s = \frac{\lambda}{4\pi N}; \; R_{AdS} = \lambda^{1/4} l_s. \tag{1.9}$$

These relations make it clear that the large N limit makes the string loops suppressed, *i.e.* $g_s \to 0$, and large λ limit corresponds to large AdS radius compared to the string scale which makes the gravity theory weakly curved and Einstein's theory becomes a good approximation.

An important aspect of this duality worth highlighting is the fact that the gravity theory lives in one higher dimension than the field theory. This extra dimension geometrizes the renormalization group (RG) flow in the dual field theory. The near boundary region in the bulk theory, *e.g.* $r \to \infty$ in eq.(1.1), correspond to the ultraviolet (UV) of the field theory. UV values of the field theory couplings correspond to the boundary condition set at asymptotic boundary of the bulk theory. Solving Einstein's equations and moving inwards in the radial bulk coordinate represents following RG flow from UV to infrared (IR) in the dual field theory. There is a vast literature on how to make this idea of holographic renormalization more precise but for what we will discuss in this thesis it is enough to have this picture in mind that the asymptotic boundary region of the bulk theory represents the UV behavior of the field theory and the deep interior in the bulk, *e.g.* the near horizon region of a black brane, describes the IR of the dual field theory.

The AdS/CFT correspondence as a holographic dictionary:

In a broader context, beyond the specific limit of large N, the AdS/CFT correspondence hints at an intricate connection between a theory of quantum gravity and gauge theories in general. Though a complete understanding of this duality is yet lacking, it is expected to shed light on the mysterious areas of quantum gravity. Despite these issues regarding more theoretical and abstract aspects of this duality, there has been a consistently growing attitude within the community of both condensed matter physicists and gravity theorists to use this correspondence as a computational tool. A holographic dictionary, or in other words a set of rules, has been set up which maps objects from one side to the other. Since in this thesis we use computational techniques heavily borrowed from the AdS/CFT correspondence, this holographic dictionary has been immensely useful and we will mention some of them relevant for the work presented in this thesis. The basic ingredient in the dictionary is that for every gauge invariant operator $\mathcal{O}$ in the quantum field theory (QFT),

[3] The 't Hooft coupling λ is related to the coupling constant g_{YM} of the SYM theory as $\lambda = g_{YM}^2 N$, in the large N limit this is this λ which is kept constant. $\mathcal{N} = 4$ SYM theory being a conformal theory the β-function vanishes and the coupling constant stops running under the renormalization group flow, and hence it serves as a parameter characterizing the theory.

there will be a corresponding field ϕ in the bulk gravitational theory. The characteristic properties of the operator $\mathcal{O}$, *e.g.* spin or charge of it, will be given by the spin or charge of the corresponding bulk field ϕ, whereas the conformal dimension of $\mathcal{O}$ will be fixed by the mass of ϕ. This field-operator map is summarized with some examples in the Table 1.1,

Boundary QFT : Operators	$\Leftrightarrow$	**Bulk Gravity : Fields**
Energy momentum tensor: $T_{\mu\nu}$	$\Leftrightarrow$	metric field: $g_{\mu\nu}$
Global current: J_μ	$\Leftrightarrow$	Maxwell gauge field: A_μ
Scalar operator: $\mathcal{O}$	$\Leftrightarrow$	Scalar field: ϕ
Fermionic operator: $\mathcal{O}_F$	$\Leftrightarrow$	Fermionic field: ψ
spin/charge of the operator	$\Leftrightarrow$	spin/charge of the field
Conformal dimension of the operator	$\Leftrightarrow$	mass of the field

Table 1.1: Holographic dictionary

Adding a source J for the operator $\mathcal{O}$ in the QFT is dual to imposing a boundary condition at infinity for the bulk field ϕ. In coordinates of eq.(1.1), the boundary value of ϕ, *i.e.* $\phi(r \to \infty) = \phi_B$, acts as the source J of the QFT upto an overall power of the radial variable r. This is summarized in the following relation equating the bulk partition function as a functional of the boundary values of the fields to the correlation functions of insertions of the operators $\mathcal{O}$ in the QFT

$$Z_{bulk}[\phi \to \phi_B] = \left\langle exp\left(i \int \phi_B \mathcal{O} \right) \right\rangle_{QFT} \tag{1.10}$$

Lastly, we would like to conclude this brief discussion of AdS/CFT correspondence as a computational tool by extending the field-operator dictionary to a statement regarding symmetries

$$\text{Global symmetries in QFT} \Leftrightarrow \text{Local gauge symmetry in bulk.} \tag{1.11}$$

This statement was implicit in the field-operator map written in Table 1.1, a gauge field in the bulk is dual to a global symmetry current in the boundary theory.

A "strong-weak" duality: the AdS/CFT correspondence as a computational tool:

The most important and notable feature of this gauge/gravity duality is the realization that it is a strong-weak duality, resulting in its enormous applicability to several other branches of physics. As it has already been mentioned, in a certain limit (large N and λ) this correspondence becomes an equivalence between a gauge theory at strong coupling in the boundary and a ordinary weakly curved two derivative Einstein gravity. As we know, strongly coupled field theories do not admit any perturbative calculation such that no simple analytic computations are possible. On the other hand, using the correspondence we can map the problem to a relatively simpler and tractable computation in the bulk Einstein gravity and hence it provides a powerful computational tool to explore strongly coupled field theories. As a consequence, research in String theory has now found its widespread application in other branches of physics as well, for example, condensed matter physics, QCD etc.; see the reviews [4, 5, 6, 7] for connections to condensed matter physics and [8] for QCD related applications. Although, it is important to note that the state of the art is still in a very immature and suggestive state and far from being decisive. But the implications obtained so far clearly demands for a more active research from the practitioners on both side.

Applictions to strongly coupled condensed matter systems:

A major portion of this thesis is devoted to using the AdS/CFT correspondence as the investigating tool for gaining insights and exploring the implications of this correspondence on the strongly coupled features of condensed matter systems. The first realization of any possible connection of this sort was pointed out in [9] that inspired a more involved research in the following years to result in a set of interesting discoveries: holographic superconductivity, holographic strange metals etc. Condensed matter systems at quantum criticality are one such promising candidates where holographic techniques might be applied [10]. In $(2+1)$-dimensions techniques of AdS/CFT correspondence are only accessible approaches to deal with strongly correlated quantum critical systems, though there are some known exceptions in $(1+1)$-dimension, [11]. Around a quantum critical point there occurs a continuous phase transition at zero temperature due to tuning some parameter of the given system. Unlike finite temperature phase transitions that are governed by thermal fluctuations, quantum phase transitions are dominated by the zero point quantum fluctuations, thus justifying the name "quantum phase transitions". In certain condensed matter systems the effects of quantum criticality persist even at finite temperatures, called the quantum critical regime. This regime to which all experiments are naturally confined, also bear key important signatures of the quantum critical point, see Fig. 1.1. There exists a mysterious class of materials called the "strange metals". The "strangeness" in this strongly coupled phase of metals is manifested in its electrical resistivity that grow linearly with temperature rather than with the square of temperature as observed in normal metals.

Another important aspect of applying holographic techniques to condensed matter systems is to understand quantum critical states at a finite chemical potential. Since condensed matter systems at finite density or chemical potential are more natural in laboratories than zero density ones, addition of finite chemical potential in the holographic studies brings the abstract theoretical understanding closer to real world systems. Landau's Fermi liquid theory is one paradigm to explain strongly coupled fermionic systems at a finite chemical potential. In recent years, a large number of experiments on various materials have discovered a plethora of "non-Fermi liquid" behaviors, *e.g.* the strange metals, where Landau's Fermi liquid theory is inadequate to explain the low energy physics of such systems. These phenomenon, being artifact of strong interactions in quantum field theory, are resilient to conventional field theoretic techniques. In view of this, applications of holographic techniques to specific condensed matter systems is well motivated. For the investigations presented in this thesis another interesting and relevant motivation for the connections between a theory of gravity and condensed matter systems can be given. As we have already mentioned, String theory has a large set of low energy vacua referred to as the landscape. This is reminiscent of a similar situation in condensed matter physics where despite having a unique microscopic theory, at large length scales governing all laboratory phenomenon, there are various emergent phases describable through effective descriptions. In chapter 2 of this thesis we will explicitly look into this connection using holography.

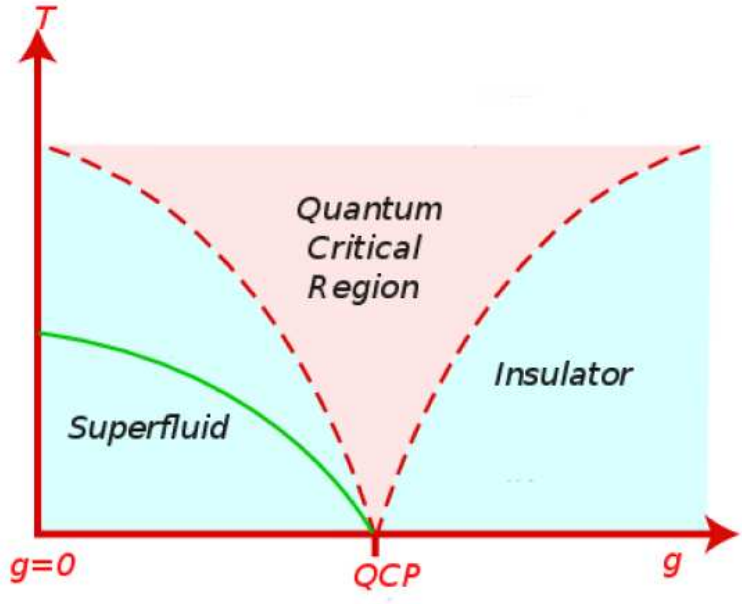

Figure 1.1: Phase diagram showing quantum critical point (QCP) and quantum critical region in superfluid-insulator transition. g is some controllable parameter in the system and T is the temperature. (*Figure adapted from [7]*)

On the dual gravity side, the primitive ingredient to consider is the black hole solutions in AdS spacetime. Through the gauge-gravity duality, a finite temperature black hole solution in AdS gravity correspond to a finite temperature state in the dual field theory. The well known Schwarzschild black hole solution represent a field theory system at zero density. Finite density states of matter require a non-zero charge density, $\langle J^t \rangle \neq 0$, for a global $U(1)$ symmetry in the field theory and that is achieved by holding the system at a non-zero chemical potential, μ. In order to impose this, in the bulk gravity theory one needs to add an extra $U(1)$ local gauge field such that there is a non-zero electric flux at infinity. Following standard AdS/CFT dictionary one can read off the values of the charge density and the chemical potential in the field theory from the near boundary behavior of the bulk gauge field. Einstein-Maxwell theory with a negative cosmological constant is the minimal framework required to describe the physics of non-zero electric flux in an asymptotically AdS spacetime. The action is written as,

$$S = \frac{1}{16\pi G_N}\int d^4x\sqrt{-g}\{R + \Lambda \; - \frac{1}{4}\, F^{\mu\nu}F_{\mu\nu}\} \tag{1.12}$$

where G_N is the Newton's constant, R is the Ricci scalar, Λ being the cosmological constant and $F_{\mu\nu} = \partial_\mu A_\nu - \partial_\nu A_\mu$ is the field strength for the $U(1)$ gauge field. This action allows for a unique solution, called the Reissner-Nordstrom (RN) black brane in AdS spacetime with the metric

$$ds^2 = -f(r)dt^2 + \frac{dr^2}{f(r)} + r^2(dx^2 + dy^2) \tag{1.13}$$

such that

$$f(r) = r^2 - \frac{M}{r} + \frac{Q^2}{r^2}. \tag{1.14}$$

The RN black brane is characterized by two parameters M and Q parameterizing the mass and the charge of the black brane respectively. The charge of the black brane represents the non-zero charge density of the boundary field theory at finite chemical potential. Truly speaking, this charge density is to be thought of as a proxy for the "stuff" of condensed matted systems, *e.g.* fluid of electrons in a metal. Despite being interesting in various aspects these RN black branes suffer from one unpleasant feature. At zero temperature extremal RN black branes have finite and large entropy which is violation of the third law of entropy. This unwanted feature of RN black branes are cured if one considers an additional scalar field, called dilaton, coupled to the Einstein-Maxwell system. Further modifications and extensions of this Einstein-Maxwell-Dilaton(EMD) system is also studied extensively in the literature and they bring in interesting features like hyperscaling violation into the dual field theory systems. In chapter 3 of this thesis, we will discuss this EMD systems in more detail and study various aspects of them.

Applications to early Universe cosmology:

Apart from the attempts to investigate the connections between a theory of gravity and strongly coupled condensed matter systems using holographic techniques, a considerable part of the study of symmetries and phases in gravity that we have undertaken in this thesis, is aimed at exploring another branch of theoretical physics, namely early Universe cosmology. Both theoretically and observationally, the physics of our Universe shortly after its birth is by itself a fascinating subject of modern day research. Our Universe is approximately homogeneous and isotropic at large enough length scales. This homogeneity and isotropy is observationally supported and is the backbone of the standard big bang cosmology - the paradigm to explain the evolution of our Universe. It successfully explains Hubble's redshift-distance relationship, the fact that our Universe is expanding with a relative velocity between two objects proportional to the distance between them. Shortly after big bang when the temperature of the Universe was larger than the ionization temperature of the atoms it was too hot for stable atoms to exist. The matter was in the state of a plasma of free electrons and nucleons (protons and neutrons). Also thermal gas of photons used to scatter off these free electrons, nucleons and hence could not propagate freely very far. As the Universe expanded and temperature cooled down to a critical point, called the "time of recombination", stable atoms started to form and the gas of photon started to stream freely. Cosmic Microwave Background (CMB) is this remnant gas of photons from early universe, more precisely a snapshot of the Universe at the time of last scattering. Earlier observations indicated that CMB is uniform, i.e. of same temperature, about 2.7 degree Kelvin, in all directions of the sky. Though further accurate observations revealed that the homogeneity and isotropy of CMB is only approximate and there are tiny fluctuations in it at the level of 1 part in 10^5. These tiny fluctuations in CMB temperature correspond to small variations in the primordial matter density which subsequently grew larger and larger in size to initiate structure formation in our Universe. Despite great successes mentioned above there are however some shortcomings of the standard model of big bang cosmology. The approximate homogeneity and isotropy of CMB temperature is not possible to explain within the framework of this standard model. It is referred to as the "Horizon problem". As shown in Fig. 1.2, the time between the big bang singularity and the last scattering surface is much smaller than the time between the latter and the present time. As a consequence two points on the last scattering surface do not have their past light cones intersecting and no causal contact between them has ever been possible. Seemingly CMB is made out of causally disconnected patches but yet it has an almost same temperature in all directions of the sky. Standard model of big bang fails to answer the puzzling question: two causally disconnected points happen to be of the same temperature.

Inflation is an attractive idea that provides a justification for the approximate uniformity in the temperature of CMB. Effectively it achieves the solution to the horizon problem by increasing the time between the singularity and the last scattering such that different points on the last scattering surface happen to be in causal contact with each other well before the big bang, see Fig. 1.3. Inflation also provides a mechanism to explain the origin of these anisotropies in CMB temperature, namely the quantum fluctuations during inflation acts as source to these tiny CMB temperature fluctuations. Besides the anisotropies in the temperature that we just mentioned, quantum fluctuations during inflation also lead to stretching of the spacetime itself. These ripples in the fabric of spacetime, also known as primordial gravitational waves, are uniquely imprinted in the polarizations of the CMB photons. Recently these primordial gravitational waves from inflation were claimed to be observed in an experiment at the South Pole, BICEP2, see [13], though it has been heavily doubted within the physics community questioning the possible contamination in the signal due to dust in our galaxy. Nevertheless, if confirmed, undoubtedly it would be a major discovery in observational cosmology since we might be seeing the first direct observational signature of the quantum fluctuations in spacetime. In inflation the rapid exponential expansion of our Universe requires a negative pressure source. In the simplest

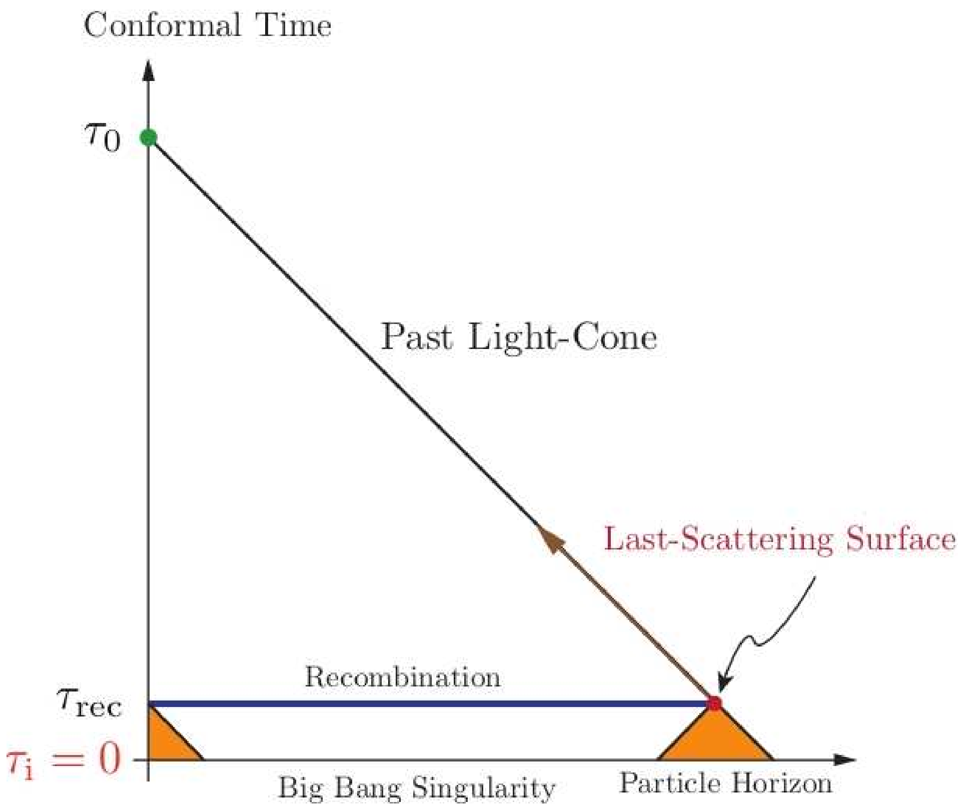

Figure 1.2: The horizon problem in standard big bang cosmology. The conformal time, τ, is defined in chapter 4 (*Figure taken from [12]*)

models it is driven by a single scalar field and the dynamics is governed by Einstein gravity coupled to a scalar field, called inflaton, with some self interacting scalar potential. The inflaton slowly rolls down the nearly flat potential such that it's potential energy dominates over the kinetic energy and it ends when they become nearly equal. CMB anisotropies are generated due to quantum fluctuations in both the scalar field or in the metric of the spacetime during inflation. In cosmology, theoretical calculations on various toy models come up with predictions that are tested against observations. In view of the abundance of models and lack of any compelling one it is more natural and conceptually appealing to adopt a viewpoint of understanding model independent features of the early Universe based on symmetry considerations alone. Interestingly, as we will see in this thesis, in some contexts for the study of early Universe the holographic principle happens to be an useful computational tool.

Organization of the Chapters:

We conclude the introduction with an overview of the chapters in this thesis:

In the next chapter of this thesis, based on [14], we address the question: what kind of phases found in nature can be realized in gravity description. With the help of a symmetry

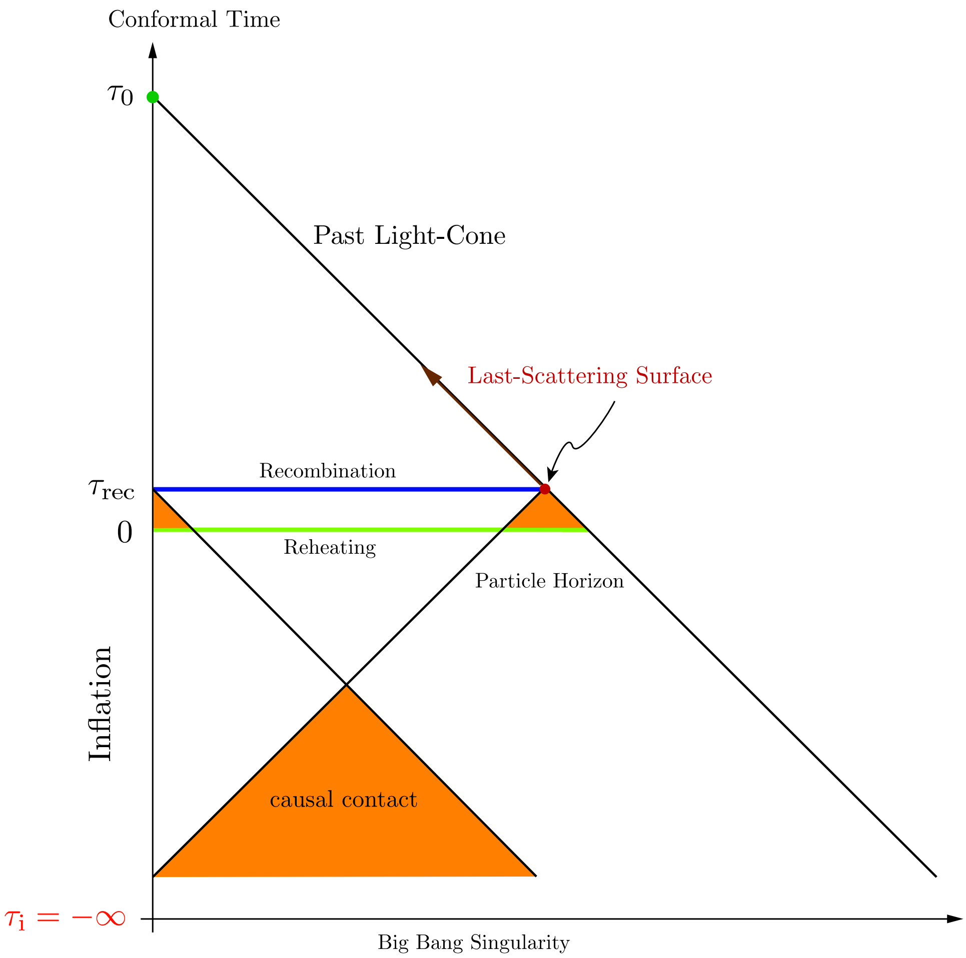

Figure 1.3: Solution to the horizon problem: Inflation. (*Figure taken from [12]*)

classification for the generalized translational symmetries, named the Bianchi classification, we find possible near horizon gravity solutions, which are homogeneous but not necessarily isotropic, falling into each class. These gravity solutions extend the existing set of a very few solutions known so far on the gravity side and correspond to similar homogeneous but possibly anisotropic phases abundantly observed in condensed matter systems.

In chapter 3, based on [15], we run our investigation the other way round and try to understand if phases in gravity are of interest in condensed matter physics. We consider a specific solution in a system of gravity coupled to scalar and gauge fields with a negative cosmological constant. It corresponds to a compressible phase on the field theory side with an unbroken global symmetry at finite chemical potential, *e.g.* Fermi liquids. We further investigate the existence of a Fermi surface in those phases by looking at its response to turning on a small magnetic field. For that we study an interesting property of the system called entanglement entropy and compute it using holography in the gravity side.

In the next chapter, based on [16], we study conformal invariance during inflation, a proposed theoretical mechanism to describe the phase of rapid expansion of our Universe at a very early epoch. The approximate de-Sitter (dS_4) spacetime during inflation has symmetries which are same as that of a 3 dimensional Euclidean conformal field theory (CFT) and that imposes non-trivial constraints on the correlation functions of the cosmological perturbations produced at that time. These correlation functions are measured directly in the sky by looking at the anisotropies in the cosmic microwave background (CMB) radiation. In slow-roll inflation we compute the four point correlator[4] of the temperature perturbations in the CMB using techniques borrowed from AdS/CFT correspondence and further investigate the non-trivial constraints on it imposed by the approximate conformal symmetry of the spacetime during inflation. The clarification of a subtle issue regarding gauge fixing leads us to the understanding of the conformal invariance of this correlator.

Finally in chapter 5 we conclude with some discussions and further comments on future prospects. There are three main appendices for each of the three chapters, where we present supplementary materials.

[4]In cosmology literature it is also known as the trispectrum.

Chapter 2

Bianchi Attractors: A Classification of Extremal Black Brane Geometries

2.1 Introduction

The Nature around us exists in a lot of various beautiful phases. As we have already mentioned in the introduction, string theory too has many varied and beautiful phases corresponding to the huge landscape of vacua in the theory. It is motivating enough to hope that a study of the phases of string theory might lead us to describe those in Nature. This hope has initiated an interesting conversation between string theory and condensed matter physics, two apparently different corners of physics. Study of black branes in gravity theories, with a particular focus on their role as holographic duals to field theories at finite temperature and/or chemical potential has shown promising sign of making this connection even stronger. Extremal branes are particularly interesting, since they correspond to zero temperature ground states. At zero temperature quantum fluctuations come into "their own", especially in strongly correlated systems, leading to interesting and novel phenomena like quantum phase transitions. The description of these ground states in terms of an extremal brane allows such effects to be studied in a non-trivial and often tractable set up.

So far only a few different kinds of extremal brane solutions have been found. The analogy with the phases of matter, mentioned above, would suggest that many more should exist. The main point of the work presented in this chapter is to show that this expectation is indeed true. We will argue below that the known types of extremal black branes are only the "tip of the iceberg", and that there is a much bigger zoo of solutions, obtainable in theories of gravity with reasonable matter, waiting to be discovered.

Symmetries are a good place to start in classifying the solutions of general relativity and also in classifying the phases of matter. The known extremal solutions mostly have the usual translational symmetries along the spatial directions in which the brane extends. The solutions we consider here differ by having a generalized version of translational invariance. Any two points along the spatial directions can still be connected by a symmetry transformation, but the generators of the symmetries now do not necessarily commute with each other. This generalized notion of translations is well known in general relativity. Spacetimes with such symmetries are said to be homogeneous. To be more precise, we will study brane solutions of the form

$$ds^2 = dr^2 - g_{00}dt^2 + g_{ij}dx^i dx^j \tag{2.1}$$

where $i, j = 1, \cdots d-1$ are the spatial directions along which the brane extends. We will find that often, for reasonable matter Lagrangians, there are brane solutions where the x^i coordinates span a homogeneous space with isometries which do not commute. Most of our discussion will be for the case $d = 4$ where the brane extends in 3 space dimensions [1]. The different kinds of generalized translational symmetries that can arise along three spatial directions are well known in general relativity. They lie in the Bianchi classification and fall into 9 different classes, *e.g.*, see [17], [18]. These classes therefore classify all homogeneous brane solutions of the type eq.(2.1).

The near-horizon geometry of extremal branes are of particular interest in the study of holography. The near-horizon geometry encodes information about the low energy dynamics of the dual field theory and often turns out to be scale invariant. The near horizon geometry is also often an attractor, with differences from the attractor geometry far away dying out as one approaches the horizon. This feature corresponds to the fact that much of the UV data in the field theory is often irrelevant in the IR. These properties mean that the near-horizon geometry is often easier to find analytically than the full solution. The attractor nature also makes the near-horizon geometry more universal than the full extremal solution. Thus one is in the happy situation that the IR region, which being more universal is of greater interest anyway, is also the region one can obtain with relative ease.

In this chapter we will focus mostly on this near-horizon region, considering solutions which are scale invariant in this region, along with being homogeneous along the spatial directions [2]. We will show that solutions lying in many of the 9 Bianchi classes mentioned above can be obtained by coupling gravity to relatively simple kinds of matter. In the examples we consider, one or two massive Abelian gauge fields in the presence of a negative cosmological constant will suffice. In one case we will also find interpolating solutions for the full extremal brane which interpolate between the scaling near-horizon region and asymptotic AdS space.

A simple example of the kind of generalized translation invariance we have in mind arises in

[1] Towards the end of this chapter we will briefly discuss examples where the time direction could also be involved in the generalized translations.

[2] The scaling symmetry will correspond to translations in the radial coordinate r. Thus, including the scaling symmetry makes the full $d+1$ dimensional space-time geometry homogeneous.

condensed matter physics when a non-zero momentum mode condenses, leading to a vector order parameter which varies in a helical manner in space with a pitch determined by the momentum of the condensed mode. For example, in spin systems this is known to happen when a spin wave of non-zero momentum condenses, resulting in the magnetization order parameter varying in a helical pattern (see [19], [20] for a discussion). In superconductors, it has been argued that such spatially modulated phases can arise due to the FFLO instability [21], [22]. Similar behavior can also occur in QCD [23] and other systems [24]. It has also been discussed recently in the context of AdS/CFT in [25], [26, 27, 28] and [29, 30, 31]. In the context of our discussion such situations lie in the Type VII class of the Bianchi classification. We will discuss this case below quite extensively since it is relatively simple and illustrates many of the features which arise in the other classes as well.

The chapter is structured as follows. We begin with a discussion of the generalized translations and various Bianchi classes in section 2.2. Then we discuss one illustrative example of a Bianchi Type VII near-horizon geometry in section 2.3. Other examples giving rise to Bianchi Types II, III, V, VI, and IX are discussed in section 2.4. A concrete example where a Type VII near-horizon geometry can arise from an asymptotically AdS spacetime is given in section 2.5. A brief discussion of subtleties which might arise when time is involved in the generalized translations is contained in section 2.6. The chapter ends with some discussion in section 2.7. Important supplementary material is contained in the Appendices A.1-A.4.

Before we proceed further it is important to comment on related existing literature. There is a formidable body of work on brane solutions in the string theory and general relativity literature; for a recent review with further references, see [32]. A classification of extremal black holes (as opposed to black branes), quite different from ours, has been discussed in [33]. Our solutions can be viewed as black branes with new kinds of "hair"; simple discussions of how branes in AdS space can violate the black hole no-hair theorems are given in the papers on holographic superconductivity, see *e.g.* [34] and [35] for discussions with additional references. Early examples of black branes with interesting horizon structure were discussed in studies of the Gregory-Laflamme instability; the original papers are [36, 37] and a recent discussion appears in [38]. As we mentioned previously, solutions with instabilities of the Type VII kind have appeared already in the context of AdS/CFT duality in the interesting papers [25, 26, 27, 28, 29, 30, 31]. Lifshitz symmetry has characterized one new type of horizon to emerge in holographic duals of field theories at finite charge density in many recent studies; this was discussed in [39] and [40] (see also [41, 42, 43, 44, 45, 46, 47] for string theory and supergravity embeddings of such solutions). The attractor mechanism has also inspired a considerable literature. The seminal paper is [48]. For a recent review with a good collection of references, see [49]. Some references on attractors without supersymmetry are [50, 51, 52, 53, 54]. A recent discussion of how the attractor mechanism may be related to new kinds of horizons for black branes, including *e.g.* Lifshitz solutions, appears in [55].

2.2 Generalized Translations and The Bianchi Classification

It is worth beginning with a simple example illustrating the kind of generalized translational symmetry we would like to explore. Suppose we are in three dimensional space described by coordinates x^1, x^2, x^3 and suppose the system of interest has the usual translational symmetries along the x^2, x^3 directions. It also has an additional symmetry but instead of being the usual translation in the x^1 direction it is now a translation accompanied by a rotation in the $x^2 - x^3$ plane. The translations along the x^2, x^3 direction are generated by the vectors fields,

$$\xi_1 = \partial_2, \quad \xi_2 = \partial_3, \tag{2.2}$$

whereas the third symmetry is generated by the vector field,

$$\xi_3 = \partial_1 + x^2\partial_3 - x^3\partial_2. \tag{2.3}$$

It is easy to see that the three transformations generated by these vectors transform any point in the three dimensional plane to any other point in its immediate neighborhood. This property, which is akin to that of usual translations, is called homogeneity. However, the symmetry group we are dealing with here is clearly different from usual translations, since the commutators of the generators, eq.(2.2,2.3) take the form

$$[\xi_1, \xi_2] = 0; \quad [\xi_1, \xi_3] = \xi_2; \quad [\xi_2, \xi_3] = -\xi_1, \tag{2.4}$$

and do not vanish, as they would have for the usual translations [3].

In the context of present chapter we will be interested in exploring such situations in more generality where the symmetries are different from the usual translations but still preserve homogeneity, allowing any point in the system of interest to be transformed to any other by a symmetry transformation [4].

When can one expect such a symmetry group to arise? Let us suppose that there is a scalar order parameter, $\phi(x)$, which specifies the system of interest. Then this order parameter must be invariant under the unbroken symmetries. The change of this order parameter under an infinitesimal transformation generated by the vector field ξ_i is given by

$$\delta\phi = \epsilon\xi_i(\phi) \tag{2.5}$$

and this would have to vanish for the transformation to be a symmetry. It is easy to see that requiring that this is true for the three symmetry generators mentioned above, eq.(2.2), eq.(2.3), leads to the condition that ϕ is a constant independent of the coordinates, x^1, x^2, x^3.

[3] In fact this symmetry group is simply the group of symmetries of the two dimensional Euclidean plane, its two translations and one rotation.

[4] In a connected space this follows from the requirement that any point is transformed to any other point in its immediate neighborhood by a symmetry transformation.

Now, such a constant configuration for ϕ is invariant under the usual translation along x^1, generated by ∂_1, besides being invariant also under a rotation in the $x^2 - x^3$ plane (and the other rotations). Thus we see that with a scalar order parameter a situation where the generalized translations are unbroken might as well be thought of as one that preserves the usual three translations along with additional rotations.

Now suppose that instead of being a scalar the order parameter specifying the system is a vector V, which we denote by $V^i\partial_i$. Under the transformation generated by a vector field ξ_i this transforms as

$$\delta V = \epsilon[\xi_i, V]. \tag{2.6}$$

Requiring that these commutators vanish for all three ξ_i's leads to the conditions,

$$V^1 = \text{constant}, \quad V^2 = V_0 \cos(x^1 + \delta), V^3 = V_0 \sin(x^1 + \delta) \tag{2.7}$$

where V_0, δ are constants independent of all coordinates. In other words the V^2, V^3 components are not constant but rotate in the $2-3$ plane as one advances along the x^1 direction. In contrast, for the usual translations all three components V^1, V^2, V^3 would be constant and the behavior of the order parameter would be different. Thus we see that with a vector order parameter, instead of a scalar, one can have situations where the generalized translational symmetries generated by eq.(2.2), eq.(2.3) are preserved but the usual translation group is not. Such a situation could also arise if the order parameter were a tensor field.

In fact situations with this type of a vector order parameter are well known to arise in condensed matter physics as was mentioned in the introduction. For example this can happen in spin systems, where the order parameter is the magnetization. In the presence of parity violation in such a system a helical spin density wave of appropriate wavelength can be set up [19], [20].

2.2.1 The Bianchi Classification

The example discussed above shares many features in common with other symmetry groups which preserve homogeneity. Luckily all such groups in three dimensions have been classified and are easily found in the physics literature since they have been of interest in the study of homogeneous situations in cosmology [17], [18]. It is known that there are 9 such inequivalent groups and they are described by the Bianchi classification. The idea behind this classification is quite simple. As we have seen above the Killing vectors which generate the symmetries form a Lie Algebra. Homogeneity requires that there should be 3 such Killing vectors in 3 dimensions. The 9 groups, and related 9 classes in the Bianchi classification, simply correspond to the 9 inequivalent real Lie Algebras one can get with 3 generators.

The familiar case of translational invariance, which includes AdS space and Lifshitz spacetimes, corresponds to the case where the three generators commute and is called Bianchi

Class I. The remaining 8 classes are different from this one and give rise to new kinds of generalized translational symmetries. The symmetry group discussed above in eq.(2.2), eq.(2.3) falls within Class VII in the Bianchi classification, with the parameter $h = 0$ in the notation of [18], see page 112. We will refer to this case as Type VII_0 below. As mentioned above it corresponds to the group of symmetries of the two-dimensional Euclidean plane. Like the example above, in the more general case as well, a scalar order parameter will not lead to a situation where the usual translations are broken. Instead a vector or more generally a tensor order parameter is needed. Such an order parameter, when it takes a suitable form, can preserve the symmetry group characterizing any of the other 8 classes.

In Appendix A.1 we give some details of the algebras for all 9 Bianchi classes. In our discussion below we will consider specific examples which lie in the Bianchi Classes, II, III, V, VI, VII and IX. Some extra details on these classes, including the generators, invariant one-forms etc, can also be found in Appendix A.1.

2.3 The Basic Set-Up Illustrated with a Simple Example

Here we turn to describing more explicitly a spacetime metric incorporating the generalized translational symmetries described above and to asking when such a metric can arise as the solution to Einstein's equations of gravity coupled with matter. Mostly we will work in 5 dimensions, this corresponds to setting $d = 4$ in eq.(2.1). In addition, to keep the discussion simple, we assume that the usual translational symmetry along the time direction is preserved so that the metric is time independent and also assume that there are no off-diagonal components between t and the other directions in the metric. This leads to

$$ds^2 = dr^2 - a(r)^2dt^2 + g_{ij}dx^i dx^j \tag{2.8}$$

with the indices i, j taking values $1, 2, 3$. For any fixed value of r, t, we get a three dimensional subspace spanned by x^i. We will take this subspace to be a homogeneous space, corresponding to one of the 9 types in the Bianchi classification.

As discussed in [18], for each of the 9 cases there are three invariant one forms, $\omega^i, i = 1, 2, 3$, which are invariant under all 3 isometries. A metric expressed in terms of these one-forms with x^i independent coefficients will be automatically invariant under the isometries. For future reference we also note that these one-forms satisfy the relations

$$d\omega^i = \frac{1}{2}C^i_{jk}\omega^j \wedge \omega^k \tag{2.9}$$

where C^i_{jk} are the structure constants of the group of isometries [18].

We take the metric to have one additional isometry which corresponds to scale invariance. An infinitesimal isometry of this type will shift the radial coordinate by $r \to r + \epsilon$. In addition we will take it to rescale the time direction with weight β_t, $t \to te^{-\beta_t \epsilon}$, and assume that it acts on the spatial coordinates x^i such that the invariant one forms, ω^i transform with weights β_i under it, [5] $\omega^i \rightarrow e^{-\beta_i \epsilon}\omega^i$.

These properties fix the metric to be of the form

$$ds^2 = R^2[dr^2 - e^{2\beta_t r}dt^2 + \eta_{ij}e^{(\beta_i+\beta_j)r}\omega^i \otimes \omega^j] \tag{2.10}$$

with η_{ij} being a constant matrix which is independent of all coordinates.

In the previous section we saw that a situation where the usual translations were not preserved but the generalized translations were unbroken requires a vector (or possibly tensor) order parameter. A simple setting in gravity, which could lead to such a situation, is to consider an Abelian gauge field coupled to gravity. We will allow the gauge field to have a mass in the discussion below. Such a theory with a massive Abelian gauge field is already known to give rise to Lifshitz spacetimes [39], [40]. Here we will find that it has in fact an even richer set of solutions, exhibiting many possible phases and patterns of symmetries, as parameters are varied.

The action of the system we consider is therefore

$$S = \int d^5x\sqrt{-g}\left\{R + \Lambda - \frac{1}{4}F^2 - \frac{1}{4}m^2A^2\right\} \tag{2.11}$$

and has two parameters, m^2, Λ. We note that in our conventions $\Lambda > 0$ corresponds to AdS space.

The three isometries along the x^i directions, time translation and scale invariance restrict the form for the gauge potential to be[6]

$$A = A_t e^{\beta_t r}dt + A_i e^{\beta_i r}\omega^i \tag{2.12}$$

where A_t, A_i are constants independent of all coordinates.

2.3.1 A Simple Example Based on Type VII

To construct a simple and explicit example we now return to the case of Type VII_0 with which we began our discussion of generalized translational symmetry in section 2.2. We will show here that a metric with this type of symmetry can arise as a solution to Einstein's equations.

The one-forms which are invariant under the isometries for this case are given, see [18],

[5]The dilatation generator could act more generally than this. A discussion of the more general case is left for the future.

[6]A possible $A_r\,dr$ term, where A_r only depends on r to be consistent with the symmetries, can always be gauged away.

page 112, by

$$\omega^1 = dx^1 \ ; \ \omega^2 = \cos(x^1)dx^2 + \sin(x^1)dx^3 \ ; \ \omega^3 = -\sin(x^1)dx^2 + \cos(x^1)dx^3. \tag{2.13}$$

As discussed above we are assuming that the x^i coordinates transform under the scaling isometry in such a way that the one-forms, ω^i, transform with definite weights. It is clear from eq.(2.13) that the only way this can happen is if x^1 is invariant, and $(x^2, x^3) \to e^{-\beta\epsilon}(x^2, x^3)$, under $r \to r+\epsilon$, so that ω^2, ω^3 have equal weights and transform as $(\omega^2, \omega^3) \to e^{-\beta\epsilon}(\omega^2, \omega^3)$. To keep the discussion simple we also assume that the metric coefficients η_{ij} which appear in eq.(2.10) are diagonal. After some rescaling this allows the metric to be written as

$$ds^2 = R^2[dr^2 - e^{2\beta_t r}dt^2 + (dx^1)^2 + e^{2\beta r}((\omega^2)^2 + \lambda^2(\omega^3)^2)]. \tag{2.14}$$

The only unknowns that remain in the metric are the two constants, R, λ and the two scaling weights, β_t and β.

Before proceeding let us comment on the physical significance of the parameter R. From eq.(2.13) we see that the coordinate distance in the x^1 direction needed to complete one full rotation in the $x^2 - x^3$ plane is 2π. From eq.(2.14) it follows that the physical distance along the x^1 direction that is needed is $2\pi R$. Thus R determines the pitch of the helix.

We will see below that a metric of the type in eq.(2.14) arises as a solution for the system, eq.(2.11), when the gauge field takes the form

$$A = e^{\beta r}\left(\sqrt{\tilde{A}_2}\,\omega^2 + \sqrt{\tilde{A}_3}\,\omega^3\right). \tag{2.15}$$

Let us begin with the gauge field equation of motion

$$d *_5 F = -\frac{1}{2}m^2 *_5 A. \tag{2.16}$$

As discussed in Appendix A.2 this gives rise to the conditions eq.(A.24), eq.(A.25) (with the index i taking values 2, 3). For the metric eq.(2.14), eq.(A.24) is met. From eq.(A.18), (A.22), (A.23) in Appendix A.2, and also from [18], page 112, we have $k^1 = 0, k^2 = k^3 = -1$. Also comparing eq.(2.14) and eq.(A.8) we see that $\lambda_1 = \lambda_2 = 1, \lambda_3 = \lambda$, and $\beta_1 = 0$, $\beta_2 = \beta_3 = \beta$. If both $\tilde{A}_2$ and $\tilde{A}_3$ are non-vanishing eq.(A.25) then gives

$$\lambda^2(m^2 - 2\beta(\beta + \beta_t)) + 2 = 0 \tag{2.17}$$
$$(m^2 - 2\beta(\beta + \beta_t)) + 2\lambda^2 = 0. \tag{2.18}$$

Assuming $\lambda \neq 1$ these conditions cannot both be met. Thus we are lead to conclude that either $\tilde{A}_2$ or $\tilde{A}_3$ must vanish. We will set $\tilde{A}_3 = 0$ without loss of generality [7], so that the

[7] From eq.(2.14) and eq.(2.13) we see that when $\lambda = 1$ the symmetries in the (x^1, x^2, x^3) directions are enhanced to the usual translations and rotations.

gauge field is given by

$$A = \sqrt{\tilde{A}_2} e^{\beta r} \omega^2 \tag{2.19}$$

and the gauge field EOM gives

$$\lambda^2(m^2 - 2\beta(\beta + \beta_t)) + 2 = 0. \tag{2.20}$$

Note that the solution we are seeking has five parameters, $R, \beta_t, \beta, \lambda$, which enter in the metric and $\tilde{A}_2$, which determines the gauge field. These are all constants.

Next, turn to the Einstein equations

$$R^\mu_\nu - \frac{1}{2}\delta^\mu_\nu R = T^\mu_\nu. \tag{2.21}$$

with

$$T^\mu_\nu = \frac{1}{2}F^\mu{}_\lambda F_\nu{}^\lambda + \frac{1}{4}m^2 A^\mu A_\nu + \frac{1}{2}\delta^\mu_\nu \left(\Lambda - \frac{1}{4}F^{\rho\sigma}F_{\rho\sigma} - \frac{1}{4}m^2 A^\rho A_\rho\right) \tag{2.22}$$

Along the tt, rr, and x^1x^1 directions these give:

$$\frac{2(1+\tilde{A}_2)}{\lambda^2} + 2\lambda^2 + \tilde{A}_2(m^2 + 2\beta^2) + 24\beta^2 - 4(1+\Lambda) = 0 \tag{2.23}$$

$$\frac{2(1+\tilde{A}_2)}{\lambda^2} + 2\lambda^2 + \tilde{A}_2(m^2 - 2\beta^2) + 8\beta(\beta + 2\beta_t) - 4(1+\Lambda) = 0 \tag{2.24}$$

$$\frac{2(1+\tilde{A}_2)}{\lambda^2} + 2\lambda^2 - \tilde{A}_2(m^2 + 2\beta^2) - 8(3\beta^2 + 2\beta_t\beta + \beta_t^2) - 4(1-\Lambda) = 0. \tag{2.25}$$

The components along the x^2, x^3 directions lead to

$$\frac{2(3+\tilde{A}_2)}{\lambda^2} - 2\lambda^2 - \tilde{A}_2(m^2 + 2\beta^2) + 8(\beta^2 + \beta_t\beta + \beta_t^2) - 4(1+\Lambda) = 0 \tag{2.26}$$

$$\frac{2(1+\tilde{A}_2)}{\lambda^2} - 6\lambda^2 - \tilde{A}_2(m^2 + 2\beta^2) - 8(\beta^2 + \beta_t\beta + \beta_t^2) + 4(1+\Lambda) = 0. \tag{2.27}$$

In obtaining these equations we have set R, which appears as the overall scale in front of the metric eq.(2.14), to be unity. The equations can then be thought of as determining the dimensionful parameters $\Lambda, m^2, \tilde{A}_2$ in terms of R. Counting eq.(2.20) these are 6 equations in all. One can check that only 5 of these are independent. These 5 equations determine the 5 parameters $(\Lambda, \beta, \beta_t, \lambda, \tilde{A}_2)$, which then completely determines the solution.

Solving, we get:

$$m^2 = \frac{2(11 + 2\lambda^2 - 10\lambda^4 + 3\lambda^6)}{\lambda^2(5\lambda^2 - 11)} \tag{2.28}$$

$$\Lambda = \frac{1}{50}\left(95\lambda^2 + \frac{25}{\lambda^2} - \frac{50}{\lambda^2 - 2} + \frac{144}{5\lambda^2 - 11} - 146\right) \tag{2.29}$$

$$\beta = \sqrt{2}\sqrt{\frac{2 - 3\lambda^2 + \lambda^4}{5\lambda^2 - 11}} \tag{2.30}$$

$$\beta_t = \frac{\lambda^2 - 3}{\sqrt{2}\,(\lambda^2 - 2)}\sqrt{\frac{2 - 3\lambda^2 + \lambda^4}{5\lambda^2 - 11}} \tag{2.31}$$

$$\tilde{A}_2 = \frac{2}{2 - \lambda^2} - 2. \tag{2.32}$$

The first of these equations can be thought of as determining λ in terms of m^2, the second then as determining Λ in terms of m^2, and so on, all in units where $R = 1$.

Requiring $\tilde{A}_2 > 0$ gives

$$1 \leq \lambda < \sqrt{2}. \tag{2.33}$$

Actually eq.(2.30) and eq.(2.31) only determine β and β_t upto an overall sign. We have chosen the sign so that in the range eq.(2.33) β_t are positive, and the g_{tt} component of the metric in particular vanishes at the horizon, $r \to -\infty$. Also we note that in this range, m^2 is a monotonic function of λ, and takes values in the range $-2 \leq m^2 < 1$, where $m^2(\lambda = 1) = -2$.

Some Concluding Remarks

We end this section with some concluding remarks.

An important question which remains is about the stability of the solution we have found above. We leave this for future study except to note that in general, negative values of m^2 do not necessarily imply an instability, as is well known from the study of AdS space, as long as the magnitude of m^2 is not very large.

It is also worth comparing our solution to the well known Lifshitz solution obtained from the same starting point eq.(2.11). This solution is discussed in Appendix A.3 for completeness. We see that with a spatially oriented gauge field the Lifshitz solution can arise only if m^2 is positive, eq.(A.49). In the parametric range $1 > m^2 > 0$ both the Type VII_0 solution and the Lifshitz solution are allowed.

Finally, it is worth noting that like the Lifshitz case, [56], while curvature invariants are finite in the solution found above the tidal forces experienced by a freely falling observer can diverge at the horizon. The curvature invariants for the solution take values

$$R^{\mu}_{\mu} = \frac{123}{25} + \frac{72}{275-125\lambda^2} + \frac{1}{\lambda^2-2} - \frac{5+39\lambda^4}{10\lambda^2} \tag{2.34}$$

$$\begin{aligned} R^{\mu\nu}R_{\mu\nu} &= \frac{(\lambda^2-1)^2}{4\lambda^4(22-21\lambda^2+5\lambda^4)^2}(1452-1804\lambda^2+8229\lambda^4 \\ &- 14304\lambda^6+10114\lambda^8-3204\lambda^{10}+381\lambda^{12}) \end{aligned} \tag{2.35}$$

$$\begin{aligned} R^{\mu\nu\sigma\rho}R_{\mu\nu\sigma\rho} &= \frac{(\lambda^2-1)^2}{4\lambda^4(22-21\lambda^2+5\lambda^4)^2}(5324-6732\lambda^2+12063\lambda^4 \\ &- 19128\lambda^6+14126\lambda^8-4700\lambda^{10}+583\lambda^{12}) \end{aligned} \tag{2.36}$$

and are indeed finite[8]. To see that the tidal forces can diverge we note that a family of geodesics can be found for the metric eq.(2.14) where x^1, x^2, x^3 take any constant values and (r,t) vary with a functional dependence on the proper time, τ, given by $(r(\tau), t(\tau))$ that is independent of these constant values. Now take any two geodesics with the same $(r(\tau), t(\tau))$ which are separated along x^2, x^3. The proper distance separating them in the x^2, x^3 directions vanishes rapidly as the geodesics go to the horizon, $r \to -\infty$ leading to a diverging tidal force.

It is worth trying to find the small temperature deformation of the Type VII solution above. Such a deformation will probably allow us to control the effects of these diverging tidal forces.

2.4 Solutions of Other Bianchi Types

The discussion so far in this chapter has mostly focused on examples of Bianchi Type VII. Solutions which lie in Bianchi Type I, *e.g.* Lifshitz solutions, are of course well known [39], [40]. In this section we will give examples of some of the other Bianchi types. Our purpose in this section is not to give a very thorough or complete discussion of these other classes, but rather to illustrate how easy it is to obtain solutions of these other types as well.

As in the discussion in section 2.3 for Type VII we focus on solutions which have in addition the usual time translational invariance as well as the scaling symmetry involving a translation in the radial direction. The presence of the scaling symmetry will simplify the analysis. Also, such scaling solutions are often the attractor end points of more complete extremal black brane geometries. Accordingly we expect the scaling solutions we discuss to be more general than the specific systems we consider, and to arise in a wide variety of settings.

A remarkable feature is that so many different types of solutions can be obtained from relatively simple gravity + matter Lagrangians. Mostly, we will consider the system described

[8] All three of the curvature scalar diverges at $\lambda = 0,\ \pm\sqrt{2},\ \pm\sqrt{\frac{11}{5}},$ but these values lie outside the range of validity of the solution given by eq.(2.33).

in eq.(2.11) consisting of only one massive Abelian gauge field and gravity. Towards the end, to get a non-trivial Type IX case, we will consider two massive gauge fields.

Our analysis has two important limitations. We will not investigate the stability of these solutions. And we will not investigate whether the scaling solutions discussed in this section can be obtained as IR end points of more general geometries which are say asymptotically AdS. We leave these questions for the future. For the Type VII case discussed in the previous section, we will construct an example in section 2.5 of a full extremal solution which asymptotes to AdS space.

The discussion in this section is a bit brief since it shares many similarities with the Type VII case studied in section 2.3.

2.4.1 Type II

We begin by considering an example which lies in Type II. The system we consider is given by eq.(2.11). The symmetry group for Type II is the Heisenberg group. The generators in a convenient basis are given in Appendix A.1. The invariant one-forms are

$$\omega^1 = dx^2 - x^1 dx^3, \quad \omega^2 = dx^3, \quad \omega^3 = dx^1. \tag{2.37}$$

We take the metric to be of the form eq.(2.10) and diagonal,

$$ds^2 = R^2[dr^2 - e^{2\beta_t r}dt^2 + e^{2(\beta_2+\beta_3)r}(\omega^1)^2 + e^{2\beta_2 r}(\omega^2)^2 + e^{2\beta_3 r}(\omega^3)^2]. \tag{2.38}$$

We take the massive gauge field to be along the time direction

$$A = \sqrt{A_t}\, e^{\beta_t r}\, dt. \tag{2.39}$$

As in the discussion of section 2.3.1 we will find it convenient to set $R = 1$. The gauge field equation of motion is

$$m^2 - 4(\beta_2 + \beta_3)\beta_t = 0. \tag{2.40}$$

The rr, tt, 11, 22, 33 components of the trace reversed Einstein equations[9] are:

[9] Trace reversed Einstein equations in $d+1$ space-time dimensions are

$$R^\mu_\nu = T^\mu_\nu - \frac{1}{d-1}\delta^\mu_\nu T\,, \quad T = T_{\mu\nu}g^{\mu\nu}\,.$$

$$6(\beta_2^2+\beta_2\beta_3+\beta_3^2)-(A_t-3)\beta_t^2-\Lambda=0 \tag{2.41}$$
$$A_t(3m^2+4\beta_t^2)+4(-3\beta_t(2(\beta_2+\beta_3)+\beta_t)+\Lambda)=0 \tag{2.42}$$
$$3+12\beta_3(\beta_2+\beta_3)+6\beta_3\beta_t+A_t\beta_t^2-2\Lambda=0 \tag{2.43}$$
$$12(\beta_2+\beta_3)^2+6(\beta_2+\beta_3)\beta_t+A_t\beta_t^2-3-2\Lambda=0 \tag{2.44}$$
$$3+12\beta_2(\beta_2+\beta_3)+6\beta_2\beta_t+A_t\beta_t^2-2\Lambda=0. \tag{2.45}$$

We have 6 parameters: $m^2,\Lambda,\beta_t,\beta_2,\beta_3,$ and A_t. There are 5 independent equations, so we will express the 5 other parameters in terms of β_t.

The solution is given as,

$$m^2=\beta_t\left(-\beta_t+\sqrt{16+\beta_t^2}\right),\qquad \Lambda=\frac{1}{16}\left(72+19\beta_t^2-3\beta_t\sqrt{16+\beta_t^2}\right), \tag{2.46}$$
$$A_t=\frac{19}{8}-\frac{3\sqrt{16+\beta_t^2}}{8\beta_t},\qquad \beta_2=\beta_3=\frac{1}{8}\left(-\beta_t+\sqrt{16+\beta_t^2}\right). \tag{2.47}$$

Note that $A_t\geq 0,\ \beta_t>0$ implies
$$\beta_t\geq\frac{3}{\sqrt{22}}. \tag{2.48}$$

2.4.2 Type VI, III and V

Next we consider the three classes Type VI, III and V. Type VI is characterized by one parameter, h. The Killing vectors take the form, see Appendix A.1,

$$\xi_1=\partial_2,\ \xi_2=\partial_3,\ \xi_3=\partial_1+x^2\partial_2+hx^3\partial_3\,. \tag{2.49}$$

When $h=0$ we get Type III and when $h=1$ we get Type V. Thus these two classes can be though of as limiting cases of Type VI.

Looking at the Killing vectors in eq.(2.49) we see that translations along the x^2,x^3 directions are of the conventional kind, but a translation along x^1 is accompanied by a rescaling along both x^2 and x^3 with weights unity and h respectively.

The invariant one-forms are

$$\omega^1=e^{-x^1}dx^2,\ \omega^2=e^{-hx^1}dx^3,\ \omega^3=dx^1. \tag{2.50}$$

We consider again the system of a massive Abelian gauge field, eq.(2.11). We take the metric to be

$$ds^2=R^2[dr^2-e^{2\beta_t r}dt^2+(\omega^3)^2+e^{2\beta_1 r}(\omega^1)^2+e^{2\beta_2 r}(\omega^2)^2] \tag{2.51}$$

and the gauge field to be

$$A = \sqrt{A_t}\, e^{\beta_t r}\, dt. \tag{2.52}$$

We also set $R = 1$ below.

The gauge field equation of motion is then

$$m^2 - 2(\beta_1 + \beta_2)\beta_t = 0. \tag{2.53}$$

The rr, tt, 11, 22, 33 component of the trace reversed Einstein equations are

$$3\beta_1^2 + 3\beta_2^2 - (A_t - 3)\beta_t^2 - \Lambda = 0 \tag{2.54}$$

$$\beta_t(\beta_1 + \beta_2 + \beta_t) - \frac{1}{12}(3A_t m^2 + 4A_t\beta_t^2 + 4\Lambda) = 0 \tag{2.55}$$

$$6 + 6h + 6\beta_1(\beta_1 + \beta_2) + 6\beta_1\beta_t + A_t\beta_t^2 - 2\Lambda = 0 \tag{2.56}$$

$$6h + 6h^2 + 6\beta_2(\beta_1 + \beta_2) + 6\beta_2\beta_t + A_t\beta_t^2 - 2\Lambda = 0 \tag{2.57}$$

$$6 + 6h^2 + A_t\beta_t^2 - 2\Lambda = 0. \tag{2.58}$$

Whereas the r3 component of Einstein's equation gives

$$\beta_1 + h\beta_2 = 0. \tag{2.59}$$

The resulting solution is conveniently expressed as follows:

$$m^2 = 2(1-h)^2(1-\beta_2^2) \tag{2.60}$$

$$\Lambda = 4h + \frac{(1-h)^2}{\beta_2^2} + 2(1-h+h^2)\beta_2^2 \tag{2.61}$$

$$A_t = \frac{2(1-h)^2 - 4(1-h+h^2)\beta_2^2}{(1-h)^2(1-\beta_2^2)} \tag{2.62}$$

$$\beta_1 = -h\beta_2 \tag{2.63}$$

$$\beta_t = \frac{(1-h)(1-\beta_2^2)}{\beta_2}. \tag{2.64}$$

Choosing the radial coordinate so that the horizon lies at $r \to -\infty$, we get $\beta_t > 0$. If we require that $\beta_1, \beta_2 \geq 0$ also, and impose that $A_t \geq 0$, as is required for the solution to exist, we get the constraints:

$$h \leq 0 \qquad \text{and} \qquad 0 < \beta_2 \leq \frac{1-h}{\sqrt{2}\sqrt{1-h+h^2}}. \tag{2.65}$$

Having chosen a value of h which satisfies eq.(2.65) and thus a Bianchi Type VI symmetry, we can then pick a value of β_2 also meeting eq.(2.65). The rest of the equations can then be thought of as follows. Eq.(2.61) determines R in units of Λ, eq.(2.60) then determines m^2 required to obtain this value of β_2 and the remaining equations determine the other parameters that enter in the solution.

Let us briefly comment on the limits which give Type V and Type III next.

Type V

To obtain this class we need to take the limit $h \to 1$. To obtain a well defined limit where A_t does not blow up requires, eq.(2.62), that $\beta_2 \to 0$ keeping $\beta_t/(1-h)$ fixed.

It is easy to see that the solution can then be expressed as follows: $m^2 \to 0$, $\beta_1 = 0$ and

$$\Lambda = 4 + \beta_t^2 \quad \text{and} \quad A_t = 2\,\frac{\beta_t^2 - 2}{\beta_t^2} \tag{2.66}$$

with the condition,

$$\beta_t^2 \geq 2. \tag{2.67}$$

After a change of coordinates $x^1 = \log(\rho)$ the metric becomes,

$$ds^2 = \left[dr^2 - e^{2\beta_t r}dt^2\right] + \left[\frac{d\rho^2 + (dx^2)^2 + (dx^3)^2}{\rho^2}\right]. \tag{2.68}$$

We see that this is simply $AdS_2 \times EAdS_3$, where $EAdS_3$ denotes the three-dimensional space of constant negative curvature obtained from the Euclidean continuation of AdS_3.

The resulting limit is in fact a one parameter family of solutions determined by the charge density. To see this note that one can think of the first equation in eq.(2.66) as determining R in terms of Λ, and the second equation as determining β_t in terms of A_t which fixes the charge density. R determines the radius of $EAdS_3$ and β_t then determines the radius of AdS_2.

Also, in this example the symmetries of the spatial manifold are enhanced from those of Type V to the full $SO(3,1)$ symmetry group of $EAdS_3$ [10].

[10] One natural way in which such a solution can be obtained is as the near horizon geometry of an extremal black brane in asymptotic AdS_5 space with non-normalizable metric deformations turned on so that the boundary theory lives in $EAdS_3$ space. One expects that the near- horizon geometry can arise without such a metric non-normalizable deformation being turned on as well.

Type III

The limit $h \to 0$ is straightforward. One gets

$$m^2 = 2(1-\beta_2^2) \tag{2.69}$$
$$\Lambda = \frac{1}{\beta_2^2} + 2\beta_2^2 \tag{2.70}$$
$$A_t = \frac{2-4\beta_2^2}{1-\beta_2^2} \tag{2.71}$$
$$\beta_1 = 0 \tag{2.72}$$
$$\beta_t = \frac{1-\beta_2^2}{\beta_2}. \tag{2.73}$$

The metric is

$$ds^2 = dr^2 - e^{2\beta_t r}dt^2 + e^{2\beta_2 r}(dx^3)^2 + \frac{1}{\rho^2}(d\rho^2 + (dx^2)^2) \tag{2.74}$$

where $x^1 = \log(\rho)$. We see that $\rho,\ x^2$ span two dimensional $EAdS_2$ space.

2.4.3 Type IX and Type VIII

In the Type IX case the symmetry group is $SO(3)$. The invariant one-forms are,

$$\omega^1 = -\sin(x^3)dx^1 + \sin(x^1)\cos(x^3)dx^2 \tag{2.75}$$
$$\omega^2 = \cos(x^3)dx^1 + \sin(x^1)\sin(x^3)dx^2 \tag{2.76}$$
$$\omega^3 = \cos(x^1)dx^2 + dx^3. \tag{2.77}$$

We consider a metric ansatz

$$ds^2 = dr^2 - e^{2\beta_t r}dt^2 + (\omega^1)^2 + (\omega^2)^2 + \ \lambda\ (\omega^3)^2. \tag{2.78}$$

This corresponds to $AdS_2 \times$ Squashed S^3. We take the system to have two gauge fields. One will be massless with only its time component turned on, and the other will have mass m^2 and an expectation value proportional to the one-form ω^3:

$$A_1 = \sqrt{A_t}e^{\beta_t r}dt, \qquad A_2 = \sqrt{A_s}\omega^3 = \sqrt{A_s}(\cos(x^1)dx^2 + dx^3). \tag{2.79}$$

The equation of motion for the first gauge field is automatically satisfied, while the equation of motion for the second yields

$$m^2 + 2\lambda = 0. \tag{2.80}$$

The independent trace reversed Einstein equations are

$$A_s + 2[(A_t - 3)\beta_t^2 + \Lambda] = 0 \tag{2.81}$$

$$6 - 2A_s - A_t\beta_t^2 - 3\lambda + 2\Lambda = 0 \tag{2.82}$$

$$A_s - A_t\beta^2 - \frac{3}{2\lambda}A_s m^2 + 3\lambda + 2\Lambda = 0. \tag{2.83}$$

Solving these four equations we express m^2, A_t, A_s, Λ in terms of β_t, λ. The solution is

$$m^2 = -2\lambda; \qquad A_t = \frac{1+2\beta_t^2}{\beta_t^2}; \tag{2.84}$$

$$A_s = 1 - \lambda; \qquad \Lambda = \frac{1}{2}(2\beta_t^2 + \lambda - 3). \tag{2.85}$$

Then, $A_s \geq 0$, $\Lambda > 0$, $\beta_t > 0$ implies

$$\lambda \leq 1; \qquad \beta_t > \sqrt{\frac{3-\lambda}{2}}. \tag{2.86}$$

Finally, let us briefly also comment on the Type VIII case [11]. Here the symmetry group is $SL(2,R)$. An example would be the case already considered in section 2.4.2 in which case the spatial directions span $EAdS_3$ and the group of symmetries of the spatial manifold is enhanced to $SO(3,1)$. However, we expect that more interesting examples, where the symmetry is only $SL(2,R)$ symmetry and not enhanced, can also easily be found. These would be the analogues of the squashed S^3 example for the Type IX case above.

2.5 An Extremal Brane Interpolating From Type VII to AdS_5

So far, our emphasis has been on finding solutions which have a scaling symmetry along with the generalized translational symmetries discussed above. One expects such scaling solutions to describe a dual field theory in the far infra-red and to arise as the near-horizon limit of non-scale invariant solutions in general. An interesting feature of the field theory, suggested by the geometric description, is that in the IR it effectively lives in a curved spacetime. For example, consider the scaling solution of Type VII type which was described in section 2.3.1. One expects, roughly, that the spacetime seen by the dual field theory is given by a hypersurface at constant $r = r_0$ with $r_0 \gg 1$. From eq.(2.14) we see that at $r = r_0$ this hypersurface is described by the metric,

$$ds^2 = R^2\left[-e^{2\beta_t r_0}dt^2 + (dx^1)^2 + e^{2\beta r_0}[(\omega^2)^2 + \lambda^2(\omega^3)^2]\right]. \tag{2.87}$$

[11] In the Type IX case studied above the spatial directions span a squashed S^3 which is compact. In the Type VIII case the corresponding manifold is non-compact and is more likely to arise starting with an asymptotic geometry where the spatial directions are along R^3 with no non-normalizable metric perturbations.

From eq. (2.13) we see that this is a non-trivial curved spacetime.

This observation raises a question: can the scaling solutions of non-trivial Bianchi type, arise in situations where the field theory in the ultraviolet is in flat spacetime? Or do they require the field theory in the UV to itself be in a curved background? The latter case would be much less interesting from the point of view of possible connections with condensed matter systems. In the gravity description when the scaling solution arises from the near-horizon limit of a geometry which is asymptotically AdS or Lifshitz, this question takes the following form: is a normalizable deformation of the metric (or its analogue in the Lifshitz case) enough? Or does one necessarily have to turn on a non-normalizable metric deformation to obtain the scaling solution of non-trivial Bianchi type in the IR?

In this section we will examine this question for the Type VII solution discussed in section 2.3.1. We will find, after enlarging the matter content to include two gauge fields, that normalizable deformations for the metric suffice. More specifically, in this example we will find solutions where the metric starts in the UV as being AdS space with a normalizable metric perturbation being turned on and ends in the IR as a scaling Type VII solution. However, the gauge fields do have a non-normalizable mode turned on in the UV[12]. From the dual field theory point of view this corresponds to being in flat space but subjecting the system to a helically varying external current. In response, the gravity solution teaches us that the field theory flows to a fixed point in the infra-red with an "emergent" non-trivial metric of the Type VII kind.

The Type VII geometry breaks parity symmetry, as was discussed in section 2.3. The Lagrangian for the example we consider preserves parity. In the solutions we find the parity violation is introduced by the non-normalizable deformations for the gauge fields, or in dual language, by the external current source.

In condensed matter physics there are often situations where the Hamiltonian itself breaks parity and the ground state of the system, in the absence of any external sources, has a helically varying order parameter. This happens for example in the cases discussed in [19], [20]. It will be interesting to examine how such situations might arise in gravitational systems as well. In 5 dimensions a Chern-Simons term can be written for a gauge field and we expect that with parity violation incorporated in this way gravity solutions showing similar behavior can also be easily found. For a discussion of helical type instabilities along these lines see [25], [26, 27, 28], [29, 30, 31].

A similar analysis, asking whether a non-trivial asymptotic metric along the spatial directions is needed in the first place, should also be carried out for the other Bianchi classes. As a first pass one can work in the thin wall approximation and ask whether the solution in the IR with the required homogeneity symmetry can be matched to AdS or a Lifshitz

[12] One of the gauge fields corresponds to a current which is a relevant operator in the IR and the other to an irrelevant operator. The current which breaks the symmetries of AdS to those of Type VII is relevant in the IR.

spacetime using a domain wall with a tension that meets reasonable energy conditions. We leave this for future work.

2.5.1 The System And The Essential Idea

We will consider a system consisting of gravity with a cosmological constant and two gauge fields A_1, A_2, with masses, m_1, m_2 described by the Lagrangian

$$S = \int d^5x\sqrt{-g}\{R + \Lambda - \frac{1}{4}F_1^2 - \frac{1}{4}F_2^2 - \frac{1}{4}m_1^2A_1^2 - \frac{1}{4}m_2^2A_2^2\}. \tag{2.88}$$

We show that this system has a scaling solution of Type VII with parameters determined by Λ, m_1^2, m_2^2. This scaling solution will be the IR end of the full solution we will construct which interpolates between the Type VII solution and asymptotic AdS_5 space in the UV.

The essential idea in constructing this full solution is as follows. It will turn out that the scaling solution, as one parameter is made small, becomes [13] $AdS_2 \times R^3$. We will call this parameter λ below. Now it is well known that $AdS_2 \times R^3$ arises as the near-horizon geometry of an extremal RN brane which asymptotes to AdS_5 space. This means the $AdS_2 \times R^3$ solution has a perturbation[14] which grows in the UV and takes it to AdS_5 space. Since the Type VII solution we find is close to $AdS_2 \times R^3$ when λ is small, it is easy to identify the corresponding perturbation in this solution as well. Starting with the Type VII solution in the IR in the presence of this perturbation, we find, by numerically integrating the solution, that it asymptotes to AdS_5 in the UV as well with only a normalizable perturbation for the metric being turned on.

The Type VII solution, for small λ, is close to $AdS_2 \times R^3$ in the following sense. At values of the radial coordinate which are not too big in magnitude the Type VII solution becomes approximately $AdS_2 \times R^3$ with a small perturbation being turned on. This means that when one starts with the Type VII solution in the IR, with the perturbation that takes it to AdS_5 being now turned on, the solution first evolves to being close to $AdS_2 \times R^3$ at moderate values of r and then further evolves to AdS_5 in the UV.

Below we first describe the Type VII solution and the limit where it becomes $AdS_2 \times R^3$. Then we describe the extreme RN geometry and its near horizon $AdS_2 \times R^3$ limit and finally we identify the perturbation in the Type VII case and numerically integrate from the IR to UV showing that the geometry asymptotes to AdS_5.

[13] In the Type VII case the symmetries are generalized translations involving a combination of the usual translations and rotations along the spatial directions. In the $AdS_2 \times R^3$ case these symmetries are enhanced to include both the usual translations and rotations along the spatial directions.

[14] These perturbations are given in eq.(2.133) and eq.(2.134) in section 2.5.3.

2.5.2 Type VII Solutions

Let us take the metric to be of the form

$$ds^2 = R^2 \left\{ dr^2 - e^{2\beta_t r} dt^2 + (dx^1)^2 + e^{2\beta r}[(\omega^2)^2 + (\lambda+1)(\omega^3)^2] \right\}. \tag{2.89}$$

This metric is the same as in eq.(2.14) and has the same symmetries. The only difference is that the parameter λ has been redefined. With our new definition when $\lambda \to 0$ the metric becomes of Lifshitz type. This follows from noting that $(\omega^2)^2 + (\omega^3)^2 = (dx^2)^2 + (dx^3)^2$, eq.(2.13). In fact, once the equations of motion are imposed in this system, we will see that the $\lambda \to 0$ limit gives $AdS_2 \times R^3$.

We take the gauge fields to have the form

$$A_2 = e^{\beta r} \sqrt{\tilde{A}_c}\, \omega^2 \tag{2.90}$$
$$A_1 = e^{\beta_t r} \sqrt{\tilde{A}_t}\, dt. \tag{2.91}$$

Note that the 6 variables, $R, \beta_t, \beta, \lambda, \tilde{A}_c, \tilde{A}_t$, are all constants and fully determine the solution. We will now solve the equations of motion to determine these constants in terms of the parameters Λ, m_1^2, m_2^2, which enter in the action eq.(2.88). As in the discussion of section 2.3 it will be convenient to work in units where $R = 1$.

The gauge field equations of motion then give

$$\sqrt{\tilde{A}_t}\left[4\beta\beta_t - m_1^2\right] = 0 \tag{2.92}$$
$$\sqrt{\tilde{A}_c}\left[2\beta(\beta_t+\beta) - \frac{2}{1+\lambda} - m_2^2\right] = 0. \tag{2.93}$$

The trace reversed Einstein equations with components along tt, rr, x^1x^1 directions give:

$$\frac{2\tilde{A}_c}{1+\lambda} + 2\tilde{A}_c\beta^2 + \tilde{A}_t(3m_1^2 + 4\beta_t^2) + 4\left[\Lambda - 3\beta_t^2 - 6\beta_t\beta\right] = 0 \tag{2.94}$$
$$\frac{\tilde{A}_c}{2(1+\lambda)} - \tilde{A}_c\beta^2 + \beta_t^2(\tilde{A}_t - 3) - 6\beta^2 + \Lambda = 0 \tag{2.95}$$
$$\frac{3\lambda^2 + 2\tilde{A}_c}{1+\lambda} + \tilde{A}_t\beta_t^2 - \tilde{A}_c\beta^2 - 2\Lambda = 0. \tag{2.96}$$

While the components with indices along the x^2, x^3 directions lead to

$$\frac{6\lambda(2+\lambda) - 2\tilde{A}_c}{1+\lambda} + 3m_2^2\tilde{A}_c + 4\beta(\tilde{A}_c\beta + 3\beta_t + 6\beta) + 2\tilde{A}_t\beta_t^2 - 4\Lambda = 0 \tag{2.97}$$
$$\frac{3\lambda(2+\lambda) - 2\tilde{A}_c}{1+\lambda} + \tilde{A}_c\beta^2 - \tilde{A}_t\beta_t^2 - 6\beta_t\beta - 12\beta^2 + 2\Lambda = 0. \tag{2.98}$$

These are 7 equations in all, but one can check that only 6 of them are independent and these 6 independent equations determine the 6 parameters mentioned above. It turns out to be convenient to express the resulting solution as follows. Working in $R = 1$ units, we express the parameters in the Lagrangian, Λ and m_2^2, along with the constants in the solution $\beta_t, \beta, \tilde{A}_t, \tilde{A}_c$, in terms of m_1^2 and λ. This gives:

$$m_2^2 = -\frac{2}{1+\lambda} + \lambda(2 - \epsilon\lambda) \tag{2.99}$$

$$\Lambda = \frac{2}{\epsilon} + 3\epsilon\lambda^2 + \lambda\left(-3 + \frac{\lambda}{1-\lambda^2}\right) \tag{2.100}$$

$$\tilde{A}_c = \frac{2\lambda}{1-\lambda} \tag{2.101}$$

$$\tilde{A}_t = \frac{4 + \lambda\left(-4 + \epsilon(5\lambda - 6)\right)}{2(\lambda - 1)(\epsilon\lambda - 1)} \tag{2.102}$$

$$\beta_t = \sqrt{\frac{2}{\epsilon}}(1 - \epsilon\lambda) \tag{2.103}$$

$$\beta = \sqrt{\frac{\epsilon}{2}}\lambda, \tag{2.104}$$

where we have introduced a new parameter ϵ (not necessarily small) which is related to m_1^2 by

$$m_1^2 = 4(1 - \epsilon\lambda)\lambda. \tag{2.105}$$

Requiring $\tilde{A}_t \geq 0$, $\tilde{A}_c \geq 0$, and also requiring that β_t, β have the same sign, leads to the conditions [15]

$$0 < \lambda < 1, \quad 0 < \epsilon \leq \frac{4}{\lambda}\frac{(1-\lambda)}{(6 - 5\lambda)}. \tag{2.106}$$

We have chosen both $\beta_t > 0, \beta \geq 0$, so that the horizon lies at $r \to -\infty$.

As in section 2.3, we leave the important question about the stability of these solutions for future work.

The Limit

Now consider the limit where $\lambda = 0$. In this limit, we get

$$m_2^2 = -2 \qquad m_1^2 = 0 \qquad \tilde{A}_c = 0 \qquad \beta = 0 \tag{2.107}$$

$$\Lambda = \frac{2}{\epsilon} \qquad \tilde{A}_t = 2 \qquad \beta_t = \sqrt{\frac{2}{\epsilon}}. \tag{2.108}$$

It is easy to see that the resulting geometry is $AdS_2 \times R^3$. It is sourced entirely by the gauge field A_1 which becomes massless. The second gauge field vanishes, since $\tilde{A}_c = 0$.

[15] The equations allow for β_t, β to have opposite sign, this would correspond to a strange dispersion relation for fluctuations though and probably would be unstable.

Next consider a Type VII solution close to the limit $\lambda \to 0$, with ϵ being held fixed and of order unity. In this limit,

$$\begin{aligned}
\beta_t &= \beta_t^{(0)} - \sqrt{2\epsilon}\lambda \quad \text{where} \quad \beta_t^{(0)} = \sqrt{\frac{2}{\epsilon}} && (2.109)\\
\beta &= \sqrt{\frac{\epsilon}{2}}\lambda && (2.110)\\
\tilde{A}_t &= 2 - \epsilon\lambda + \mathcal{O}(\lambda^2) && (2.111)\\
\tilde{A}_c &= 2\lambda + \mathcal{O}(\lambda^2). && (2.112)
\end{aligned}$$

Also we note that in this limit it follows from eq.(2.99), eq.(2.100), eq.(4.3) that

$$\begin{aligned}
m_2^2 &= -2 + 4\lambda && (2.113)\\
\Lambda &= \frac{2}{\epsilon} - 3\lambda && (2.114)\\
m_1^2 &= 4\lambda && (2.115)
\end{aligned}$$

up to $O(\lambda^2)$ corrections.

Now consider an intermediate range for the radial variable where

$$|r| \ll \frac{1}{\lambda}. \qquad (2.116)$$

In this intermediate region we can expand various components of the metric. E.g.,

$$e^{2\beta r} \simeq 1 + 2\beta r \qquad (2.117)$$

etc. This gives for the metric

$$\begin{aligned}
ds^2 &= \left[dr^2 - e^{2\sqrt{\Lambda}r}dt^2 + (dx^1)^2 + (dx^2)^2 + (dx^3)^2\right] + \delta ds^2 && (2.118)\\
A_1 &= \sqrt{2}e^{\sqrt{\Lambda}r}dt + \delta A_1 && (2.119)\\
A_2 &= \delta A_2 && (2.120)
\end{aligned}$$

where

$$\begin{aligned}
\delta ds^2 &= (\lambda r)\left[\sqrt{\frac{\epsilon}{2}}e^{2\sqrt{\Lambda}r}dt^2 + \sqrt{2\epsilon}((dx^2)^2 + (dx^3)^2)\right] + \lambda(\omega^3)^2 && (2.121)\\
\delta A_1 &= -\left[\lambda r\frac{\sqrt{\epsilon}}{2} + \frac{\lambda\epsilon}{\sqrt{8}}\right]e^{\sqrt{\Lambda}r}dt && (2.122)\\
\delta A_2 &= \sqrt{2\lambda}\omega^2. && (2.123)
\end{aligned}$$

In obtaining these expressions we have used eq.(2.109) and eq.(2.114) to express $\beta_t^{(0)}$ in terms of Λ.

We see that when $\lambda \ll 1$ and eq.(2.116) is met the solution does reduce to $AdS_2 \times R^3$ with only A_1 being turned on. There are additional perturbations in the metric and gauge fields, given by eq.(2.121), eq.(2.122), eq.(2.123). These are small in this region.

2.5.3 Extremal RN Brane

In this subsection we turn off the gauge field A_2 and consider a system consisting of just gravity, with Λ, and A_1, with no mass. It is well known that this system has an extremal Reissner Nordstrom black brane solution with metric

$$ds^2 = -a(\tilde{r})dt^2 + \frac{1}{a(\tilde{r})}d\tilde{r}^2 + b(\tilde{r})[dx^2 + dy^2 + dz^2] \tag{2.124}$$

where

$$a(\tilde{r}) = \frac{(\tilde{r} - \tilde{r}_h)^2(\tilde{r} + \tilde{r}_h)^2(\tilde{r}^2 + 2\tilde{r}_h^2)\Lambda}{12\tilde{r}^4}; \qquad b(\tilde{r}) = \tilde{r}^2 \tag{2.125}$$

and gauge field

$$A = A_t dt \tag{2.126}$$

where

$$A_t(\tilde{r}) = -\tilde{r}_h\sqrt{\frac{\Lambda}{2}}\left(\frac{\tilde{r}_h^2}{\tilde{r}^2} - 1\right). \tag{2.127}$$

The parameter $\tilde{r}_h$ determines the location of the horizon and is determined by the charge density carried by the extremal brane.

Near the horizon, as $\tilde{r} \to \tilde{r}_h$, the geometry becomes of $AdS_2 \times R^3$ type. As discussed in Appendix A.4 by changing variables

$$r = \int \frac{d\tilde{r}}{\sqrt{a(\tilde{r})}} \tag{2.128}$$

one can express the metric and gauge fields for $\tilde{r} \to \tilde{r}_h$ as

$$ds^2 = dr^2 - e^{2\sqrt{\Lambda}r}\left(1 - \frac{14}{3}e^{\sqrt{\Lambda}r}\right)dt^2 + \left(1 + 2e^{\sqrt{\Lambda}r}\right)(dx^2 + dy^2 + dz^2) \tag{2.129}$$

$$A_t = \sqrt{2}e^{\sqrt{\Lambda}r}\left(1 - \frac{8}{3}e^{\sqrt{\Lambda}r} + \cdots\right)dt. \tag{2.130}$$

It is useful to write these expressions as the leading terms

$$ds^2 = dr^2 - e^{2\sqrt{\Lambda}r}dt^2 + (dx^1)^2 + (dx^2)^2 + (dx^3)^2 \tag{2.131}$$

$$A_{1t} = \sqrt{2}e^{\sqrt{\Lambda}r}, \tag{2.132}$$

which correspond to $AdS_2 \times R^3$ sourced by a gauge field in the time-like direction, and corrections,

$$\begin{aligned} \delta ds^2 &= \frac{14}{3}e^{3\sqrt{\Lambda}r}dt^2 + 2e^{\sqrt{\Lambda}r}\left((dx^1)^2 + (dx^2)^2 + (dx^3)^2\right) && (2.133) \\ \delta A_{1t} &= -\frac{8}{3}\sqrt{2}e^{2\sqrt{\Lambda}r}. && (2.134) \end{aligned}$$

We see that the perturbations are small if

$$e^{\sqrt{\Lambda}r} \ll 1, \qquad (2.135)$$

which is the condition for being close enough to the horizon of the extremal brane. Note that this condition requires that r be negative.

2.5.4 The Perturbation in Type VII

We can now identify the perturbation in Type VII, with small λ, which becomes eq.(2.133), eq.(2.134) in the $\lambda \to 0$ limit. We write

$$\begin{aligned} ds^2 &= dr^2 - f(r)dt^2 + g(r)(dx^1)^2 + h(r)(\omega^2)^2 + j(r)(\omega^3)^2 && (2.136) \\ A_1 &= A_{1t}(r)dt && (2.137) \\ A_2 &= A_2(r)\omega^2, && (2.138) \end{aligned}$$

with

$$\begin{aligned} f(r) &= e^{2\beta_t r}(1 + \tilde{\epsilon} f_c e^{\nu r}) && (2.139) \\ g(r) &= 1 + \tilde{\epsilon} g_c e^{\nu r} && (2.140) \\ h(r) &= e^{2\beta r}(1 + \tilde{\epsilon} h_c e^{\nu r}) && (2.141) \\ j(r) &= e^{2\beta r}(\lambda + 1)(1 + \tilde{\epsilon} j_c e^{\nu r}) && (2.142) \\ A_{1t}(r) &= \sqrt{\tilde{A}_t} e^{\beta_t r}(1 + \tilde{\epsilon} A_{1c} e^{\nu r}) && (2.143) \\ A_2(r) &= \sqrt{\tilde{A}_c} e^{\beta r}(1 + \tilde{\epsilon} A_{2c} e^{\nu r}). && (2.144) \end{aligned}$$

The parameters $\beta_t, \beta, A_{1c}, A_{2c}$ take values given in eq.(2.109), eq.(2.110), eq.(2.111), eq.(2.112), and $\tilde{\epsilon}$ is the small parameter which keeps the perturbation small.

It is easy to see that there is a solution to the resulting coupled linearized equations in which

$$\nu = \sqrt{\frac{2}{\epsilon}}\left(1 - \lambda\frac{20}{9}\epsilon\right). \qquad (2.145)$$

By shifting r we can always rescale f_c. For comparing with eq.(2.133), eq.(2.134) we take

$$\tilde{\epsilon} f_c = -\frac{14}{3}. \qquad (2.146)$$

The other parameters then take the values

$$\tilde{\epsilon} g_c = 2\left(1+\lambda\,\frac{\epsilon}{378}(167+54\epsilon)\right) \tag{2.147}$$
$$\tilde{\epsilon} h_c = 2\left(1+\lambda\,\frac{\epsilon(548-\epsilon(89+81\epsilon))}{756(\epsilon-1)}\right) \tag{2.148}$$
$$\tilde{\epsilon} j_c = 2\left(1+\lambda\,\frac{\epsilon(170-\epsilon(467+81\epsilon))}{756(\epsilon-1)}\right) \tag{2.149}$$
$$\tilde{\epsilon} A_{1c} = -\frac{8}{3}\left(1+\lambda\,\frac{(32-27\epsilon)\epsilon}{2016}\right) \tag{2.150}$$
$$\tilde{\epsilon} A_{2c} = -\frac{1}{2}\epsilon + O(\lambda). \tag{2.151}$$

Note the $O(\lambda)$ correction to A_{2c} will contribute at higher order since $\tilde{A}_c$ is or order λ.

It is easy to see that as $\lambda \to 0$ this perturbation becomes exactly the one given in eq.(2.133), eq.(2.134).

2.5.5 The Interpolation

We are finally ready to consider what happens if we start with the Type VII solution we have found in section 2.5.2 but now with the perturbation identified in the previous section being turned on. We work with the cases where $\lambda \ll 1$.

Since $\nu > 0$ we see that as $r \to -\infty$ the effects of the perturbation becomes very small and the solutions becomes the Type VII solution discussed in section 2.5.2.

In the region where r is negative and both conditions eq.(2.116) and eq.(2.135) are met we see that the resulting solution can be thought of as being approximately $AdS_2 \times R^3$ with only A_1 being turned on along the time direction. There are corrections to this approximate solution given by the sum of the perturbations in eq.(2.121), eq.(2.122),eq.(2.123) and eq.(2.133), eq.(2.134).

To numerically integrate we will start in this region and then go further out to larger values of r. We take the metric and gauge fields to be given by eq.(2.136), eq.(2.137), eq.(2.138).

We are interested in a solution which asymptotes to AdS_5. It is best to work with values of ϵ for which m_2^2 lies above the AdS_5 BF bound. This condition gives $m_2^2/\Lambda > -\frac{1}{6}$. Working with the leading order terms in eq.(2.113), eq.(2.114) this condition is met if

$$\epsilon < \frac{1}{6}. \tag{2.152}$$

In the figures which are included below we have taken $\epsilon = \frac{1}{7}$. In addition, we take $\lambda = 10^{-2}$. And we start the numerical integration at $r = -3$, which meets the conditions eq.(2.116), eq.(2.135). Varying these parameters, within a range of values, does not change our results in any essential way.

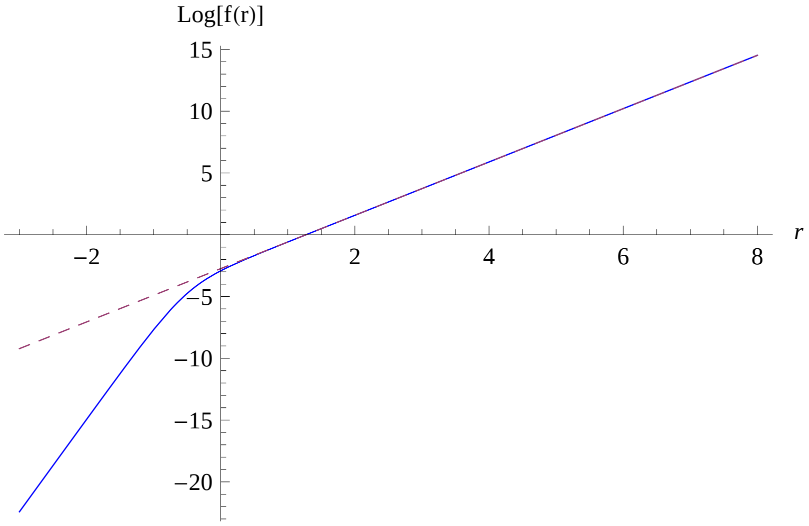

Figure 2.1: Numerical solution for metric component $\log f(r)$.

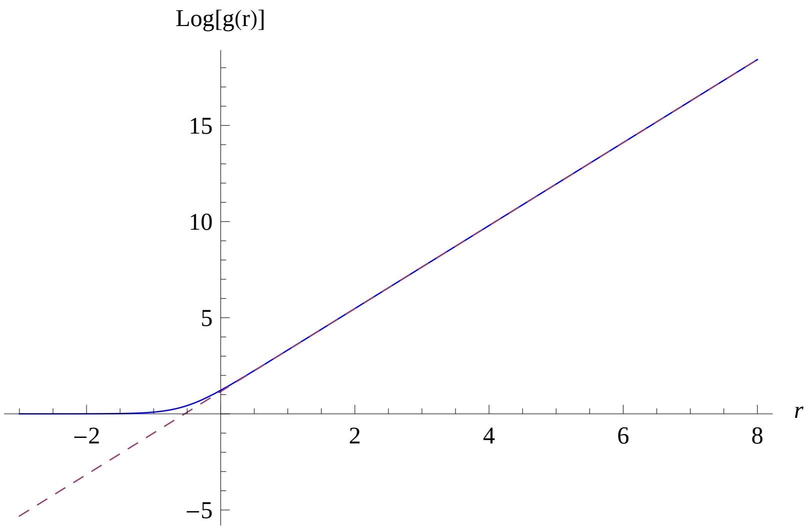

Figure 2.2: Numerical solution for metric component $\log g(r)$.

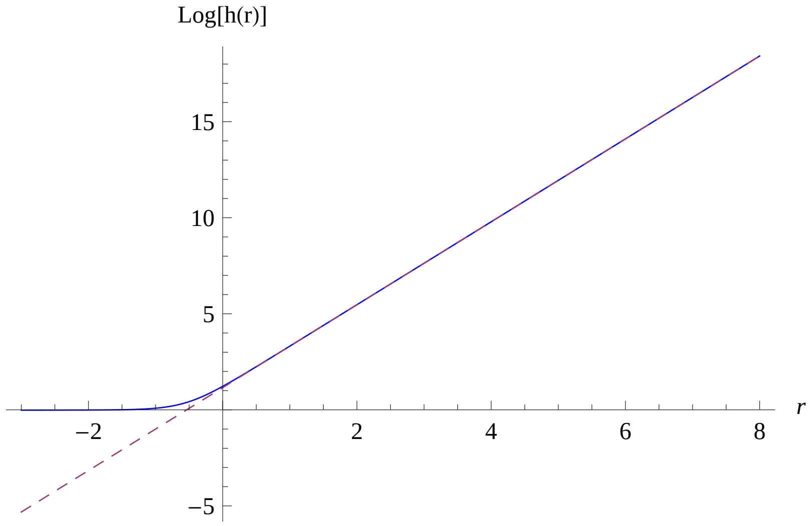

Figure 2.3: Numerical solution for metric component $\log h(r)$.

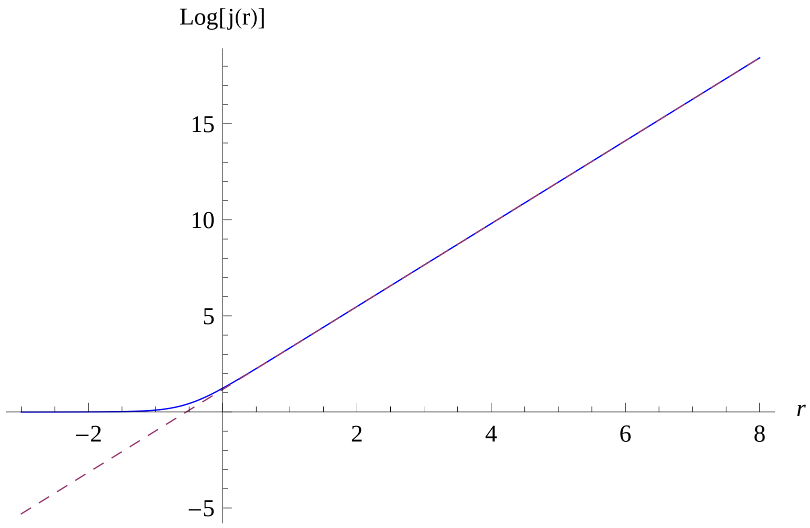

Figure 2.4: Numerical solution for metric component $\log j(r)$.

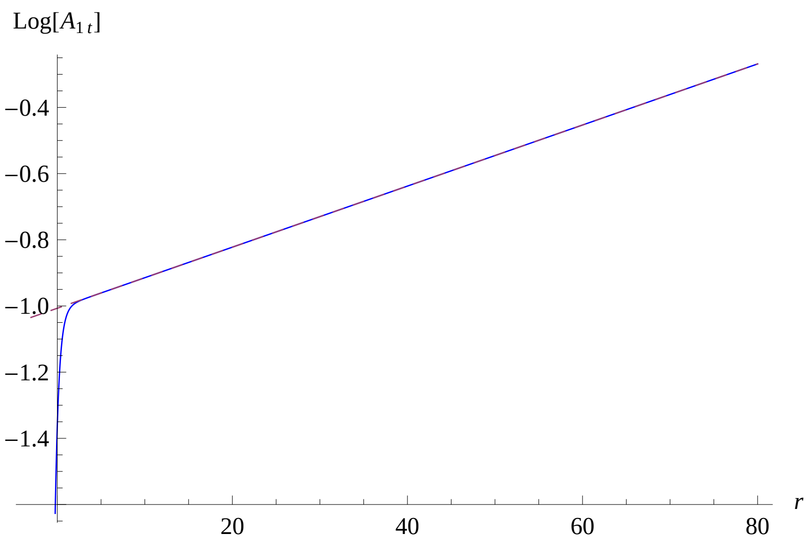

Figure 2.5: Numerical solution for gauge field $\log A_{1t}(r)$.

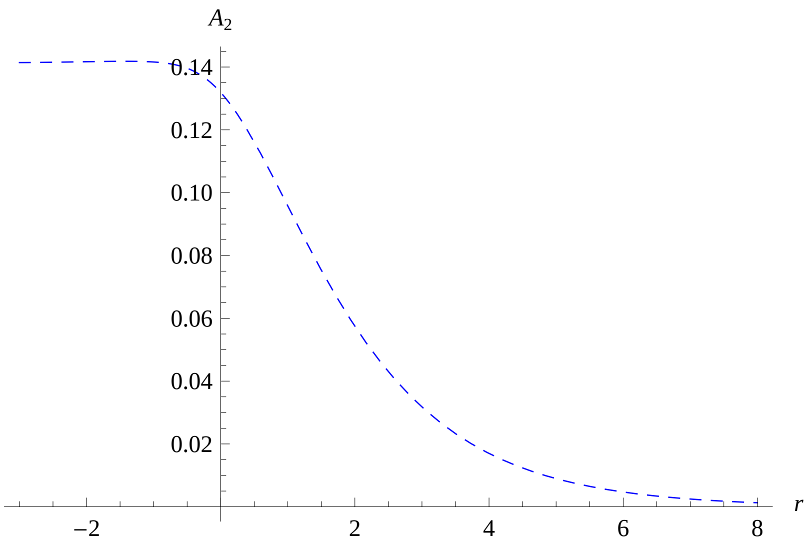

Figure 2.6: Numerical solution for gauge field $A_2(r)$.

The reader will see from Fig.(2.1), (2.2), (2.3), (2.4), that the metric coefficients $f(r)$, $g(r)$, $h(r)$, $j(r)$, become exponential in r as $r \to \infty$. We have fitted the slope and find agreement with the behavior in AdS space with cosmological constant given in eq.(2.114).

Notice that when λ is small and positive the gauge field A_1 has a small and positive m^2, eq.(2.115). In asymptotic AdS_5 space such a gauge field has two solutions behaving like

$$A_1 \sim e^{\left(-\sqrt{\frac{\Lambda}{12}} \pm \sqrt{\frac{\Lambda}{12}+\frac{m_1^2}{2}}\right)r}. \tag{2.153}$$

In particular one branch grows exponentially as $r \to \infty$. It is easy to see that this behavior agrees with the Fig.(2.5) at large r. The small value of m_1^2 means one has to go out to relatively large values of r to see this behavior. In contrast, since A_2 has negative m^2 both the solutions asymptotically die out, which agrees with Fig.(2.6).

One comment is worth making here. The reader might wonder why the asymptotically growing A_1 gauge field does not back react and lead to a departure from AdS_5 space. The reason is that m_1^2 is very slightly positive, *i.e.*, $m_1^2/\Lambda \ll 1$, and as a result the stress energy due to this field is still sub dominant compared to the cosmological term at large r.

In summary, the numerical integration shows that the resulting geometry is asymptotically AdS_5 with small corrections which correspond to normalizable perturbations being turned on. The gauge fields in contrast have both their normalizable and non-normalizable modes turned on. This is clear in the A_1 case which grows exponentially, but it is also true for A_2 which has negative m^2 so that both modes for it die away asymptotically.

We have thus established that the Type VII geometry discussed in section 2.5.2 can arise starting from a flat boundary metric with non-normalizable gauge field deformations turned on.

2.6 Generalized Translations Involving Time and Closed Time-Like Curves

So far, we have been discussing examples where the usual time translation symmetry is preserved and the generalized translations only involve the spatial directions. However, one can also have situations where the generalized translations involve the time direction in a non-trivial manner. For example, a case of Type VII_0 type can arise when a translation in the time direction is accompanied by a rotation in a spatial two-plane. This could happen if there is a vector order parameter which is time dependent and rotates in the spatial two-plane as time advances. The time dependent order parameter might arise as a response to a suitable periodic time dependent external source.

We should note that a situation where time gets non-trivially involved in the generalized translations does not necessarily require the spacetime to be time dependent. For example it could have been that one has the standard translational symmetry along time and all the spatial directions except for one, x^1, and in the x^1 direction the translation is accompanied by a boost in the t, x^2 plane. In this case the metric would depend on x^1 but not t, just as in the case of Type VII discussed in section 2.3.1 the metric depended on x^1 but not x^2, x^3. Another example will be presented below where this point will also become clear.

Here, as in the discussion earlier, we will be interested in geometries which have scale invariance, along with the generalized translational symmetries mentioned above. Such gravitational solutions, from the point of view of possible connections with condensed matter physics, could describe dynamical critical phenomenon which arise when a system is subjected to time varying external forces.

In general, in the 9 Bianchi classes, the three generators of the symmetry algebra are inequivalent. Once we allow for the generalized translations to also involve time one typically finds that each Bianchi class gives rise to more than one physically distinct possibility depending on the role time translations play in the symmetry algebra.

We have not systematically examined which of the many resulting cases arising in this way can be realized by coupling reasonable kinds of matter fields to gravity, or even examined systematically which of these cases are allowed by the various energy conditions. These conditions could well impose fairly stringent restrictions in these cases where time is more non-trivially involved.

A few simple examples which we have constructed already illustrate some novel aspects which arise in such situations and we will limit ourselves to commenting on them here. In particular we will discuss below one example in which the resulting space-time may be physically unacceptable since it involves closed time-like curves. This example illustrates the need to proceed with extra caution in dealing with situations where the generalized translations also involve time.

The case we have in mind is most simply discussed in 4 total spacetime dimensions and is based on the Bianchi Type II algebra, which involves translations of a generalized sort along t, x^1, x^2, generated by Killing vectors

$$\xi_1 = \partial_t, \quad \xi_2 = \partial_1, \quad \xi_3 = \partial_2 + x^1 \partial_t. \tag{2.154}$$

The invariant one-forms are given by (see Appendix A.1)

$$\omega^1 = dt - x^2 dx^1 \ ; \ \omega^2 = dx^1 \ ; \ \omega^3 = dx^2. \tag{2.155}$$

We assume the full metric to be also invariant under a translation in r accompanied by a rescaling of t, x^1, x^2. Also we will take the metric to be diagonal in the basis of the invariant one-forms given above which gives [16]

$$ds^2 = R^2 \left[dr^2 - e^{2\beta_1 r}(dt - x^2 dx^1)^2 + e^{\beta_1 r}((dx^1)^2 + (dx^2)^2) \right]. \tag{2.156}$$

The gauge field is taken to be along the invariant one-form ω^1 given in eq.(2.155) and of the form

$$A = \sqrt{A_1} e^{\beta_1 r} \omega^1. \tag{2.157}$$

The gauge field equation of motion for this system gives

$$m^2 - 2(1 + \beta_1^2) = 0. \tag{2.158}$$

The trace reversed Einstein equations along r, t, x^1 respectively are

$$A_1 - 6\beta_1^2 + A_1\beta_1^2 + 2\Lambda = 0 \tag{2.159}$$
$$-2 + A_1 + A_1 m^2 - 8\beta_1^2 + A_1\beta_1^2 + 2\Lambda = 0 \tag{2.160}$$
$$2 - A_1 - 4\beta_1^2 - A_1\beta_1^2 + 2\Lambda = 0. \tag{2.161}$$

The Einstein equation along x^2 gives the same equation as along x^1.

It can be easily verified that the solution to these equations is

$$m^2 = 2(1 + \beta_1^2) \qquad \Lambda = \frac{1}{2}(5\beta_1^2 - 1) \qquad A_1 = 1. \tag{2.162}$$

So we see that reasonable matter in the form of a massive Abelian gauge field, in the presence of a cosmological constant, can give rise to a geometry of Type II where time enters in a non-trivial way in the generalized translations.

However, as we will now see, this metric has closed time-like curves. This is a cause for physical concern, although similar solutions were investigated in [57] and suggestions about how CTCs may sometimes be acceptable features in such solutions were described there.

With a redefinition of the form,

$$t - \frac{x^1 x^2}{2} \to t \quad ; \quad x^1 \to \rho \sin\theta \quad ; \quad x^2 \to \rho\cos\theta \tag{2.163}$$

the metric becomes

$$ds^2 = dr^2 - e^{2\beta_1 r} dt^2 + e^{\beta_1 r} d\rho^2 + e^{\beta_1 r}\rho^2 \left(1 - \frac{\rho^2}{4} e^{\beta_1 r}\right) d\theta^2 + \rho^2 e^{2\beta_1 r} d\theta dt. \tag{2.164}$$

Here the coordinate θ is periodic with period 2π. Now notice that for $\left(1 - \frac{\rho^2}{4} e^{\beta_1 r}\right) < 0$, θ

[16] Note that this metric is not time dependent, also note that for simplicity we are assuming that both spatial coordinates x^1 and x^2 scale similarly, but in general that is not required.

becomes time-like and the closed curve, $\theta = [0, 2\pi]$, becomes a closed time-like curve.

2.7 Discussion

In the analysis discussed in this chapter, we argued that black branes need not be translationally invariant along the spatial directions in which they extend, and could instead have the less restrictive property of homogeneity. We showed that such black brane solutions in $4+1$ dimensions are classified by the Bianchi classification and fall into 9 classes. We mostly considered extremal black branes and focused on their near-horizon attractor region, which we took to be of scale invariant type. We found that such scale invariant solutions, realizing many of the non-trivial Bianchi classes, can arise in relatively simple gravitational systems with a negative cosmological constant and one or two massive Abelian gauge fields as matter. From the point of view of the holographically dual field theory, and of possible connections with condensed matter physics, these solutions correspond to new phases of matter which can arise when translational invariance is broken[17].

It is clear that our analysis has merely scratched the surface in exploring these new homogeneous brane solutions, and much more needs to be done to understand them better. Some extensions of our work already performed and also a few directions for future work are as follows:

- One would like to analyze the stability properties of the near-horizon solutions we have found in more detail. In the examples we constructed, sometimes solutions in two different classes are allowed for the same range of parameters. For example, with one gauge field, both Lifshitz and Type VII can arise for the same mass range. In such cases especially one would like to know if both solutions are stable or if one of them has an instability.
- It seems reasonable to suggest that the scaling solutions we have obtained arise as the near-horizon limits of extremal black brane solutions. For the case of Type VII we showed that this was indeed true by obtaining a full extremal black brane solution which asymptotes to AdS space at large distance. In the follow up work, in [58], we explored if this is true for the other classes as well. There we argued that there is at least no constraints in principle from null and weak energy considerations to have an interpolation for most of the other Bianchi geometries. Though we couldn't construct any specific interpolation of those attractors in a given model.
- One would like to find the small temperature deformation of these solutions. This can be done working in the near-horizon limit itself. This is important in characterizing the

[17] Massive gauge fields in the bulk correspond to currents in the boundary theory which are not conserved. One expects that similar solutions should also arises when the symmetry is spontaneously broken in the bulk, corresponding to a superfluid in the boundary. It will be interesting to check if superfluids found in nature exhibit all of the phases we have found.

thermodynamics of these systems better, and also in establishing that the solutions are the end points of non-extremal solutions. It is known that while curvature invariants are finite in the Lifshitz solutions, tidal forces do blow up (for a recent discussion of the nature of Lifshitz singularities, see *e.g.* [56]). We saw that this was also true in the Type VII case investigated in section 2.3.1, and expect it to be true in many solutions in the other Bianchi classes as well. It would be worth investigating this issue further. If a finite temperature deformation exists, it would probably allow us to control the effects due to these large tidal forces.

- One should understand these solutions more deeply from the point of view of the attractor mechanism. The solutions are tightly constrained by symmetries, since they have the generalized translational invariances and scaling invariance (this involves a translation along the radial direction). These symmetries are enough to determine the solution completely up to a few constants, *e.g.* R, β_1, β_i, A_t in eq.(2.10), eq.(2.12). It should be straightforward to formulate an entropy function for any given Bianchi class which can be extremised to obtain these constants, thereby determining the full solution from purely algebraic considerations. It would also be interesting to ask when a given scaling solution is an attractor in terms of varying the asymptotic data and studying how the solution changes, and to understand how to encode the attractor behavior (or lack thereof) in terms of suitable near-horizon data. We hope to report on this development soon.

- Going beyond solutions with scaling symmetry, it is interesting to allow for the possibility that the near-horizon geometry does not have a scaling isometry, but instead has a conformal Killing vector corresponding to a shift of the radial direction and a rescaling of the other directions. Such metrics have been analyzed in [59], [60], [61], [62], [63], [64], [65] and shown to lead to interesting behaviors. In a follow up work we, in [66], we constructed explicit examples for some classes of the Bianchi attractors with hyperscaling violation and also stripped version of them.

- It is quite amazing to us that even the relatively simple matter systems we have explored here, consisting of a just a couple of massive gauge fields, can yield such a large diversity of solutions. It would be fascinating to explore within a simple system of this type, which of the solutions are related to each other by RG flow.

- Naturally, one would like to know whether the kinds of simple gravitational systems we have analyzed here (with their required values of parameters) can arise in string theory[18]. To be even more ambitious, one would ultimately like to ask about all of the phases that can be realized in gravitational systems which admit a consistent UV completion. The homogeneous phases we have investigated here are many more than

[18] Some brane solutions of supergravity theories with instabilities which break translational invariance have been identified in the literature [26, 27, 28], [29, 30, 31]. It would also be interesting to ask whether the attractor solutions we have found describe the end points for these instabilities.

were previously considered, but one suspects that even they are only a tiny subset of all possibilities!

Chapter 3

Entangled Dilaton Dyons

3.1 Introduction

In the previous chapter we saw that possible interesting connections could arise between gravitation and condensed matter physics. Specifically, an insight from the condensed matter systems, namely the abundance of varied phases in nature, inspired us to find possible similar phases in the gravity theory. It was also important to note that the AdS/CFT correspondence played a crucial role in establishing that connection.

In this chapter we are interested in running our investigation of the interesting connection between condensed matter system and a theory of gravity in the other way round. More precisely, we try to consider a specific solution in a gravitational theory coupled to matter and examine if it is possible to gain insight about any corresponding phase in condensed matter physics. On the gravity side, the Einstein-Maxwell-Dilaton (EMD) system consisting of gravity and a Maxwell gauge field coupled to a neutral scalar (the Dilaton) is of considerable interest from the point of view of realizing an important class of systems in condensed matter physics consisting of fermions at finite density with strong correlations. Landau Fermi liquid theory is one paradigm that often describes such systems, but it can fail. The resulting Non-Fermi liquid behavior is poorly understood and believed to be of considerable interest, *e.g.*, in the study of High T_c superconductors in $2+1$ dimensions. Fermions in the boundary theory carry a conserved charge - fermion number- so it is natural to include a gauge field in the bulk. The presence of a neutral scalar allows for promising new phases to arise where the entropy vanishes at non-zero chemical potential and zero temperature, as was discussed in [67], [68], [59]. These phases correspond to compressible states of matter with unbroken fermion number symmetry, see [69]. It was found that the thermodynamics and transport properties of these systems, while showing the existence of gapless excitations, do not fit those of a Landau Fermi liquid. For example, the specific heat is typically not linear in the temperature (T), at small temperatures, and the electric resistivity also does not have the required T^2 dependence [1].

In a different context, study of entanglement between degrees of freedom of a quantum system specifically near quantum critical point, has inspired considerable interest among physicists. The most studied measure of such an entanglement is called the entanglement entropy. A more formal definition of this quantity is discussed in section 3.5. Apart from several interesting issues regarding calculation of entanglement entropy in quantum field theories, a fascinating connection of holography and this quantity has been established. We will also discuss about this explicitly in section 3.5. More relevant to our discussions in this chapter is an exciting recent development leading to the claim that for an appropriate range parameters such an EMD system could give rise to an entanglement entropy which reproduces the behavior expected of a system with a Fermi surface. If we take a sufficiently big region in space in a system with a Fermi surface it is believed that the entanglement entropy goes like

$$S_{entangled} \sim A \log(A) \tag{3.1}$$

where A is the area of the boundary of this region [2],[3]. The log enhancement is believed to be the tell-tale signature of a Fermi surface. Exactly such a behavior was shown to arise for appropriate choices of parameters in the EMD system in [63], see also [64]. In addition, it was argued that the specific heat, at small temperatures, could be understood on the basis of gapless excitations which dispersed with a non-trivial dynamical exponent.

Taken together, these developments suggest that for an appropriate range of parameters the EMD system could perhaps describe phases where a Fermi surface does form but where the resulting description is not of Landau Fermi liquid type. While this is a promising possibility it is far from being definitely established. In fact, as has been known for some time now, at large N (classical gravity) the system does not exhibit some of the standard characteristics expected of a system with a Fermi surface. For example there are no oscillations in the magnetization and other properties as the magnetic field is varied (the de Haas-van Alphen effect) , nor are there any $2k_F$ Friedel oscillation [4]. More recently the non-zero momentum current-current two point function has been calculated and found to have suppressed weight at small frequency [77].

In this chapter we will continue to study this class of systems from the gravity side by

[1] These results refer to the case when the boundary theory is $2+1$ dimensional with a $3+1$ dimensional bulk dual.

[2] Strictly speaking this behavior has only been proven for free or weakly coupled fermions [70],[71] but it is expected to be more generally true due to the locus of gapless excitations which arises in the presence of a Fermi surface. Additional evidence has also been obtained in [72], [73], [74].

[3] It is important to remember that this logarithmic behavior is the leading contribution in entanglement entropy when the UV cut off energy scale is of the same order as the Fermi energy, which is quite common in condensed matter physics. On the other hand for analysis in high energy physics the UV cut off scale is generally considered as much higher than the Fermi energy and we get the area law in entanglement entropy as the leading divergent contribution. Besides this divergent term, there is however a finite term which gives a logarithmic contribution as in eq.(3.1).

[4] At one loop de Hass- van Alphen type oscillations are seen, [75]. For some recent discussion of Friedel oscillations in $(1+1)$ dim. see [76].

turning on an additional magnetic field and determining the resulting response. In our work the magnetic field will be kept small compared to charge density in the boundary theory. We will be more specific about what this means in terms of the energy scales of the boundary theory shortly. For now let us note that without a magnetic field the purely electric theory has a scaling-type solution (more correctly a hyperscaling violating solution). The magnetic field is kept small so that its effects are a small perturbation compared to the electric field in the ultraviolet (UV) of this scaling solution.

The chapter is planned as follows. We start with a brief description of the dilatonic system and the hyperscaling violating metrics in section 3.2. The effects of a magnetic field are discussed in section 3.3. The resulting thermodynamics is discussed in section 3.4 and the entanglement entropy in section 3.5. We end with a discussion of results and some concluding comments in section 3.6. Appendix B.1 contains important details about the numerical analysis.

Before ending the introduction let us also comment on some related literature. For a discussion of probe fermions in the extremal RN geometry and the resulting non-Fermi liquid behavior see, [78],[79], [80],[81],[41],[82]. The EMD system has been studied in [67],[68],[59],[60],[83],[84],[85],[61],[62],[86]. The subject of entanglement entropy has received considerable attention in the literature lately, for a partial list of references see [87],[88],[89], [90],[91], for early work; and for a discussion within the context of the AdS/CFT correspondence see [92],[93] [5].

3.2 The Einstein Maxwell Dilaton Gravity System

We work in $3 + 1$ dimensions in the gravity theory with an action

$$S = \int d^4x\sqrt{-g}[R - 2(\nabla\phi)^2 - f(\phi)F_{\mu\nu}F^{\mu\nu} - V(\phi)]. \tag{3.2}$$

Much of our emphasis will be on understanding the near horizon region of the black brane solutions which arise in this system. This region is more universal, often having the properties of an attractor, and also determines the IR behavior of the system. In this region, in the solutions of interest, the dilaton will become large, $\phi \to \pm\infty$. The potential and gauge coupling function take the approximate forms

$$f(\phi) = e^{2\alpha\phi} \tag{3.3}$$

$$V = -|V_0|e^{2\delta\phi} \tag{3.4}$$

[5] Two papers in particular have overlap with the work reported here. While their motivations were different the analysis carried out in these papers is similar to ours. The EMD system with the inclusion of possible higher order corrections was analyzed in [94] and it was found that sometimes these corrections could change the behavior of the geometry resulting in an $AdS_2 \times R^2$ region in the deep IR. This analysis was generalized to the case with hyperscaling violation in the work [95] which appeared while the work presented in this chapter was being completed.

along this direction of field space. The two parameters, α, δ, govern the behavior of the system. For example the thermodynamic and transport properties and also the entanglement properties crucially depend on these parameters. The action in eq. (4.1) has a symmetry under which the sign of ϕ, α, δ are reversed. Without loss of generality we will therefore choose $\delta > 0$ in the discussion which follows.

Our analysis will build on the earlier investigations in [59] and [61], and our conventions will be those in [61]. We will work in coordinates where the metric is,

$$ds^2 = -a(r)^2 dt^2 + \frac{dr^2}{a(r)^2} + b(r)^2(dx^2 + dy^2) \tag{3.5}$$

The horizon of the extremal black brane will be taken to lie at $r = 0$.

The gauge field equation of motion gives,

$$F = \frac{Q_e}{f(\phi)b^2} dt \wedge dr + Q_m dx \wedge dy. \tag{3.6}$$

The remaining equations of motion can be conveniently expressed in terms of an effective potential [53]

$$V_{\text{eff}} = \frac{1}{b^2}\left(e^{-2\alpha\phi}Q_e^2 + e^{2\alpha\phi}Q_m^2\right) - \frac{b^2|V_0|}{2}e^{2\delta\phi}, \tag{3.7}$$

and are given by,

$$(a^2b^2)'' = 2|V_0|e^{2\delta\phi}b^2 \tag{3.8}$$

$$\frac{b''}{b} = -\phi'^2 \tag{3.9}$$

$$(a^2b^2\phi')' = \frac{1}{2}\partial_\phi V_{\text{eff}} \tag{3.10}$$

$$a^2b'^2 + \frac{1}{2}a^{2\prime}b^{2\prime} = a^2b^2\phi'^2 - V_{\text{eff}}. \tag{3.11}$$

3.2.1 Solutions With Only Electric Charge

Next let us briefly review the solutions with Q_m set to zero which carry only electric charge. The solution in the near-horizon region take the form,

$$a = C_a r^\gamma \qquad b = r^\beta \qquad \phi = k\log r \tag{3.12}$$

where the coefficients C_a, γ, β, k and the electric charge Q_e are given by

$$\beta = \frac{(\alpha+\delta)^2}{4+(\alpha+\delta)^2} \qquad \gamma = 1 - \frac{2\delta(\alpha+\delta)}{4+(\alpha+\delta)^2} \qquad k = -\frac{2(\alpha+\delta)}{4+(\alpha+\delta)^2} \tag{3.13}$$

$$C_a^2 = |V_0|\frac{\left(4+(\alpha+\delta)^2\right)^2}{2\left(2+\alpha(\alpha+\delta)\right)\left(4+(3\alpha-\delta)(\alpha+\delta)\right)} \qquad Q_e^2 = |V_0|\frac{2-\delta(\alpha+\delta)}{2\left(2+\alpha(\alpha+\delta)\right)}. \tag{3.14}$$

It might seem strange at first that the electric charge Q_e is fixed, this happens because in the near-horizon metric we work with the the time (and spatial coordinates) which have been rescaled compared to their values in the UV.

The following three conditions must be satisfied for this solution to be valid : $Q_e^2 > 0, C_a^2 > 0, \gamma > 0$. These give the constraints,

$$
\begin{aligned}
2 - \delta(\alpha+\delta) &> 0 \qquad (3.15)\\
2 + \alpha(\alpha+\delta) &> 0 \qquad (3.16)\\
4 + (3\alpha-\delta)(\alpha+\delta) &> 0 \qquad (3.17)\\
4 + (\alpha-3\delta)(\alpha+\delta) &> 0. \qquad (3.18)
\end{aligned}
$$

The last of these conditions follow from the requirement that

$$2\gamma - 1 > 0 \qquad (3.19)$$

so that the specific heat is positive. Fig.(3.1) shows the the region in the (δ, α) plane, with $\delta > 0$, allowed by the above constraints.

To summarize our discussion, the metric in the purely electric solution takes the form

$$ds^2 = -C_a^2 r^{2\gamma} dt^2 + \frac{dr^2}{C_a^2 r^{2\gamma}} + r^{2\beta}(dx^2 + dy^2). \qquad (3.20)$$

And the dilaton is given in eq.(3.12,3.13) While this solution is not scale invariant it does admit a conformal killing vector. This follows from noting that under the transformation

$$
\begin{aligned}
r &= \lambda \tilde{r} \qquad (3.21)\\
t &= \lambda^{1-2\gamma} \tilde{t} \qquad (3.22)\\
\{x, y\} &= \lambda^{1-\gamma-\beta}\{\tilde{x}, \tilde{y}\} \qquad (3.23)
\end{aligned}
$$

the metric eq.(3.20) remains invariant upto a overall scaling,

$$ds^2 = \lambda^{2-2\gamma}\{-C_a^2 \tilde{r}^{2\gamma} d\tilde{t}^2 + \frac{d\tilde{r}^2}{C_a^2 \tilde{r}^{2\gamma}} + \tilde{r}^{2\beta}(d\tilde{x}^2 + d\tilde{y}^2)\}. \qquad (3.24)$$

The dilaton also changes under this rescaling by an additive constant,

$$\phi = k\ ln(\tilde{r}) + k\ ln(\lambda) \qquad (3.25)$$

The two exponents γ, β which appear in the metric are related to the dynamic exponent with which gapless excitations disperse and hyperscaling violations, as was explained in [64].

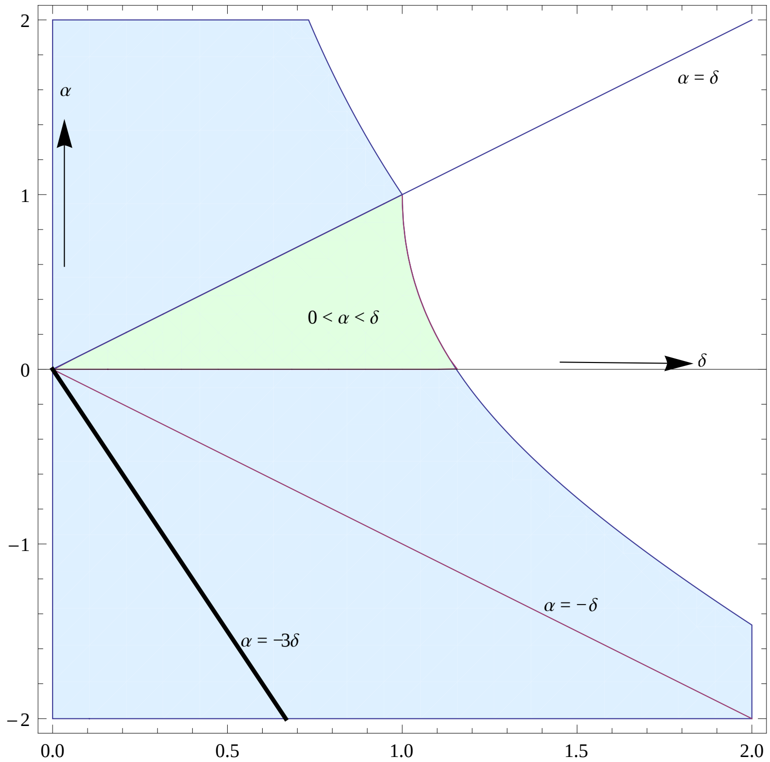

Figure 3.1: The blue and green shaded regions are allowed by the various positivity and thermodynamics constraints for the electric scaling solutions. The straight lines in the (δ, α) plane demarcate various regions which will be relevant for the discussion in the following sections.

Under the coordinate change,

$$r = \tilde{r}^{-\frac{1}{\beta}} \tag{3.26}$$

$$t = \frac{1}{\beta C_a^2}\tilde{t} \tag{3.27}$$

$$(x, y) = \frac{1}{\beta C_a}(\tilde{x}, \tilde{y}), \tag{3.28}$$

the metric eq.(3.20) becomes

$$ds^2 = \frac{1}{\beta^2 C_a^2}\frac{1}{\tilde{r}^2}\left\{-\frac{d\tilde{t}^2}{\tilde{r}^{\frac{4(z-1)}{2-\theta}}} + \tilde{r}^{\frac{2\theta}{2-\theta}}d\tilde{r}^2 + d\tilde{x}^2 + d\tilde{y}^2\right\}. \tag{3.29}$$

Where,

$$z = \frac{2\gamma - 1}{\beta + \gamma - 1} \qquad\qquad \theta = \frac{2(\gamma - 1)}{\beta + \gamma - 1}. \tag{3.30}$$

This is the form of the metric discussed in [64] (upto the overall $\frac{1}{\beta^2 C_a^2}$ factor which was set to unity by a choice of scale). The exponent z is the dynamic exponent, as we can see from the scaling weights of the t and x, y directions in eq.(3.22), eq.(3.23). The exponent θ is the hyperscaling violation exponent, we will also explain this further in section 3.4.

Let us end this section with some more comments. In eq.(3.6) the two-form F is dimensionless, so that Q_e, Q_m have dimensions of $[Mass]^2$. The chemical potential μ is related to Q_e by

$$Q_e \sim \mu^2 \tag{3.31}$$

and has dimensions of mass.

The near-horizon geometry of the type being discussed here can be obtained by starting from an asymptotically AdS space in the UV for a suitable choice of the potential $V(\phi)$. This was shown, *e.g.*, in [61], for additional discussion see Appendix B.1. It is simplest to consider situations where the asymptotic AdS space has only one scale, μ, which characterizes both the chemical potential of the boundary theory and any breaking of conformal invariance due to a non-normalisable mode for the dilaton being turned on. In our subsequent discussion we will have such a situation in mind and the scale μ will often enter the discussion of the thermodynamics and entanglement.

Also note that the parameter N^2 which will enter for example in the entropy eq.(3.52) is given in terms of the potential eq.(3.4) by

$$N^2 \sim \frac{1}{G_N|V_0|}. \tag{3.32}$$

Again to keep the discussion simple we will take the cosmological constant for the asymptotic AdS to be of order V_0 so that N^2 is also number of the degrees of freedom in the UV[6].

The solutions we have considered can have curvature singularities as $r \to 0$, when such singularities are absent tidal forces can still diverge near the horizon, *e.g.*, see [7], [56]. These divergences can be cut-off by heating the system up to a small temperature as discussed in [68], [61]. Also, as we will see shortly, adding a small magnetic field can alter the behavior of the geometry in the deep IR again removing the singular region.

3.3 The Effect of the Magnetic field on the Gravity Solution

Now that we have understood the solutions obtained with only electric charge we are ready to study the effects of adding a small magnetic field.

The presence of the magnetic field gives rise to an additional term in the effective potential eq.(3.7). The magnetic field is a small perturbation if this term is small compared to the

[6] The examples studied in [61] are of this type. There the full potential was taken to be $V(\phi) = -2|V_0|\cosh(2\delta\phi)$ (see eq.(F.1 of [61]). As a result in the asymptotic region $r \to \infty$ the potential goes to its maximum value, $V \to V_\infty = -2|V_0| \sim -|V_0|$.

[7] Sometimes the geometries can be regular with no singularities or diverging tidal forces, [96].

electric charge term, giving rise to the condition

$$\left(\frac{Q_m}{Q_e}\right)^2 \ll e^{-4\alpha\phi}. \tag{3.33}$$

From eq.(3.12) and eq.(3.13) we see that

$$e^{-4\alpha\phi} = r^{-4\alpha k} \tag{3.34}$$

so eq.(3.33) in fact gives rise to a condition on the radial coordinate

$$\left(\frac{Q_m}{Q_e}\right)^2 \ll r^{-4\alpha k}. \tag{3.35}$$

By a small magnetic field we mean more precisely choosing a suitable value of Q_m and starting at a value of the radial coordinate r where eq.(3.35) is met. We will be then interested in asking if this magnetic perturbation continues to be small in the IR, *i.e.*, even smaller values of r, or if its effects grow [8].

The requirement that the magnetic field is small can be stated more physically as follows. Consider a purely electric solution which asymptotes to AdS space in the far UV and let μ be the only scale characterizing the boundary theory which is dual to this electric theory as discussed in the previous section. Then the magnetic field is small if it satisfies the condition

$$|Q_m| \ll \mu^2, \tag{3.36}$$

so that its effects can be neglected in the UV and continue to be small all the way to the electric scaling region.

Our discussion breaks up into different cases depending on the values of the parameters α, δ. We will choose $\delta \geq 0$ in the discussion below without any loss of generality. Let us also note that although we do not always mention them for an electric solution to exist the additional conditions eq.(3.15)-eq.(3.18) must also be met.

We now turn to the various cases.

3.3.1 Case I. $-\delta < \alpha < 0$

In this case the magnetic perturbation is irrelevant in the infrared. From eq.(3.13) we see that $\alpha k > 0$ so that

$$e^{-4\alpha\phi} = r^{-4\alpha k} \to \infty \tag{3.37}$$

[8] As is clear from eq.(3.35) and we will study this shortly in more detail, the magnetic field is relevant in the IR when $\alpha k < 0$. It is easy to see from eq.(3.13), eq.(3.14) that when this condition is met the coupling $g^2 = e^{-2\alpha\phi}$ in the purely electric solution is weakly coupled in the IR since $g^2 \to 0$ as $r \to 0$.

as $r \to 0$. Thus choosing a value of Q_m, r, where eq.(3.33) is met and going to smaller values of r, eq.(3.33) will continue to hold and therefore the effects of the magnetic field will continue to be small [9]. In this range of parameters then the low temperature behavior of the system and its low frequency response will be unchanged from the purely electric case. Also the entanglement entropy in the boundary theory of a region of sufficient large volume will be unchanged and be given as we shall see in section 3.5 by eq.(3.81).

3.3.2 Case II. $|\alpha| > \delta$

In this case the magnetic perturbation is relevant in the infrared and in the deep infrared the solution approaches an attractor of the extremal RN type. The dilaton is drawn to a fixed and finite value ϕ_0 and does not run-away and the near-horizon geometry is $AdS_2 \times R^2$ with the metric components eq.(3.5), being

$$b = b_0 \tag{3.38}$$

$$a^2 = \frac{r^2}{R_2^2}, \tag{3.39}$$

where b_0, R_2^2 are constants with R_2 being the radius of AdS_2.. Note that in this attractor region of the spacetime the effects of the electric and magnetic fields are comparable.

To establish this result we first show that eq.(3.8), eq.(3.9), eq.(3.10) and eq.(3.11) allow for such an attractor solution. Next, starting with this attractor solution we identify appropriate perturbations and establish numerically that the solution flows to the electric scaling solution in the UV.

It is easy to check that the equations of motion allow for a solution of the type described above. Eq.(3.10) and eq.(3.11) are met with ϕ being constant and b being constant as long as the conditions $V_{eff} = \partial_\phi V_{eff} = 0$ are met. This gives rise to the conditions

$$e^{-2\alpha\phi_0} Q_e^2 + e^{2\alpha\phi_0} Q_m^2 = \frac{b_0^4 |V_0|}{2} e^{2\delta\phi_0} \tag{3.40}$$

$$-e^{-2\alpha\phi_0} Q_e^2 + e^{2\alpha\phi_0} Q_m^2 = \left(\frac{\delta}{\alpha}\right) \frac{b_0^4 |V_0|}{2} e^{2\delta\phi_0} \tag{3.41}$$

which determine ϕ_0, b_0. Eliminating b_0 between the two equations gives

$$e^{4\alpha\phi_0} = \frac{Q_e^2}{Q_m^2} \frac{1 + \frac{\delta}{\alpha}}{1 - \frac{\delta}{\alpha}} \tag{3.42}$$

The LHS must be positive, this gives a constraint $|\frac{\delta}{\alpha}| < 1$ which is indeed true for Case II.

[9] On the other hand the magnetic field gets increasingly more important at large r, *i.e.*, in the UV. However from numerical solutions one sees that for a suitable $V(\phi)$, when $Q_m^{/}\mu^2 \ll 1$ its effects continue to be small all the way upto the asymptotic AdS region.

Substituting eq.(3.42) in eq.(3.40) next determines b_0 in terms of ϕ_0 to be

$$b_0^4 = \frac{4Q_e^2 e^{-2\phi_0(\alpha+\delta)}}{|V_0|\left(1-\frac{\delta}{\alpha}\right)}. \tag{3.43}$$

Of the remaining equations eq.(3.9) is trivially satisfied while eq.(3.8) determines R_2 to be

$$R_2^2 = \frac{1}{|V_0|}(|\frac{\alpha-\delta}{\alpha+\delta}|)^{\frac{\delta}{2\alpha}}(\frac{Q_m^2}{Q_e^2})^{\frac{\delta}{2\alpha}}. \tag{3.44}$$

We see that for $\alpha > 0$, $R_2 \to 0$ as $Q_m \to 0$, making the AdS_2 highly curved, while for $\alpha < 0$, $R_2 \to \infty$ as $Q_m \to 0$.

Appendix B.1 contains some discussion of the two perturbations in this $AdS_2 \times R^2$ solution which grow in the UV. Starting with an appropriate choice of these two perturbations we find that the solution flows to the electric scaling solution in the UV. This can be seen in Fig.(B.2) and (B.3). For an appropriate choice of potential going out even further in the UV one finds that the solution becomes asymptotically AdS_4, as shown in Fig.(B.5) and (B.6).

The $AdS_2 \times R^2$ near-horizon geometry changes the IR behavior of the system completely. As discussed in the introduction there is now an extensive thermodynamic entropy and the entanglement entropy also scales like the volume, for large enough volume. For additional discussion of the thermodynamics see section 3.4 .

3.3.3 Case III. $0 < \alpha < \delta$

In this case also we will see that the magnetic perturbation is relevant in the IR. Our analysis for what the end point is in the IR will not be complete, however.

We do identify a candidate "run-away" attractor as the IR end point of the system. In this attractor solution the magnetic field dominates and the effects of the electric field are negligible in comparison. As a result a solution taking the hyperscaling violating form eq.(3.12), for an appropriate choice of exponents, exists. We will refer to this solution as the magnetic scaling solution below. Unfortunately, we have not been able to satisfactorily establish that starting with the electric solution of interest one does indeed end in this magnetic scaling solution in the IR. This requires additional numerical work.

To see that the magnetic perturbation is relevant in the IR note that $\alpha k < 0$ in this region so that eventually, for small enough values of r, condition eq.(3.35) will no longer hold and the effects of the magnetic field will become significant.

To identify the candidate run-away attractor let us begin by noting that the effective potential eq.(3.7) and thus the equations of motion are invariant under the transformation, $Q_m \leftrightarrow Q_e$ accompanied by $\alpha \to -\alpha$ with the other parameters staying the same. Under this transformation the region discussed in Case I maps to the region $0 < \alpha < \delta$. The discussion for Case I above then shows that, with Q_m present, in this region of parameter space there is a consistent solution where the effects of the electric charge in the deep IR can be neglected. The solution takes the form, eq.(3.12) and eq.(3.13), eq.(3.14), with $Q_e \to Q_m$ and $\alpha \to -\alpha$. This is the magnetic scaling solution referred to above. Actually, this solution exists only if $(-\alpha, \delta)$ meet the conditions eq.(3.15)-eq.(3.18). In Fig.(3.1) the region for Case III where all the conditions eq.(3.15)-eq.(3.18) are met is shown in green. It is easy to see that for any point in this allowed green region the corresponding point $(-\alpha, \delta)$ automatically lies in the allowed blue region.

Assuming that we have identified the correct IR end point we see that the thermodynamic entropy at extremality continues to vanish once the magnetic perturbation is added. It is also easy to see that the entanglement entropy is of the form eq.(3.81).

A more complete analysis of the system in this region of (α, δ) parameter space is left for the future.

3.3.4 Additional Comments

We end this section with some comments. It is sometimes useful to think of the solutions we have been discussing as being embedded in a more complete one which asymptotes to AdS space in the UV. The dual field theory then lives on the boundary of AdS space and standard rules of AdS/CFT can be used to understand its behavior. We take this theory to have one scale, μ, as discussed in section 3.2. In addition the magnetic field is also turned on with $Q_m/\mu^2 \ll 1$. The full metric for this solution will be of the form eq.(3.5) and in the UV will become AdS space [10] :

$$ds^2 = -r^2 dt^2 + \frac{1}{r^2} dr^2 + r^2(dx^2 + dy^2) \tag{3.45}$$

Starting with this geometry for $r \to \infty$ it will approach the electric scaling solution when $r \lesssim \mu$.

The magnetic field becomes a significant effect when its contribution to the effective potential eq.(3.7) is roughly comparable to the electric field. This gives a condition for the dilaton

$$e^{-4\alpha\phi} \sim \frac{Q_m^2}{Q_e^2} \tag{3.46}$$

Using eq.(3.13) this happens at a radial location $r \sim r_*$ where

$$r_* \sim \mu \left(\frac{Q_m^2}{Q_e^2} \right)^{\frac{-1}{4\alpha k}} \tag{3.47}$$

Here we have introduced the parameter μ which was set equal to unity in eq.(3.12), eq.(3.13), eq.(3.14). For Case II and III where the magnetic perturbation is relevant in the IR, $\alpha k < 0$,

[10] We have set $R_{AdS} = 1$.

and the magnetic field continues to be important for all $r < r_*$. In Case II for $r \ll r_*$ the solution becomes $AdS_2 \times R^2$. In Case III we have not identified the IR endpoint with certainty when $r \ll r_*$. For Case I the magnetic perturbation is irrelevant in the IR.

Second, Fig.(3.2) shows a plot of various regions in the (δ, α) plane, with $\delta > 0$. Region C corresponds to Case I. Regions A, D and E correspond to Case II. And region B corresponds to Case III. The line $\alpha = -3\delta$ which is of special interest is the thick black line separating regions E and D. These regions are also described in terms of the parameters β, γ, eq.(3.13), eq.(3.14) in Table (3.1). The corresponding values of the parameters (θ, z) can be obtained from eq.(3.30).

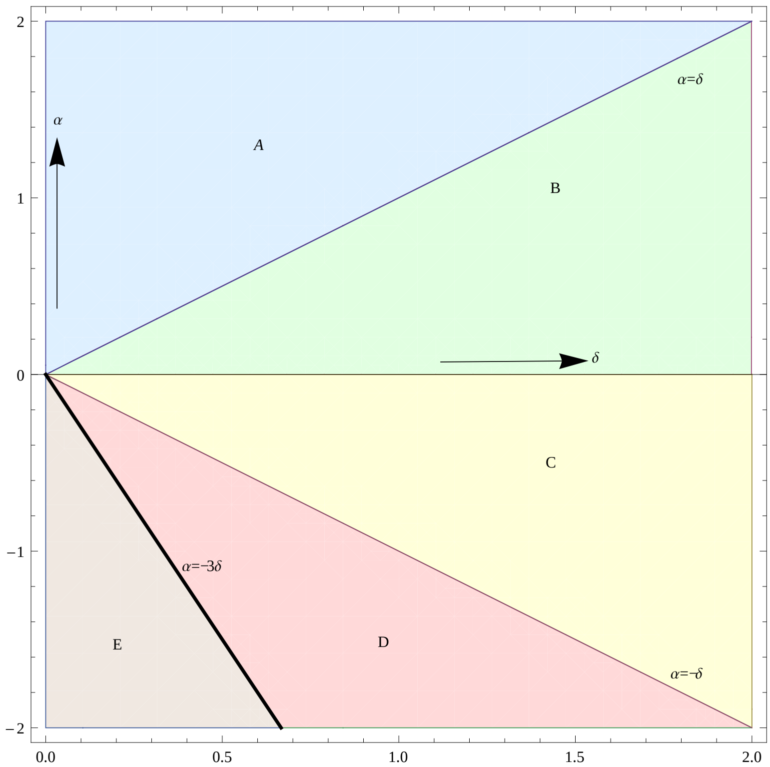

Figure 3.2: Figure showing various region in (δ, α) space. Details of these regions can be found in Table (1)

Region	δ,α	$\beta,\ \gamma$
A	$\alpha > \delta$	$1+\beta > \gamma > 1-\beta$
B	$0 < \alpha < \delta$	$\gamma < 1-\beta$
C	$0 > \alpha > -\delta$	$\gamma < 1-\beta$
D	$-3\delta < \alpha < -\delta$	$\gamma > 1+\beta$
E	$\alpha < -3\delta$	$1+\beta > \gamma > 1-\beta$

Table 3.1: Various Regions in (δ, α) space

3.4 A Detailed Discussion of Thermodynamics

In this section we will discuss the thermodynamic behavior in the presence of the magnetic field in some more detail. The introduction of a small magnetic field in the dilaton system can have a significant effect on the IR behavior as we have already discussed. Here we will study some additional aspects of the resulting thermodynamics.

In our system the role of the Fermi energy is played by the chemical potential μ. Let us start with the purely electric theory first at a small temperature T

$$T/\mu \ll 1 \tag{3.48}$$

As discussed in [59], [61] the entropy density $s = S/V$ goes like

$$s \sim N^2 T^{\frac{2\beta}{2\gamma-1}}. \tag{3.49}$$

Under the scaling symmetry equations, (3.21), (3.22), (3.23), s has dimensions of $L^{\theta-2}$, where θ is defined in eq.(3.30) and L transforms in the same way as the (x, y) coordinates do in eq.(3.23). Thus θ is the exponent related to hyperscaling violation.

Now we can consider introducing a small magnetic field Q_m. Since the stress energy of the electromagnetic field is quadratic in Q_m^2 this should result in a correction to the entropy which is of order Q_m^2. The scaling symmetry eq.(3.22), eq.(3.23) then fixes the resulting temperature dependence of this correction so that s is given by

$$s \sim N^2\mu^2 \left(\frac{T}{\mu}\right)^{\frac{2\beta}{2\gamma-1}} \left(1 + s_1 \left(\frac{Q_m}{\mu^2}\right)^2 \left(\frac{T}{\mu}\right)^{\frac{4\alpha k}{2\gamma-1}}\right) \tag{3.50}$$

where k is defined in eq.(3.12), eq.(3.13) and s_1 is a μ independent constant. We see that the magnetic field can be regarded as a small perturbation only for temperatures meeting the condition

$$\left(\frac{Q_m}{\mu^2}\right)^2 \left(\frac{T}{\mu}\right)^{\frac{4\alpha k}{2\gamma-1}} \ll 1 \tag{3.51}$$

We have numerically verified that the coefficient s_1 indeed does not vanish for generic values of (α, δ).

The condition eq.(3.51) is in agreement with the discussion of section section 3.2 where we found that the magnetic field is irrelevant or relevant in the IR depending on the sign of αk. Since $2\gamma - 1 > 0$, eq.(3.19), we see from eq.(3.50) that when $\alpha k > 0$ the effects of the magnetic field on the entropy vanish as $T \to 0$. On the other hand when $\alpha k < 0$ these effects grow as $T \to 0$.

3.4.1 More on Case II.

One region of the parameter space where $\alpha k < 0$ corresponds to Case II. As discussed in section 3.2 in this case the resulting geometry for $T = 0$ in the deep IR is of the extreme RN type and the entropy at extremality does not vanish. From eq.(3.43) this entropy is given by

$$S = s_0 V N^2 \mu^2 \left(\frac{Q_m}{\mu^2}\right)^{\frac{\alpha+\delta}{2\alpha}} \tag{3.52}$$

where s_0 is a dimensionless constant, V is the volume and we have used eq.(3.31). The remaining region of parameter space where $\alpha k < 0$ corresponds to Case III. For this case as discussed in section 3.2 our analysis is not complete. If the IR in the gravity theory is an attractor of the magnetic scaling type described in 3.3.3 then the entropy vanishes at extremality.

It is also worth commenting on the behavior of some of the other thermodynamic variables for Case II. We start with the case where both Q_m, T vanish, then first introduce a small $Q_m/\mu^2 \ll 1$ and finally a small temperature. The temperature we consider meets the condition $T/\mu \ll 1$. In fact it is taken small enough to meet the more stringent condition

$$\frac{Q_m^2}{\mu^4} \gg \left(\frac{T}{\mu}\right)^{\frac{-4\alpha k}{2\gamma-1}} \tag{3.53}$$

so that eq.(3.51) does not hold and the near horizon geometry is that of a near- extremal RN black brane at a small non-zero temperature.

The discussion of thermodynamics is conceptually simplest if we think of the gravity solution being asymptotic in the deep UV to AdS space with a possible non-normalisable mode for the dilaton turned on, as was discussed in 3.2.1. In the absence of a magnetic field the dual field theory is a relativistic theory with the coupling constant dual to the dilaton being turned on and thus scale invariance being broken. The energy density ρ and pressure P for such a system at zero temperature are given by

$$\rho = c_1 N^2 \mu^3 + \rho_0 \tag{3.54}$$

$$P = \frac{c_1}{2} N^2 \mu^3 - \rho_0 \tag{3.55}$$

where the ρ_0 term arises due to the cosmological constant induced by to the breaking of scale invariance when the non-normalisable mode of the dilaton is turned on.

On introducing a small magnetic field the geometry changes for Case II significantly in the deep IR. However one expects that the resulting change in ρ, p, which are determined by the normalisable mode of gravity at the boundary, is small. Since the stress-energy in the bulk changes at quadratic order in Q_m, as was discussed above, this correction should be of order Q_m^2. Thus the pressure, working still at zero temperature, would become

$$P = \frac{c_1}{2} N^2 \mu^3 - \rho_0 + a_1 N^2 \frac{Q_m^2}{\mu} \tag{3.56}$$

where a_1 is a dimensionless constant. The resulting magnetization can be obtained using the thermodynamic relation

$$SdT + Nd\mu - VdP + MdQ_m = 0. \tag{3.57}$$

Keeping $T = 0$ and μ fixed gives

$$\frac{M}{V} = \frac{dP}{dQ_m} = 2a_1 N^2 \frac{Q_m}{\mu} \tag{3.58}$$

We expect this magnetization to be diamagnetic.

Introducing a small temperature next will result in a temperature dependence in the pressure and the magnetization. The change in the pressure keeping μ, Q_m fixed and increasing T slightly is given from eq.(3.57) by

$$\Delta P = \int sdT = s_0 N^2 \mu^2 \left(\frac{Q_m}{\mu^2}\right)^{\frac{\alpha+\delta}{2\alpha}} T \tag{3.59}$$

where we have used eq.(3.52). Adding this to eq.(3.56) gives the total pressure to be

$$P = \frac{c_1}{2} N^2 \mu^3 - \rho_0 + a_1 N^2 \frac{Q_m^2}{\mu} + s_0 N^2 \mu^2 \left(\frac{Q_m}{\mu^2}\right)^{\frac{\alpha+\delta}{2\alpha}} T \tag{3.60}$$

The resulting magnetization also acquires a linear dependence on temperature

$$\frac{M}{V} = 2a_1 N^2 \frac{Q_m}{\mu} + s_o N^2 \left(\frac{\alpha+\delta}{2\alpha}\right) T \left(\frac{Q_m}{\mu^2}\right)^{\frac{\delta-\alpha}{2\alpha}} \tag{3.61}$$

Notice that in Case II $|\alpha| > \delta$ and therefore the exponent $\frac{\delta-\alpha}{2\alpha}$ in the second term on the RHS is negative. Since $Q_m/\mu^2 \ll 1$ this means that the coefficient of the term linear in T in the magnetization is enhanced. As a result at a small temperature of order

$$\frac{T}{\mu} \sim \left(\frac{Q_m}{\mu^2}\right)^{\frac{3\alpha-\delta}{2\alpha}} \tag{3.62}$$

this term will become comparable to the zero temperature contribution.

A case of particular interest is when $\alpha = -3\delta$. This corresponds to $\theta = 1$, eq.(3.30), and gives rise to the logarithmic enhancement of entropy eq.(3.1). The pressure and magnetization etc can be obtained for this case by substituting this relation between α, δ in the the equations above.

Let us end this section some comments. It is important to note that after turning on the magnetic field the state is still compressible. The compressibility is defined by $\kappa = -\frac{1}{V}\frac{\partial V}{\partial P}|_{TQ_mN}$ and can be related to the change in charge or number density n as μ is changed,

$$\kappa = \frac{1}{n^2}(\frac{\partial n}{\partial \mu})|_{TQ_m} \tag{3.63}$$

From eq.(3.57) and eq.(3.60) we see that

$$n = \frac{\partial P}{\partial \mu}|_{TQ_m} = \frac{3}{2}c_1 N^2 \mu^2 + \cdots \tag{3.64}$$

where the first term on the RHS arises from the first term in P in eq.(3.60) and the ellipses denote corrections which are small. Thus the charge density is only slightly corrected by the addition of Q_m and therefore the state remains compressible. Our discussion above for the magnetization etc has been for Case II. The analysis in case I where the magnetic field is irrelevant in the IR is straightforward. For Case III we do not have a complete analysis of what happens in the gravity theory in the deep IR. A candidate attractor was identified in section 3.3, if this attractor is indeed the IR end point then starting from it the resulting thermodynamics can be worked out at small Q_m, T along the lines above.

3.5 Entanglement Entropy and the Effect of Magnetic Field

As was mentioned in the introduction, entanglement entropy is an interesting property of any quantum system characterizing the correlation between the degrees of freedom of the system. It has several interesting applications. For example in condensed matter systems, *e.g.* quantum spin chains, entanglement entropy is a diagnostic characterize quantum critical points and is believed to serve as a order parameter for quantum phase transition whereas in quantum information theory it appears as a computational resource.

In quantum field theory consider a pure quantum state described by the wave function $|\psi\rangle$ and the Hilbert space of the whole quantum system is divided into two parts, say A and B. The density matrix corresponding to the total system is obtained as $\rho_{tot} = |\psi\rangle\langle\psi|$. The reduced density matrix for the subsystem A is $\rho_A = Tr_B(\rho_{tot})$, which can be obtained as one traces out the subsystem B. The entanglement entropy is simply the von Neumann entropy associated with this reduced density matrix ρ_A for the subsystem A.

$$S_A = -Tr_A\left(\rho_A \log \rho_A\right) \tag{3.65}$$

Analytic computation of entanglement entropy in general quantum field theories for arbitrary dimensions is notoriously complicated. For lower dimensional theories and in special situations like conformal field theories there are several known methods to compute it. In an interesting development using holographic techniques a general prescription for calculating entanglement entropy for field theories admitting dual gravity description has been proposed, see [92] and [93]. Following the prescription, consider a circular region, **R**, in the dual field theory such that it's boundary, $\partial\mathbf{R}$, is a circle of radius L. To compute the entanglement entropy of **R** we work on a fixed constant time slice and find the surface in the bulk which has minimum area subject to the condition that it terminates in $\partial\mathbf{R}$ at the boundary of AdS. The entanglement entropy is then computed as

$$S_{EE} = \frac{A_{min}}{4G_N}, \tag{3.66}$$

where A_{min} is the area of this surface in the bulk and G_N is the Newton's constant, see Fig.3.3 The entanglement entropy for the hyperscaling violating metrics we have been

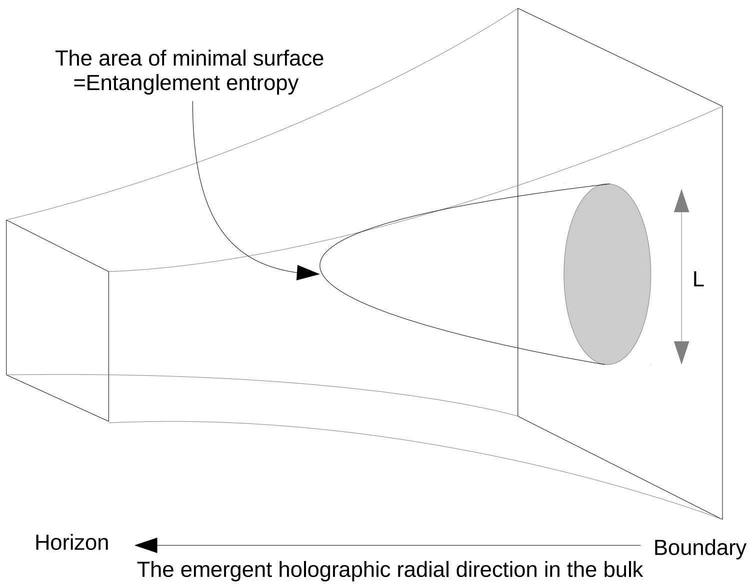

Figure 3.3: Holographic entanglement entropy.

considering has already been worked out in [63], see also [64]. Knowing these results, the behavior of the entanglement entropy for our system of interest, in the presence of a small magnetic field, can be easily deduced.

To keep the discussion self contained we first review the calculation of the entanglement entropy for hyperscaling violating metrics and then turn to the system of interest.

3.5.1 Entanglement Entropy in Hyperscaling Violating Metrics

We will be considering a metric of the form

$$ds^2 = -r^{2\gamma}dt^2 + \frac{dr^2}{r^{2\gamma}} + r^{2\beta}(dx^2 + dy^2) \tag{3.67}$$

(this is the same form as eq.(3.12) except that we have dropped the constant C_a^2 by appropriately scaling the metric). In the discussion below it will be useful to think of this metric as arising in the IR starting with an AdS metric in the UV. This could happen for an appropriately chosen potential as was discussed in section 3.2, [61]. The field theory of interest then lives on the boundary of AdS space. We will again restrict ourselves to a circular region **R** in the field theory of radius L. We will work in a coordinate system of the form eq.(3.5) which as $r \to 0$ becomes eq.(3.67) and as $r \to \infty$ becomes AdS space

$$ds^2 = r^2(-dt^2) + \frac{dr^2}{r^2} + r^2(dx^2 + dy^2). \tag{3.68}$$

Replacing (x, y) by (ξ, θ) the metric eq.(3.5) can be rewritten as

$$ds^2 = -a^2dt^2 + \frac{dr^2}{a^2} + b^2(d\xi^2 + \xi^2 d\theta^2). \tag{3.69}$$

We expect the minimum area bulk surface to maintain the circular symmetry of the boundary circle. Such a circularly symmetric surface has area

$$A_{bulk} = 2\pi \int \sqrt{b^2\left(\frac{d\xi}{dr}\right)^2 + \frac{1}{a^2}}\, \xi(r)b(r)dr \tag{3.70}$$

where $\xi(r)$ is the radius of the circle which varies with r. To obtain A_{min} we need to minimize A_{bulk} subject to the condition that as $r \to \infty$, $\xi \to L$. The resulting equation for $\xi(r)$ is

$$\frac{d}{dr}\left(\frac{b^3\xi\frac{d\xi}{dr}}{\sqrt{b^2(\frac{d\xi}{dr})^2 + \frac{1}{a^2}}}\right) - \sqrt{b^2\left(\frac{d\xi}{dr}\right)^2 + \frac{1}{a^2}}\, b = 0. \tag{3.71}$$

Let us note that the circle on the boundary of **R** has area[11]

$$A = 2\pi L \tag{3.72}$$

It is easy to see that as $r \to \infty$ the $b^2(\frac{d\xi}{dr})^2$ term in the square root in eq.(3.70) cannot dominate over the $\frac{1}{a^2}$ term. The contribution to A_{bulk} from the $r \to \infty$ region can then be estimated easily to give

$$\delta_1 A_{bulk} = A r_{max} \tag{3.73}$$

[11] As mentioned earlier we will persist in calling this the area although it is of course the perimeter.

where r_{max} is the IR cutoff in the bulk which should be identified with a UV cutoff in the boundary. This is the expected universal contribution to entanglement which arises from very short distance modes entangled across the boundary of **R**.

Now one would expect that as L is increased the bulk surface penetrates deeper into the IR eventually entering the scaling region eq.(3.67). For large enough L one expects that the radial variable ξ stays approximately constant in the UV and undertakes most of its excursion from L to 0 in this scaling region. We will make these assumption here and proceed. These assumptions can be verified numerically for the interesting range of parameters and we will comment on this further below.

With these assumptions the contribution from the scaling region for the minimal area surface $\delta_2 A_{bulk}$ can be estimated by a simple scaling argument. We can neglect the change in ξ before the surface enters the scaling region and take its value at the boundary of the scaling region[12] which we denote as ξ_0 to be L. Under the scaling symmetry eq.(3.21)-eq.(3.23), which takes

$$r \to \lambda r, \xi \to \lambda^{1-\beta-\gamma}\xi, \tag{3.74}$$

we see from eq.(3.70) that

$$\delta_2 A_{bulk} \to \lambda^{2(1-\gamma)}\delta_2 A_{bulk} \tag{3.75}$$

Now by choosing λ in eq.(3.74) to be

$$\lambda = L^{\frac{1}{\gamma+\beta-1}} \tag{3.76}$$

we can set the rescaled value for ξ_0 to be unity. In terms of the rescaled variable the minimization problem has no scale left and $\delta_2 A_{bulk}$ must be order unity. This tells us that when $\xi_0 = L$

$$\delta_2 A_{bulk} \sim L L^{\frac{\gamma-\beta-1}{\gamma+\beta-1}}. \tag{3.77}$$

Note also that with ξ_0 set equal to unity the surface would reach a minimum value at a radial value of r_{min} which is of order unity. Thus before the rescaling

$$r_{min} \sim \lambda = L^{-(\frac{1}{\beta+\gamma-1})}. \tag{3.78}$$

Now we are ready to consider different regions in the (γ, β) parameter space. From eq.(3.13) we see that $\beta > 0$ and from eq.(3.19) that $\gamma > 1/2$.

- $\gamma > 1 + \beta$: In this case we see from eq.(3.77) and (3.73) that $\delta_2 A_{bulk} > \delta_1 A_{bulk}$ for sufficiently big L and fixed UV cutoff r_0. Thus the dominant contribution to the area

[12] By the boundary of the scaling region we mean the region where the metric begins to significantly depart from eq.(3.67). This happens as we go to larger values of r; for even larger values the metric becomes AdS space.

for sufficiently big L comes the scaling region. The entanglement is then given by

$$S_{EE} \sim N^2 (L\mu)(L\mu)^{\frac{\gamma-\beta-1}{\gamma+\beta-1}} \tag{3.79}$$

with an additional term proportional to L in units of the UV cutoff r_0. In eq.(3.79) we have introduced the scale μ to make up the dimensions. We remind the reader that this scale stands for the chemical potential which is the only length scale in the boundary theory. We see from eq.(3.79) that the entanglement grows with L with a power faster than unity. Also notice that from eq.(3.78) r_{min} decreases with increasing L in accord with our expectation that the surface penetrates further into the scaling region as L is increased.

- A special case of importance is when $1+\beta=\gamma$. Here the term $(L\mu)^{\frac{\gamma-\beta-1}{\gamma+\beta-1}}$ is replaced by a log, [63], resulting in eq.(3.79) being replaced by

$$S_{EE} \sim N^2 (L\mu)\log(L\mu) \tag{3.80}$$

- $1+\beta > \gamma > 1-\beta$: In this case we see from eq.(3.77) and eq.(3.73) that the contribution $\delta_2 A_{bulk}$ grows with L with a power less than unity and therefore the contribution made by the scaling region to the total area is less significant than $\delta_1 A$ which is linear in [13]L. In this region of parameter space the entanglement entropy is therefore dominated by the short distance contributions and given by

$$S_{EE} \sim N^2 \frac{L}{a} \tag{3.81}$$

where $a = \frac{1}{r_{max}}$ is an UV cutoff in the system.

- $\gamma < 1-\beta$: In this case r_{min} does not decreases with increasing L, actually the surface stops entering the scaling region and our considerations based on the scaling symmetry are not relevant. The entanglement entropy is again given by eq.(3.81).

One can calculate the minimal area surface numerically for cases when $\gamma > 1+\beta$ and also $1+\beta > \gamma > 1-\beta$. This gives agreement with the above discussion including the scaling behavior for r_{min} eq.(3.78) in these regions of parameter space.

Let us make some more comments now. In the case where the near horizon geometry is of extreme RN type, *i.e.*, $AdS_2 \times R^2$ we have $\beta=0, \gamma=1$. This case needs to be dealt with separately. Here the entanglement entropy scales like the volume and equals the Beckenstein-Hawking entropy of the corresponding region in the boundary theory.

$$S_{EE} \sim N^2 (L\mu)^2 \tag{3.82}$$

[13] We should note that the scaling argument tells us that r_{min} does decrease with increasing L, eq.(3.78), so that the surface does get further into the scaling region as L increases.

The discussion in section 3.2 was in terms of the parameters (α, δ) while here we have used (β, γ). The relation between these parameters is obtained from eq.(3.14) and summarized in Table 1. We see that $\gamma > 1+\beta$ corresponds to Region D. The line $\gamma = 1+\beta$ corresponds to $\alpha = -3\delta$ at the interface between D and E. The condition $1+\beta > \gamma > 1-\beta$ corresponds to A and E and finally $\gamma < 1-\beta$ to B and C.

3.5.2 Entanglement with a Small Magnetic Field

We are now ready to consider the effects of a small magnetic field. The behavior of the gravity solutions was discussed in section 3.2 where it was shown that the analysis breaks up into various cases. In all cases we will take the solution to approach AdS space in the UV. The resulting behavior of the solution was discussed for the various cases in subsection 3.3.4. For $r \gg \mu$ the solution is AdS space while for $r_* \ll r \ll \mu$ it is of electric scaling type (r_* is defined in eq.(3.47)). What happens for $r \ll r_*$ depends on the various cases.

- Case II. $|\alpha| > \delta$: In this case the geometry for $r \ll r_*$ is $AdS_2 \times R^2$. Let us start with a boundary circle of very small radius and slowly increase its size. When the radius $L\mu \ll 1$ the entanglement entropy is given by eq.(3.81). When $L\mu \sim 1$ the surface begins to penetrate the electric scaling region and as L increases we see from eq.(3.78) that r_{min} decreases. When r_{min} reaches r_* the surface begins to enter the region where the magnetic field has an appreciable effect on the geometry. Using eq.(3.78) this corresponds to

$$L \sim L_* = \frac{1}{\mu}\left(\frac{Q_e^2}{Q_m^2}\right)^{-\frac{1}{(4\alpha k)(\beta+\gamma-1)}}. \tag{3.83}$$

  For

$$L_* \gg L \gg \frac{1}{\mu} \tag{3.84}$$

  the entanglement entropy is given by the calculation in the electric solution. Thus for $-3\delta < \alpha < -\delta$ it grows faster than L with an additional fractional power while for $\alpha = -3\delta$ it is logarithmically enhanced. For other values of (α, δ) which lie in this region the entanglement entropy is proportional to L and is dominated by the UV contribution.

  Finally, when $L \gg L_*$ the surface enters into the near-horizon $AdS_2 \times R^2$ geometry. Now the entanglement entropy grows like L^2 and is given by

$$S \sim L^2 N^2 \mu^2 \left(\frac{Q_m}{\mu^2}\right)^{\frac{\alpha+\delta}{2\alpha}} \tag{3.85}$$

  This is an expression analogous to the Beckenstein-Hawking entropy, eq.(3.52), but with L^2 now being the volume of the region of interest. For the case of special interest,

$\alpha = -3\delta$, this becomes

$$S \sim L^2 N^2 \mu^2 \left(\frac{Q_m}{\mu^2}\right)^{\frac{1}{3}}. \tag{3.86}$$

- Case III. $0 < \alpha < \delta$: In this case the magnetic field is important at small r. For $L_* \gg L \gg \frac{1}{\mu}$ the entanglement is given by the electric theory, it goes like eq.(3.81) and arises dominantly due to short distance correlations. The geometry in the deep IR could be the magnetic scaling solution discussed in subsection 3.3.3. If this is correct for $L \gg L_*$ the entanglement will continue to go like eq.(3.81).

- Case I. $-\delta < \alpha < 0$: In this case the magnetic field is not important in the IR and the the entanglement entropy is given by eq.(3.81) both when $L < \frac{1}{\mu}$ and $L > \frac{1}{\mu}$.

3.6 Discussion

In the work presented in this chapter we have studied a system of gravity coupled to an Abelian gauge field and a dilaton. This system is of interest from the point of view of studying fermionic matter at non-zero charge density. Firstly we will summarize some of our key results. We find that in the dilaton system even a small magnetic field can have an important effect at long distances since the magnetic field can become relevant in the Infra-red (IR). The resulting thermodynamic and entanglement entropy can then change significantly. In particular this happens for the whole range of parameters where the entanglement entropy is of the form eq.(3.1).

More specifically, the EMD system we analyze is characterized by two parameters (α, δ) which are defined in [14] eq.(3.3), eq.(3.4). When $|\alpha| > |\delta|$ we show that the magnetic field is relevant in the IR and the geometry in the deep infra-red (small values of the radial coordinate r we use) flows to an $AdS_2 \times R^2$ attractor. As a result the system acquires a non-zero extensive entropy even at zero temperature. The entanglement entropy also changes and grows like the volume of the region of interest [15] (for large enough volume). In particular, this happens for the values $\alpha = -3\delta$ where the purely electric theory gives rise to an entanglement of the form eq.(3.1).

We also analyze the thermodynamics and some transport properties of the resulting state. The system continues to be compressible in the presence of a magnetic field and its specific heat is linear at small temperatures. Both these facts indicate the presence of gapless excitations. In general the system has a magnetization which is linear in the magnetic field and which is expected to be diamagnetic. The $AdS_2 \times R^2$ attractor leads to the magnetization having a temperature dependence, at small T, which can become important

[14] The relation of (α, δ) to the parameters (θ, z) now more conventionally used in the literature is given in eq.(3.30). In particular $\alpha = -3\delta$ corresponds to $\theta = d - 1 = 1$.

[15] A potential confusion with our terminology arises because we are in two dimensions. Thus the volume of the region of interest is actually its area and the area of the boundary of this region is the perimeter.

even for small magnetic fields, eq.(3.62).

The summary is that for parameters where the electric theory has an entanglement of the form eq.(3.1), suggesting that it is a non-Landau Fermi liquid, the magnetic field is a relevant perturbation in the IR. As a result even a small magnetic field has a significant effect on the state of the system at long distances. The state continues to be compressible, with a linear specific heat, but the thermodynamic entropy at zero temperature is now extensive and the entanglement entropy scales like the volume of the region of interest, this behavior also being linked to the extensive ground state entropy [16]. At intermediate length scales for which the relevant region of the geometry is still reasonably well approximated by the hyperscaling violating type metric and the effects of the magnetic field are small, the behavior of the system continues to be essentially what it was in the absence of the magnetic field. In particular the thermodynamics is essentially unaffected by the magnetic field and the entanglement entropy also stays unchanged. Similar results for the existence of an $AdS_2 \times R^2$ attractor and associated changes in thermodynamic and entanglement entropy etc are true in the whole region where $|\alpha| > |\delta|$.

The behavior mentioned above is roughly analogous to what happens in a weakly coupled system with a Fermi surface. While in this case the introduction of a small magnetic field leads to the formation of Landau levels, at intermediate energies still low compared to the Fermi energy but big compared to the spacing of the Landau levels, and correspondingly at intermediate length scales smaller than the magnetic length, the behavior continues to be essentially that of a system with a Fermi surface. In particular the thermodynamics is essentially unchanged by the small magnetic field and the entanglement entropy is also expected to have the $A\log(A)$ behavior at these length scales. Going to much lower energies of order the spacing between the Landau level and correspondingly to distance scales of order or longer the magnetic length though the behavior of the system can change. For example in the free fermion theory, depending on the fermion density, a Landau level can be fully or partially filled, and partial filling would result in an extensive ground state entropy.

In other regions of parameter space where $|\alpha| < |\delta|$ the magnetic perturbation is either not relevant in the IR and thus essentially leaves the low-energy and large distance behavior of the system unchanged. Or it is relevant but we have not been able to completely establish the resulting geometry to which the system flows in the deep IR.

We end in this section with some concluding comments and future directions.

- For the case $|\alpha| > \delta$ (Case II in our terminology) we saw that the magnetic field is a relevant perturbation in the IR and the inclusion of a small magnetic field changes the behavior significantly making the zero temperature thermodynamic entropy extensive and the entanglement grow like the volume. In particular this happens along the line

[16] More generally from the fact that the magnetic field is a relevant perturbation in the IR we learn that the compressible state described by the purely electric solution "anti-screens" the effects of the magnetic field making them grow at larger distances.

$\alpha = -3\delta$ ($\theta = 1$, eq.(3.30)), where the electric theory has an entanglement entropy of the form eq.(3.1) suggesting the presence of a Fermi surface.

- It is well known that an extensive ground state entropy can arise in the presence of a magnetic field due to partially filled Landau levels. When this happens in a free fermionic theory the entropy scales like Q_m while, in contrast, for the dilaton system the dependence on the the magnetic field is typically more exotic, eq.(3.85). For example, with $\alpha = -3\delta$ the entropy goes like $Q_m^{1/3}$, eq(3.86). Such a non-trivial exponent suggests that the ground state is more interesting and strange.

- A notable feature about how the entanglement entropy behaves in all the cases we have studied is that it never decreases in the IR, *i.e.*, as one goes to regions of larger and larger size (L)in the boundary. For instance, consider the case where $-3\delta \leq \alpha < -\delta$. In this case for very small L is it given by eq.(3.81) and dominated by short distance correlations of the CFT. At intermediate values of L, meeting the condition eq.(3.84), it goes like eq.(3.79) and is enhanced compared to the L dependence by an additional fractional power of L or a $\log(L)$, eq.(3.80). Finally at very large values of L it grows like the volume L^2, eq.(3.82). We see that as L increases the entanglement increases monotonically [17] . In other cases while the detailed behavior is different this feature is still true. These observations are in agreement with [97] where a renormalized version of the entanglement entropy was defined and it was suggested that in $2+1$ dimensions this entropy would monotonically increase. It is easy to see that the behavior of the entanglement entropy we have found implies that the renormalized entanglement entropy of [97] is monotonic and increasing.

- In [61] the behavior of a probe fermion in the bulk in the electric hyperscaling violating geometry was discussed. This corresponds to calculating the two point function of a gauge invariant fermionic correlator in the boundary. It is notable that the region in parameter space where Fermi liquid behavior was found to occur for this correlator is exactly the region $|\alpha| > \delta$ for which we have found that the geometry flows to an $AdS_2 \times R^2$ endpoint in the IR [18]. It would be worth understanding this seeming coincidence more deeply. It is also worth mentioning that in [61] marginal Fermi liquid behavior was found when $|\alpha| = \delta$. This region lies at the boundary of the region $|\alpha| > \delta$ where an $AdS_2 \times R^2$ endpoint arise [19].

[17] Our scaling argument does not directly fix the sign of the entanglement entropy in eq.(3.79) and eq.(3.80). However it is clear that the sign must be positive since the corresponding contribution to the surface area is bigger than the contribution from the UV for fixed r_{max} as $L \to \infty$, and the total surface area must be positive.

[18] The remaining region $|\alpha| < \delta$ does not exhibit Fermi liquid behavior, this includes Case I of section 3.2 where the magnetic field is irrelevant and also Case III of section 3.2 where it is relevant but where we have not identified a definite IR end point to which the solution flows.

[19] In fact the nature of the attractor changes at this boundary. E.g. in the purely electric case when $\alpha = -\delta$ the dilaton is a flat direction of the attractor potential and not fixed to a unique value in the IR, similarly for $\alpha = \delta$ in the purely magnetic case.

- Our focus in this chapter was on taking an electrically charged system and including a small magnetic field. However, it is worth pointing out that the magnetic solutions with no electric field present ($Q_e = 0$) are also of considerable interest in their own right. These solutions can be obtained by taking

$$Q_e \to Q_m \tag{3.87}$$

  and $\alpha \to -\alpha$ in the solutions eq.(3.13), eq.(3.14). For a choice of parameters, which now meet the condition $\alpha = 3\delta$, the resulting entanglement entropy has the form eq.(3.1) which suggests the presence of a Fermi surface even though the charge density is now vanishing. It would be worth understanding the resulting state better in the field theory. The transformation eq.(3.87) is an electromagnetic duality transformation, and should act by exchanging charged particles with vortices in the field theory [98],[99]. These vortices perhaps form a Fermi surface resulting in the logarithmic enhancement of the entropy.

- We have not included an axion field in our analysis. Such a field is natural to include once the dilaton is present and it can have important consequences once the magnetic field is also turned on as was discussed in [83]. For example it was shown in [83] for the case $\delta = 0$ that in the presence of the axion the entropy at extremality continues to vanishes in the presence of a magnetic field. Once the axion is included we need to allow for the potential to also depend on it, this leads to considerable choice in the kinds of models one can construct. To remove some of this arbitrariness it would be worth including the axion within the context of models which arise in string theory or at least gauged supergravity.

- More generally, the time seems now ripe to systematically embed models of this type in string theory and supergravity. Some papers in this direction have already appeared [65], [100],[101],[102], [103],[104]. It would be worth understanding these constructions better and also gaining a better understanding of their dual field theory descriptions.

Chapter 4

Conformal Invariance and the Four Point Scalar Correlator in Slow-Roll Inflation

4.1 Introduction

The main theme of this thesis is to study different phases in a theory of gravity guided by symmetry principles to gain insights about other branches of physics. In the previous two chapters, we have considered applying our studies of gravity into different aspects of condensed matter systems. In this chapter, we continue our study of phases in gravity, constrained by symmetry principles, to learn about a different area of physics, namely Early Universe Cosmology.

As we have already discussed in the introduction, inflation is the most successful idea to address the shortcomings of the standard Big Bang cosmology. Apart from explaining the approximate homogeneity and isotropy of the early Universe, inflation also provides a mechanism for the production of perturbations which lead to a small breaking of these symmetries. The simplest model of inflation involves a scalar field, called the inflaton, with a potential which is positive and slowly varying during the inflationary era. The positive and approximately constant potential gives rise to a spacetime which is well described, upto small corrections, by four dimensional de Sitter space (dS_4). This spacetime is homogeneous and isotropic, in fact highly symmetric, with symmetry group $SO(4,1)$. Quantum effects, due to the rapid expansion of the Universe during inflation, give rise to small perturbations in this spacetime. These perturbations are of two types: tensor perturbations, or gravity waves, and scalar perturbations, which owe their origin to the presence of the inflaton.

Impressive advances in observational cosmology in recent years, such as the measurement of the cosmic microwave background, increasingly constrain some of the parameters which appear in the inflationary dynamics. This includes a determination of the amplitude of the two-point correlator for scalar perturbations, and more recently, a measurement of the tilt in this correlator and a bound on magnitude of the scalar three point function [105], [106]. In fact, observations are now able to rule out several models of inflation, see for *e.g.* [105].

A more detailed theoretical study of the higher point correlation functions for perturbations produced during inflation is generally motivated by these observational advancements. There are theoretical developments also which make this an opportune time to carry out such a study. Assuming that the $SO(4,1)$ symmetries of de Sitter space are shared by the full inflationary dynamics, including the scalar field, to good approximation, this symmetry group can be used to characterize and in some cases significantly constrain the correlation functions of perturbations produced during inflation. Although the idea of inflation is quite old, such a symmetry based analysis, which can sometimes lead to interesting model independent consequences, has received relatively little attention, until recently.

Another interesting aspect of the study of correlations between cosmological perturbations, carried out in this chapter, is worth mentioning. As we have mentioned earlier, the physics of inflationary cosmology is described by approximate dS_4 spacetime. Einstein gravity in the presence of a positive cosmological constant admits dS_4 as a unique solution, in contrast to the AdS_4 solution which requires a negative cosmological constant. Theoretical development coming from the recent intensive study of the AdS/CFT correspondence in string theory and gravity therefore generally raises the question: if the techniques of AdS/CFT correspondence can be helpful in dS_4 case as well. The reason behind such a hope being that four dimensional AdS space, AdS_4, is related, by analytic continuation to dS_4, and its symmetry group $SO(3,2)$ on continuation becomes the $SO(4,1)$ symmetry of dS_4. As we will see explicitly in this chapter, many of the techniques which have been developed to study correlators in AdS space can be adapted to the study of correlators in de Sitter space. It is well known that the $SO(3,2)$ symmetries of AdS_4 are also those of a $2+1$ dimensional conformal field theory. It then follows that the $SO(4,1)$ symmetries of dS_4 are the same as those of a 3 dimensional Euclidean Conformal Field Theory. This connection, between symmetries of dS_4 and a 3 dimensional CFT, is often a useful guide in organizing the discussion of de Sitter correlation functions. A deeper connection between de Sitter space and CFTs, analogous to the AdS/CFT correspondence, is much more tentative at the moment. We will therefore not assume that any such deeper connection exists in the discussion below. Instead, our analysis will only use the property that dS_4 and CFT_3 share the same symmetry group.

More specifically, in the work presented in this chapter, we will use some of more recent theoretical developments referred to above, to calculate the four point correlator for scalar perturbations produced during inflation. We will work in the simplest model of inflation mentioned above, consisting of a slowly varying scalar coupled to two-derivative gravity, which is often referred to as the slow-roll model of inflation. This model is characterized by three parameters, the Hubble constant during inflation, H, and the two slow-roll parameters, denoted by ϵ, η, which are a measure of the deviation from de Sitter invariance. These parameters are defined in eq.(4.3), eq.(4.4). In our calculation, which is already quite complicated, we will work to leading order in ϵ, η. In this limit the effects of the slow variation of the potential can be neglected and the calculation reduces to one in dS space. The tilt of the two-point scalar correlator, as measured for example by the Planck experiment, suggest that ϵ, η are of order a few percent, and thus that the deviations from de Sitter invariance are small, so that our approximation should be a good one.

In the slow-roll model of inflation we consider, one knows before hand, from straightforward estimates, that the magnitude of the four point scalar correlator is very small. The calculation we carry out is therefore not motivated by the hope of any immediate contact with observations. Rather, it is motivated by more theoretical considerations mentioned above, namely, to explore the connection with calculations in AdS space and investigate the role that conformal symmetry can play in constraining the inflationary correlators.

In fact, the calculation of the four point function in this model of inflation has already been carried out in [107], using the so called "in-in" or Schwinger-Keldysh formalism. Quite surprisingly, it turns out that the result obtained in [107] does not seem to satisfy the Ward identities of conformal invariance. This is a very puzzling feature of the result. It seemed to us that it was clearly important to understand this puzzle further since doing so would have implications for other correlation functions as well, and this in fact provided one of the main motivations for our work.

The result we obtain for the four point function using, as we mentioned above, techniques motivated by the AdS/CFT correspondence, agrees with that obtained in [107]. Since the final answer is quite complicated, this agreement between two calculations using quite different methods is a useful check on the literature.

But, more importantly, the insights from AdS/CFT also help us resolve the puzzle regarding conformal invariance mentioned above. In fact techniques motivated from AdS/CFT are well suited for the study of symmetry related questions in general, since these techniques naturally lead to the wave function of the Universe which is related to the partition function in the CFT.

We find that the wave function, calculated upto the required order for the four point function calculation, is indeed invariant under conformal transformations. However our calculation also reveals a subtlety, which is present in the de Sitter case and which does not have an analogue in the AdS case. This subtlety, which holds the key to the resolution, arises because one needs to proceed differently in calculating a correlation function from a wave function as opposed to the partition function (in the presence of sources). Given a wave function, as in the de Sitter case, one must carry out a further sum over all configurations weighting them with the square of the wave function, as per the standard rules of quantum mechanics, to obtain the correlation functions.

This sum also runs over possible values of the metric. This is a sign of the fact that the metric is itself a dynamical variable on the late-time surface on which we are evaluating the wave function. We emphasize that this is not in contradiction with the fact that the metric perturbation becomes time independent at late times. Rather, the point is that there is also a non-zero amplitude for this time-independent value to be non-trivial. In contrast, in the AdS case, where the boundary value of the metric (the non-normalizable mode) is a source, one does not carry out this further sum; instead correlation functions are calculated by taking derivatives with respect to the boundary metric.

From a calculational perspective, this further sum over all configurations in the de Sitter case requires a more complete fixing of gauge for the metric. This is not surprising since even defining local correlators in a theory without a fixed background metric requires a choice of gauge. This resulting gauge is not preserved in general by a conformal transformation. As a result, a conformal transformation must be accompanied by a suitable coordinate parameterization before it becomes a symmetry in the chosen gauge. Once this additional parameterization is included, we find that the four point function does indeed meet the resulting Ward identities of conformal invariance. We expect this to be true for other correlation functions as well.

There is another way to state the fact above. The correlation functions that are commonly computed in the AdS/CFT correspondence can be understood to be limits of bulk correlation functions, where only normalizable modes are turned on [108]. However, as emphasized in [109], the expectation values of de-Sitter perturbations that we are interested in cannot be obtained in this way as a limit of bulk correlation functions. As a result, they do not directly satisfy the Ward identities of conformal invariance, although a signature of this symmetry remains in the wave function of the Universe from which they originate.

The Ward identities of conformal invariance, once they have been appropriately understood, serve as a highly non-trivial test on the result especially when the correlation function is a complicated one, as in the case of the scalar four point function considered here. The AdS/CFT point of view also suggests other tests, including the flat-space limit where we check that the AdS correlator reduces to the flat space scattering amplitude of four scalars in the appropriate limit. In a third series of checks, we test the behavior of the correlator in suitable limits that are related to the operator product expansion in a conformal field theory. Our result meets all these checks.

Before proceeding let us discuss some of the other related literature on the subject. For a current review on the present status of inflation and future planned experiments, see [110]. Two reviews which discuss non-Gaussianity from the CMB and from large scale structure are, [111], and [112] respectively. The scalar four point function in single field inflation has been discussed in [107, 113, 114, 115, 116]. The general approach we adopt is along the lines of the seminal work of Maldacena [117]. (See also [118].) Some other references which contain a discussion of conformal invariance and its implications for correlators in cosmology are [119, 120, 121, 122, 123, 124, 125, 126, 127, 128, 129, 130, 131, 132]. Some discussion of consistency conditions which arise in the squeezed limit can be found in [118, 133, 134, 135, 136, 137, 138, 139, 140, 141, 142, 143, 144, 145]. An approach towards holography in inflationary backgrounds is given in [146, 147].

This chapter is structured as follows. Some basic concepts which are useful in the calculation are discussed in section 4.2, including the connection between the wave function in dS space and the partition function in AdS space. Issues related to conformal invariance are discussed in section 4.3. A term in the wave function needed for the four point correlator is then calculated in section 4.4, leading to the final result for the correlator in section 4.5. Important tests of the result are carried out in section 4.6 including a discussion of the Ward identities of conformal invariance. Finally, we end with a discussion in section 4.7. There are six important appendices which contain useful supplementary material.

4.2 Basic Concepts and Strategy for the Calculation

We will consider a theory of gravity coupled to a scalar field, the inflaton, with action

$$S = \int d^4x\sqrt{-g}M_{Pl}^2\left[\frac{1}{2}R - \frac{1}{2}(\nabla\phi)^2 - V(\phi)\right]. \tag{4.1}$$

Note we are using conventions in which ϕ is dimensionless. Also note that in our conventions the relation between the Planck mass and the gravitational constant is

$$M_{Pl}^2 = \frac{1}{8\pi G_N}. \tag{4.2}$$

If the potential is slowly varying, so that the slow-roll parameters are small,

$$\epsilon \equiv \left(\frac{V'}{2V}\right)^2 \ll 1 \tag{4.3}$$

and

$$\eta \equiv \frac{V''}{V} \ll 1, \tag{4.4}$$

then the system has a solution which is approximately de Sitter space, with metric,

$$ds^2 = -dt^2 + a^2(t)\sum_{i=1}^{3} dx^i dx^i, \tag{4.5}$$

$$a^2(t) = e^{2Ht}, \tag{4.6}$$

where the Hubble constant is,

$$H = \sqrt{\frac{V}{3}}. \tag{4.7}$$

This solution describes the exponentially expanding inflationary Universe.

The slow-roll parameters introduced above can be related to time derivatives of the Hubble constant, in the slow-roll approximation, as follows,

$$\epsilon = -\frac{\dot{H}}{H^2}, \tag{4.8}$$

while η is given by,

$$\eta = \epsilon - \frac{\ddot{H}}{2H\dot{H}}. \tag{4.9}$$

Using the slow-roll approximation we can also express ϵ in terms of the rate of change of the scalar as,

$$\epsilon = \frac{1}{2}\frac{\dot{\phi}^2}{H^2}. \tag{4.10}$$

de Sitter space is well known to be a highly symmetric space with symmetry group $SO(1,4)$. We will refer to this group as the conformal group because it is also the symmetry group of a conformal field theory in 3 dimensions. This group is ten dimensional. It consists of 3 rotations and 3 translations in the x^i directions, which are obviously symmetries of the metric, eq.(4.5); a scale transformations of the form,

$$x^i \to \lambda x^i, t \to t - \frac{1}{H}\log(\lambda); \tag{4.11}$$

and 3 special conformal transformations whose infinitesimal form is

$$x^i \to x^i - 2(b_j x^j)x^i + b^i\left(\sum_j (x^j)^2 - \frac{e^{-2Ht}}{H^2}\right), \tag{4.12}$$

$$t \to t + 2\frac{b_j x^j}{H}, \tag{4.13}$$

where $b^i, i = 1,2,3$ are infinitesimal parameters. This symmetry group will play an important role in our discussion below.

As mentioned above during the inflationary epoch the Hubble constant varies with time and de Sitter space is only an approximation to the space-time metric. The time varying Hubble constant also breaks some of the symmetries of de Sitter space. While translations and rotations in the x^i directions are left unbroken, the scaling and special conformal symmetries are broken. However, as long as the slow-roll parameters ϵ, η, are small this breaking is small and the resulting inflationary spacetime is still approximately conformally invariant.

4.2.1 The Perturbations

Next we turn to describing perturbation in the inflationary spacetime. Following, [117], we write the metric in the ADM form,

$$ds^2 = -N^2dt^2 + h_{ij}(dx^i + N^i dt)(dx^j + N^j dt). \tag{4.14}$$

By suitable coordinate transformations we can set the lapse function

$$N = 1 \tag{4.15}$$

and the shift functions to vanish,

$$N_i = 0. \tag{4.16}$$

The metric then takes the form,

$$ds^2 = -dt^2 + h_{ij}dx^i dx^j. \tag{4.17}$$

We will work in this gauge throughout in the following discussion.

The metric of dS space can be put in this form, eq.(4.5) with

$$h_{ij} = e^{2Ht}\delta_{ij}. \tag{4.18}$$

Perturbations about dS space take the form

$$h_{ij} = e^{2Ht}g_{ij}, \tag{4.19}$$

with

$$g_{ij} = \delta_{ij} + \gamma_{ij}, \tag{4.20}$$

$$\gamma_{ij} = 2\zeta\delta_{ij} + \widehat{\gamma}_{ij}. \tag{4.21}$$

By definition the metric perturbation $\widehat{\gamma}_{ij}$ meets the condition,

$$\widehat{\gamma}_{ii} = 0. \tag{4.22}$$

The tensor modes are given by $\widehat{\gamma}_{ij}$. Let us note here that the expansion in eq.(4.21) is true to lowest order in the perturbations, higher order corrections will be discussed in Appendix C.4 and will be shown to be unimportant to the order we work.

Besides perturbations in the metric there are also perturbations in the inflaton,

$$\phi = \bar{\phi}(t) + \delta\phi \tag{4.23}$$

where $\bar{\phi}(t)$ is the background value of the inflaton.

The metric of dS space, eq.(4.17), eq.(4.18) is rotationally invariant with $SO(3)$ symmetry in the x^i directions. This invariance can be used to classify the perturbations. There are two types of perturbations, scalar and tensor, which transform as spin 0 and spin 2 under the rotation group respectively. The tensor perturbations arise from the metric, $\widehat{\gamma}_{ij}$. The scalar perturbation physically arises due to fluctuations in the inflaton field.

We turn to describing these perturbations more precisely next.

Gauge 1

We will be especially interested in understanding the perturbations at sufficiently late time, when their wavelength becomes bigger than the Horizon scale H. At such late times the perturbations become essentially time independent. It turns out that the coordinate transformations used to bring the metric in the form eq.(4.14) meeting conditions, eq.(4.15), eq.(4.16), does not exhaust all the gauge invariance in the system for describing such time independent perturbations. Additional spatial reparameterizations of the kind

$$x^i \to x^i + v^i(\boldsymbol{x}) \tag{4.24}$$

can be carried out which keep the form of the metric fixed. These can be used to impose the condition

$$\partial_i \widehat{\gamma}_{ij} = 0. \tag{4.25}$$

From eq.(4.22), eq.(4.25) we see that $\widehat{\gamma}_{ij}$ is now both transverse and traceless, as one would expect for the tensor perturbations.

In addition, a further coordinate transformation can also be carried out which is a time parameterization of the form,

$$t \to t + \epsilon(\boldsymbol{x}). \tag{4.26}$$

Strictly speaking to stay in the gauge eq.(4.15), eq.(4.16), this time parameterization must be accompanied by a spatial parameterization

$$x^i \to x^i + v^i(t, \boldsymbol{x}), \tag{4.27}$$

where to leading order in the perturbations

$$v^i = -\frac{1}{2H}(\partial_i \epsilon) e^{-2Ht}. \tag{4.28}$$

However, at late time we see that $v^i \to 0$ and thus the spatial parameterization vanishes. As a result this additional coordinate transformation does not change $\widehat{\gamma}_{ij}$ which continues to be transverse, upto exponentially small corrections.

By suitably choosing the parameter ϵ in eq.(4.26) one can set the perturbation in the inflaton to vanish,

$$\delta\phi = 0. \tag{4.29}$$

This choice will be called gauge 1 in the subsequent discussion. The value of ζ, defined in eq.(4.21), in this gauge, then corresponds to the scalar perturbation. It gives rise to fluctuations of the spatial curvature.

Gauge 2

Alternatively, having fixed the spatial reparameterizations so that $\widehat{\gamma}_{ij}$ is transverse, eq.(4.25), we can then choose the time parameterization, ϵ, defined in eq.(4.26) differently, so that

$$\zeta = 0, \tag{4.30}$$

and it is the scalar component of the metric perturbation, instead of $\delta\phi$, that vanishes. This choice will be referred to as gauge 2. The scalar perturbations in this coordinate system are then given by fluctuations in the inflaton $\delta\phi$.

This second gauge is obtained by starting with the coordinates in which the perturbations take the form given in gauge 1, where they are described by $\zeta, \widehat{\gamma}_{ij}$, and carrying out a time reparameterization

$$t \to t + \frac{\zeta}{H}, \tag{4.31}$$

to meet the condition eq.(4.30). The tensor perturbation $\widehat{\gamma}_{ij}$ is unchanged by this coordinate transformation. If the background value of the inflaton in the inflationary solution is

$$\phi = \bar{\phi}(t), \tag{4.32}$$

the resulting value for the perturbation $\delta\phi$ this gives rise to is [1]

$$\delta\phi = -\frac{\dot{\bar{\phi}}\zeta}{H}. \tag{4.33}$$

Using eq.(4.10) we can express this relation as

$$\delta\phi = -\sqrt{2\epsilon}\zeta. \tag{4.34}$$

For purposes of calculating the 4-pt scalar correlator at late time, once the modes have crossed the horizon, it will be most convenient to first use gauge 2, where the perturbation is described by fluctuations in the scalar, $\delta\phi$, and then transform the resulting answer to gauge 1, where the perturbation is given in terms of fluctuation in the metric component,

[1] There are corrections involving higher powers of the perturbation in this relation, but these will not be important in our calculation of the four point function.

ζ. This turns out to be a convenient thing to do for tracing the subsequent evolution of scalar perturbations, since a general argument, following essentially from gauge invariance, says that ζ must be a constant once the mode crosses the horizon. This fact is discussed in [148, 149, 150, 151, 152, 153], for a review see section [5.4] of [154].

4.2.2 Basic Aspects of the Calculation

Let us now turn to describing some basic aspects of the calculation. Our approach is based on that of [117]. We will calculate the wave function of the Universe as a functional of the scalar and tensor perturbations. Once this wave function is known correlation functions can be calculated from it in a straightforward manner.

In particular we will be interested in the wave function at late times, when the modes of interest have crossed the horizon so that their wavelength $\lambda \gg H$. At such late times the Hubble damping results in the correlation functions acquiring a time independent form. Since the correlation functions become time independent the wave function also becomes time independent at these late enough times.

The perturbations produced during inflation in the slow-roll model are known to be approximately Gaussian. This allows the wave function, which is a functional of the perturbations in general, to be written as a power series expansion of the form,

$$\begin{aligned}\psi[\chi(\boldsymbol{x})] = \exp\Bigg[&-\frac{1}{2}\int d^3x d^3y \chi(\boldsymbol{x})\chi(\boldsymbol{y})\langle O(\boldsymbol{x})O(\boldsymbol{y})\rangle \\ &+\frac{1}{6}\int d^3x d^3y d^3z\, \chi(\boldsymbol{x})\chi(\boldsymbol{y})\chi(\boldsymbol{z})\langle O(\boldsymbol{x})O(\boldsymbol{y})O(\boldsymbol{z})\rangle + \cdots \Bigg].\end{aligned} \tag{4.35}$$

This expression is schematic, with χ standing for a generic perturbation which could be a scalar or a tensor mode, and the coefficients $\langle O(\boldsymbol{x})O(\boldsymbol{y})\rangle, \langle O(\boldsymbol{x})O(\boldsymbol{y})O(\boldsymbol{z})\rangle$ being functions which determine the two-point three point etc correlators. Let us also note, before proceeding, that the coefficient functions will transform under the $SO(1,4)$ symmetries like correlation functions of appropriate operators in a Euclidean Conformal Field Theory, and we have denoted them in this suggestive manner to emphasize this feature.

For our situation, we have the tensor perturbation, γ_{ij}, and the scalar perturbation, which in gauge 1 is given by $\delta\phi$. With a suitable choice of normalization the wave function takes the form[2]

$$\begin{aligned}
\psi[\delta\phi,\gamma_{ij}] = \exp\Bigg[\frac{M_{Pl}^2}{H^2}\Bigg(& -\frac{1}{2}\int d^3x\sqrt{g(\boldsymbol{x})}\; d^3y\sqrt{g(\boldsymbol{y})}\;\delta\phi(\boldsymbol{x})\delta\phi(\boldsymbol{y})\langle O(\boldsymbol{x})O(\boldsymbol{y})\rangle \\
& -\frac{1}{2}\int d^3x\sqrt{g(\boldsymbol{x})}\; d^3y\sqrt{g(\boldsymbol{y})}\;\gamma_{ij}(\boldsymbol{x})\gamma_{kl}(\boldsymbol{y})\langle T^{ij}(\boldsymbol{x})T^{kl}(\boldsymbol{y})\rangle \\
& -\frac{1}{4}\int d^3x\sqrt{g(\boldsymbol{x})}\; d^3y\sqrt{g(\boldsymbol{y})}\; d^3z\sqrt{g(\boldsymbol{z})} \\
& \qquad \delta\phi(\boldsymbol{x})\delta\phi(\boldsymbol{y})\gamma_{ij}(\boldsymbol{z})\langle O(\boldsymbol{x})O(\boldsymbol{y})T^{ij}(\boldsymbol{z})\rangle \\
& +\frac{1}{4!}\int d^3x\sqrt{g(\boldsymbol{x})}\; d^3y\sqrt{g(\boldsymbol{y})}\; d^3z\sqrt{g(\boldsymbol{z})}\; d^3w\sqrt{g(\boldsymbol{w})} \\
& \qquad \delta\phi(\boldsymbol{x})\delta\phi(\boldsymbol{y})\delta\phi(\boldsymbol{z})\delta\phi(\boldsymbol{w})\langle O(\boldsymbol{x})O(\boldsymbol{y})O(\boldsymbol{z})O(\boldsymbol{w})\rangle + \cdots\Bigg)\Bigg].
\end{aligned} \tag{4.36}$$

Where $g(\boldsymbol{x}) = \det[g_{ij}(\boldsymbol{x})]$ and g_{ij} is given in eq.(4.20).

The terms which appear explicitly on the RHS of eq.(4.36) are all the ones needed for calculating the four point scalar correlator of interest in this work. The ellipses indicate additional terms which will not enter the calculation of this correlation function, in the leading order approximation in $\frac{M_{pl}^2}{H^2}$, where loop effects can be neglected. The graviton two-point correlator and the graviton-scalar-scalar three point function are relevant because they contribute to the scalar four point correlator after integrating out the graviton at tree level as we will see below in more detail in sec 4.5.

In fact only a subset of terms in eq.(4.36) are relevant for calculating the 4-pt scalar correlator. As was mentioned in subsection 4.2.1 we will first calculate the result in gauge 2. Working in this gauge, where $\zeta = 0$, and expanding the metric g_{ij} in terms of the perturbation γ_{ij}, eq.(4.20), one finds that the terms which are relevant are

$$\begin{aligned}
\psi[\delta\phi(\boldsymbol{k}),\gamma^s(\boldsymbol{k})] = \exp\Bigg[\frac{M_{Pl}^2}{H^2}\Bigg(& -\frac{1}{2}\int\frac{d^3\boldsymbol{k_1}}{(2\pi)^3}\frac{d^3\boldsymbol{k_2}}{(2\pi)^3}\delta\phi(\boldsymbol{k_1})\delta\phi(\boldsymbol{k_2})\langle O(-\boldsymbol{k_1})O(-\boldsymbol{k_2})\rangle \\
& -\frac{1}{2}\int\frac{d^3\boldsymbol{k_1}}{(2\pi)^3}\frac{d^3\boldsymbol{k_2}}{(2\pi)^3}\gamma^s(\boldsymbol{k_1})\gamma^{s'}(\boldsymbol{k_2})\langle T^s(-\boldsymbol{k_1})T^{s'}(-\boldsymbol{k_2})\rangle \\
& -\frac{1}{4}\int\frac{d^3\boldsymbol{k_1}}{(2\pi)^3}\frac{d^3\boldsymbol{k_2}}{(2\pi)^3}\frac{d^3\boldsymbol{k_3}}{(2\pi)^3}\delta\phi(\boldsymbol{k_1})\delta\phi(\boldsymbol{k_2})\gamma^s(\boldsymbol{k_3})\langle O(-\boldsymbol{k_1})O(-\boldsymbol{k_2})T^s(-\boldsymbol{k_3})\rangle \\
& +\frac{1}{4!}\int\prod_{J=1}^{4}\left\{\frac{d^3\boldsymbol{k}_J}{(2\pi)^3}\delta\phi(\boldsymbol{k}_J)\right\}\langle O(-\boldsymbol{k_1})O(-\boldsymbol{k_2})O(-\boldsymbol{k_3})O(-\boldsymbol{k_4})\rangle\Bigg)\Bigg].
\end{aligned} \tag{4.37}$$

In eq.(4.37) we have shifted to momentum space, with

$$\delta\phi(\boldsymbol{x}) = \int\frac{d^3k}{(2\pi)^3}\delta\phi(\boldsymbol{k})e^{i\boldsymbol{k}\cdot\boldsymbol{x}} \tag{4.38}$$

and similarly for γ_{ij} and all the coefficient functions appearing in eq.(4.37). Also, since γ_{ij}

[2]The coefficient functions include contact terms, which are analytic in some or all of the momenta.

is transverse we can write

$$\gamma_{ij}(\boldsymbol{k}) = \sum_{s=1}^{2} \gamma_s(\boldsymbol{k})\epsilon^s_{ij}(\boldsymbol{k}), \tag{4.39}$$

where $\epsilon^s_{ij}(k),\ s = 1, 2$, is a basis of polarization tensors which are transverse and traceless. Some additional conventions pertaining to our definition for ϵ^s_{ij} etc are given in Appendix C.1.

Of the four coefficient functions which appear explicitly on the RHS of eq.(4.37), two, the coefficient functions $\langle O(\boldsymbol{k_1})O(\boldsymbol{k_2})\rangle$ and $\langle T^s(\boldsymbol{k_1})T^{s'}(\boldsymbol{k_2})\rangle$ are well known. The function $\langle O(\boldsymbol{k_1})O(\boldsymbol{k_2})T^s(\boldsymbol{k_3})\rangle$ was obtained in [117], for the slow-roll model of inflation being considered here, and also obtained from more general considerations in [131], see also [125]. These coefficient functions are also summarized in Appendix C.1. This only leaves the $\langle O(\boldsymbol{k_1})O(\boldsymbol{k_2})O(\boldsymbol{k_3})O(\boldsymbol{k_4})\rangle$ coefficient function. Calculating it will be one of the major tasks in this chapter.

Conventions: Before proceeding it is worth summarizing some of our conventions. Vectors with components in the x^i directions will be denoted as boldface, *e.g.*, $\boldsymbol{x}, \boldsymbol{k}$, while their magnitude will be denoted without the boldface, *e.g.*, $x = |\boldsymbol{x}|, k = |\boldsymbol{k}|$. Components of such vectors will be denoted without bold face, *e.g.*, k^i. The Latin indices on these components will be raised and lowered using the flat space metric, so that $k^i = k_i$, $x^i = x_i$, and also $\boldsymbol{k} \cdot \boldsymbol{x} = k_i x_i$.

4.2.3 The Wave Function

The wave function as a functional of the late time perturbations can be calculated by doing a path integral,

$$\psi[\chi(\boldsymbol{x})] = \int^{\chi(\boldsymbol{x})} D\chi e^{iS}, \tag{4.40}$$

where S is the action and χ stands for the value a generic perturbation takes at late time.

To make the path integral well defined one needs to also specify the boundary conditions in the far past. In our discussions in this chapter we take these boundary conditions to correspond to the standard Bunch Davies boundary conditions. In the far past, the perturbations had a wavelength much shorter than the Hubble scale, the short wavelengths of the modes makes them insensitive to the geometry of de Sitter space and they essentially propagate as if in Minkowski spacetime. The Bunch Davies vacuum corresponds to taking the modes to be in the Minkowski vacuum at early enough time.

An elegant way to impose this boundary condition in the path integral above, as discussed in [117], is as follows. Consider de Sitter space in conformal coordinates,

$$ds^2 = \frac{1}{H^2\eta^2}(-d\eta^2 + \sum_{i=1}^{3}(dx^i)^2), \tag{4.41}$$

with the far past being $\eta \to -\infty$, and late time being $\eta \to 0$. Continue η so that it acquires a small imaginary part $\eta \to \eta(1-i\epsilon), \epsilon > 0$. Then the Bunch Davies boundary condition is correctly imposed if the path integral is done over configurations which vanish at early times when $\eta \to -\infty(1-i\epsilon)$. Note that in general the resulting path integral is over complex field configurations.

As an example, for a free scalar field with equation,

$$\nabla^2 \phi = 0, \tag{4.42}$$

a mode with momentum $\boldsymbol{k}$, $\phi = f_{\boldsymbol{k}}(\eta) e^{i\boldsymbol{k}\cdot\boldsymbol{x}}$ which meets the required boundary condition is

$$f_{\boldsymbol{k}} = c_1(\boldsymbol{k})(1 - ik\eta)e^{ik\eta}. \tag{4.43}$$

The second solution,

$$f_{\boldsymbol{k}} = c_2(\boldsymbol{k})(1 + ik\eta)e^{-ik\eta} \tag{4.44}$$

is not allowed. Since $f_{\vec{k}} \neq f^*_{\vec{k}}$ the resulting configuration which dominates the saddle point is complex.

With the Bunch Davies boundary conditions the path integral is well defined as a functional of the boundary values of the fields at late time.

We will evaluate the path integral in the leading saddle-point approximation. Corrections corresponding to quantum loop effects are suppressed by powers of H/M_{Pl} and are small as long as $H/M_{Pl} \ll 1$. In this leading approximation the procedure to be followed is simple. We expand the action about the zeroth order inflationary background solution. Next, extremize the resulting corrections to the action as a function of the perturbations, to get the equations which must be satisfied by the perturbations. Solve these equations subject to the Bunch Davies boundary conditions, in the far past, and the given boundary values of the perturbations at late times. And finally evaluate the correction terms in the action on-shell, on the resulting solution for the perturbations, to obtain the action as a functional of the late time boundary values of the perturbations. This gives, from eq.(4.40)

$$\psi[\chi(x)] = e^{iS^{dS}_{\text{on-shell}}[\chi(x)]}. \tag{4.45}$$

This procedure is further simplified by working in the leading slow-roll approximation, as we will do. In this approximation, as was mentioned above, the metric becomes that of de Sitter space, eq.(4.5) with constant H. Since the slow-roll parameters, eq.(4.3), eq.(4.4) are put to zero, the potential V, eq.(4.1), can be taken to be a constant, related to the Hubble constant by eq.(4.7). The resulting action for the small perturbations is then given by

$$S = \int d^4x \sqrt{-\det(\bar{g}_{\mu\nu} + \delta g_{\mu\nu})} M_{Pl}^2 \left[\frac{1}{2} R(\bar{g}_{\mu\nu} + \delta g_{\mu\nu}) - V - \frac{1}{2}(\nabla \delta\phi)^2\right]. \tag{4.46}$$

Here $\bar{g}_{\mu\nu}$ denotes the background value for the metric in de Sitter space, eq.(4.5), and V is constant, as mentioned above. $\delta g_{\mu\nu}$ is the metric perturbation, and $\delta\phi$ is the perturbation for the scalar field, eq.(4.23).

Notice that the action for the perturbation of the scalar, is simply that of a minimally coupled scalar field in de Sitter space. In particular self interaction terms coming from expanding the potential, for example a $(\delta\phi)^4$ term which would be of relevance for the four-point function, can be neglected in the leading slow-roll approximation. One important consequence of this observation is that the correlation functions to leading order in the slow-roll parameters must obey the symmetries of de Sitter space. In particular, this must be true for the scalar 4-point function.

4.2.4 The Partition Function in AdS and the Wave Function in dS

The procedure described above for calculating the wave function in de Sitter space is very analogous to what is adopted for calculating the partition function AdS space. In fact this connection allows us to conveniently obtain the wave function in de Sitter space from the partition function in AdS space, after suitable analytic continuation, as we now explain.

Euclidean AdS_4 space has the metric (in Poincare coordinates):

$$ds^2 = R_{\text{AdS}}^2 \frac{1}{z^2}(dz^2 + \sum_{i=1}^{3}(dx^i)^2) \tag{4.47}$$

with $z \in [0, \infty]$. R is the radius of AdS space.

After continuing z, H to imaginary values,

$$z = -i\eta, \tag{4.48}$$

and,

$$R_{\text{AdS}} = \frac{i}{H} \tag{4.49}$$

where $\eta \in [-\infty, 0]$ and H is real, this metric becomes that of de Sitter space given in eq.(4.41).

The partition function in AdS space is defined as a functional of the boundary values that fields take as $z \to 0$. In the leading semi-classical approximation it is given by

$$Z[\chi(x)] = e^{-S_{\text{on-shell}}^{\text{AdS}}} \tag{4.50}$$

where $S_{\text{on-shell}}^{\text{AdS}}$ is the on shell action which is obtained by substituting the classical solution for fields which take the required boundary values, $z \to 0$, into the action. We denote these boundary values generically as $\chi(x)$ in eq.(4.50).

Besides the boundary conditions at $z \to 0$ one also needs to impose boundary conditions as $z \to \infty$ to make the calculation well defined. This boundary condition is imposed by requiring regularity for fields as $z \to \infty$.

For example, for a free scalar field with momentum $\boldsymbol{k}$, $\phi = f_{\boldsymbol{k}} e^{i\boldsymbol{k}\cdot\boldsymbol{x}}$, the solution to the wave equation, eq.(4.42) is,

$$f_{\boldsymbol{k}} = c_1(\boldsymbol{k})(1+kz)e^{-kz} + c_2(\boldsymbol{k})(1-kz)e^{kz}. \tag{4.51}$$

Regularity requires that c_2 must vanish, and the solution must be

$$f_{\boldsymbol{k}} = c_1(\boldsymbol{k})(1+kz)e^{-kz}. \tag{4.52}$$

At $z \to 0$ the solution above goes to a z independent constant

$$f_{\boldsymbol{k}} = c_1(\boldsymbol{k}). \tag{4.53}$$

More generally a solution is obtained by summing over modes of this type,

$$\phi(z, \boldsymbol{x}) = \int \frac{d^3k}{(2\pi)^3} \phi(\boldsymbol{k})(1+kz)e^{-kz} e^{i\boldsymbol{k}\cdot\boldsymbol{x}}. \tag{4.54}$$

Towards the boundary, as $z \to 0$, this becomes,

$$\phi(\boldsymbol{x}) = \int \frac{d^3k}{(2\pi)^3} \phi(\boldsymbol{k}) e^{i\boldsymbol{k}\cdot\boldsymbol{x}}. \tag{4.55}$$

The AdS on-shell action is then a functional of $\phi(\boldsymbol{k})$.

The reader will notice that the relation between the partition function and on-shell action in AdS space, eq.(4.50), is quite analogous to that between the wave function and on shell action in dS space eq.(4.45). We saw above that after the analytic continuation, eq.(4.48), eq.(4.49), the AdS metric goes over to the metric in dS space. It is easy to see that this analytic continuation also takes the solutions for fields in AdS space which meet the regularity condition as $z \to \infty$, to those in dS space meeting the Bunch Davies boundary conditions. For example, the free scalar which meets the regularity condition, as $z \to 0$, in AdS, is given in eq.(4.52), and this goes over to the solution meeting the Bunch Davies boundary condition in dS space, eq.(4.43). Also after the analytic continuation the boundary value of a field as $z \to 0$ in AdS, becomes the boundary value at late times, as $\eta \to 0$ in dS, as is clear from comparing eq.(4.53) with the behavior of the solution in eq.(4.43) at $\eta \to 0$.

These facts imply that the on-shell action in AdS space when analytically continued gives the on-shell action in dS space. For example, for a massless scalar field the action in AdS space is a functional of the boundary value for the field $\phi(\boldsymbol{k})$, eq.(4.55), and also on the

AdS radius $R_{\rm AdS}$. We denote

$$S^{\rm AdS}_{\text{on-shell}} = S^{\rm AdS}_{\text{on-shell}}[\phi(\boldsymbol{k}), R_{\rm AdS}]. \tag{4.56}$$

to make this dependence explicit. The on shell action in dS space is then obtained by taking $R_{\rm AdS} \to i/H$,

$$S^{ds}_{\text{on-shell}}[\phi(\boldsymbol{k}), H] = -i\ S^{\rm AdS}_{\text{on-shell}}\big[\phi(\boldsymbol{k}), \frac{i}{H}\big]. \tag{4.57}$$

Note that on the LHS in this equation $\phi(\boldsymbol{k})$ refers to the late time value of the scalar field in dS space. The factor of i on the RHS arises because the analytic continuation eq.(4.48) leads to an extra factor of i when the z integral involved in evaluating the AdS action is continued to the η integral in dS space.

Two more comments are worth making here. First, it is worth being more explicit about the analytic continuation, eq.(4.48), eq.(4.49). To arrive at dS space with the Bunch Davies conditions correctly imposed one must start with regular boundary condition in AdS space, $z \to \infty$, and then continue z from the positive real axis to the negative imaginary axis by setting

$$z = |z|e^{i\phi} \tag{4.58}$$

and taking ϕ to go from 0 to $\pi/2$. In particular when $\phi = \pi/2 - \epsilon$, $\eta = iz$ is given by

$$\eta = -|z|(1 - i\epsilon) = -|\eta|(1 - i\epsilon), \tag{4.59}$$

so that η has a small positive imaginary part. Imposing the regularity condition then implies that fields vanish when $\eta \to \infty$, this is exactly the condition required to impose the Bunch Davies boundary condition.

Second, one subtlety we have not discussed is that the resulting answers for correlation functions can sometimes have divergences and needs to be regulated by introducing a suitable cutoff in the infra-red. Physical answers do not depend on the choice of cut-off procedure and in any case this issue will not arise for the calculation of interest here, which is to obtain the scalar four-point correlator.

4.2.5 Feynman-Witten Diagrams in *AdS*

As we mentioned above, the wave function of the Universe helps to elucidate the role of various symmetries, such as conformal invariance. This itself makes the on-shell action in AdS a useful quantity to consider. However, there is another advantage in first doing the calculation in anti-de Sitter space.

The various coefficient functions in the wave function of the Universe can be computed by a set of simple diagrammatic rules. These Feynman diagrams in AdS are sometimes called “Witten diagrams”. They are closely related to flat-space Feynman diagrams, except that flat space propagators must be replaced by the appropriate Green functions in AdS. Taking the limit where the external points of the correlators reach the boundary, we obtain correlators in one-lower dimension, which are conformally invariant.

These correlators have been extensively studied in the AdS/CFT literature, where several powerful techniques have been devised to calculate them, and check their consistency. We will bring some of these techniques to bear upon this calculation below. In fact, the four point scalar correlator that we are interested in, has been computed in position space in [155] and in [156]. Here we will compute this quantity in momentum space.

Although, in principle, we could have obtained this answer by Fourier transforming the position space answers, it is much more convenient to do the calculation directly using momentum space Feynman-Witten diagrams. The use of momentum space is particularly convenient in odd boundary dimensions, since the propagators simplify greatly, and exchange interactions can be evaluated by a straightforward algebraic procedure of computing residues of a complex function, as we will see below.

4.2.6 Basic Strategy for the Calculation

Now that we have discussed all the required preliminaries in some detail, we are ready to spell out the basic strategy that we will adopt in our calculation of the scalar four point function. First, we will calculate the coefficient function $\langle O(\boldsymbol{x}_1)O(\boldsymbol{x}_2)O(\boldsymbol{x}_3)O(\boldsymbol{x}_4)\rangle$, which, as was discussed in section 4.2.2, is the one coefficient function which is not already known. This correlator is given by a simple set of Feynman-Witten diagrams that we can evaluate in momentum space. With this coefficient function in hand, all the relevant terms in the on-shell AdS action are known, and we can analytically continue the Euclidean AdS result of section 4.4.1 to de Sitter space in section 4.4.2. We then proceed to calculate the four point scalar correlator from it as discussed in section 4.5. Before embarking on the calculation though we let us first pause to discuss some general issues pertaining to conformal invariance in the next section.

4.3 Conformal Invariance and the Issue of Gauge Fixing

Working in the ADM formalism, with metric, eq.(4.14), the action, eq.(4.1), is given by

$$S = \frac{M_{Pl}^2}{2}\int\sqrt{-h}\Big[NR^{(3)} - 2NV + \frac{1}{N}(E_{ij}E^{ij} - E^2) + \frac{1}{N}(\partial_t\phi - N^i\partial_i\phi)^2 \\ - Nh^{ij}\partial_i\phi\partial_j\phi\Big] \tag{4.60}$$

where

$$\begin{aligned} E_{ij} =& \frac{1}{2}(\partial_t h_{ij} - \nabla_i N_j - \nabla_j N_i), \\ E =& E^i_i. \end{aligned} \tag{4.61}$$

The equations of motion of N_i, N give rise to the constraints

$$\nabla_i[N^{-1}(E^i_j - \delta^i_j E)] = 0, \tag{4.62}$$

$$R^{(3)} - 2V - \frac{1}{N^2}(E_{ij}E^{ij} - E^2) - \frac{1}{N^2}(\partial_t\phi - N^i\partial_i\phi)^2 - h^{ij}\partial_i\phi\partial_j\phi = 0 \tag{4.63}$$

respectively.

The constraints obtained by varying the shift functions, N_i, leads to invariance under spatial reparameterizations, eq.(4.24). The constraint imposed by varying the lapse function, N, leads to invariance under time reparameterizations, eq.(4.26). Physical states must meet these constraints. In the quantum theory this implies that the wave function must be invariant under the spatial reparameterizations and the time reparameterization, eq.(4.24),eq.(4.26), for a pedagogical introduction see [157]. We will see that these conditions give rise to the Ward identities of interest.

Under the spatial parameterization, eq.(4.24) the metric and scalar perturbations transform as

$$\gamma_{ij} \to \gamma_{ij} + \delta\gamma_{ij} = \gamma_{ij} - \nabla_i v_j - \nabla_j v_i, \tag{4.64}$$

$$\delta\phi \to \delta\phi + \delta(\delta\phi) = \delta\phi - v^k\partial_k\delta\phi. \tag{4.65}$$

Requiring that the wave function is invariant under the spatial parameterization imposes the condition that

$$\psi[\gamma_{ij} + \delta\gamma_{ij}, \delta\phi + \delta(\delta\phi)] = \psi[\gamma_{ij}, \delta\phi]. \tag{4.66}$$

For the wave function in eq.(4.36) imposing this condition in turn leads to constraints on the coefficient functions. For example, it is straightforward to see, as discussed in Appendix C.2 that we get the condition,

$$\partial_i\langle T_{ij}(\boldsymbol{x})O(\boldsymbol{y_1})O(\boldsymbol{y_2})\rangle = \delta^3(\boldsymbol{x}-\boldsymbol{y_1})\langle\partial_{y_1^j}O(\boldsymbol{y_1})O(\boldsymbol{y_2})\rangle + \delta^3(\boldsymbol{x}-\boldsymbol{y_2})\langle O(\boldsymbol{y_1})\partial_{y_2^j}O(\boldsymbol{y_2})\rangle. \tag{4.67}$$

Similar conditions rise for other correlation functions. These conditions are exactly the Ward identities due to translational invariance in the conformal field theory.

Under the time reparameterizations, eq.(4.26), the metric transforms as

$$\gamma_{ij} \to \gamma_{ij} + 2H\epsilon(\boldsymbol{x})\delta_{ij}. \tag{4.68}$$

The scalar perturbation, $\delta\phi$, at late times is independent of t and thus is invariant under time parameterization. The invariance of the wave function then gives rise to the condition

$$\psi[\gamma_{ij} + 2H\epsilon(\boldsymbol{x}), \delta\phi] = \psi[\gamma_{ij}, \delta\phi] \tag{4.69}$$

which also imposes conditions on the coefficient functions. For example from eq.(4.37) we get that the condition

$$\langle T_{ii}(\boldsymbol{x})O(\boldsymbol{y}_1)O(\boldsymbol{y}_2)\rangle = -3\delta^3(\boldsymbol{x}-\boldsymbol{y}_1)\langle O(\boldsymbol{y}_1)O(\boldsymbol{y}_2)\rangle - 3\delta^3(\boldsymbol{x}-\boldsymbol{y}_2)\langle O(\boldsymbol{y}_1)O(\boldsymbol{y}_2)\rangle \tag{4.70}$$

must be true, as shown in Appendix C.2. Similarly other conditions also arise; these are all exactly the analogue of the Ward identities in the CFT due to Weyl invariance, with O being an operator of dimension 3.

The isometries corresponding to special conformal transformations were discussed in eq.(4.12), eq.(4.13). We see that at late times when $e^{-2Ht} \to 0$ these are given by

$$x^i \to x^i - 2(b_j x^j)x^i + b^i \sum_j (x^j)^2, \tag{4.71}$$

$$t \to t + 2\frac{b_j x^j}{H}. \tag{4.72}$$

We see that this is a combination of a spatial parameterization, eq.(4.24) and a time parameterization, eq.(4.26). The invariance of the wave function under the special conformal transformations then follows from our discussion above. It is easy to see, as discussed in Appendix C.2 that the invariance of the wave function under conformal transformations leads to the condition that the coefficient functions must be invariant under the transformations,

$$\begin{aligned} &O(\boldsymbol{x}) \to O(\boldsymbol{x}) + \delta O(\boldsymbol{x}), \\ &\delta O(\boldsymbol{x}) = -6(\boldsymbol{x}\cdot\boldsymbol{b})O(\boldsymbol{x}) + DO(\boldsymbol{x}), \\ &D \equiv x^2(\boldsymbol{b}\cdot\boldsymbol{\partial}) - 2(\boldsymbol{b}\cdot\boldsymbol{x})(\boldsymbol{x}\cdot\boldsymbol{\partial}). \end{aligned} \tag{4.73}$$

and

$$\begin{aligned} &T_{ij}(\boldsymbol{x}) \to T_{ij} + \delta T_{ij}, \\ &\delta T_{ij} = -6(\boldsymbol{x}\cdot\boldsymbol{b})T_{ij} - 2M^k{}_i T_{kj} - 2M^k{}_j T_{ik} + DT_{ij}, \\ &M^k{}_i \equiv (x^k b^i - x^i b^k), \\ &D \equiv x^2(\boldsymbol{b}\cdot\boldsymbol{\partial}) - 2(\boldsymbol{b}\cdot\boldsymbol{x})(\boldsymbol{x}\cdot\boldsymbol{\partial}). \end{aligned} \tag{4.74}$$

The resulting conditions on the coefficient functions agree exactly with the Ward identities for conformal invariance which must be satisfied by correlation function in the conformal field theory.

Specifically for the scalar four point function of interest here, the relevant terms in the wave function are given in eq.(4.37) in momentum space. The momentum space versions of eq.(4.73), eq.(4.74) are given in the Appendix C.2.2 in eq.(C.25), eq.(C.27), eq.(C.29), eq.(C.30). It is easy to check that the two point functions, $\langle O(\boldsymbol{k_1})O(\boldsymbol{k_2})\rangle$ and $\langle T_{ij}(\boldsymbol{k_1})T_{kl}(\boldsymbol{k_2})\rangle$ are both invariant under these transformations. The invariance of $\langle O(\boldsymbol{k_1})O(\boldsymbol{k_2})T^s(\boldsymbol{k_3})\rangle$ was discussed *e.g.* in [125, 131]. In order to establish conformal invariance for the wave function it is then enough to prove that the coefficient function $\langle O(\boldsymbol{k_1})O(\boldsymbol{k_2})O(\boldsymbol{k_3})O(\boldsymbol{k_4})\rangle$ is invariant under the transformation eq.(C.29). We will see that the answer we calculate in section 4.4 does indeed have this property.

4.3.1 Further Gauge Fixing and Conformal Invariance

We now come to an interesting subtlety which arises when we consider the conformal invariance of correlation functions, as opposed to the wave function, in the de Sitter case. This subtlety arises because one needs to integrate over the metric and scalar perturbations, to calculate the correlation functions from the wave function. In order to do so the gauge symmetry needs to be fixed more completely, as we will see in the subsequent discussion. However, once this additional gauge fixing is done a general conformal transformation does not preserve the choice of gauge. Thus, to test for conformal invariance of the resulting correlation functions, the conformal transformation must be accompanied by a compensating coordinate transformation which restores the choice of gauge. As we describe below, this compensating transformation is itself field-dependent. The invariance of the correlation functions under the combined conformal transformation and compensating coordinate transformation is then the signature of the underlying conformal invariance.

Let us note here that this subtlety does not have a corresponding analogue in the AdS case, where one computes the partition function, and the boundary value of the metric is a source which is non-dynamical. It is also worth emphasizing, before we go further, that due to these complications it is in fact easier to test for the symmetries in the wave function itself rather than in the correlators which are calculated from it. Calculating the wave function by itself does not require the additional gauge fixing mentioned above. Thus the wave function should be invariant separately under conformal transformations and spatial reparameterizations. Once this is shown to be true the invariance of the probability distribution function $P[\delta\phi]$ and all correlation functions under the combined conformal transformation and gauge restoring parameterization then follows.

We will now discuss this issue in more detail. Let us begin by noting, as was discussed in section 4.2, that the conditions, eq.(4.15), eq.(4.16), do not fix the gauge completely. One has the freedom to do spatial reparameterizations of the form eq.(4.24), and at late times, also a time parameterization of the form, eq.(4.26). Using this freedom one can then fix the gauge further, for example, leading to gauge 1 or gauge 2 in section 4.2. In fact it is necessary to do so in order to calculate correlation functions from the wave function, otherwise one would end up summing over an infinite set of copies of the same physical configuration.

As a concrete example, consider the case where we make the choice of gauge 2 of subsection 4.2.1. In this gauge $\zeta = 0$ and the metric γ_{ij} is both traceless and transverse. On carrying out a conformal transformation, the coordinates x^i, t transform as given in eq.(4.71) and eq.(4.72) respectively. As shown in Appendix C.2 eq.(C.20),

$$\delta\gamma_{ij}(x) = 2M^m{}_j\gamma_{im} + 2M^m{}_i\gamma_{mj} - (x^2 b^m - 2x^m(\boldsymbol{x}\cdot\boldsymbol{b}))\frac{\partial\gamma_{ij}(\boldsymbol{x})}{\partial x^m}, \tag{4.75}$$

where $\delta\gamma_{ij} = \gamma'_{ij}(x) - \gamma_{ij}(x)$ is the change in γ_{ij} and $M^m{}_j = x^m b^j - x^j b^m$.

Since $\delta\gamma_{ii} = 0$, γ'_{ij} remains traceless and ζ continues to vanish. However

$$\partial_i\delta\gamma_{ij} = -6b^k\gamma_{kj} \neq 0, \tag{4.76}$$

so we see that $\gamma'_{ij}(x)$ is not transverse anymore.

Now, upon carrying out a further coordinate transformation

$$x^i \to x^i + v^i(\boldsymbol{x}) \tag{4.77}$$

γ_{ij} transforms as

$$\begin{aligned}\gamma_{ij}(\boldsymbol{x}) &\to \gamma_{ij}(\boldsymbol{x}) + \delta\gamma_{ij},\\ \delta\gamma_{ij} &= -\partial_i v_j - \partial_j v_i.\end{aligned} \tag{4.78}$$

Choosing

$$v^j(\boldsymbol{x}) = \frac{-6b^k\gamma_{kj}(\boldsymbol{x})}{\partial^2} \tag{4.79}$$

it is easy to see that transformed metric perturbation γ_{ij} continues to be traceless and also now becomes transverse. The combination of the conformal transformation, eq.(4.71) and the compensating spatial parameterization eq.(4.77), eq.(4.79), thus keep one in gauge 2. Let us note here that we will work with perturbation with non-zero momentum, thus $\frac{1}{\partial^2} = -\frac{1}{k^2}$ will be well defined.

The scalar perturbation $\delta\phi$ transforms like a scalar under both the conformal transformation, eq.(4.71) and the compensation parameterization eq.(4.77) with eq.(4.79). It then follows that under the combined transformation which leaves one in gauge 2 it transforms as follows:

$$\delta\phi \to \delta\phi + \delta(\delta\phi), \tag{4.80}$$

$$\delta(\delta\phi) = \delta^C(\delta\phi) + \delta^R(\delta\phi), \tag{4.81}$$

where $\delta^C(\delta\phi)$ is the change in $\delta\phi$ due to conformal transformation eq.(4.71),

$$\delta^C\big(\delta\phi(\boldsymbol{x})\big) = -(x^2 b^i - 2x^i(\boldsymbol{x}\cdot\boldsymbol{b}))\frac{\partial}{\partial x^i}\delta\phi(\boldsymbol{x}) \tag{4.82}$$

and $\delta^R(\delta\phi)$ is the change in $\delta\phi$ under spatial parameterization eq.(4.77) with eq.(4.79)

$$\delta^R\big(\delta\phi(\boldsymbol{x})\big) = -v^i(\boldsymbol{x})\partial_i\delta\phi(\boldsymbol{x}). \tag{4.83}$$

It is important to note that the coordinate transformation parameter v^i, eq.(4.78) is itself dependent on the metric perturbation, γ_{ij}, eq.(4.79). As a result the change in $\delta\phi$ under the spatial parameterization is non-linear in the perturbations, $\gamma_{ij}, \delta\phi$. This is in contrast to $\delta^C(\delta\phi)$ which is linear in $\delta\phi$. As we will see in section 4.6.1 when we discuss the four point function in more detail, a consequence of this non-linearity is that terms in the probability distribution function which are quadratic in $\delta\phi$ will mix with those which are quartic, thereby ensuring invariance under the combined transformation, eq.(4.81).

The momentum space expression for $\delta^C\big(\delta\phi(\boldsymbol{x})\big)$ is given in eq.(C.28) of Appendix C.2.2. We write here the momentum space expression for v^i and $\delta^R\big(\delta\phi(\boldsymbol{x})\big)$

$$v_i(\boldsymbol{k}) = \frac{6b^k\gamma_{ki}(\boldsymbol{k})}{k^2}, \tag{4.84}$$

$$\delta^R\big(\delta\phi(\boldsymbol{k})\big) = i6b^k k^i \int \frac{d^3k_2}{(2\pi)^3}\frac{\gamma_{ki}(\boldsymbol{k}-\boldsymbol{k_2})}{|\boldsymbol{k}-\boldsymbol{k_2}|^2}\delta\phi(\boldsymbol{k_2}). \tag{4.85}$$

4.3.2 Conformal Invariance of the Four Point Correlator

Now consider the four point scalar correlator in gauge 2. It can be calculated from $\psi[\delta\phi,\gamma_{ij}]$ by evaluating the functional integral:

$$\langle\delta\phi(\boldsymbol{x}_1)\delta\phi(\boldsymbol{x}_2)\delta\phi(\boldsymbol{x}_3)\delta\phi(\boldsymbol{x}_4)\rangle = \mathcal{N}\int \mathcal{D}[\delta\phi]\mathcal{D}[\gamma_{ij}]\prod_{i=1}^{4}\delta\phi(\boldsymbol{x}_i)\ |\psi[\delta\phi,\gamma_{ij}]|^2. \tag{4.86}$$

The normalization $\mathcal{N}$ is given by

$$\mathcal{N}^{-1} = \int \mathcal{D}[\delta\phi]\mathcal{D}[\gamma_{ij}]\ |\psi[\delta\phi,\gamma_{ij}]|^2. \tag{4.87}$$

The integral over the field configurations in eq.(4.86) can be done in two steps. We can first integrate out the metric to obtain a probability distribution which is a functional of $\delta\phi$ alone,

$$P[\delta\phi(\boldsymbol{x})] = \mathcal{N}\int \mathcal{D}[\gamma_{ij}]\ |\psi[\delta\phi,\gamma_{ij}]|^2, \tag{4.88}$$

and then use $P[\delta\phi(x)]$ to compute correlations of $\delta\phi$, in particular the correlator,

$$\langle\delta\phi(\boldsymbol{x}_1)\delta\phi(\boldsymbol{x}_2)\delta\phi(\boldsymbol{x}_3)\delta\phi(\boldsymbol{x}_4)\rangle = \int \mathcal{D}[\delta\phi]\prod_{i=1}^{4}\delta\phi(\boldsymbol{x}_i)P[\delta\phi]. \tag{4.89}$$

Note that the integral over the metric γ_{ij} is well defined only because of the further gauge fixing which was done leading to gauge 2.

The invariance of the wave function under conformal transformations and compensating spatial reparameterizations implies that the probability distribution $P[\delta\phi]$ must be invariant under the combined transformation generated by the conformal transformation and compensating parameterization which leaves one in the gauge 2. This gives rise to the condition

$$P[\delta\phi + \delta(\delta\phi)] = P[\delta\phi] \tag{4.90}$$

where $\delta(\delta\phi)$ is given in eq.(4.81) with eq.(4.82) and eq.(4.83). We will see in section 4.6.1 that our final answer for $P[\delta\phi]$ does indeed meet this condition.

4.4 Computation of the $\langle O(\boldsymbol{x}_1)O(\boldsymbol{x}_2)O(\boldsymbol{x}_3)O(\boldsymbol{x}_4)\rangle$ Coefficient Function

We now compute the coefficient of the quartic term in the wave function of the Universe. This coefficient is the same as the four point correlation function of marginal scalar operators in anti-de Sitter space. As explained above, this calculation has the advantage that it can be done by standard Feynman-Witten diagram techniques. In the next section, we put this correlator together with other known correlators to obtain the wave function of the Universe at late times. This can then easily be used to compute the expectation value in de Sitter space that we are interested in.

Additional Conventions: Some additional conventions we will use are worth stating here. The Greek indices $\mu, \nu, \cdots$, take 4 values in the $z, x^i, i = 1, 2, 3,$ directions. The inverse of the back ground metric $\bar{g}_{\mu\nu}$ is denoted by $\bar{g}^{\mu\nu}$, while indices for the metric perturbation $\delta g_{\mu\nu}$ are raised or lowered using the flat space metric, so that, *e.g.*, $\delta g^{\mu\nu} = \eta^{\mu\rho}\delta g_{\rho\kappa}\eta^{\kappa\nu}$.

4.4.1 The Calculation in AdS Space

We are now ready to begin our calculation of the $\langle O(\boldsymbol{x}_1)O(\boldsymbol{x}_2)O(\boldsymbol{x}_3)O(\boldsymbol{x}_4)\rangle$ coefficient function. As discussed in subsection 4.2.6 we will first calculate the relevant term in the partition function in Euclidean AdS space and then continue the answer to obtain this coefficient function in dS space. This will allow us to readily use some of the features recently employed in AdS space calculations. However, it is worth emphasizing at the outset itself that it is not necessary to do the calculation in this way. The problem of interest is well posed in de Sitter space and if the reader prefers, the calculation can be directly done in de Sitter space, using only minor modifications in the AdS calculation.

The perturbations in dS space we are interested in can be studied with the action given in eq.(4.46). For the analogous problem in AdS space we start with the action

$$S = \frac{M_{Pl}^2}{2}\int d^4x\sqrt{g}\Big[R - 2\Lambda - (\nabla\delta\phi)^2\Big] \tag{4.91}$$

where $g_{\mu\nu}$ here is a Euclidean signature metric, and Λ, the cosmological constant. AdS space arises as the solution of this system with metric, eq.(4.47), and with the scalar $\delta\phi = 0$. The radius $R_{\rm AdS}$ in eq.(4.47) is related to Λ [3] by

$$\Lambda = -\frac{3}{R_{\rm AdS}^2}. \tag{4.92}$$

To simplify the analysis it is convenient to set $R_{\rm AdS} = 1$, the dependence on $R_{\rm AdS}$ can be restored by noting that the action is dimensionless, so that the prefactor which multiples the action must appear in the combination $\frac{M_{Pl}^2 R_{\rm AdS}^2}{2}$. The metric in eq.(4.47) then becomes

$$ds^2 = \frac{dz^2 + (dx^i)^2}{z^2} \tag{4.93}$$

where the index i takes values, $i = 1, 2, 3$.

For studying the small perturbations we expand the metric by writing

$$g_{\mu\nu} = \bar{g}_{\mu\nu} + \delta g_{\mu\nu} \tag{4.94}$$

where $\bar{g}_{\mu\nu}$ is the AdS metric given in eq.(4.93) and $\delta g_{\mu\nu}$ is the metric perturbation. Expanding the action, eq.(4.91) in powers of the perturbations $\delta g_{\mu\nu}$ and $\delta\phi$ then gives,

$$S = S_0 + S^{(2)}_{\rm grav} - \frac{M_{Pl}^2}{2}\int d^4x\sqrt{\bar{g}}\ \bar{g}^{\mu\nu}\ \partial_\mu(\delta\phi)\partial_\nu(\delta\phi) + S_{\rm int}. \tag{4.95}$$

S_0 in eq.(4.95) is the action for the background AdS space with metric eq.(4.93). $S^{(2)}_{\rm grav}$ is the quadratic part of the metric perturbation. Using the action given in [158] (see also eq.(98) in [159]), and using the first order equations of motion the quadratic action for the graviton can be simplified to [160]

$$S^{(2)}_{\rm grav} = \frac{M_{Pl}^2}{8}\int d^4\boldsymbol{x}\sqrt{\bar{g}}\left(\widetilde{\delta g}^{\mu\nu}\Box\delta g_{\mu\nu} + 2\widetilde{\delta g}^{\mu\nu}R_{\mu\rho\nu\sigma}\delta g^{\rho\sigma} + 2\nabla^\rho\widetilde{\delta g}_{\rho\mu}\nabla^\sigma\widetilde{\delta g}^{\mu}_{\sigma}\right), \tag{4.96}$$

with $\widetilde{\delta g}^{\mu\nu} = \delta g^{\mu\nu} - \frac{1}{2}\bar{g}^{\mu\nu}\delta g^\alpha_\alpha$. We also expand $S_{\rm int}$ to linear order in $\delta g_{\mu\nu}$, since higher order terms are not relevant to our calculation.

$$S_{\rm int} = \frac{M_{Pl}^2}{2}\int d^4x\sqrt{\bar{g}}\ \frac{1}{2}\ \delta g^{\mu\nu}T_{\mu\nu}, \tag{4.97}$$

where the scalar stress energy is

$$T_{\mu\nu} = 2\partial_\mu(\delta\phi)\partial_\nu(\delta\phi) - \bar{g}_{\mu\nu}\bar{g}^{\alpha\beta}\partial_\alpha(\delta\phi)\partial_\beta(\delta\phi). \tag{4.98}$$

[3] Note that in our conventions $\Lambda < 0$ corresponds to AdS space.

Let us note that the quadratic term, eq.(4.96), can also be written as, see eq.(98) in [159],

$$
\begin{aligned}
S^{(2)}_{grav} =& \frac{M_{Pl}^2}{2}\int d^4x\sqrt{\bar{g}}\Big[-2\Lambda\Big\{-\frac{1}{4}\delta g_{\alpha\beta}\delta g^{\alpha\beta}+\frac{1}{8}(\delta g^{\alpha}_{\alpha})^2\Big\}+\Big\{-R\Big(\frac{1}{8}(\delta g^{\alpha}_{\alpha})^2 \\
&-\frac{1}{4}\delta g_{\alpha\beta}\delta g^{\alpha\beta}\Big)-\delta g^{\nu\beta}\delta g_{\beta\alpha}R^{\alpha\nu}+\frac{1}{2}\delta g^{\alpha}_{\alpha}\delta g^{\nu\beta}R_{\nu\beta}-\frac{1}{4}\nabla_{\mu}\delta g_{\alpha\beta}\nabla^{\mu}\delta g^{\alpha\beta} \\
&+\frac{1}{4}\nabla_{\mu}\delta g^{\alpha}_{\alpha}\nabla^{\mu}\delta g^{\beta}_{\beta}-\frac{1}{2}\nabla_{\beta}\delta g^{\alpha}_{\alpha}\nabla_{\mu}\delta g^{\beta\mu}+\frac{1}{2}\nabla^{\alpha}\delta g^{\nu\beta}\nabla_{\nu}\delta g_{\alpha\beta}\Big\}\Big].
\end{aligned}
\tag{4.99}
$$

From eq.(4.95) we see that the scalar perturbation is a free field with only gravitational interactions. The four point function arises from S_{int} due to single graviton exchange. The scalar perturbation gives rise to a stress energy which sources a metric perturbation. Using the action eq.(4.95) we can solve for $\delta g_{\mu\nu}$ in terms of this source and a suitable Green's function. Then substitute the solution for the metric perturbation back into the action to obtain the on-shell action as a function of $\phi_{\boldsymbol{k}_i}$.

From eq.(4.95) we see that to leading order the scalar perturbation, $\delta\phi$, satisfies the free equation in AdS space. For a mode with momentum dependence $e^{i\boldsymbol{k}\cdot\boldsymbol{x}}$ the solution, which is regular as $z\to\infty$ is given by

$$
\delta\phi = (1+kz)e^{-kz}e^{i\boldsymbol{k}\cdot\boldsymbol{x}}. \tag{4.100}
$$

A general solution is obtained by linearly superposing solutions of this type. For calculating the four point scalar correlator we take

$$
\delta\phi = \sum_{i=1}^{4}\phi(\boldsymbol{k}_i)(1+k_iz)e^{-k_iz}e^{i\boldsymbol{k}_i\cdot\boldsymbol{x}} \tag{4.101}
$$

so that it is a sum of four modes with momenta $\boldsymbol{k_1},\cdots\boldsymbol{k_4}$, with coefficients $\phi(\boldsymbol{k}_i)$.

Notice that towards the boundary of AdS space, as $z\to 0$,

$$
\delta\phi = \sum_{i=1}^{4}\phi(\boldsymbol{k}_i)e^{i\boldsymbol{k}\cdot\boldsymbol{x}}. \tag{4.102}
$$

Thus the procedure above yields the partition function in AdS space as a function of the external scalar source, eq.(4.102). On suitably analytically continuing this answer we will then obtain the wave function in de Sitter space as a functional of the boundary value of the scalar field given in eq.(4.102) from where the four point correlator can be obtained.

To proceed we must fix a gauge for the metric perturbations, because it is only after doing so we can solve for the metric uniquely in terms of the matter stress tensor. Alternately stated, the Feynman diagram for graviton exchange involves the graviton propagator, which is well defined only after a choice of gauge for the graviton. We will choose the gauge

$$\delta g_{zz} = 0, \quad \delta g_{zi} = 0, \tag{4.103}$$

with $i = 1, 2, 3$, taking values over the x^i directions. We emphasize that, at this stage, our final answer for the correlation function in anti-de Sitter space, or the on shell action is gauge invariant and independent of our choice of gauge above. After the analytic continuation, eq.(4.48), this gauge goes over to the gauge eq.(4.15), eq.(4.16) discussed in section 4.2.1 in the context of dS space. [4]

The on-shell action, with boundary values set for the various perturbations, has an expansion precisely analogous to (4.37). As we mentioned there, the only unknown coefficient is the four-point correlation function $\langle O(\boldsymbol{x_1})O(\boldsymbol{x_2})O(\boldsymbol{x_3})O(\boldsymbol{x_4})\rangle$. Although, at tree-level this correlator can be computed by solving the classical equations of motion, it is more convenient to simply evaluate the Feynman-Witten diagrams shown in Fig.(4.1). The answer is then simply

$$\begin{aligned} S^{\text{AdS}}_{\text{on-shell}} = \frac{M_{\text{pl}}^2 R_{\text{AdS}}^2}{8} \int \frac{dz_1}{z_1^4}\frac{dz_2}{z_2^4} d^3x_1 d^3x_2 \bar{g}^{i_1i_2}\bar{g}^{j_1j_2} T_{i_1j_1}(x_1,z_1) G^{\text{grav}}_{i_2j_2,k_2l_2}(x_1,z_1,x_2,z_2) \\ \bar{g}^{k_1k_2}\bar{g}^{l_1l_2} T_{k_1l_1}(x_2,z_2). \end{aligned} \tag{4.104}$$

In this equation the scalar stress-tensor T_{ij} is given in (4.98), and the graviton propagator G^{grav} is given by [160, 161]

$$G^{\text{grav}}_{ij,kl} = \int \frac{d^3\boldsymbol{k}}{(2\pi)^3} e^{i\boldsymbol{k}\cdot(\boldsymbol{x}_1-\boldsymbol{x}_2)} \int_0^\infty \frac{dp^2}{2} \left[\frac{J_{\frac{3}{2}}(pz_1) J_{\frac{3}{2}}(pz_2)}{\sqrt{z_1 z_2}\,(\boldsymbol{k}^2+p^2)} \frac{1}{2} \left(\mathcal{T}_{ik}\mathcal{T}_{jl} + \mathcal{T}_{il}\mathcal{T}_{jk} - \mathcal{T}_{ij}\mathcal{T}_{kl} \right) \right], \tag{4.105}$$

where

$$\mathcal{T}_{ij} = \delta_{ij} + \frac{k_i k_j}{p^2}. \tag{4.106}$$

Since the x-integrals in (4.104) just impose momentum conservation in the boundary directions, the entire four-point function calculation boils down to doing a simple integral in the radial (z) direction. Here, the factors of $\frac{1}{z^4}$ come from the determinant of the metric to give the appropriate volume factor.

Note that the projector that appears in the graviton propagator is not transverse and traceless. As we also discuss in greater detail below in section 4.6.2, this is the well known analogue of the fact that the axial gauge propagator in flat space also has a longitudinal component. For calculational purposes it is convenient to break up our answer into the contribution from the transverse graviton propagator, and the longitudinal propagator. This leads us to write the graviton propagator in a form that was analyzed in [162] (see eq.

[4]The conformal time η in eq.(4.48) is related to t in eq.(4.14) by $\eta = e^{-Ht}$.

4.14 of that paper), and we find that the four point correlation function

$$S^{\text{AdS}}_{\text{on-shell}} = \frac{M_{Pl}^2 R_{\text{AdS}}^2}{2}\frac{1}{4}[\widetilde{W} + 2R], \tag{4.107}$$

where, $\widetilde{W}$ is obtained from the scalar stress tensor, eq.(4.98), and the transverse graviton Greens function, $\widetilde{G}_{ij,kl}(z_1, \boldsymbol{x}_1; z_2, \boldsymbol{x}_2)$.

$$\widetilde{W} = \int dz_1 d^3\boldsymbol{x}_1 dz_2 d^3\boldsymbol{x}_2 T_{i_1j_1}(z_1,\boldsymbol{x}_1)\delta^{i_1i_2}\delta^{j_1j_2}\widetilde{G}_{i_2j_2,k_2l_2}(z_1,\boldsymbol{x}_1;z_2,\boldsymbol{x}_2)\delta^{k_1k_2}\delta^{l_1l_2}T_{k_1l_1}(z_2,\boldsymbol{x}_2)\,. \tag{4.108}$$

In the expression above, we have also canceled off the volume factors of $\frac{1}{z^4}$ in (4.104) with the two factors of z^2 in the raised metric. The transverse graviton Green function is almost the same as (4.105)

$$\begin{aligned}\widetilde{G}_{ij,kl}(z_1,\boldsymbol{x}_1;z_2,\boldsymbol{x}_2) = \int \frac{d^3\boldsymbol{k}}{(2\pi)^3}e^{i\boldsymbol{k}\cdot(\boldsymbol{x}_1-\boldsymbol{x}_2)}\int_0^\infty \frac{dp^2}{2}\Bigg[\frac{J_{\frac{3}{2}}(pz_1)J_{\frac{3}{2}}(pz_2)}{\sqrt{z_1z_2}\,(\boldsymbol{k}^2+p^2)}\frac{1}{2} \\ \left(\widetilde{\mathcal{T}}_{ik}\widetilde{\mathcal{T}}_{jl}+\widetilde{\mathcal{T}}_{il}\widetilde{\mathcal{T}}_{jk}-\widetilde{\mathcal{T}}_{ij}\widetilde{\mathcal{T}}_{kl}\right)\Bigg],\end{aligned} \tag{4.109}$$

except that $\widetilde{\mathcal{T}}_{ij}$, which appears here, is a projector onto directions perpendicular to $\boldsymbol{k}$,

$$\widetilde{\mathcal{T}}_{ij} = \delta_{ij} - \frac{k_ik_j}{k^2}. \tag{4.110}$$

After momentum conservation is imposed on the intermediate graviton, we have $\boldsymbol{k} = \boldsymbol{k_1}+\boldsymbol{k_2}$. Details leading to eq.(4.108) are discussed in Appendix C.3.

The other term on the RHS of eq.(4.107), R, arises from the longitudinal graviton contribution (which is just the difference between (4.105) and (4.109)) and it is convenient for us to write it as a sum of three terms,

$$R = R_1 + R_2 + R_3, \tag{4.111}$$

with,

$$\begin{aligned}R_1 &= -\int \frac{d^3\boldsymbol{x}_1dz_1}{z_1^2}T_{zj}(\boldsymbol{x}_1,z_1)\frac{1}{\partial^2}T_{zj}(\boldsymbol{x}_1,z_1),\\ R_2 &= -\frac{1}{2}\int \frac{d^3\boldsymbol{x}_1dz_1}{z_1}\;\partial_jT_{zj}(\boldsymbol{x}_1,z_1)\frac{1}{\partial^2}T_{zz}(\boldsymbol{x}_1,z_1),\\ R_3 &= -\frac{1}{4}\int \frac{d^3\boldsymbol{x}_1dz_1}{z_1^2}\;\partial_jT_{zj}(\boldsymbol{x}_1,z_1)\left(\frac{1}{\partial^2}\right)^2\partial_iT_{zi}(\boldsymbol{x}_1,z_1),\end{aligned} \tag{4.112}$$

where $\frac{1}{\partial^2}$ denotes the inverse of $\partial_{x^i}\partial_{x^j}\delta^{ij}$.

Substituting for $\delta\phi$ from eq.(4.102) in the stress tensor eq.(4.98) one can calculate both these contributions. The resulting answer is the sum of three terms shown in Fig.(4.1), which can be thought of as corresponding to S, T, and U channel contributions respectively. In the S channel exchange the momentum carried by the graviton along the x^i directions is,

$$\boldsymbol{k} = \boldsymbol{k_1} + \boldsymbol{k_2}. \tag{4.113}$$

The contributions of the T, U channels can be obtained by replacing $\boldsymbol{k_2} \leftrightarrow \boldsymbol{k_3}$, and $\boldsymbol{k_2} \leftrightarrow \boldsymbol{k_4}$ respectively.

The S channel contribution for $\widetilde{W}$ which we denote by $\widetilde{W}^S(\boldsymbol{k_1}, \boldsymbol{k_2}, \boldsymbol{k_3}, \boldsymbol{k_4})$ turns out to be

$$\widetilde{W}^S(\boldsymbol{k_1}, \boldsymbol{k_2}, \boldsymbol{k_3}, \boldsymbol{k_4}) = 16(2\pi)^3\ \delta^3\Big(\sum_{J=1}^{4} \boldsymbol{k}_J\Big)\Big(\prod_{I=1}^{4} \phi(\boldsymbol{k}_I)\Big)\widehat{W}^S(\boldsymbol{k_1}, \boldsymbol{k_2}, \boldsymbol{k_3}, \boldsymbol{k_4}) \tag{4.114}$$

where

$$\begin{aligned}
&\widehat{W}^S(\boldsymbol{k_1}, \boldsymbol{k_2}, \boldsymbol{k_3}, \boldsymbol{k_4}) = -2\Bigg[\Bigg\{\boldsymbol{k_1}.\boldsymbol{k_3} + \frac{\{(\boldsymbol{k_2}+\boldsymbol{k_1}).\boldsymbol{k_1}\}\{(\boldsymbol{k_4}+\boldsymbol{k_3}).\boldsymbol{k_3}\}}{|\boldsymbol{k_1}+\boldsymbol{k_2}|^2}\Bigg\} \\
&\Bigg\{\boldsymbol{k_2}.\boldsymbol{k_4} + \frac{\{(\boldsymbol{k_1}+\boldsymbol{k_2}).\boldsymbol{k_2}\}\{(\boldsymbol{k_3}+\boldsymbol{k_4}).\boldsymbol{k_4}\}}{|\boldsymbol{k_1}+\boldsymbol{k_2}|^2}\Bigg\} + \Bigg\{\boldsymbol{k_1}.\boldsymbol{k_4} + \frac{\{(\boldsymbol{k_2}+\boldsymbol{k_1}).\boldsymbol{k_1}\}\{(\boldsymbol{k_4}+\boldsymbol{k_3}).\boldsymbol{k_4}\}}{|\boldsymbol{k_1}+\boldsymbol{k_2}|^2}\Bigg\} \\
&\Bigg\{\boldsymbol{k_2}.\boldsymbol{k_3} + \frac{\{(\boldsymbol{k_2}+\boldsymbol{k_1}).\boldsymbol{k_2}\}\{(\boldsymbol{k_4}+\boldsymbol{k_3}).\boldsymbol{k_3}\}}{|\boldsymbol{k_1}+\boldsymbol{k_2}|^2}\Bigg\} - \Bigg\{\boldsymbol{k_1}.\boldsymbol{k_2} - \frac{\{(\boldsymbol{k_2}+\boldsymbol{k_1}).\boldsymbol{k_1}\}\{(\boldsymbol{k_1}+\boldsymbol{k_2}).\boldsymbol{k_2}\}}{|\boldsymbol{k_1}+\boldsymbol{k_2}|^2}\Bigg\} \\
&\Bigg\{\boldsymbol{k_3}.\boldsymbol{k_4} - \frac{\{(\boldsymbol{k_3}+\boldsymbol{k_4}).\boldsymbol{k_4}\}\{(\boldsymbol{k_4}+\boldsymbol{k_3}).\boldsymbol{k_3}\}}{|\boldsymbol{k_1}+\boldsymbol{k_2}|^2}\Bigg\}\Bigg] \times \\
&\Bigg[\Bigg\{\frac{k_1k_2(k_1+k_2)^2\left((k_1+k_2)^2 - k_3^2 - k_4^2 - 4k_3k_4\right)}{(k_1+k_2-k_3-k_4)^2(k_1+k_2+k_3+k_4)^2(k_1+k_2-|\boldsymbol{k_1}+\boldsymbol{k_2}|)(k_1+k_2+|\boldsymbol{k_1}+\boldsymbol{k_2}|)} \\
&\Big(-\frac{k_1+k_2}{2k_1k_2} - \frac{k_1+k_2}{-(k_1+k_2)^2+k_3^2+k_4^2+4k_3k_4} + \frac{k_1+k_2}{|\boldsymbol{k_1}+\boldsymbol{k_2}|^2-(k_1+k_2)^2} \\
&+ \frac{1}{-k_1-k_2+k_3+k_4} - \frac{1}{k_1+k_2+k_3+k_4} + \frac{3}{2(k_1+k_2)}\Big) + (1,2 \leftrightarrow 3,4)\Bigg\} \\
&- \frac{|\boldsymbol{k_1}+\boldsymbol{k_2}|^3\left(-k_1^2 - 4k_2k_1 - k_2^2 + |\boldsymbol{k_1}+\boldsymbol{k_2}|^2\right)\left(-k_3^2 - 4k_4k_3 - k_4^2 + |\boldsymbol{k_1}+\boldsymbol{k_2}|^2\right)}{2\left(-k_1^2 - 2k_2k_1 - k_2^2 + |\boldsymbol{k_1}+\boldsymbol{k_2}|^2\right)^2\left(-k_3^2 - 2k_4k_3 - k_4^2 + |\boldsymbol{k_1}+\boldsymbol{k_2}|^2\right)^2}\Bigg],
\end{aligned} \tag{4.115}$$

The S channel contribution for R is denoted by $R^S(\boldsymbol{k_1}, \boldsymbol{k_2}, \boldsymbol{k_3}, \boldsymbol{k_4})$ and is given by

$$R^S(\boldsymbol{k_1}, \boldsymbol{k_2}, \boldsymbol{k_3}, \boldsymbol{k_4}) = 16(2\pi)^3\ \delta^3\big(\sum_{J=1}^{4} \boldsymbol{k}_J\big)\Big[\prod_{I=1}^{4} \phi(\boldsymbol{k}_I)\Big]\widehat{R}^S(\boldsymbol{k_1}, \boldsymbol{k_2}, \boldsymbol{k_3}, \boldsymbol{k_4}), \tag{4.116}$$

where

$$\begin{aligned}
\widehat{R}^S(\boldsymbol{k_1}, \boldsymbol{k_2}, \boldsymbol{k_3}, \boldsymbol{k_4}) =& \frac{A_1(\boldsymbol{k_1}, \boldsymbol{k_2}, \boldsymbol{k_3}, \boldsymbol{k_4})}{(k_1+k_2+k_3+k_4)} + \frac{A_2(\boldsymbol{k_1}, \boldsymbol{k_2}, \boldsymbol{k_3}, \boldsymbol{k_4})}{(k_1+k_2+k_3+k_4)^2} \\
&+ \frac{A_3(\boldsymbol{k_1}, \boldsymbol{k_2}, \boldsymbol{k_3}, \boldsymbol{k_4})}{(k_1+k_2+k_3+k_4)^3}
\end{aligned} \tag{4.117}$$

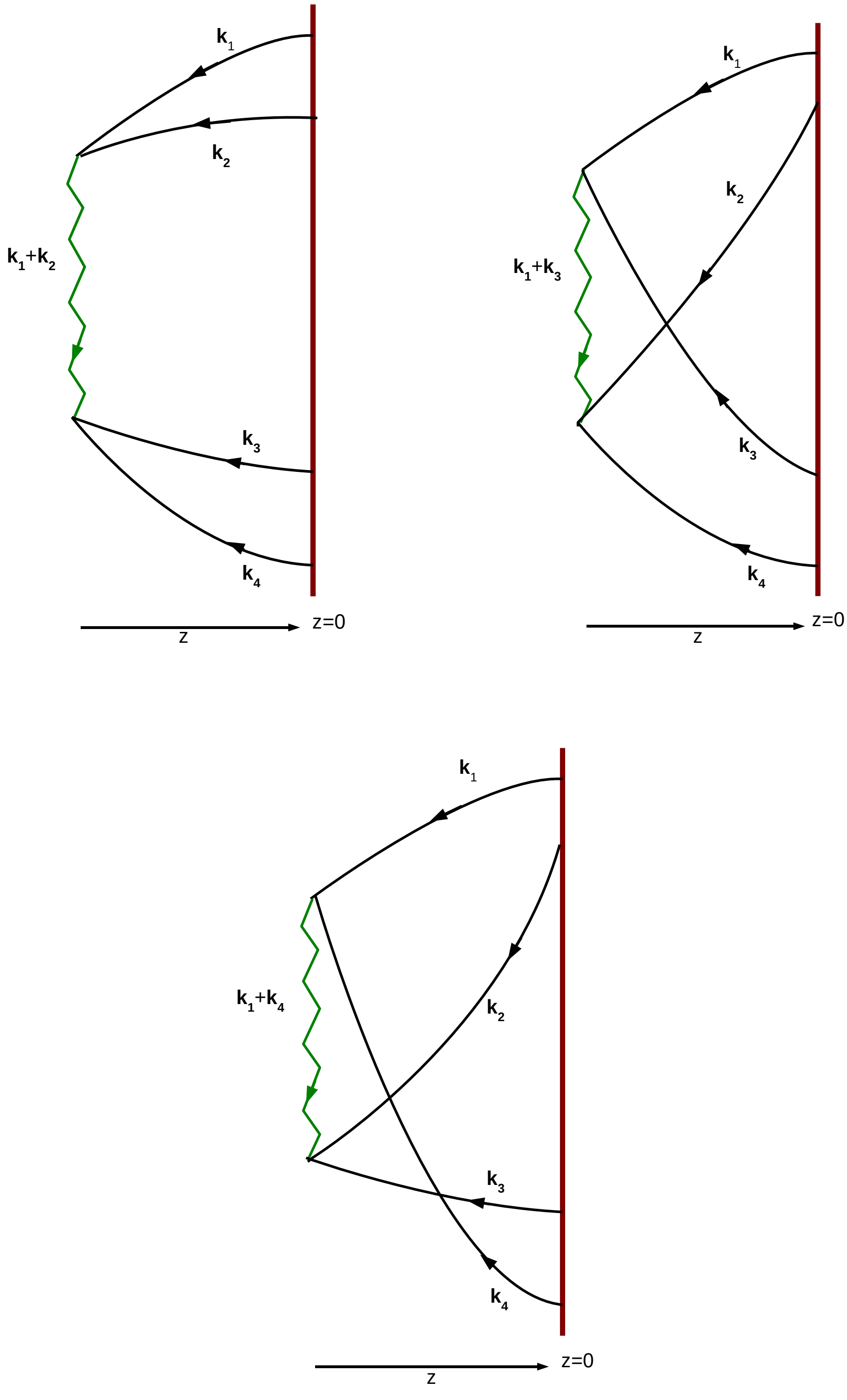

Figure 4.1: Three different contribution corresponding to S,T and U-channel to the scalar four point correlator are shown in the three figures. The brown solid vertical line represents the 3-dimensional boundary of AdS_4 at $z = 0$, the black solid lines are boundary to bulk scalar propagators whereas the green wavy lines are graviton propagators in the bulk.

with

$$A_1(\boldsymbol{k_1},\boldsymbol{k_2},\boldsymbol{k_3},\boldsymbol{k_4}) = \Bigg[\frac{\boldsymbol{k_3}\cdot\boldsymbol{k_4}\left(\boldsymbol{k_1}\cdot\boldsymbol{k_2}\left(k_1^2+k_2^2\right)+2k_1^2k_2^2\right)}{8|\boldsymbol{k_1}+\boldsymbol{k_2}|^2} + \{1,2\Leftrightarrow 3,4\}\Bigg]$$
$$- \frac{k_1^2\boldsymbol{k_2}\cdot\boldsymbol{k_3}k_4^2 + k_1^2\boldsymbol{k_2}\cdot\boldsymbol{k_4}k_3^2 + \boldsymbol{k_1}\cdot\boldsymbol{k_3}k_2^2k_4^2 + \boldsymbol{k_1}\cdot\boldsymbol{k_4}k_2^2k_3^2}{2|\boldsymbol{k_1}+\boldsymbol{k_2}|^2}$$
$$- \frac{\left(\boldsymbol{k_1}\cdot\boldsymbol{k_2}\left(k_1^2+k_2^2\right)+2k_1^2k_2^2\right)\left(\boldsymbol{k_3}\cdot\boldsymbol{k_4}\left(k_3^2+k_4^2\right)+2k_3^2k_4^2\right)}{8|\boldsymbol{k_1}+\boldsymbol{k_2}|^4}, \quad (4.118)$$

$$A_2(\boldsymbol{k_1},\boldsymbol{k_2},\boldsymbol{k_3},\boldsymbol{k_4}) = -\frac{1}{8|\boldsymbol{k_1}+\boldsymbol{k_2}|^4}\Bigg[k_3k_4(k_3+k_4)\left(\boldsymbol{k_1}\cdot\boldsymbol{k_2}\left(k_1^2+k_2^2\right)+2k_1^2k_2^2\right)$$
$$(k_3k_4+\boldsymbol{k_3}\cdot\boldsymbol{k_4}) + k_1k_2(k_1+k_2)(k_1k_2+\boldsymbol{k_1}\cdot\boldsymbol{k_2})\left(\boldsymbol{k_3}\cdot\boldsymbol{k_4}\left(k_3^2+k_4^2\right)+2k_3^2k_4^2\right)\Bigg]$$
$$-\frac{1}{2|\boldsymbol{k_1}+\boldsymbol{k_2}|^2}\Bigg[k_1^2\boldsymbol{k_2}\cdot\boldsymbol{k_3}k_4^2(k_2+k_3) + k_1^2\boldsymbol{k_2}\cdot\boldsymbol{k_4}k_3^2(k_2+k_4)$$
$$+\boldsymbol{k_1}\cdot\boldsymbol{k_3}k_2^2k_4^2(k_1+k_3) + \boldsymbol{k_1}\cdot\boldsymbol{k_4}k_2^2k_3^2(k_1+k_4)\Bigg]$$
$$+\Bigg[\frac{\boldsymbol{k_1}\cdot\boldsymbol{k_2}}{8|\boldsymbol{k_1}+\boldsymbol{k_2}|^2}\Big((k_1+k_2)\left(\boldsymbol{k_3}\cdot\boldsymbol{k_4}\left(k_3^2+k_4^2\right)+2k_3^2k_4^2\right)$$
$$+k_3k_4(k_3+k_4)(k_3k_4+\boldsymbol{k_3}\cdot\boldsymbol{k_4})\Big) + \{1,2\Leftrightarrow 3,4\}\Bigg], \quad (4.119)$$

$$A_3(\boldsymbol{k_1},\boldsymbol{k_2},\boldsymbol{k_3},\boldsymbol{k_4}) = -\frac{k_1k_2k_3k_4(k_1+k_2)(k_3+k_4)(k_1k_2+\boldsymbol{k_1}\cdot\boldsymbol{k_2})(k_3k_4+\boldsymbol{k_3}\cdot\boldsymbol{k_4})}{4|\boldsymbol{k_1}+\boldsymbol{k_2}|^4}$$
$$-\frac{k_1k_2k_3k_4(k_1\boldsymbol{k_2}\cdot\boldsymbol{k_3}k_4 + k_1\boldsymbol{k_2}\cdot\boldsymbol{k_4}k_3 + \boldsymbol{k_1}\cdot\boldsymbol{k_3}k_2k_4 + \boldsymbol{k_1}\cdot\boldsymbol{k_4}k_2k_3)}{|\boldsymbol{k_1}+\boldsymbol{k_2}|^2}$$
$$+\frac{1}{4|\boldsymbol{k_1}+\boldsymbol{k_2}|^2}\Bigg[k_1k_2(k_1k_2+\boldsymbol{k_1}\cdot\boldsymbol{k_2})\left(\boldsymbol{k_3}\cdot\boldsymbol{k_4}\left(k_3^2+k_4^2\right)+2k_3^2k_4^2\right)$$
$$+\boldsymbol{k_1}\cdot\boldsymbol{k_2}k_3k_4(k_1+k_2)(k_3+k_4)(k_3k_4+\boldsymbol{k_3}\cdot\boldsymbol{k_4}) + \{1,2\Leftrightarrow 3,4\}\Bigg]$$
$$+\frac{3k_1k_2k_3k_4(k_1k_2+\boldsymbol{k_1}\cdot\boldsymbol{k_2})(k_3k_4+\boldsymbol{k_3}\cdot\boldsymbol{k_4})}{4|\boldsymbol{k_1}+\boldsymbol{k_2}|^2}., \quad (4.120)$$

Details leading to these results are given in Appendix C.3. The full answer for $S^{\text{AdS}}_{\text{on-shell}}$ is obtained by adding the contributions of the S, T, U channels. This gives, from eq.(4.107),

$$S^{\text{AdS}}_{\text{on-shell}} = \frac{M_{\text{pl}}^2R_{\text{AdS}}^2}{4}\Bigg[\frac{1}{2}\Big\{\widetilde{W}^S(\boldsymbol{k_1},\boldsymbol{k_2},\boldsymbol{k_3},\boldsymbol{k_4}) + \widetilde{W}^S(\boldsymbol{k_1},\boldsymbol{k_3},\boldsymbol{k_2},\boldsymbol{k_4}) + \widetilde{W}^S(\boldsymbol{k_1},\boldsymbol{k_4},\boldsymbol{k_3},\boldsymbol{k_2})\Big\}$$
$$+R^S(\boldsymbol{k_1},\boldsymbol{k_2},\boldsymbol{k_3},\boldsymbol{k_4}) + R^S(\boldsymbol{k_1},\boldsymbol{k_3},\boldsymbol{k_2},\boldsymbol{k_4}) + R^S(\boldsymbol{k_1},\boldsymbol{k_4},\boldsymbol{k_3},\boldsymbol{k_2})\Bigg] \quad (4.121)$$

where $\widetilde{W}^S(\boldsymbol{k_1},\boldsymbol{k_2},\boldsymbol{k_3},\boldsymbol{k_4})$ is given in eq.(4.114) and $R^S(\boldsymbol{k_1},\boldsymbol{k_2},\boldsymbol{k_3},\boldsymbol{k_4})$ is given in eq.(4.116).

4.4.2 Analytic Continuation to de Sitter Space

As we explained in section 4.2.4, the on-shell action $S^{\text{AdS}}_{\text{on-shell}}$ obtained above can be analytically continued to the de Sitter space on-shell action $S^{dS}_{\text{on-shell}}$. So, the AdS correlator that we have computed above continues directly to the coefficient function in the wave function of the Universe at late times on de Sitter space. More precisely, the result of eq.(4.121) is just the Fourier transform of the coefficient function we are interested in by

$$\langle O(\boldsymbol{x}_1)O(\boldsymbol{x}_2)O(\boldsymbol{x}_3)O(\boldsymbol{x}_4)\rangle = \int \prod_{I=1}^{4} \frac{d^3k_I}{(2\pi)^3} e^{i(\boldsymbol{k}_I\cdot\boldsymbol{x}_I)} \langle O(\boldsymbol{k_1})O(\boldsymbol{k_2})O(\boldsymbol{k_3})O(\boldsymbol{k_4})\rangle \tag{4.122}$$

where

$$\begin{aligned}\langle O(\boldsymbol{k_1})O(\boldsymbol{k_2})O(\boldsymbol{k_3})O(\boldsymbol{k_4})\rangle = -4(2\pi)^3\delta^3(\sum_{i=1}^{3}\boldsymbol{k}_i)\Bigg[\frac{1}{2}\Bigg\{&\widehat{W}^S(\boldsymbol{k_1},\boldsymbol{k_2},\boldsymbol{k_3},\boldsymbol{k_4})\\ +\widehat{W}^S(\boldsymbol{k_1},\boldsymbol{k_3},\boldsymbol{k_2},\boldsymbol{k_4})+\widehat{W}^S(\boldsymbol{k_1},\boldsymbol{k_4},\boldsymbol{k_3},\boldsymbol{k_2})\Bigg\}&+\widehat{R}^S(\boldsymbol{k_1},\boldsymbol{k_2},\boldsymbol{k_3},\boldsymbol{k_4})\\ +\widehat{R}^S(\boldsymbol{k_1},\boldsymbol{k_3},\boldsymbol{k_2},\boldsymbol{k_4})+\widehat{R}^S(\boldsymbol{k_1},\boldsymbol{k_4},\boldsymbol{k_3},\boldsymbol{k_2})\Bigg]&\end{aligned} \tag{4.123}$$

where $\widehat{W}^S(\boldsymbol{k_1},\boldsymbol{k_2},\boldsymbol{k_3},\boldsymbol{k_4})$ is given in eq.(4.115) and $\widehat{R}^S(\boldsymbol{k_1},\boldsymbol{k_2},\boldsymbol{k_3},\boldsymbol{k_4})$ is given in eq.(4.117). As was mentioned in subsection 4.2.2, once the coefficient function $\langle O(\boldsymbol{x}_1)O(\boldsymbol{x}_2)O(\boldsymbol{x}_3)O(\boldsymbol{x}_4)\rangle$ is obtained in eq.(4.122), eq.(4.123), we now know all the relevant terms in the wave function in eq.(4.37).

4.5 Computation of the Four Point Scalar Correlator in de Sitter Space

With the wave function eq.(4.37), in our hand we can proceed to calculate the scalar four point correlator $\langle\delta\phi(\boldsymbol{x}_1)\delta\phi(\boldsymbol{x}_2)\delta\phi(\boldsymbol{x}_3)\delta\phi(\boldsymbol{x}_4)\rangle$ which was defined in eq.(4.86). As was discussed in subsection 4.3.1 we need to fix the gauge more completely for this purpose. We will work below first in gauge 2, described in subsection 4.2.1 and then at the end of the calculation transform the answer to be in gauge 1, section 4.2.1.

In gauge 2 the metric perturbation γ_{ij} is transverse and traceless. Working in this gauge we follow the strategy outlined in subsection 4.3.1 and first integrate out the metric perturbation to obtain a probability distribution $P[\delta\phi]$ defined in eq.(4.88). The functional integral over γ_{ij} is quadratic. Integrating it out gives, in momentum space,

$$\gamma_{ij}(k) = -\frac{1}{2k^3}\int \frac{d^3k_1}{(2\pi)^3}\frac{d^3k_2}{(2\pi)^3}\delta\phi(\boldsymbol{k_1})\delta\phi(\boldsymbol{k_2})\langle O(-\boldsymbol{k_1})O(-\boldsymbol{k_2})T^{lm}(\boldsymbol{k})\rangle\widehat{P}_{lmij}(\boldsymbol{k}) \tag{4.124}$$

where

$$\begin{aligned} \widehat{P}_{ijkl}(\boldsymbol{k}) &= \widetilde{\mathcal{T}}_{ik}(\boldsymbol{k})\widetilde{\mathcal{T}}_{jl}(\boldsymbol{k}) + \widetilde{\mathcal{T}}_{il}(\boldsymbol{k})\widetilde{\mathcal{T}}_{jk}(\boldsymbol{k}) - \widetilde{\mathcal{T}}_{ij}(\boldsymbol{k})\widetilde{\mathcal{T}}_{kl}(\boldsymbol{k}), \\ \text{with } \widetilde{\mathcal{T}}_{ik}(\boldsymbol{k}) &= \delta_{ik} - \frac{k_i k_k}{k^2}. \end{aligned} \tag{4.125}$$

Eq.(4.124) determines the $\gamma_{ij}(k)$ in terms of the scalar perturbation $\delta\phi(k)$. Substituting back then leads to the expression,

$$\begin{aligned} P[\delta\phi(\boldsymbol{k})] = \exp\Bigg[\frac{M_{Pl}^2}{H^2}\Bigg(&-\int \frac{d^3k_1}{(2\pi)^3}\frac{d^3k_2}{(2\pi)^3}\ \delta\phi(\boldsymbol{k_1})\delta\phi(\boldsymbol{k_2})\langle O(-\boldsymbol{k_1})O(-\boldsymbol{k_2})\rangle \\ &+\int\prod_{J=1}^{4}\left\{\frac{d^3k_J}{(2\pi)^3}\delta\phi(\boldsymbol{k}_J)\right\}\Bigg\{\frac{1}{12}\langle O(-\boldsymbol{k_1})O(-\boldsymbol{k_2})O(-\boldsymbol{k_3})O(-\boldsymbol{k_4})\rangle \\ &+\frac{1}{8}\langle O(-\boldsymbol{k_1})O(-\boldsymbol{k_2})T_{ij}(\boldsymbol{k_1}+\boldsymbol{k_2})\rangle'\langle O(-\boldsymbol{k_3})O(-\boldsymbol{k_4})T_{kl}(\boldsymbol{k_3}+\boldsymbol{k_4})\rangle' \\ &(2\pi)^3\delta^3\Big(\sum_{J=1}^{4}\boldsymbol{k}_J\Big)\widehat{P}_{ijkl}(\boldsymbol{k_1}+\boldsymbol{k_2})\frac{1}{|\boldsymbol{k_1}+\boldsymbol{k_2}|^3}\Bigg\}\Bigg)\Bigg] \end{aligned} \tag{4.126}$$

with $\widehat{P}_{ijkl}(\boldsymbol{k_1}+\boldsymbol{k_2})$ being defined in eq.(4.125) and the prime in $\langle O(\boldsymbol{k_1})O(\boldsymbol{k_2})T_{ij}(\boldsymbol{k_3})\rangle'$ signifies that a factor of $(2\pi)^3\delta^3\big(\sum_{l=1}^4 \boldsymbol{k}_l\big)$ is being stripped off from the unprimed correlator $\langle O(\boldsymbol{k_1})O(\boldsymbol{k_2})T_{ij}(\boldsymbol{k_3})\rangle$, *i.e.*

$$\langle O(\boldsymbol{k_1})O(\boldsymbol{k_2})T_{ij}(\boldsymbol{k_3})\rangle = (2\pi)^3\delta^3\Big(\sum_{J=1}^{4}\boldsymbol{k}_J\Big)\langle O(\boldsymbol{k_1})O(\boldsymbol{k_2})T_{ij}(\boldsymbol{k_3})\rangle'. \tag{4.127}$$

We see that in the exponent on the RHS of eq.(4.126) there are two terms which are quartic in $\delta\phi$, the first is proportional to the $\langle O(\boldsymbol{k_1})O(\boldsymbol{k_2})O(\boldsymbol{k_3})O(\boldsymbol{k_4})\rangle$ coefficient function, and the second is an extra term which arises in the process of integration out γ_{ij} to obtain the probability distribution, $P[\delta\phi]$.

The four function can now be calculated from $P[\delta\phi(\boldsymbol{k})]$ using eq.(4.89). The answer consists of two terms which come from the two quartic terms mentioned above respectively and are straightforward to compute. We will refer to these two contributions with the subscript "*CF*" and "*ET*" respectively below. The $\langle O(\boldsymbol{k_1})O(\boldsymbol{k_2})O(\boldsymbol{k_3})O(\boldsymbol{k_4})\rangle$ coefficient function in eq.(4.126) gives the contribution,

$$\begin{aligned} \langle\delta\phi(\boldsymbol{k_1})\delta\phi(\boldsymbol{k_2})\delta\phi(\boldsymbol{k_3})\delta\phi(\boldsymbol{k_4})\rangle_{CF} &= -8(2\pi)^3\delta^3\Big(\sum_{J=1}^{4}\boldsymbol{k}_J\Big)\frac{H^6}{M_{Pl}^6}\frac{1}{\prod_{J=1}^4(2k_J^3)} \\ &\Bigg[\frac{1}{2}\Big\{\widehat{W}^S(\boldsymbol{k_1},\boldsymbol{k_2},\boldsymbol{k_3},\boldsymbol{k_4})+\widehat{W}^S(\boldsymbol{k_1},\boldsymbol{k_3},\boldsymbol{k_2},\boldsymbol{k_4})+\widehat{W}^S(\boldsymbol{k_1},\boldsymbol{k_4},\boldsymbol{k_3},\boldsymbol{k_2})\Big\} \\ &+\widehat{R}^S(\boldsymbol{k_1},\boldsymbol{k_2},\boldsymbol{k_3},\boldsymbol{k_4})+\widehat{R}^S(\boldsymbol{k_1},\boldsymbol{k_3},\boldsymbol{k_2},\boldsymbol{k_4})+\widehat{R}^S(\boldsymbol{k_1},\boldsymbol{k_4},\boldsymbol{k_3},\boldsymbol{k_2})\Bigg] \end{aligned} \tag{4.128}$$

where $\widehat{W}^S(\boldsymbol{k_1},\boldsymbol{k_2},\boldsymbol{k_3},\boldsymbol{k_4})$ is given in eq.(4.115) and $\widehat{R}^S(\boldsymbol{k_1},\boldsymbol{k_2},\boldsymbol{k_3},\boldsymbol{k_4})$ is given in eq.(4.117).

While the ET term which arises due to integration out γ_{ij} gives,

$$\begin{aligned}\langle\delta\phi(\boldsymbol{k_1})\delta\phi(\boldsymbol{k_2})\delta\phi(\boldsymbol{k_3})\delta\phi(\boldsymbol{k_4})\rangle_{ET} = 4(2\pi)^3\delta^3\Big(\sum_{J=1}^{4}\boldsymbol{k}_J\Big)\frac{H^6}{M_{Pl}^6}\frac{1}{\prod_{J=1}^{4}(2k_J^3)} \\ \Big[\widehat{G}^S(\boldsymbol{k_1},\boldsymbol{k_2},\boldsymbol{k_3},\boldsymbol{k_4})+\widehat{G}^S(\boldsymbol{k_1},\boldsymbol{k_3},\boldsymbol{k_2},\boldsymbol{k_4})+\widehat{G}^S(\boldsymbol{k_1},\boldsymbol{k_4},\boldsymbol{k_3},\boldsymbol{k_2})\Big]\end{aligned} \quad (4.129)$$

where

$$\begin{aligned}\widehat{G}^S(\boldsymbol{k_1},\boldsymbol{k_2},\boldsymbol{k_3},\boldsymbol{k_4}) = \frac{S(\widetilde{\boldsymbol{k}},\boldsymbol{k_1},\boldsymbol{k_2})S(\widetilde{\boldsymbol{k}},\boldsymbol{k_3},\boldsymbol{k_4})}{|\boldsymbol{k_1}+\boldsymbol{k_2}|^3}\Bigg[\Bigg\{\boldsymbol{k_1}.\boldsymbol{k_3}+\frac{\{(\boldsymbol{k_2}+\boldsymbol{k_1}).\boldsymbol{k_1}\}\{(\boldsymbol{k_4}+\boldsymbol{k_3}).\boldsymbol{k_3}\}}{|\boldsymbol{k_1}+\boldsymbol{k_2}|^2}\Bigg\} \\ \Bigg\{\boldsymbol{k_2}.\boldsymbol{k_4}+\frac{\{(\boldsymbol{k_1}+\boldsymbol{k_2}).\boldsymbol{k_2}\}\{(\boldsymbol{k_3}+\boldsymbol{k_4}).\boldsymbol{k_4}\}}{|\boldsymbol{k_1}+\boldsymbol{k_2}|^2}\Bigg\}+\Bigg\{\boldsymbol{k_1}.\boldsymbol{k_4}+\frac{\{(\boldsymbol{k_2}+\boldsymbol{k_1}).\boldsymbol{k_1}\}\{(\boldsymbol{k_4}+\boldsymbol{k_3}).\boldsymbol{k_4}\}}{|\boldsymbol{k_1}+\boldsymbol{k_2}|^2}\Bigg\} \\ \Bigg\{\boldsymbol{k_2}.\boldsymbol{k_3}+\frac{\{(\boldsymbol{k_2}+\boldsymbol{k_1}).\boldsymbol{k_2}\}\{(\boldsymbol{k_4}+\boldsymbol{k_3}).\boldsymbol{k_3}\}}{|\boldsymbol{k_1}+\boldsymbol{k_2}|^2}\Bigg\}-\Bigg\{\boldsymbol{k_1}.\boldsymbol{k_2}-\frac{\{(\boldsymbol{k_2}+\boldsymbol{k_1}).\boldsymbol{k_1}\}\{(\boldsymbol{k_1}+\boldsymbol{k_2}).\boldsymbol{k_2}\}}{|\boldsymbol{k_1}+\boldsymbol{k_2}|^2}\Bigg\} \\ \Bigg\{\boldsymbol{k_3}.\boldsymbol{k_4}-\frac{\{(\boldsymbol{k_3}+\boldsymbol{k_4}).\boldsymbol{k_4}\}\{(\boldsymbol{k_4}+\boldsymbol{k_3}).\boldsymbol{k_3}\}}{|\boldsymbol{k_1}+\boldsymbol{k_2}|^2}\Bigg\}\Bigg]\end{aligned} \quad (4.130)$$

with

$$S(\widetilde{\boldsymbol{k}},\boldsymbol{k_1},\boldsymbol{k_2}) = (k_1+k_2+k_3)-\frac{\sum_{i>j}k_ik_j}{(k_1+k_2+k_3)}-\frac{k_1k_2k_3}{(k_1+k_2+k_3)^2}\Bigg|_{\widetilde{\boldsymbol{k}}=-(\boldsymbol{k_1}+\boldsymbol{k_2})}. \quad (4.131)$$

The full answer for the four point correlator in gauge 2 is then given by combining eq.(4.128) and eq.(4.129),

$$\begin{aligned}\langle\delta\phi(\boldsymbol{k_1})\delta\phi(\boldsymbol{k_2})\delta\phi(\boldsymbol{k_3})\delta\phi(\boldsymbol{k_4})\rangle = &\langle\delta\phi(\boldsymbol{k_1})\delta\phi(\boldsymbol{k_2})\delta\phi(\boldsymbol{k_3})\delta\phi(\boldsymbol{k_4})\rangle_{CF} \\ &+\langle\delta\phi(\boldsymbol{k_1})\delta\phi(\boldsymbol{k_2})\delta\phi(\boldsymbol{k_3})\delta\phi(\boldsymbol{k_4})\rangle_{ET}.\end{aligned} \quad (4.132)$$

Let us end this subsection with one comment. We see from eq.(4.126) that the ET contribution is determined by the $\langle OOT_{ij}\rangle$ correlator. As discussed in [131] this correlator is completely fixed by conformal invariance, so we see conformal symmetry completely fixes the ET contribution to the scalar 4 point correlator.

4.5.1 Final Result for the Scalar Four Point Function

We can now convert the result to gauge 1 defined in 4.2.1 using the relation [5] in eq.(4.34).

[5] The relation in eq.(4.34) has corrections in involving higher powers of ζ which could lead to additional contributions in eq.(4.133) that arise from the two point correlator of $\delta\phi$. However these corrections are further suppressed in the slow-roll parameters as discussed in Appendix C.4.

This gives

$$
\begin{aligned}
\langle\zeta(\boldsymbol{k_1})\zeta(\boldsymbol{k_2})\zeta(\boldsymbol{k_3})\zeta(\boldsymbol{k_4})\rangle = (2\pi)^3\delta^3\Big(\sum_{J=1}^{4}\boldsymbol{k}_J\Big)\frac{H^6}{M_{Pl}^6\epsilon^2}\frac{1}{\prod_{J=1}^{4}(2k_J^3)}& \\
\Big[\widehat{G}^S(\boldsymbol{k_1},\boldsymbol{k_2},\boldsymbol{k_3},\boldsymbol{k_4})+\widehat{G}^S(\boldsymbol{k_1},\boldsymbol{k_3},\boldsymbol{k_2},\boldsymbol{k_4})+\widehat{G}^S(\boldsymbol{k_1},\boldsymbol{k_4},\boldsymbol{k_3},\boldsymbol{k_2})& \\
-\widehat{W}^S(\boldsymbol{k_1},\boldsymbol{k_2},\boldsymbol{k_3},\boldsymbol{k_4})-\widehat{W}^S(\boldsymbol{k_1},\boldsymbol{k_3},\boldsymbol{k_2},\boldsymbol{k_4})-\widehat{W}^S(\boldsymbol{k_1},\boldsymbol{k_4},\boldsymbol{k_3},\boldsymbol{k_2})& \\
-2\Big\{\widehat{R}^S(\boldsymbol{k_1},\boldsymbol{k_2},\boldsymbol{k_3},\boldsymbol{k_4})+\widehat{R}^S(\boldsymbol{k_1},\boldsymbol{k_3},\boldsymbol{k_2},\boldsymbol{k_4})+\widehat{R}^S(\boldsymbol{k_1},\boldsymbol{k_4},\boldsymbol{k_3},\boldsymbol{k_2})\Big\}\Big]&
\end{aligned}
\tag{4.133}
$$

where $\widehat{W}^S(\boldsymbol{k_1},\boldsymbol{k_2},\boldsymbol{k_3},\boldsymbol{k_4})$ is given in eq.(4.115), $\widehat{R}^S(\boldsymbol{k_1},\boldsymbol{k_2},\boldsymbol{k_3},\boldsymbol{k_4})$ is given in eq.(4.117) and $\widehat{G}^S(\boldsymbol{k_1},\boldsymbol{k_2},\boldsymbol{k_3},\boldsymbol{k_4})$ is given in eq.(4.130).

Eq.(4.133) is one of the main results of this chapter. The variables $\boldsymbol{k}_i, i=1,2,3,4$ refer to the spatial momenta carried by the perturbations, The scalar perturbation ζ is defined in eq.(4.21), see also subsection 4.2.1, with $\zeta(\boldsymbol{k})$ being related to $\zeta(\boldsymbol{x})$ by a relation analogous to eq. (4.38). H is the Hubble constant during inflation defined in eq.(4.6), eq.(4.7). Our conventions for M_{Pl} are given in eq.(4.1), eq. (4.2). And the slow-roll parameter ϵ is defined in eq.(4.3), eq.(4.10).

The result, eq.(4.133), was derived in the leading slow-roll approximation. One way to incorporate corrections is to take H in eq.(4.133) to be the Hubble parameter when the modes cross the horizon, at least for situations where all momenta, $\boldsymbol{k}_i, i=1,\cdots 4$, are comparable in magnitude. Additional corrections which depend on the slow-roll parameters, ϵ,η, eq.(4.3), eq.(4.4), will also arise.

Comparison with previous results

Our result, eq.(4.133), agrees with that obtained in [107]. The result in [107] consists of two terms, the CI term and the ET term, see eq.(4.7). The CI term agrees with the $\hat{R}^S$ terms in eq.(4.133) which arise due the longitudinal graviton propagator, eq.(4.116). The $\hat{W}$ terms in eq.(4.133) arise from the transverse graviton propagator, eq.(4.108), while the G^S terms arise from the extra contribution due to integrating out the metric perturbation, eq.(4.130); these two together agree with the ET term in [107]. This comparison is carried out in a Mathematica file that is included with the source of the arXiv version of the paper [16] on which this chapter is based on.

4.6 Consistency Checks of the Result and Behavior in Some Limits

We now turn to carrying out some tests on our result for the four point function and examining its behavior in some limits. We will first verify that the result is consistent with the conformal invariance of de Sitter space in subsection 4.6.1, and then examine its behavior in various limits in subsection 4.6.3 and show that this agrees with expectations.

4.6.1 Conformal Invariance

Our calculation for the 4 point function was carried out at leading order in the slow-roll approximation, where the action governing the perturbations is that of a free scalar in de Sitter space, eq.(4.42). Therefore the result must be consistent with the full symmetry group of dS_4 space which is $SO(1,4)$ as was discussed in section 4.2. In fact the wave function, eq.(4.37), in this approximation itself should be invariant under this symmetry, as was discussed in section 4.3, see also, [117], [118] and [131].

For the four point function we are discussing, as was discussed towards the end of section eq.(4.3) after eq.(4.74), given the checks in the literature already in place only one remaining check needs to be carried out to establish the invariance of all relevant terms in the wave function. This is to check the invariance of the $\langle O(\boldsymbol{k_1})O(\boldsymbol{k_2})O(\boldsymbol{k_3})O(\boldsymbol{k_4})\rangle$ coefficient defined in eq.(4.122) and eq.(4.123). Conformal invariance of the coefficient function $\langle O(\boldsymbol{k_1})O(\boldsymbol{k_2})O(\boldsymbol{k_3})O(\boldsymbol{k_4})\rangle$ gives rise to the equation

$$\begin{aligned}&\langle \delta O(\boldsymbol{k_1})O(\boldsymbol{k_2})O(\boldsymbol{k_3})O(\boldsymbol{k_4})\rangle + \langle O(\boldsymbol{k_1})\delta O(\boldsymbol{k_2})O(\boldsymbol{k_3})O(\boldsymbol{k_4})\rangle \\ &+ \langle O(\boldsymbol{k_1})O(\boldsymbol{k_2})\delta O(\boldsymbol{k_3})O(\boldsymbol{k_4})\rangle + \langle O(\boldsymbol{k_1})O(\boldsymbol{k_2})O(\boldsymbol{k_3})\delta O(\boldsymbol{k_4})\rangle = 0\end{aligned} \tag{4.134}$$

where $\delta O(\boldsymbol{k})$ is given in Appendix C.2.2, eq.(C.29), and depends on $\boldsymbol{b}$ which is the parameter specifying the conformal transformation.

The coefficient function $\langle O(\boldsymbol{k_1})O(\boldsymbol{k_2})O(\boldsymbol{k_3})O(\boldsymbol{k_4})\rangle$ contains an overall delta function which enforces momentum conservation, eq.(4.123). As was argued in [118] all terms in eq.(4.134) where the derivatives act on this delta function sum to zero, so the effect of the derivative operators acting on it can be neglected. We can also use rotational invariance so take $\boldsymbol{b}$ to point along the x^1 direction. Our answer for $\langle O(\boldsymbol{k_1})O(\boldsymbol{k_2})O(\boldsymbol{k_3})O(\boldsymbol{k_4})\rangle$ is given in eq.(4.123). The complicated nature of the answer makes it very difficult to check analytically whether eq.(4.134) is met. However, it is quite simple to check this numerically. Using Mathematica [163], one finds that the LHS of eq.(4.134) does indeed vanish with the four point function given in eq.(4.123), there by showing that our result for $\langle O(\boldsymbol{k_1})O(\boldsymbol{k_2})O(\boldsymbol{k_3})O(\boldsymbol{k_4})\rangle$ does meet the requirement of conformal invariance. This then establishes that all terms in the wave function relevant for the four point function calculation are invariant under conformal symmetry.

A further subtlety having to do with gauge fixing, arises in discussing the conformal invariance of correlation functions, as opposed to the wave function, as discussed in section 4.3.1. The relevant terms in the probability distribution $P[\delta\phi]$ were obtained in eq.(4.126). The scalar four point function would be invariant if $P[\delta\phi]$ is invariant under the combined conformal transformation, eq.(4.71), eq.(4.72) and compensating coordinate transformation, eq.(4.77). From eq.(4.124) and eq.(4.79) we see that the compensating coordinate transformation in this case is specified by

$$v_i(\boldsymbol{k}) = -\frac{3b^k}{k^5}\int \frac{d^3k_1}{(2\pi)^3}\frac{d^3k_2}{(2\pi)^3}\delta\phi(\boldsymbol{k_1})\delta\phi(\boldsymbol{k_2})\langle O(-\boldsymbol{k_1})O(-\boldsymbol{k_2})T^{lm}(\boldsymbol{k})\rangle \widehat{P}_{lmki}(\boldsymbol{k}) \tag{4.135}$$

with $\widehat{P}_{lmki}(\boldsymbol{k})$ being given in eq.(4.125).

Thus the total change in $\delta\phi$, given in eq.(4.81) becomes,

$$\delta(\delta\phi(\boldsymbol{k})) = \delta^C(\delta\phi(\boldsymbol{k})) + \delta^R(\delta\phi(\boldsymbol{k})) \tag{4.136}$$

where $\delta^C(\delta\phi(\boldsymbol{k}))$ is given in eq.(C.28) of Appendix C.2.2. Using eq.(4.124) in eq.(4.85), $\delta^R(\delta\phi(\boldsymbol{k}))$ becomes,

$$\begin{aligned}\delta^R(\delta\phi(\boldsymbol{k})) = &-3ik^ib^k\int \frac{d^3\boldsymbol{k_1}}{(2\pi)^3}\frac{d^3\boldsymbol{k_2}}{(2\pi)^3}\frac{d^3\boldsymbol{k_3}}{(2\pi)^3}\frac{\widehat{P}_{lmki}(\boldsymbol{k}-\boldsymbol{k_2})}{|\boldsymbol{k}-\boldsymbol{k_2}|^5}\\ &\delta\phi(\boldsymbol{k_1})\delta\phi(\boldsymbol{k_2})\delta\phi(\boldsymbol{k_3})\langle O(-\boldsymbol{k_1})O(-\boldsymbol{k_2})T_{lm}(-\boldsymbol{k}+\boldsymbol{k_2})\rangle .\end{aligned} \tag{4.137}$$

Note in particular that v^i given in eq.(4.135) is quadratic in the scalar perturbation and as a result $\delta^R(\delta\phi)$ in eq.(4.137) is cubic in $\delta\phi$.

The probability distribution, $P[\delta\phi]$ upto quartic order in $\delta\phi$ is given in eq.(4.126) and consists of quadratic terms and quartic terms. In Appendix C.5 we show that, upto quartic order,

$$P[\delta\phi(\boldsymbol{k})] = P[\delta\phi(\boldsymbol{k}) + \delta\big(\delta\phi(\boldsymbol{k})\big)] \tag{4.138}$$

where $\delta\big(\delta\phi(\boldsymbol{k})\big)$ is given in eq.(4.136), so that $P[\delta\phi]$ is invariant under $\delta(\delta\phi)$ upto this order. This invariance arises as follows. The quadratic term in $P[\delta\phi]$ gives rise to a contribution going like $\delta\phi^4$, since $\delta^R(\delta\phi)$ is cubic in $\delta\phi$. This is canceled by a contribution coming from the quartic term due to $\delta^C(\delta\phi)$ which is linear in $\delta\phi$. Eq.(4.138) establishes that the probability distribution function and thus also the four point scalar correlator calculated from it are conformally invariant.

4.6.2 Flat Space Limit

We now describe another strong check on our computation of the four point correlator: its "flat space limit." This is the statement that, in a particular limit, this correlation function reduces to the flat space scattering amplitude of four minimally coupled scalars in four dimensions! More precisely, we use the flat space limit developed in [164, 165], which involves an analytic continuation of the momenta. In our context, the limit reads

$$\lim_{k_1+k_2+k_3+k_4\to 0}\frac{(k_1+k_2+k_3+k_4)^3}{k_1k_2k_3k_4}\langle O(\boldsymbol{k_1})O(\boldsymbol{k_2})O(\boldsymbol{k_3})O(\boldsymbol{k_4})\rangle' = \mathcal{N}S_4(\tilde{\boldsymbol{k}}_{\boldsymbol{1}},\tilde{\boldsymbol{k}}_{\boldsymbol{2}},\tilde{\boldsymbol{k}}_{\boldsymbol{3}},\tilde{\boldsymbol{k}}_{\boldsymbol{4}}) \tag{4.139}$$

where S_4 is the four-point scattering amplitude of scalars minimally coupled to gravity, and the on-shell four-momenta of these scalars are related to the three-momenta of the correlators by $\tilde{\boldsymbol{k}}_{\boldsymbol{n}} = (ik_n, \boldsymbol{k_n})$. This means that we add an additional planar direction to the three boundary directions, and use ik_n for the this component of the four-dimensional momentum (which we call the z-component) and $\boldsymbol{k_n}$ for the other three components. An intuitive way to understand this limit is as follows. The four-point flat space scattering amplitude conserves four-momentum, whereas the CFT correlator conserves just three-momentum. The point where $\sum k_n = 0$ corresponds to the point in kinematic space, where the four-momentum is conserved. The claim is that the CFT correlator has a pole at this point, and the residue is just the flat space scattering amplitude.

Note that, consistent with our conventions, the prime on the correlator indicates that a factor involving the delta function has been stripped off. Similarly, on the right hand side, S_4 is the flat-space scattering amplitude *without* the momentum conserving delta function. Here, $\mathcal{N}$ is an unimportant numerical factor (independent of all the momenta) that we will not keep track of, which just depends on the conventions we use to normalize the correlator and the amplitude.

Before we show this limit, let us briefly describe the flat space scattering amplitude of four minimally coupled scalars. In fact, the Feynman diagrams that contribute to this amplitude are very similar to the Witten diagrams of Fig.(4.1). The s-channel diagram is shown in Fig.(4.2), and of course, the t and u-channel diagrams also contribute to the amplitude. So,

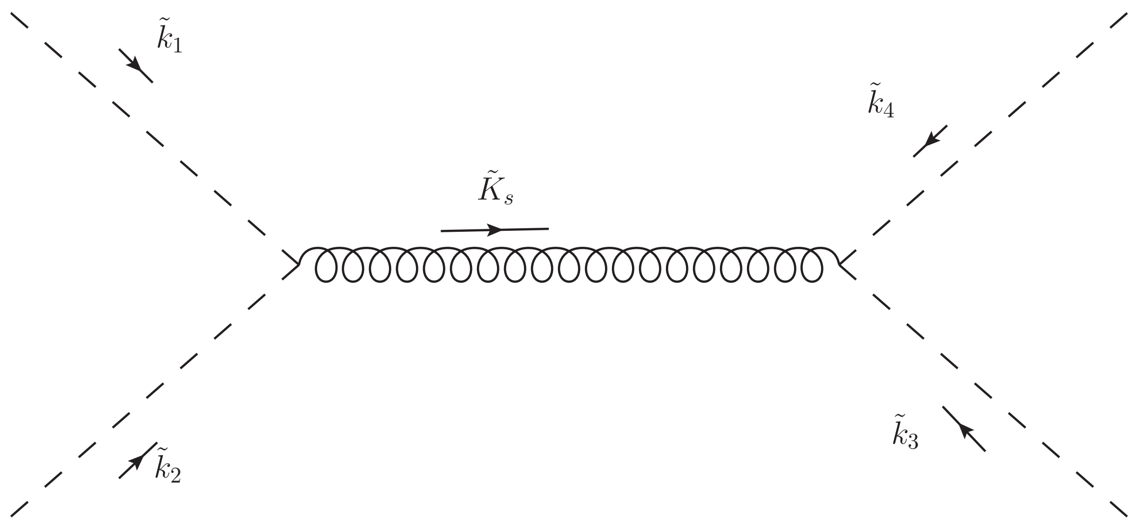

Figure 4.2: S-channel Feynman diagram for scattering of minimally coupled scalars .

the flat-space amplitude using the diagram in Fig.(4.2) evaluates to

$$S_4 = T^{\text{flat}}_{ij}(\tilde{\boldsymbol{k}}_{\boldsymbol{1}}, \tilde{\boldsymbol{k}}_{\boldsymbol{2}}) G^{\text{flat-grav}}_{ijkl}(\tilde{\boldsymbol{K}}_{\boldsymbol{s}}) T^{\text{flat}}_{kl}(\tilde{\boldsymbol{k}}_{\boldsymbol{3}}, \tilde{\boldsymbol{k}}_{\boldsymbol{4}}) + \text{t+u-channels} \tag{4.140}$$

where $\tilde{\boldsymbol{K}}_{\boldsymbol{s}} = \tilde{\boldsymbol{k}}_{\mathbf{1}} + \tilde{\boldsymbol{k}}_{\mathbf{2}}$ and

$$\begin{aligned} T^{\text{flat}}_{i,j}(\tilde{\boldsymbol{k}}_{\mathbf{1}}, \tilde{\boldsymbol{k}}_{\mathbf{2}}) &= \tilde{k}_1^i \tilde{k}_2^j - \frac{1}{2}(\tilde{\boldsymbol{k}}_{\mathbf{1}} \cdot \tilde{\boldsymbol{k}}_{\mathbf{2}})\delta^{ij}, \\ G^{\text{flat-grav}}_{ijkl}(\tilde{\boldsymbol{K}}_{\boldsymbol{s}}) &= \frac{1}{\tilde{\boldsymbol{K}}_{\boldsymbol{s}}{}^2 - i\epsilon} \frac{1}{2}\left[\left(\mathcal{T}^{\text{flat}}_{ik}\mathcal{T}^{\text{flat}}_{jl} + \mathcal{T}^{\text{flat}}_{il}\mathcal{T}^{\text{flat}}_{jk} - \mathcal{T}^{\text{flat}}_{ij}\mathcal{T}^{\text{flat}}_{kl}\right)\right], \\ \mathcal{T}^{\text{flat}}_{ij} &= \delta_{ij} + \frac{\tilde{K}_{si}\tilde{K}_{sj}}{(\tilde{K}_s{}^0)^2} \end{aligned} \tag{4.141}$$

and we emphasize that in (4.140) the Latin indices are contracted only over the spatial directions. In (4.141), $\tilde{K}_s{}^0$ indicates the z-component of the exchanged momentum. The reader should compare this formula to our starting formula for the four-point correlator in (4.104). In fact, if we consider the pole in the p-integral at $p = i(k_1 + k_2)$, in this integral, we see that we will get the right flat space limit. However, in our calculation it was convenient to divide the expression in (4.104) into two parts: a transverse graviton contribution given in (4.108), and a longitudinal graviton contribution that we wrote as a remainder comprised of three terms in (4.111).

We can make the same split for the flat-space amplitude, by replacing the graviton propagator with a simplified version $\widetilde{G}^{\text{flat-grav}}_{ijkl}$, by replacing each $\mathcal{T}^{\text{flat}}_{ij}$ with

$$\widetilde{\mathcal{T}}^{\text{flat}}_{ij} = \delta_{ij} - \frac{\tilde{K}_{si}\tilde{K}_{sj}}{(\boldsymbol{K}_{\boldsymbol{s}})^2}. \tag{4.142}$$

and then writing

$$S_4 = \tilde{S}_4 + 2R^{\text{flat}} \tag{4.143}$$

where $\tilde{S}_4$ is given by an expression analogous to (4.140)

$$\tilde{S}_4 = T^{\text{flat}}_{ij}(\tilde{\boldsymbol{k}}_{\mathbf{1}}, \tilde{\boldsymbol{k}}_{\mathbf{2}})\tilde{G}^{\text{flat-grav}}_{ijkl}(\tilde{\boldsymbol{K}}_{\boldsymbol{s}})T^{\text{flat}}_{kl}(\tilde{\boldsymbol{k}}_{\mathbf{3}}, \tilde{\boldsymbol{k}}_{\mathbf{4}}) + \text{t+u-channels} = \tilde{k}_{1i}\tilde{k}_{2j}\widehat{P}^{ijkl}(\tilde{\boldsymbol{K}}_{\boldsymbol{s}})\tilde{k}_{3k}\tilde{k}_{4l}. \tag{4.144}$$

The second equality follows because projector in this simplified propagator now projects onto traceless tensors that are transverse to $\tilde{K}_s$, which we have denoted by $\widehat{P}^{ijkl}(\tilde{\boldsymbol{K}}_{\boldsymbol{s}})$, as in (4.125).

Now, consider the expression in (4.115). We see that the *third order* pole at $k_t = (k_1 + k_2 + k_3 + k_4)$ is given by

$$\begin{aligned} \widehat{W}^S &= \frac{k_{1i}k_{2j}k_{3k}k_{4l}P^{ijkl}}{k_t^3}\left[\left\{\frac{k_1k_2(k_1+k_2)^2\left((k_1+k_2)^2 - k_3^2 - k_4^2 - 4k_3k_4\right)}{(k_1+k_2-k_3-k_4)^2((k_1+k_2)^2 - |\boldsymbol{k_1}+\boldsymbol{k_2}|^2)}\right]\right. + \mathrm{O}\left(\frac{1}{k_t^2}\right) \\ &= \frac{1}{k_t^3}\frac{k_1k_2k_3k_4}{(k_1+k_2)^2 - |\boldsymbol{k_1}+\boldsymbol{k_2}|^2}k_{1i}k_{2j}k_{3k}k_{4l}P^{ijkl} + \mathrm{O}\left(\frac{1}{k_t^2}\right) \\ &= \frac{k_1k_2k_3k_4}{k_t^3}\tilde{S}_4 + \mathrm{O}\left(\frac{1}{k_t^2}\right). \end{aligned} \tag{4.145}$$

All that remains to establish the flat space limit is to show that

$$\lim_{k_1+k_2+k_3+k_4 \to 0} \frac{(k_1+k_2+k_3+k_4)^3}{k_1 k_2 k_3 k_4} \widehat{R}^S = R^{\text{flat}}. \tag{4.146}$$

The algebra leading to this is a little more involved but as we verify in the included Mathematica file [163] this also remarkably turns out to be true.

So, we find that our complicated answer for the four-point scalar correlator reduces in this limit precisely to the flat space scalar amplitude. This is a very non-trivial check on our answer.

4.6.3 Other Limits

In this subsection we consider our result for the four point function for various other limiting values of the external momenta. The first limit we consider in subsection 4.6.3 is when one of the four momenta goes to zero. Without any loss of generality we can take this to be $\boldsymbol{k_4} \to 0$. The second limit we consider in subsection 4.6.3 is when two of the momenta, say $\boldsymbol{k_1}, \boldsymbol{k_2}$ get large and nearly opposite to each other, while the others, $\boldsymbol{k_3}, \boldsymbol{k_4}$, stay fixed, so that, $\boldsymbol{k_1} \simeq -\boldsymbol{k_2}$, and $k_1, k_2 \gg k_3, k_4$. In both cases we will see that the result agrees with what is expected from general considerations. Finally, in subsection 4.6.3 we consider the counter-collinear limit where the sum of two momenta vanish, say $|\boldsymbol{k_1}+\boldsymbol{k_2}| \to 0$. In this limit we find that the result has a characteristic third order pole singularity resulting in a characteristic divergence, as noted in [107].

Limit I : $\boldsymbol{k_4} \to 0$

This kind of a limit was first considered in [117] and is now referred to as a squeezed limit in the literature. It is convenient to think about the behavior of the four point function in this limit by analyzing what happens to the wave function eq.(4.37). For purposes of the present discussion we can write the wave function, eq.(4.37), as,

$$\begin{aligned}\psi[\delta\phi(\boldsymbol{k})] = \exp\Bigg[\frac{M_{Pl}^2}{H^2}\bigg(& -\frac{1}{2}\int \frac{d^3\boldsymbol{k_1}}{(2\pi)^3}\frac{d^3\boldsymbol{k_2}}{(2\pi)^3}\delta\phi(\boldsymbol{k_1})\delta\phi(\boldsymbol{k_2})\langle O(-\boldsymbol{k_1})O(-\boldsymbol{k_2})\rangle \\ & + \frac{1}{3!}\int \frac{d^3\boldsymbol{k_1}}{(2\pi)^3}\frac{d^3\boldsymbol{k_2}}{(2\pi)^3}\frac{d^3\boldsymbol{k_3}}{(2\pi)^3}\delta\phi(\boldsymbol{k_1})\delta\phi(\boldsymbol{k_2})\delta\phi(\boldsymbol{k_3}) \\ & \langle O(-\boldsymbol{k_1})O(-\boldsymbol{k_2})O(-\boldsymbol{k_3})\rangle \\ & + \frac{1}{4!}\int \frac{d^3\boldsymbol{k_1}}{(2\pi)^3}\frac{d^3\boldsymbol{k_2}}{(2\pi)^3}\frac{d^3\boldsymbol{k_3}}{(2\pi)^3}\frac{d^3\boldsymbol{k_4}}{(2\pi)^3}\delta\phi(\boldsymbol{k_1})\delta\phi(\boldsymbol{k_2})\delta\phi(\boldsymbol{k_3})\delta\phi(\boldsymbol{k_4}) \\ & \langle O(-\boldsymbol{k_1})O(-\boldsymbol{k_2})O(-\boldsymbol{k_3})O(-\boldsymbol{k_4})\rangle + \cdots \bigg)\Bigg].\end{aligned} \tag{4.147}$$

Here terms dependent on the tensor perturbations have not been shown explicitly since they are not relevant for the present discussion. We have also explicitly included a three point function on the RHS. This three point function vanishes in the slow-roll limit, [117], but it is important to include it for the general argument we give now, since the slow -roll limit for this general argument is a bit subtle.

In the limit when $\boldsymbol{k_4} \to 0$, $\delta\phi(\boldsymbol{k_4})$ becomes approximately constant and its effect is to rescale the metric by taking h_{ij}, eq.(4.18), to be, eq.(4.20), eq.(4.21),

$$h_{ij} = e^{2Ht}(1+2\zeta)\delta_{ij} \tag{4.148}$$

where $\zeta(\boldsymbol{k_4})$ is related to $\delta\phi(\boldsymbol{k_4})$ by, eq.(4.34),

$$\delta\phi(\boldsymbol{k_4}) = -\sqrt{2\epsilon}\zeta(\boldsymbol{k_4}). \tag{4.149}$$

The effect on the wave function in this limit can be obtained by first considering the wave function in the absence of the $\delta\phi(\boldsymbol{k_4})$ perturbation and then rescaling the momenta to incorporate the dependence on $\delta\phi(\boldsymbol{k_4})$. The coefficient of the term which is trilinear in $\delta\phi$ on the RHS of eq.(4.147) is denoted by $\langle O(\boldsymbol{k_1}O(\boldsymbol{k_2})O(\boldsymbol{k_3})\rangle$. Under the rescaling which incorporates the effects of $\delta\phi(\boldsymbol{k_4})$ this coefficient will change as follows:

$$\delta\langle O(\boldsymbol{k_1})O(\boldsymbol{k_2})O(\boldsymbol{k_3})\rangle \sim \frac{\delta\phi(\boldsymbol{k_4})}{\sqrt{\epsilon}}\left(\sum_{i=1}^{3}\boldsymbol{k}_i\cdot\partial_{\boldsymbol{k}_i}\right)\langle O(\boldsymbol{k_1})O(\boldsymbol{k_2})O(\boldsymbol{k_3})\rangle. \tag{4.150}$$

As a result the trilinear term now depends on four powers of $\delta\phi$ and gives a contribution to the four point function. We see that the resulting value of the coefficient of the term quartic in $\delta\phi$ is therefore

$$\lim_{\boldsymbol{k_4}\to 0}\langle O(\boldsymbol{k_1})O(\boldsymbol{k_2})O(\boldsymbol{k_3})O(\boldsymbol{k_4})\rangle \sim \frac{1}{\sqrt{\epsilon}}\left(\sum_{i=1}^{3}\boldsymbol{k}_i\cdot\partial_{\boldsymbol{k}_i}\right)\langle O(\boldsymbol{k_1})O(\boldsymbol{k_2})O(\boldsymbol{k_3})\rangle. \tag{4.151}$$

The three point function in this slow-roll model of inflation was calculated in [117] and the result is given in eq.(4.5), eq.(4.6) of [117]. From this result it is easy to read-off the value of $\langle O(\boldsymbol{k_1})O(\boldsymbol{k_2})O(\boldsymbol{k_3})\rangle$. One gets that

$$\langle O(\boldsymbol{k_1})O(\boldsymbol{k_2})O(\boldsymbol{k_3})\rangle \propto (2\pi)^3\delta(\sum_i k_i)\frac{1}{\sqrt{\epsilon}}A \tag{4.152}$$

where

$$A = 2\frac{\ddot{\phi}_*}{\dot{\phi}_* H}\sum_{i=1}^{3}k_i^3 + \frac{\dot{\phi}_*^2}{H^2}\left[\frac{1}{2}\sum_{i=1}^{3}k_i^3 + \frac{1}{2}\sum_{i\neq j}k_i k_j^2 + 4\frac{\sum_{i>j}k_i^2 k_j^2}{k_t}\right] \tag{4.153}$$

where the subscript $*$ means values of the corresponding object to be evaluated at the time of horizon crossing and $k_t = k_1 + k_2 + k_3$. 4 Substituting in eq.(4.151) gives

$$\lim_{\boldsymbol{k_4}\to 0}\langle O(\boldsymbol{k_1})O(\boldsymbol{k_2})O(\boldsymbol{k_3})O(\boldsymbol{k_4})\rangle \sim \frac{1}{\epsilon}\left[\sum_{i=1}^{3}\boldsymbol{k}_i\cdot\partial_{\boldsymbol{k}_i}\right]\left[\delta(\sum_i k_i)A\right]. \tag{4.154}$$

Now, it is easy to see that due to the $\dot{\phi}_*, \ddot{\phi}_*$ dependent prefactors A is of order the slow-roll parameters ϵ, η, eq.(4.9), eq.(4.10). Thus in the limit where $\epsilon \sim \eta$ and both tend to zero the $\frac{1}{\epsilon}$ prefactor on the RHS will cancel the dependence in A due to the prefactors. However, note that there is an additional suppression since A is trilinear in the momenta and therefore $\delta(\sum_i k)A$ will be invariant under rescaling all the momenta to leading order in the slow-roll approximation,

$$\left[\sum_{i=1}^{3}\boldsymbol{k}_i\cdot\partial_{\boldsymbol{k}_i}\right]\left[\delta(\sum_i k_i)A\right] = 0. \tag{4.155}$$

As a result the RHS of eq.(4.154) and thus the four point function will vanish in this limit in the leading slow-roll approximation. To subleading order in the slow-roll approximation the condition in eq.(4.155) will not be true any more since the Hubble constant H and $\dot{\phi}_*, \ddot{\phi}_*$ which appears in eq.(4.153) will also depend on k and should be evaluated to take the values they do when the modes cross the horizon.

For our purpose it is enough to note that the behavior of the four point function in the leading slow-roll approximation is that it vanishes when $\boldsymbol{k_4} \to 0$. It is easy to see that the result in eq.(4.123) does have this feature in agreement with the general analysis above. In fact expanding eq.(4.123) for small momentum we find it vanishes linearly with k_4.

Limit II : k_1, k_2 get large

Next, we consider a limit where two of the momenta, say $\boldsymbol{k_1}, \boldsymbol{k_2}$, get large in magnitude and approximately cancel, so that their sum, $|\boldsymbol{k_1} + \boldsymbol{k_2}|$, is held fixed. The other two momenta, $\boldsymbol{k_3}, \boldsymbol{k_4}$, are held fixed in this limit. Note that this limit is a very natural one from the point of view of the CFT. In position space in the CFT in this limit two operators come together, at the same spatial location and the behavior can be understood using the operator product expansion (OPE). We will see below that our result for the four point function reproduces the behavior expected from the OPE in the CFT.

It is convenient to start the analysis first from the CFT point of view and then compare with the four point function result we have obtained [6]. Consider the four point function of an operator O of dimension 3 in a CFT:

$$\langle O(\boldsymbol{x}_1)O(\boldsymbol{x}_2)O(\boldsymbol{x}_3)O(\boldsymbol{x}_4)\rangle. \tag{4.156}$$

[6] One expects to justify the OPE from the bulk itself, but we will not try to present a careful derivation along those lines here.

The momentum space correlator is

$$\langle O(\boldsymbol{k_1})O(\boldsymbol{k_2})O(\boldsymbol{k_3})O(\boldsymbol{k_4})\rangle = \int d^3\boldsymbol{x}_1 d^3\boldsymbol{x}_2 d^3\boldsymbol{x}_3 d^3\boldsymbol{x}_4 \; e^{-i(\boldsymbol{k_1}\cdot\boldsymbol{x}_1+\boldsymbol{k_2}\cdot\boldsymbol{x}_2+\boldsymbol{k_3}\cdot\boldsymbol{x}_3+\boldsymbol{k_4}\cdot\boldsymbol{x}_4)}$$
$$\langle O(\boldsymbol{x}_1)O(\boldsymbol{x}_2)O(\boldsymbol{x}_3)O(\boldsymbol{x}_4)\rangle$$
$$= (2\pi)^3\delta^{(3)}(\sum_I \boldsymbol{k_I}) \int d^3\boldsymbol{y}_2 d^3\boldsymbol{y}_3 d^3\boldsymbol{y}_4 \; e^{-i(\boldsymbol{k_2}\cdot\boldsymbol{y}_2+\boldsymbol{k_3}\cdot\boldsymbol{y}_3+\boldsymbol{k_4}\cdot\boldsymbol{y}_4)}$$
$$\langle O(\boldsymbol{0})O(\boldsymbol{y}_2)O(\boldsymbol{y}_3)O(\boldsymbol{y}_4)\rangle \tag{4.157}$$

where in the last line on the RHS above

$$\boldsymbol{y}_2 = \boldsymbol{x}_2 - \boldsymbol{x}_1, \;\; \boldsymbol{y}_3 = \boldsymbol{x}_3 - \boldsymbol{x}_1, \;\; \boldsymbol{y}_4 = \boldsymbol{x}_4 - \boldsymbol{x}_1. \tag{4.158}$$

We are interested in the limit where $\boldsymbol{k_3}, \boldsymbol{k_4}$ are held fixed while

$$k_2 \to \infty \text{ and } k_1 = |-(\boldsymbol{k_2}+\boldsymbol{k_3}+\boldsymbol{k_4})| \to \infty \tag{4.159}$$

In position space in this limit $\boldsymbol{x}_1 \to \boldsymbol{x}_2$ so that

$$\boldsymbol{y}_2 \to 0. \tag{4.160}$$

The operator product expansion can be used when the condition in eq.(4.160) is met, to expand

$$O(\boldsymbol{0})O(\boldsymbol{y_2}) = C_1 \frac{y_2^i y_2^j}{y_2^5} T_{ij}(\boldsymbol{y_2}) + \dots \tag{4.161}$$

where C_1 is a constant that depends on the normalization of O. In general there are extra contact terms which can also appear on the RHS of the OPE. We are ignoring such terms and considering the limit when y_2 is small but not vanishing.

Using eq.(4.161) in the RHS of eq.(4.157) we get

$$\lim_{\boldsymbol{k_2}\to\infty} \langle O(\boldsymbol{k_1})O(\boldsymbol{k_2})O(\boldsymbol{k_3})O(\boldsymbol{k_4})\rangle' = \int d^3\boldsymbol{y_2}\; d^3\boldsymbol{y}_3\; d^3\boldsymbol{y}_4\; C_1 \frac{y_2^i y_2^j}{y_2^5}\; e^{-i(\boldsymbol{k_2}\cdot\boldsymbol{y}_2+\boldsymbol{k_3}\cdot\boldsymbol{y}_3+\boldsymbol{k_4}\cdot\boldsymbol{y}_4)}$$
$$\langle T_{ij}(\boldsymbol{y}_2)O(\boldsymbol{y}_3)O(\boldsymbol{y}_4)\rangle' \tag{4.162}$$

where by the lim on the LHS we mean more precisely the limit given in eq.(4.159) and the symbol $\langle O(\boldsymbol{k_1})O(\boldsymbol{k_2})O(\boldsymbol{k_3})O(\boldsymbol{k_4})\rangle'$ with the prime superscript stands of the four point correlator $\langle O(\boldsymbol{k_1})O(\boldsymbol{k_2})O(\boldsymbol{k_3})O(\boldsymbol{k_4})\rangle$ without the factor of $(2\pi)^3\delta^3(\sum_i \boldsymbol{k}_i)$. The variable $\boldsymbol{k_1}$ which appears in the argument on the LHS of eq.(4.162) is understood to take the value $\boldsymbol{k_1} = -(\boldsymbol{k_2}+\boldsymbol{k_3}+\boldsymbol{k_4})$.

Now in the limit of interest when $k_2 \to \infty$, the support for the integral on the RHS of eq.(4.162) comes from the region where $y_2 \to 0$. Thus the integral in eq.(4.162) can be approximated to be

$$\begin{aligned}&\int d^3\boldsymbol{y}_2\, d^3\boldsymbol{y}_3\, d^3\boldsymbol{y}_4\, C_1 \frac{y_2^i y_2^j}{y_2^5}\, e^{-i(\boldsymbol{k_2}\cdot\boldsymbol{y}_2+\boldsymbol{k_3}\cdot\boldsymbol{y}_3+\boldsymbol{k_4}\cdot\boldsymbol{y}_4)}\langle T_{ij}(\boldsymbol{y}_2)O(\boldsymbol{y}_3)O(\boldsymbol{y}_4)\rangle' \\ &= C_1 D_1 \frac{k_2^i k_2^j}{k_2^2}\int d^3\boldsymbol{y}_3\, d^3\boldsymbol{y}_4 e^{-i(\boldsymbol{k_3}\cdot\boldsymbol{y}_3+\boldsymbol{k_4}\cdot\boldsymbol{y}_4)}\langle T_{ij}(\boldsymbol{0})O(\boldsymbol{y}_3)O(\boldsymbol{y}_4)\rangle',\end{aligned} \tag{4.163}$$

where the prefactor is due to

$$\frac{k_2^i k_2^j}{k_2^2} = D_1 \int d^3 y_2 \frac{y_2^i y_2^j}{y_2^5} e^{i\boldsymbol{k_2}\cdot y_2}. \tag{4.164}$$

Finally doing the integral in eq.(4.163) gives us,

$$\int d^3\boldsymbol{y}_3\, d^3\boldsymbol{y}_4\, e^{-i(\boldsymbol{k_3}\cdot\boldsymbol{y}_3+\boldsymbol{k_4}\cdot\boldsymbol{y}_4)}\langle T_{ij}(\boldsymbol{0})O(\boldsymbol{y}_3)O(\boldsymbol{y}_4)\rangle' = \langle T_{ij}(-\boldsymbol{k_3}-\boldsymbol{k_4})O(\boldsymbol{k_3})O(\boldsymbol{k_4})\rangle' \tag{4.165}$$

where the prime superscript again indicates the absence of the momentum conserving delta function, and using eq.(4.162), eq.(4.163), and eq.(4.165), we get

$$\lim_{\boldsymbol{k_2}\to\infty}\langle O(\boldsymbol{k_1})O(\boldsymbol{k_2})O(\boldsymbol{k_3})O(\boldsymbol{k_4})\rangle' = C_1 D_1 \frac{k_2^i k_2^j}{k_2^2}\langle T_{ij}(-\boldsymbol{k_3}-\boldsymbol{k_4})O(\boldsymbol{k_3})O(\boldsymbol{k_4})\rangle'. \tag{4.166}$$

From eq.(4.166) we see that in this limit the behavior of the scalar four point function gets related to the three point $\langle T_{ij}(-\boldsymbol{k_3}-\boldsymbol{k_4})O(\boldsymbol{k_3})O(\boldsymbol{k_4})\rangle$ correlator. For the slow-roll model we are analyzing this three point function was calculated in [117] and has been studied more generally in [131], see also [125], [130]. These results give the value of the $\langle T_{ij}(-\boldsymbol{k_3}-\boldsymbol{k_4})O(\boldsymbol{k_3})O(\boldsymbol{k_4})\rangle$ correlator after contracting with the polarization of the graviton, $e^{s,ij}$, to be,

$$e^{s,ij}\langle T_{ij}(-\boldsymbol{k_3}-\boldsymbol{k_4})O(\boldsymbol{k_3})O(\boldsymbol{k_4})\rangle' = -2e^{s,ij}k_{3i}k_{4j}S(\tilde{k},k_3,k_4) \tag{4.167}$$

where the momentum

$$\tilde{\boldsymbol{k}} = -(\boldsymbol{k_3}+\boldsymbol{k_4}), \tag{4.168}$$

is the argument of T_{ij}.[7] Note that the polarization $e^{s,ij}$ is a traceless tensor perpendicular to $\tilde{\boldsymbol{k}}$ and $S(\widetilde{k},k_3,k_4)$ is given in eq.(4.131).

By choosing $\boldsymbol{k_2}\perp(\boldsymbol{k_3}+\boldsymbol{k_4})$ we use eq.(4.167) to obtain from eq.(4.166)

$$\lim_{\boldsymbol{k_2}\to\infty}\langle O(\boldsymbol{k_1})O(\boldsymbol{k_2})O(\boldsymbol{k_3})O(\boldsymbol{k_4})\rangle' = C_1 D_1 \frac{k_2^i k_2^j}{k_2^2}k_{3i}k_{4j}S(\tilde{k},k_3,k_4). \tag{4.169}$$

The numerical constant $C_1 D_1$ in eq.(4.169) can be obtained independently looking at

[7] The reader should not confuse this with the four-momentum that was introduced in subsection 4.6.2. Here $\tilde{\boldsymbol{k}}$ is a three-vector.

the correlator $\langle OOT_{ij}\rangle$. This correlator was completely fixed after contracting with the polarization of the graviton, $e^{s,ij}$, by conformal invariance in [131]. Comparing the behavior of $\langle OOT_{ij}\rangle$ in the limit when two of the O's come together in position space with the expectations from CFT one can obtain,

$$C_1 D_1 = \frac{3}{2}. \tag{4.170}$$

For the correlator $\langle O(\boldsymbol{k_1})O(\boldsymbol{k_2})O(\boldsymbol{k_3})O(\boldsymbol{k_4})\rangle$, to compare this expectation from CFT in eq.(4.169) with our result in eq.(4.123), it is convenient to parameterize $\boldsymbol{k_2} = \boldsymbol{a}/\epsilon$ and then take the limit $\epsilon \to 0$, with $\boldsymbol{k_3}, \boldsymbol{k_4}$ held fixed and $\boldsymbol{k_1} = -(\boldsymbol{k_2} + \boldsymbol{k_3} + \boldsymbol{k_4})$. For comparison purposes we also consider the situation when $\boldsymbol{k_2} \perp (\boldsymbol{k_3} + \boldsymbol{k_4})$. As discussed in Appendix C.6.1 in this limit and also for the cases when $\boldsymbol{k_2}$ is perpendicular to $\boldsymbol{k_3} + \boldsymbol{k_4}$, we find that eq.(4.123) becomes

$$\lim_{\boldsymbol{k_2}\to\infty} \langle O(\boldsymbol{k_1})O(\boldsymbol{k_2})O(\boldsymbol{k_3})O(\boldsymbol{k_4})\rangle' = \frac{3}{2}\frac{k_2^i k_2^j}{k_2^2} k_{3i}k_{4j} S(\tilde{k}, k_3, k_4). \tag{4.171}$$

Comparing eq.(4.169) with eq.(4.171) it is obvious that, in this limit, our result for the four point function agrees precisely with the expectation from OPE in the CFT. The agreement is upto contact terms which have been neglected in our discussion based on CFT considerations above anyways.

Limit III: Counter-Collinear Limit

Finally, we consider a third limit in which the sum of two momenta vanish while the magnitudes of all individual momenta, $k_i, i = 1, \cdots 4$, are non-vanishing. Below we consider the case where

$$\boldsymbol{k}_{12} \equiv \boldsymbol{k_1} + \boldsymbol{k_2} \to 0. \tag{4.172}$$

Note that by momentum conservation it then follows that $(\boldsymbol{k_3} + \boldsymbol{k_4})$ also vanishes. This limit is referred to as the counter-collinear limit in the literature. As we will see, in this limit our result, eq.(4.133), has a divergence which arises from a pole in the propagator of the graviton which is exchanged to give rise to the term, eq.(4.129). This divergence is a characteristic feature of the result and could potentially be observationally interesting. Towards the end of this subsection we will see that the counter-collinear limit can in fact be obtained as a special case of the limit considered in the previous subsection.

It is easy to see that in the limit eq.(4.172) the contribution of the CF term eq.(4.128) is finite while that of the ET contribution term eq.(4.129) has a divergence arising from the

$G^S(\boldsymbol{k_1}, \boldsymbol{k_2}, \boldsymbol{k_3}, \boldsymbol{k_4})$ term, leading to,

$$\begin{split}\langle\delta\phi(\boldsymbol{k_1})\delta\phi(\boldsymbol{k_2})\delta\phi(\boldsymbol{k_3})\delta\phi(\boldsymbol{k_4})\rangle_{ET} \to & 4(2\pi)^3\delta^3\Big(\sum_J \boldsymbol{k}_J\Big)\frac{H^6}{M_{Pl}^6}\frac{1}{\prod_{J=1}^4(2k_J^3)}\frac{9}{4}\frac{k_1^3k_3^3}{k_{12}^3} \\ & \sin^2(\theta_1)\sin^2(\theta_3)\cos(2\chi_{12,34}).\end{split} \tag{4.173}$$

The RHS arises as follows. In this limit $k_1 \simeq k_2$ and $k_3 \simeq k_4$, and from eq.(4.131)

$$S(k_1, k_2) \simeq \frac{3}{2}k_1, \tag{4.174}$$

and similarly, $S(k_3, k_4) \simeq \frac{3}{2}k_3$. As explained in Appendix C.6.2, eq.(4.129) then gives rise to eq.(4.173), where θ_1 is the angle between $\boldsymbol{k_1}$ and $\boldsymbol{k}_{12}$ θ_3 is the angle between $\boldsymbol{k_3}$ and $\boldsymbol{k}_{12}$, and $\chi_{12,34}$ is the angle between the projections of $\boldsymbol{k_1}, \boldsymbol{k_3}$ on the plane orthogonal to $\boldsymbol{k}_{12}$.

From eq.(4.173) it then follows that in this limit

$$\begin{split}\langle\zeta(\boldsymbol{k_1})\zeta(\boldsymbol{k_2})\zeta(\boldsymbol{k_3})\zeta(\boldsymbol{k_4})\rangle_{ET} \to & 4(2\pi)^3\delta^3\Big(\sum_J \boldsymbol{k}_J\Big)\frac{1}{4\epsilon^2}\frac{H^6}{M_{Pl}^6}\frac{1}{\prod_{J=1}^4(2k_J^3)}\frac{9}{4}\frac{k_1^3k_3^3}{k_{12}^3} \\ & \sin^2(\theta_1)\sin^2(\theta_3)\cos(2\chi_{12,34}).\end{split} \tag{4.175}$$

Some comments are now in order. First, as was noted in subsection 4.5 after eq.(4.132) the ET contribution term is completely fixed by conformal invariance and therefore the $1/k_{12}^3$ divergence in eq.(4.175) is also fixed by conformal symmetry and is model independent. The model dependence in the result above could arise from the fact that the CF term makes no contribution in the slow-roll case. The behavior of the CF term (like that of the ET term, see below) in this limit depends on contact terms which arise in the OPE. We have not studied these contact terms carefully and it could perhaps be that in other models the CF term also gives rise to a divergent contribution comparable to eq.(4.175). Of course departures from the result above can also arise in models where conformal invariance is not preserved.

Second, the two factors $S(k_1, k_2), S(k_3, k_4)$ in eq.(4.130) arise from the two factors of $\langle OOT_{ij}\rangle$ in the ET contribution to $P[\delta\phi]$, eq.(4.126), since $\langle OOT_{ij}\rangle$ when contracted with a polarization tensor can be expressed in terms of S, eq.(C.8) in Appendix C.1. In the three point function $\langle OOT_{ij}\rangle$ the limit where $\boldsymbol{k_1} + \boldsymbol{k_2}$ vanishes is a squeezed limit. This limit was investigated in [131], subsection 4.2, and it follows from eq.(4.174) and eq.(C.8) in Appendix C.1 that in this limit

$$\langle O(\boldsymbol{k_1})O(\boldsymbol{k_2})T_{ij}(\boldsymbol{k_3})\rangle' e^{s,ij} = -2e^{s,ij}k_{1i}k_{2j}\frac{3}{2}k_1 \tag{4.176}$$

and is a contact term since it is analytic in $\boldsymbol{k_2}$. However it is easy to see from eq.(4.173) that the contribution that the product of two of these three point functions make to the four point scalar correlator in the counter-collinear limit is no longer a contact term. This example illustrates the importance of keeping track of contact terms carefully even for the purpose of eventually evaluating non-contact terms in the correlation function.

Finally, we note that due to conformal invariance an equivalent way to phrase the counter-collinear limit is to take the four momenta, $\boldsymbol{k_1}, \boldsymbol{k_2}, \boldsymbol{k_3}, \boldsymbol{k_4}$, all large while keeping the sum, $\boldsymbol{k_1} + \boldsymbol{k_2} = -\boldsymbol{k_3} + \boldsymbol{k_4}$, fixed. This makes it clear that the counter-collinear limit is a special case of the limit considered in the previous subsection. However in our discussion of the previous section we did not keep track of contact terms. Here, in obtaining the leading divergent behavior it is important to keep these terms, as we have noted above. In fact without keeping the contact term contributions in $\langle OOT_{ij} \rangle$ the ET contribution would vanish in this limit.

4.7 Discussion

In the analysis presented in this chapter we have calculated the primordial four point correlation function for scalar perturbations in the canonical model of slow-roll inflation, eq.(4.1). We worked to leading order in the slow-roll approximation where the calculations can be done in de Sitter space. Our final answer is given in eq.(4.133). This answer agrees with the result obtained in [107], which was obtained using quite different methods.

The resulting answer is small, as can be seen from the prefactor in eq.(4.133) which goes like $\frac{H^6}{M_{Pl}^6 \epsilon^2} \sim P_\zeta^3 \epsilon$, where $P_\zeta \sim 10^{-10}$ is the power in the scalar perturbation, eq.(C.6). And it is a complicated function of the magnitudes of three independent momenta and three angles.

The smallness of the answer is expected, since it can be easily estimated without any detailed calculation by noting, for example, that the coefficient of the $\langle OOOO \rangle$ term, eq.(4.37), is not expected to vanish [8]. In discussions related to observations, it is conventional to consider the four point correlator (also called the trispectrum) to be of the local form and parameterize it by two coefficients τ_{NL}, g_{NL}. This local form arises by taking the perturbation to be of the type,

$$\zeta = \zeta_g + \frac{1}{2}\sqrt{\tau_{NL}}(\zeta_g^2 - \langle \zeta_g^2 \rangle) + \frac{9}{25} g_{NL} \zeta_g^3, \tag{4.177}$$

where ζ_g is a Gaussian field. The answer we get is not of this local type[9] and so it is not possible to directly compare our result with the experimental bounds quoted in the literature, see [106], [166], $\tau_{NL} < 2800$. However, to get some feel for the situation, we note that the non-Gaussian term proportional to $\sqrt{\tau_{NL}}$ in eq.(4.177) would give rise to a four point correlator of order $\sim \tau_{NL} P_\zeta^3$. Thus, as a very rough estimate the slow-roll model gives rise to $\tau_{NL} \sim \epsilon \sim 10^{-2}$ which is indeed small and very far from the experimental bound

[8] In contrast the $\langle OOO \rangle$ coefficient function vanishes to leading order in the slow-roll approximation leading to $f_{NL} \sim \epsilon$. This vanishing of $\langle OOO \rangle$ is expected from general considerations of CFT.

[9] We clarify that we are not excluding any local type terms from the answer for the four point function, but rather that the full answer is not of the form obtained by making the ansatz in eq.(4.177).

mentioned above.

As mentioned in the introduction, one of the main motivations of this work was to use techniques drawn from the AdS/CFT correspondence for calculating correlation functions of perturbations produced during inflation, and to analyze how the Ward identities of conformal invariance get implemented on these correlation functions. The four point scalar correlator provides a concrete and interesting setting for these purposes.

As the analysis above has hopefully brought out the calculation could be done quite easily by continuing the result from AdS space. In fact doing the calculation in this way naturally gives rise to the wave function. And the wave function is well suited for studying how the symmetries, including conformal invariance, are implemented, since the symmetries of the wave function are automatically symmetries of all correlators calculated from it. We found that the wave function, calculated upto the required order for the four point scalar correlator, is conformally invariant and also invariant under spatial reparameterizations. The Ward identities for conformal invariance follow from this, and it also follows that the four point function satisfies these Ward identities, this is discussed further in the next paragraph. Given the complicated nature of the result these Ward identities serve as an important and highly non-trivial check on the result. An additional set of checks was also provided by comparing the behavior of the result in various limits to what is expected from the operator product expansion in a conformal field theory.

Our analysis helped uncover an interesting general subtlety with regard to the Ward identities of conformal invariance. This subtlety arises in de Sitter space, more generally inflationary backgrounds, and does not have an analogue in AdS space, and is a general feature for other correlation functions as well. In the dS case one computes the wave function as a functional of the boundary values for the scalar and the tensor perturbations, in contrast to the partition function in AdS space. As a result, calculating the correlation functions in dS space requires an additional step of integrating over all boundary values of the scalar and tensor perturbations. This last step is well defined only if we fix the gauge completely.

The resulting correlation functions are then only invariant under a conformal transformation accompanied by a compensating coordinate transformation that restores the gauge. Failure to include this additional coordinate transformation results in the wrong Ward identities. It is also worth emphasizing that due to these complications it is actually simpler to check for conformal invariance in the wave function, before correlation functions are computed from it. The wave function is well defined without the additional gauge fixing mentioned above, and on general grounds can be argued to be invariant under both conformal transformations and general spatial reparameterizations. Once this is ensured the correlation functions calculated from it automatically satisfy the required Ward identities.

Going beyond the canonical slow-roll model we have considered, one might ask what constraints does conformal symmetry impose on the 4 point correlator in general? Our answer, eq.(4.133), arises from a sum of two terms, see eq.(4.132). The second contribution, the extra term (ET), eq.(4.129), is completely determined by conformal invariance and is model independent. This follows by noting that the boundary term is obtained from the $\langle OOT_{ij}\rangle$ correlator[10], and the $\langle OOT_{ij}\rangle$ correlator in turn is completely fixed by conformal invariance, *e.g.* as discussed in [131]. The first contribution to the answer though, the $\langle OOOO\rangle$ dependent CF term, is more model dependent and is related to the 4 point function of a dimension 3 scalar operator O in a CFT. In 3 dimensional CFT there are 3 cross-ratios for the 4 point function in position space which are conformally invariant, and any function of these cross ratios is allowed by conformal invariance. This results in a rather weak constraint on the CF term.

However, some model independent results can arise in various limits. For example, in the counter-collinear limit considered in section 4.6.3, our full answer has a characteristic pole and is dominated by the ET contribution. In contrast the contribution from the CF term is finite and sub-dominant. The difference in behavior can be traced to contact terms in the OPE of two O operators. While we have not studied these contact terms in enough detail, it seems to us reasonable that in a large class of models the ET term should continue to dominate in this limit and the resulting behavior of the correlator should then be model independent and be a robust prediction that follows just from conformal invariance. A similar model independent result may also arise in another limit which was discussed in section section 4.6.3, in which two of the momenta grow large. In this limit again the behavior of $\langle OOOO\rangle$, upto contact terms, is determined by the $\langle OOT_{ij}\rangle$ correlator, eq.(4.166), eq.(4.169), which is model independent. A better understanding of the extent of model independence in this limit also requires a deeper understanding of the relevant contact terms which we leave for the future.

[10]See eq.(4.126) and related discussion leading to eq.(4.129) in section 4.5.

Chapter 5

Conclusions

In this concluding chapter of the thesis we aim at summarizing our discussions so far. We will comment on the main results of our analysis presented in the earlier chapters and also mention some of the future open questions.

The primary goal of this thesis was to study various aspects of symmetries in different phases of gravitation. The AdS/CFT correspondence played an important role in our analysis since the main computational technique we used was heavily borrowed from it. We found useful applications of our analysis to different branches of physics, namely condensed matter physics and Early Universe Cosmology. The first two chapters were devoted to exploring the relatively new connection between gravity theory and strongly coupled field theories. In the third chapter we turned to a significantly different area of theoretical physics, Early Universe Cosmology. In all the three chapters, the importance of symmetry principles and the existence of various phases in the study of gravity was highlighted. Apart from this, use of the holographic principle as a computational tool also happened to be a common feature in all of them.

In chapter 2, we examined if different phases found in nature, more specifically in condensed matter systems, could be realized in simple models of Einstein gravity coupled to sensible matter. We found that the existing set of translationally invariant black brane solutions can be extended by relaxing the property of isotropy. Using the classification of real 3 dimensional algebra studied in Mathematics, namely the *i.e.* Bianchi classification, we constructed near horizon solutions corresponding to homogeneous, but not necessarily isotropic, geometries. Truly speaking, our solutions are not of the most general type as we had only obtained a restricted set of them, namely scale invariant ones. Further, we also considered a somewhat simplified situation where the symmetry algebra remains unchanged along the radial flow of the geometry, or in other words, the radial direction does not take part in the symmetry algebra of each of the Bianchi classes. The type -VII geometry is indeed realized in condensed matter systems with a helical symmetry, *e.g.* in spin density waves. In order to have the dual field theory, with the Bianchi solutions as their IR fixed points, living in flat space we constructed a numerical interpolation of the near horizon Bianchi type-VII attractor to asymptotically AdS spacetime.

Among possible future directions, one of the most interesting extensions of our work will be to try and relax the extremal nature of the black brane solutions, which will allow us to study transport properties like conductivity and other finite temperature artefacts in these anisotropic solutions in general. In the follow up work, in [66], we have found examples of Bianchi attractors with reduced symmetry properties, *e.g.* the near horizon geometry does not has exact scaling invariance but instead has a conformal Killing vector and also studied the possibility of a more general classification where the radial direction of the geometry gets non-trivially involved in the symmetry algebra such that the natural mathematics is that of real four-algebras with three dimensional sub-algebras. In another extension of this work, we also explored the possibility of interpolating Bianchi attractors, other than type-VII one, to asymptotic AdS spacetime in [58].

Next, in chapter 3, we continued with our attempts to find connections between a theory of gravity and condensed matter systems but used the gauge-gravity duality in the reversed way. We explored the possibility: whether some specific gravity solution can provide insights for condensed matter physics. We considered the hyperscaling violating solutions in dilatonic gravity models as they provide a set up for studying strongly correlated aspects of field theories, *e.g.* non-Fermi liquid behavior etc. More precisely, we wanted to examine the claim that the existence of Fermi Surface leads to specific significant imprint in the behavior of the entanglement entropy of the system. In a holographic set-up we subjected our system of electrically charged hyperscaling violating black brane to turning on a small magnetic field and studied its response. As it has been already mentioned in the discussion of chapter 3, we found some interesting similarity in our holographic analysis with regards to a condensed matter system namely a Fermi surface, and, its response to a small magnetic field.

One interesting future direction to explore is to understand the "IR-completion" of these near extremal hyperscaling violating attractors in these Einstein-Maxwell-Dilaton gravity systems. The typical logarithmic running of the dilaton close to the horizons of these attractors modifies the deep IR geometry. Also the extensive ground state entropy of the $AdS_2 \times R^2$ geometries we found, as a response to turning on a small magnetic field, hints at possible instabilities. Taken together, all these suggests that the true ground state of these attractors is yet not identified, [30], [94], [95]. It is quite natural, therefore, to say that the lesson we learn from our study in this thesis is that though there are promising hopes, a lot has to be understood in order to establish a connection between phases in gravity and condensed matter systems on a firm footing.

In chapter 4, we shifted our focus to find applications of our study of symmetries to a significantly different subject of physics from condensed matter systems, namely the physics of our Universe shortly after its birth. From a somewhat more abstract viewpoint, we were interested in the following question, how the conformal symmetries of a CFT constraints the correlation functions of operators in the theory. As it is well known, the constraints coming from the conformal symmetry is realized in terms of Ward identities involving correlation functions of the operators. These general lessons from a conformal field theory were then applied to learn about the correlations between the cosmological perturbations encoded in the CMB radiation. More specifically, we were interested in the four point function of the scalar perturbations produced during the exponential expansion of our universe, also known as inflation. Our investigation clarified the way in which conformal invariance of the approximate de Sitter spacetime of our Universe is realized for this particular correlator, also known as trispectrum in the cosmology community, in slow-roll inflation. The question of conformal invariance becomes subtle since one needs to take care of gauge fixing simultaneously, owing to the fact that gravity is a gauge theory. As we have already discussed, there is no immediate hope of any observational confirmation of our investigation for the four point scalar correlator of cosmological perturbations because of very small magnitude of it. Despite that, we believe that our analysis would serve as an important conceptual advancement in the understanding of the physics of early Universe based on symmetry considerations alone. Also it is worth mentioning that our analysis is robust in the sense that it does not depend on any particular model. Most interestingly, the use of computational techniques borrowed from holography in our investigation also follows from symmetry considerations, as isometry group of both dS_4 and Euclidean AdS_4 are same. This enables one to make use of the well studied methods of AdS/CFT correspondence into de Sitter cosmology. A further connection of the isometries of both dS_4 and Euclidean AdS_4 to the conformal symmetry group of three dimensional CFT's also enabled us to use well studied methods available there. Therefore, we concluded this chapter with enough evidences emerging out from our investigations justifying the significance of a study of symmetries in the inflationary phase describing very early stages of our Universe.

Appendix A

Appendices for Chapter 2: *Bianchi Attractors: A Classification of Extremal Black Brane Geometries*

A.1 Three Dimensional Homogeneous spaces

A three dimensional homogeneous space has three linearly independent Killing vector fields, ξ_i, $i = 1, 2, 3$. The infinitesimal transformations generated by these Killing vectors take any point in the space to any other point in its immediate vicinity. The Killing vectors satisfy a three dimensional real algebra with commutation relations

$$[\xi_i, \xi_j] = C^k_{ij}\xi_k. \tag{A.1}$$

As discussed in [17], [18] there are 9 different such algebras, up to basis redefinitions, and thus 9 different classes of such homogeneous spaces. This classification is called the Bianchi classification and the 9 classes are the 9 Bianchi classes.

Also, as is discussed in [17],[18], in each case there are three linearly independent invariant vector fields, X_i, which commute with the three Killing vectors

$$[\xi_i, X_j] = 0. \tag{A.2}$$

The X_i's in turn satisfy the algebra

$$[X_i, X_j] = -C^k_{ij}X_k. \tag{A.3}$$

There are also three one-forms, ω^i, which are dual to the invariant vectors X_i. The Lie derivatives of these one-forms along the ξ_i directions also vanish making them invariant along the ξ directions as well. The ω^i's satisfy the relations

$$d\omega^i = \frac{1}{2} C^i_{jk} \omega^j \wedge \omega^k. \tag{A.4}$$

Below we give a list which contains the structure constants for the 9 Bianchi algebras, in a particular basis of generators. For all the classes that arise in the analysis in this chapter we also give the Killing vector fields, invariant one-forms and invariant vector fields, in a particular coordinate basis. See [18] for more details.

- **Type I**: $C^i_{jk} = 0$

$$\xi_i = X_i = \partial_i,\ \omega^i = dx^i,\ d\omega^i = 0 \tag{A.5}$$

- **Type II**: $C^1_{23} = -C^1_{32} = 1$ and rest $C^i_{j,k} = 0$

$$\begin{array}{cccc} \xi_1 = \partial_2 & X_1 = \partial_2 & \omega^1 = dx^2 - x^1 dx^3 & d\omega^1 = \omega^2 \wedge \omega^3 \\ \xi_2 = \partial_3 & X_2 = x^1\partial_2 + \partial_3 & \omega^2 = dx^3 & d\omega^2 = 0 \\ \xi_3 = \partial_1 + x^3\partial_2 & X_3 = \partial_1 & \omega^3 = dx^1 & d\omega^3 = 0 \end{array}$$

- **Type III**: $C^1_{13} = -C^1_{31} = 1$ and rest $C^i_{j,k} = 0$

$$\begin{array}{cccc} \xi_1 = \partial_2 & X_1 = e^{x^1}\partial_2 & \omega^1 = e^{-x^1} dx^2 & d\omega^1 = \omega^1 \wedge \omega^3 \\ \xi_2 = \partial_3 & X_2 = \partial_3 & \omega^2 = dx^3 & d\omega^2 = 0 \\ \xi_3 = \partial_1 + x^2\partial_2 & X_3 = \partial_1 & \omega^3 = dx^1 & d\omega^3 = 0 \end{array}$$

- **Type V**: $C^1_{13} = -C^1_{31} = 1$, $C^2_{23} = -C^2_{32} = 1$ and rest $C^i_{j,k} = 0$

$$\begin{array}{cccc} \xi_1 = \partial_2 & X_1 = e^{x^1}\partial_2 & \omega^1 = e^{-x^1} dx^2 & d\omega^1 = \omega^1 \wedge \omega^3 \\ \xi_2 = \partial_3 & X_2 = e^{x^1}\partial_3 & \omega^2 = e^{-x^1} dx^3 & d\omega^2 = \omega^2 \wedge \omega^3 \\ \xi_3 = \partial_1 + x^2\partial_2 + x^3\partial_3 & X_3 = \partial_1 & \omega^3 = dx^1 & d\omega^3 = 0 \end{array}$$

- **Type VI**: $C^1_{13} = -C^1_{31} = 1$, $C^2_{23} = -C^2_{32} = h$ with $(h \neq 0, 1)$ and rest $C^i_{j,k} = 0$

$$\begin{array}{cccc} \xi_1 = \partial_2 & X_1 = e^{x^1}\partial_2 & \omega^1 = e^{-x^1} dx^2 & d\omega^1 = \omega^1 \wedge \omega^3 \\ \xi_2 = \partial_3 & X_2 = e^{hx^1}\partial_3 & \omega^2 = e^{-hx^1} dx^3 & d\omega^2 = h\omega^2 \wedge \omega^3 \\ \xi_3 = \partial_1 + x^2\partial_2 + hx^3\partial_3 & X_3 = \partial_1 & \omega^3 = dx^1 & d\omega^3 = 0 \end{array}$$

- **Type $\mathbf{VII_0}$**: $C^1_{23} = -C^1_{32} = -1$, $C^2_{13} = -C^2_{31} = 1$ and

  rest $C^i_{j,k} = 0$.

$$\begin{array}{cc} \xi_1 = \partial_2 & X_1 = \cos(x^1)\partial_2 + \sin(x^1)\partial_3 \\ \xi_2 = \partial_3 & X_2 = -\sin(x^1)\partial_2 + \cos(x^1)\partial_3 \\ \xi_3 = \partial_1 - x^3\partial_2 + x^2\partial_3 & X_3 = \partial_1 \end{array}$$

  And also,

$$\begin{array}{cc} \omega^1 = \cos(x^1)dx^2 + \sin(x^1)dx^3 & d\omega^1 = -\omega^2 \wedge \omega^3 \\ \omega^2 = -\sin(x^1)dx^2 + \cos(x^1)dx^3 & d\omega^2 = \omega^1 \wedge \omega^3 \\ \omega^3 = dx^1 & d\omega^3 = 0 \end{array}$$

- **Type IX**: $C^1_{23} = -C^1_{32} = 1$, $C^2_{31} = -C^2_{13} = 1$, $C^3_{12} = -C^3_{21} = 1$ and rest are zero.

$$\begin{aligned} \xi_1 &= \partial_2 \\ \xi_2 &= \cos(x^2)\partial_1 - \cot(x^1)\sin(x^2)\partial_2 + \tfrac{\sin(x^2)}{\sin(x^1)}\partial_3 \\ \xi_3 &= -\sin(x^2)\partial_1 - \cot(x^1)\cos(x^2)\partial_2 + \tfrac{\cos(x^2)}{\sin(x^1)}\partial_3 \end{aligned}$$

With

$$\begin{aligned} X_1 &= -\sin(x^3)\partial_1 + \tfrac{\cos(x^3)}{\sin(x^1)}\partial_2 - \cot(x^1)\cos(x^3)\partial_3 \\ X_2 &= \cos(x^3)\partial_1 + \tfrac{\sin(x^3)}{\sin(x^1)}\partial_2 - \cot(x^1)\sin(x^3)\partial_3 \\ X_3 &= \partial_3 \end{aligned}$$

And also,

$$\begin{aligned} \omega^1 &= -\sin(x^3)dx^1 + \sin(x^1)\cos(x^3)dx^2; & d\omega^1 &= \omega^2\wedge\omega^3 \\ \omega^2 &= \cos(x^3)dx^1 + \sin(x^1)\sin(x^3)dx^2; & d\omega^2 &= \omega^3\wedge\omega^1 \\ \omega^3 &= \cos(x^1)dx^2 + dx^3; & d\omega^3 &= \omega^1\wedge\omega^2 \end{aligned}$$

For Types IV and VIII we give the structure constants only. For more explicit data on these Types, see [18]

- **Type IV**: $C^1_{13} = -C^1_{31} = 1$, $C^1_{23} = -C^1_{32} = 1$, $C^2_{23} = -C^2_{32} = 1$ and rest $C^i_{j,k} = 0$

- **Type VII$_\mathbf{h}$ ($\mathbf{0 < h^2 < 4}$)**: $C^2_{13} = -C^2_{31} = 1$, $C^1_{23} = -C^1_{32} = -1$, $C^2_{23} = -C^2_{32} = h$ and rest $C^i_{j,k} = 0$

- **Type VIII**: $C^1_{23} = -C^1_{32} = -1$, $C^2_{31} = -C^2_{13} = 1$, $C^3_{12} = -C^3_{21} = 1$ and rest $C^i_{j,k} = 0$

A.2 Gauge Field Equation of Motion

In this appendix we will consider a system with action eq.(2.11) and metric of form

$$ds^2 = dr^2 - e^{2\beta_t r}dt^2 + \eta_{ij}(r)\omega^i\omega^j \tag{A.6}$$

and derive the equation of motion for the gauge field. In eq.(A.6) $\omega^i, i = 1,2,3$, are the three invariant one-forms along the spatial directions in which the brane extends.

To preserve the generalised translation symmetries along the spatial directions the gauge potential must take the form

$$A = \sum_i f_i(r)\omega^i + A_t(r)dt. \tag{A.7}$$

Eventually, we will take η_{ij} to be diagonal

$$\eta_{ij} = (\lambda_1^2 e^{2\beta_1 r}, \lambda_2^2 e^{2\beta_2 r}, \lambda_3^2 e^{2\beta_3 r}) \tag{A.8}$$

and the functions appearing in the gauge field to be of the form

$$f_i(r) = \tilde{A}_i e^{\beta_i r}, \quad A_t(r) = A_t e^{\beta_t r}. \tag{A.9}$$

where $\lambda_i, \beta_i, \beta_t, \tilde{A}_i, A_t$ are all constants independent of all coordinates. For now though, we keep them to be general and proceed.

The gauge field equation of motion is

$$d *_5 F = -\frac{1}{2} m^2 *_5 A. \tag{A.10}$$

Only two cases are relevant for the discussion above. Either the gauge field has components only along the spatial directions or only along time. We discuss them in turn below.

A.2.1 Gauge Field With Components Along Spatial Directions

Using $d\omega^i = \frac{1}{2} C^i{}_{jk} \omega^j \wedge \omega^k$, we get the field strength to be[1]

$$F = dA = f_i'(r) dr \wedge \omega^i + \frac{1}{2} f_i(r) C^i{}_{jk}\, \omega^j \wedge \omega^k. \tag{A.11}$$

With a choice of orientation so that in the basis $(\omega^1, \omega^2, \omega^3, dr, dt)$, $\epsilon_{123rt} > 0$, we have the following Hodge dualities:

$$*_5 \omega^i = \frac{e^{\beta_t r}}{2} \sqrt{\eta}\, \eta^{ij} \epsilon_{jkl}\, \omega^k \wedge \omega^l \wedge dr \wedge dt \tag{A.12}$$

$$*_5 (\omega^j \wedge \omega^k) = \frac{e^{\beta_t r}}{\sqrt{\eta}} \eta_{il}\, \epsilon^{jkl}\, \omega^i \wedge dr \wedge dt \tag{A.13}$$

$$*_5 (dr \wedge \omega^i) = -\frac{\sqrt{\eta} e^{\beta_t r}}{2} \eta^{ij} \epsilon_{jkl}\, \omega^k \wedge \omega^l \wedge dt. \tag{A.14}$$

Here we are using notation such that $\epsilon^{ijk} = \epsilon_{ijk} = 1$.

Thus the R.H.S of the gauge field equation, eq(A.10), becomes,

$$-\frac{1}{2} m^2 *_5 A = -\frac{1}{4} m^2 f_i(r) \eta^{ij} \sqrt{\eta} e^{\beta_t r} \epsilon_{jnp}\, \omega^n \wedge \omega^p \wedge dr \wedge dt. \tag{A.15}$$

[1] Note in our convention $F = \frac{1}{2} F_{\mu\nu} dx^\mu \wedge dx^\nu$.

The L.H.S of the gauge field equation, eq(A.10), becomes,

$$
\begin{aligned}
d *_5 F &= d\left(-\frac{\sqrt{\eta}e^{\beta_t r}}{2} f_i'(r)\eta^{ij}\epsilon_{jkl}\,\omega^k\wedge\omega^l\wedge dt + \frac{e^{\beta_t r}}{2\sqrt{\eta}} f_i(r) C^i{}_{jk}\,\eta_{le}\,\epsilon^{ejk}\omega^l\wedge dr\wedge dt\right)\\
&= \left[-\frac{1}{2}\left(f_i'(r)e^{\beta_t r}\sqrt{\eta}\eta^{ij}\right)'\epsilon_{jnp} + \frac{1}{4\sqrt{\eta}} f_i(r)e^{\beta_t r}C^i{}_{jk}\eta_{le}C^l{}_{np}\epsilon^{ejk}\right]\,\omega^n\wedge\omega^p\wedge dr\wedge dt\\
&\quad -\frac{1}{2}f_i'(r)e^{\beta_t r}\sqrt{\eta}\eta^{ij}\epsilon_{jkl}C^k{}_{qn}\,\omega^q\wedge\omega^n\wedge\omega^l\wedge dt. \qquad \text{(A.16)}
\end{aligned}
$$

Comparing eq.(A.15), eq.(A.16) we see that

$$
f_i'(r)e^{\beta_t r}\sqrt{\eta}\eta^{ij}\epsilon_{jkl}C^k{}_{qn}\epsilon^{qnl} = 0. \qquad \text{(A.17)}
$$

Defining

$$
\begin{aligned}
\epsilon^{ijl}C^k{}_{ij} &\equiv 2C^{lk} \qquad \text{(A.18)}\\
\epsilon_{ijk}C^{ij} &\equiv 2a_k \qquad \text{(A.19)}
\end{aligned}
$$

as in [17], we get the condition that

$$
\text{either} \quad a_k = 0 \qquad \text{or} \qquad f_i'(r)e^{\beta_t r}\sqrt{\eta}\eta^{ij}(r)a_j = 0. \qquad \text{(A.20)}
$$

Here we consider the case when $a_k = 0$, this includes Type I, II, III, VII$_0$, VIII, IX. In particular it covers all cases discussed in the main text where A is oriented along the spatial directions.

Now comparing the $\omega\wedge\omega\wedge dr\wedge dt$ terms in eq.(A.15), eq.(A.16) and multiplying by ϵ^{mnp} on both sides we get

$$
\frac{1}{2}m^2\sqrt{\eta}f_i(r)e^{\beta_t r}\eta^{im} = (f_i'(r)e^{\beta_t r}\sqrt{\eta}\eta^{im})' - \frac{e^{\beta_t r}}{\sqrt{\eta}}f_i(r)C^{ji}C^{ml}\eta_{lj}. \qquad \text{(A.21)}
$$

To proceed let us consider the metric to be of form eq.(A.8). Also note that the gauge field is assumed to be of form as in eq.(A.9) but with $A_t = 0$. Also we take C^{ji} to be diagonal of form

$$
C^{ji} = \delta^{ji}k^j \quad \text{(with no sum over the index } j\text{)}, \qquad \text{(A.22)}
$$

for some constants k^j such that $2a_k = \epsilon_{ijk}C^{ij} = 0$. This is equivalent to

$$
C^i{}_{jk} = \epsilon_{ijk}k^i \quad \text{(with no sum over the index } i\text{)}. \qquad \text{(A.23)}
$$

Then eq.(A.21) says that for every value of the index $i = 1, 2, 3$, such that $\tilde{A}_i$ is non-vanishing, following two conditions must be met:

$$\sum_j \beta_j = 2\beta_i \tag{A.24}$$

and

$$\left[\frac{1}{2}m^2 - \beta_i(-\beta_i + \beta_t + \sum_j \beta_j)\right] = -\frac{\lambda_i^4}{\tilde{\lambda}^2}(k^i)^2, \tag{A.25}$$

where $\tilde{\lambda} = \lambda_1\lambda_2\lambda_3$.

A.2.2 Gauge Field With Components Only Along Time

Next take the case where the gauge field has only a component along the time direction,

$$A = A_t(r)dt. \tag{A.26}$$

The field strength becomes

$$F = dA = A_t'(r)dr \wedge dt. \tag{A.27}$$

Using the Hodge star relations,

$$\begin{aligned} *_5(dr \wedge dt) &= -\frac{\sqrt{\eta}e^{-\beta_t r}}{6}\epsilon_{ijk}\, \omega^i \wedge \omega^j \wedge \omega^k && \text{(A.28)} \\ *_5(dt) &= \frac{\sqrt{\eta}e^{-\beta_t r}}{6}\epsilon_{ijk}\, dr \wedge \omega^i \wedge \omega^j \wedge \omega^k, && \text{(A.29)} \end{aligned}$$

we get

$$\begin{aligned} d *_5 F &= -\frac{\epsilon_{ijk}}{6}\left(\sqrt{\eta}e^{-\beta_t r}A_t'(r)\right)'\, dr \wedge \omega^i \wedge \omega^j \wedge \omega^k && \text{(A.30)} \\ *_5 A &= A_t(r)\frac{\sqrt{\eta}e^{-\beta_t r}}{6}\epsilon_{ijk}\, dr \wedge \omega^i \wedge \omega^j \wedge \omega^k. && \text{(A.31)} \end{aligned}$$

Thus the gauge field equation of motion eq.(A.10) becomes

$$\left(\sqrt{\eta}e^{-\beta_t r}A_t'(r)\right)' = \frac{m^2}{2}A_t(r)\sqrt{\eta}e^{-\beta_t r}. \tag{A.32}$$

With a metric eq.(A.8) and gauge field

$$A_t(r) = A_t e^{\beta_t r}, \tag{A.33}$$

we get

$$2\beta_t \sum_i \beta_i = m^2, \tag{A.34}$$

where $\tilde{\lambda} = \lambda_1\lambda_2\lambda_3$.

A.3 Lifshitz Solutions

In this appendix we examine Lifshitz solutions which are known to arise in the system, eq.(2.11). Let us consider an ansatz,

$$ds^2 = dr^2 - e^{2\beta_t r} dt^2 + e^{2\beta_i r}(dx^i)^2 \tag{A.35}$$

where $i = 1, 2, 3$. Let us first turn on the gauge field along time direction,

$$A = \sqrt{A_t} e^{\beta_t r} dt. \tag{A.36}$$

The Maxwell equation gives

$$m^2 = 2\beta_t(\beta_1 + \beta_2 + \beta_3) \tag{A.37}$$

and the trace reversed Einstein equations give

$$\begin{aligned}
A_t\beta_t^2 - 3(\beta_t^2 + \beta_1^2 + \beta_2^2 + \beta_3^2) + \Lambda &= 0 & \text{(A.38)}\\
A_t(3m^2 + 4\beta_t^2) - 12\beta_t(\beta_t + \beta_1 + \beta_2 + \beta_3) + 4\Lambda &= 0 & \text{(A.39)}\\
A_t\beta_t^2 + 6\beta_1(\beta_t + \beta_1 + \beta_2 + \beta_3) - 2\Lambda &= 0 & \text{(A.40)}\\
A_t\beta_t^2 + 6\beta_2(\beta_t + \beta_1 + \beta_2 + \beta_3) - 2\Lambda &= 0 & \text{(A.41)}\\
A_t\beta_t^2 + 6\beta_3(\beta_t + \beta_1 + \beta_2 + \beta_3) - 2\Lambda &= 0. & \text{(A.42)}
\end{aligned}$$

The last three equations show $\beta_i = \beta$ for all i. Using this in the Maxwell equation we get

$$m^2 = 6\beta\beta_t. \tag{A.43}$$

Then solving the other equation of motion gives the solution as

$$\begin{aligned}
\beta_i &= \beta \;\forall\; i & \text{(A.44)}\\
m^2 &= 6\beta\beta_t & \text{(A.45)}\\
\Lambda &= \beta_t^2 + 2\beta\beta_t + 9\beta^2 & \text{(A.46)}\\
A_t &= 2(1 - \frac{\beta}{\beta_t}). & \text{(A.47)}
\end{aligned}$$

If $\beta_t > 0, \beta_i > 0$,then m^2 is always positive. For the gauge field to be real, $\beta_t > \beta$.

Now, with the same metric ansatz, we choose the gauge field to be oriented along any one of x^i directions. Without loss of generality, let us choose it to be oriented along x^1:

$$A = \sqrt{A_1} e^{\beta_1 r} dx^1. \tag{A.48}$$

The equation of motion can be obtained from the previous case by $\beta_t \leftrightarrow \beta_1$ and $A_t \to -A_1$.

Then solving the equation of motion gives

$$\begin{aligned}
\beta_t = \beta_i &= \beta \ \forall\ i \neq 1 && \text{(A.49)}\\
m^2 &= 6\beta\beta_1 && \text{(A.50)}\\
\Lambda &= \beta_1^2 + 2\beta\beta_1 + 9\beta^2 && \text{(A.51)}\\
A_1 &= 2(\frac{\beta}{\beta_1} - 1). && \text{(A.52)}
\end{aligned}$$

Again, if $\beta_t > 0, \beta_i > 0$, then m^2 is always positive. For the gauge field to be real $\beta > \beta_1$.

A.4 Extremal RN solution

Starting with the action eq.(2.11), and setting $m^2 = 0$, one gets the well known Reissner Nordstrom black brane solution.

It has the metric

$$ds^2 = -a(\tilde{r})dt^2 + \frac{1}{a(\tilde{r})}d\tilde{r}^2 + b(\tilde{r})[dx^2 + dy^2 + dz^2] \tag{A.53}$$

with

$$a(\tilde{r}) = \frac{Q^2}{12\tilde{r}^4} + \frac{\tilde{r}^2\Lambda}{12} - \frac{M}{\tilde{r}^2} \qquad b(\tilde{r}) = \tilde{r}^2 \tag{A.54}$$

and the gauge field,

$$A = -\left(\frac{Q}{2\tilde{r}^2} - \frac{Q}{2\tilde{r}_h^2}\right) dt. \tag{A.55}$$

Here Q is charge and M is the mass of the black brane.

In the extremal limit we get $a'(\tilde{r}_h) = 0$ and also $a(\tilde{r}_h) = 0$. This allows us to solve for Q and M in terms of $\tilde{r}_h$,

$$\begin{aligned}
M &= \frac{\tilde{r}_h^4\Lambda}{4} && \text{(A.56)}\\
Q^2 &= 2\tilde{r}_h^6\Lambda, && \text{(A.57)}
\end{aligned}$$

giving eq.(2.125), eq.(2.127).

Now consider a new radial coordinate, $\tilde{r}$, given by eq.(2.128).. The relation between the coordinates near $\tilde{r} = \tilde{r}_h$ is given by

$$\sqrt{\Lambda}r = \log\left(\frac{\tilde{r} - \tilde{r}_h}{\tilde{r}_h}\right) + \frac{7}{6}\frac{\tilde{r} - \tilde{r}_h}{\tilde{r}_h} + \cdots . \tag{A.58}$$

This can be inverted (as $\tilde{r} \to \tilde{r}_h$, $r \to -\infty$) to give

$$\frac{\tilde{r} - \tilde{r}_h}{\tilde{r}_h} = e^{\sqrt{\Lambda}r}\left[1 - \frac{7}{6}e^{\sqrt{\Lambda}r} + \cdots\right]. \tag{A.59}$$

In the new coordinates the metric near $r = -\infty$ becomes

$$\begin{aligned} ds^2 &= dr^2 - \tilde{r}_h^2 \Lambda e^{2\sqrt{\Lambda} r}\left(1 - \frac{14}{3} e^{\sqrt{\Lambda} r} + \cdots\right) dt^2 \\ &+ \tilde{r}_h^2 \left(1 + 2 e^{\sqrt{\Lambda} r} + \cdots\right)(dx^2 + dy^2 + dz^2) \end{aligned} \tag{A.60}$$

and the gauge field becomes

$$A = \tilde{r}_h \sqrt{\Lambda}\sqrt{2} e^{\sqrt{\Lambda} r}\left(1 - \frac{8}{3} e^{\sqrt{\Lambda} r} + \cdots\right) dt. \tag{A.61}$$

If we rescale the coordinates as $t \to \frac{t}{\tilde{r}_h \sqrt{\Lambda}}$ and $\{x, y, z\} \to \frac{1}{\tilde{r}_h}\{x, y, z\}$, then the solution up to first order in deviation near $r = -\infty$ can be written as, eq.(2.129), eq.(2.130).

Appendix B

Appendices for Chapter 3: *Entangled Dilaton Dyons*

B.1 Numerical Interpolation

In this appendix we consider Case II solutions which were discussed in section 3.3.2 and establish that the deep IR solution is indeed $AdS_2 \times R^2$. We establish this numerically by integrating outwards from the $AdS_2 \times R^2$ near horizon solution discussed in subsection 3.3.2 and showing that the system approaches the electric scaling solution. For a suitable potential we find that the electric scaling solution in turn finally asymptotes to AdS_4 in the UV. Our numerical work is done using the Mathematica package.

We divide the discussion into three parts. In the first part we identify two perturbations in the $AdS_2 \times R^2$ region that grow towards the UV. In the second part, by choosing an appropriate combination of these two perturbation, we numerically integrate outwards taking the scalar potential to be $V(\phi) = -|V_0|e^{2\delta\phi}$, eq.(3.4). At moderately large radial distances we get the electric scaling solution. In the last part, taking the potential to be of the form $V(\phi) = -2|V_0|\cosh(2\delta\phi)$ [1], we continue the numerical integration towards larger r and show that the geometry asymptotes to AdS_4.

B.1.1 The perturbations

To identify the perturbations in the $AdS_2 \times R^2$ solution discussed in 3.3.2 we consider perturbations of this solution of the following form for the metric components and the

[1] Note, for this last part we present results for the case where $\alpha > \delta$ so that in the electric scaling solution $\phi \to \infty$ in the deep IR. As a result the modified potential $-2|V_0|\cosh(2\delta\phi)$ can be approximated by $-|V_0|e^{2\delta\phi}$ in the IR. In the UV we then find that the modified potential allows for an AdS_4 solution. A similar analysis can be done when $\alpha < -\delta$, using a suitably modified potential.

dilaton,

$$a(r) = C_a r \left[1 + a_{c1} r^{\nu} + \mathcal{O}(r^{2\nu})\right] \tag{B.1}$$
$$b(r) = b_0 \left[1 + b_{c1} r^{\nu} + \mathcal{O}(r^{2\nu})\right] \tag{B.2}$$
$$\phi(r) = \phi_0 + \log\left[1 + \phi_{c1} r^{\nu} + \mathcal{O}(r^{2\nu})\right]. \tag{B.3}$$

Note that this is a perturbation series in r^{ν} which is valid in the near horizon region where $r \ll 1$. Equations (3.8-3.11) can be solved to leading order in r^{ν} to find perturbations which are relevant towards the UV, i.e with $\nu > 0$. We find two such perturbations parametrized by their strengths $\phi_{c1}^{(1)}, a_{c1}^{(2)}$ which are given below :

$$a_{c1}^{(1)} = \frac{2\delta}{1+\alpha^2-\delta^2+\sqrt{1+4\alpha^2-4\delta^2}}\phi_{c1}^{(1)} \tag{B.4}$$
$$b_{c1}^{(1)} = 0 \tag{B.5}$$
$$\nu_1 = \frac{1}{2}(-1+\sqrt{1+4\alpha^2-4\delta^2}) \tag{B.6}$$

and

$$b_{c1}^{(2)} = -\frac{3(-2+\alpha^2-\delta^2)}{2(-2+\alpha^2-2\delta^2)}a_{c1}^{(2)} \tag{B.7}$$
$$\phi_{c1}^{(2)} = -\frac{3\delta}{(-2+\alpha^2-2\delta^2)}a_{c1}^{(2)} \tag{B.8}$$
$$\nu_2 = 1 \tag{B.9}$$

Note that $b_{c1}^{(1)}$ vanishes in the first of the above perturbations, as a result the first correction to $b(r)$ starts at second order. Actually, we found it important to go to second order in the first of the above perturbations for carrying out the numerical integration satisfactorily. We will not provide the detailed expressions for these second order corrections here since they are cumbersome.

B.1.2 Scaling symmetries

The system of equations eq.(3.8)-eq.(3.11) has two scaling symmetries.

$$a^2 \to \lambda_1 a^2, \qquad r^2 \to \lambda_1 r^2 \tag{B.10}$$
$$(Q_e^2, Q_m^2) \to \lambda_2(Q_e^2, Q_m^2), \qquad b^2 \to \lambda_2 b^2 \tag{B.11}$$

The first scaling symmetries can be used to set [2] $a_{c1}^{(2)} = -1$. The second scaling symmetry can then be used to set $Q_e = 1$. In addition we can choose units so that $|V_0| = 1$. With these choices the system of equations has two parameters, $\phi_{c1}^{(1)}$, which characterises the first

[2]We cannot change the sign of $a_{c1}^{(2)}$ by using the symmetries. The above sign is necessary for the solution to flow to the electric scaling solution in the UV.

perturbation, eqn. (B.4), and Q_m. Numerical analysis shows that for a given choice of $Q_m \ll \mu^2$, $\phi_{c1}^{(1)}$ needs to be tuned very precisely to ensure that the solution flows to the electric scaling solution. Otherwise, for example with the modified potential considered in subsection B.1.4 below, the solution can flow from the $AdS_2 \times R^2$ region in the IR directly to AdS_4, as $r \to \infty$, without passing close to the electric scaling solution at intermediate values of r.

B.1.3 Numerics : $AdS_2 \times R^2$ to the Electric Scaling Solution

We will illustrate the fact that the solution evolves from the $AdS_2 \times R^2$ geometry to the electric scaling solution once the values of $\phi_{c1}^{(1)}$ is suitably chosen with one example here. Similar behaviour is found for other values of (α, δ), which lie in Case II [3]

The example we present here has $\alpha = 1, \delta = 0.6$ (satisfying $|\alpha| > \delta$). We will present the data here for the case when $Q_m = 10^{-4}$ the behaviour for other values of $Q_m \ll \mu^2$ is similar. It turns out that in this case we have to fine tune the value of this parameter to be near $\phi_{c1}^{(1)} = -0.3173$ so as to obtain an electric scaling solution at intermediate r.

Evidence for the electric scaling solution can be obtained by examining the relative contributions that various terms make in the effective potential eq.(3.7). In the electric scaling region the contribution that the Q_m^2 dependent term makes must be smaller than the Q_e^2 dependent term and the scalar potential which in turn must scale in the same way. Fig.(B.1) shows the different contributions to V_{eff} made by the terms, $e^{-2\alpha\phi}Q_e^2, e^{2\alpha\phi}Q_m^2$ and $b^4(r)\frac{e^{2\delta\phi}}{2}$ in a Log-Log plot. Clearly the Q_e^2 term is growing as the same power of r as the scalar potential $e^{2\delta\phi}$ term and Q_m^2 is subdominant.

Fig.(B.2) and Fig.(B.3) show the plots of metric components $a(r), b(r)$ and the scalar $\phi(r)$ obtained numerically. Each of them is fitted to a form given in eq(3.13). We see that the fitted parameters agree well with the analytic values for β, γ and k obtained from eq.(3.14) with $(\alpha, \delta) = (1, 0.6)$. This confirms that the system flows to the electric scaling solution.

B.1.4 Numerics : $AdS_2 \times R^2 \to$ Electric Scaling $\to AdS_4$.

Here we show that on suitably modifying the potential so that the IR behaviour is essentially left unchanged the solution which evolves from the $AdS_2 \times R^2$ geometry in the deep IR to the electric scaling solution can be further extended to become asymptotic AdS_4 in the far UV.

We will illustrate this for the choice made in the previous subsection: $(\alpha, \delta) = (1, 0.6)$, $(Q_e = 1, Q_m = 10^{-4})$. For this choice of (α, δ) it is easy to see from eq.(3.13), eq.(3.14) that $\phi \to \infty$ in the IR of the electric scaling solution, and from eq.(3.42) that it continues to be

[3] The example we choose here has $\alpha, \delta > 0$. Similar results are also obtained when $\alpha < 0, \delta > 0$.

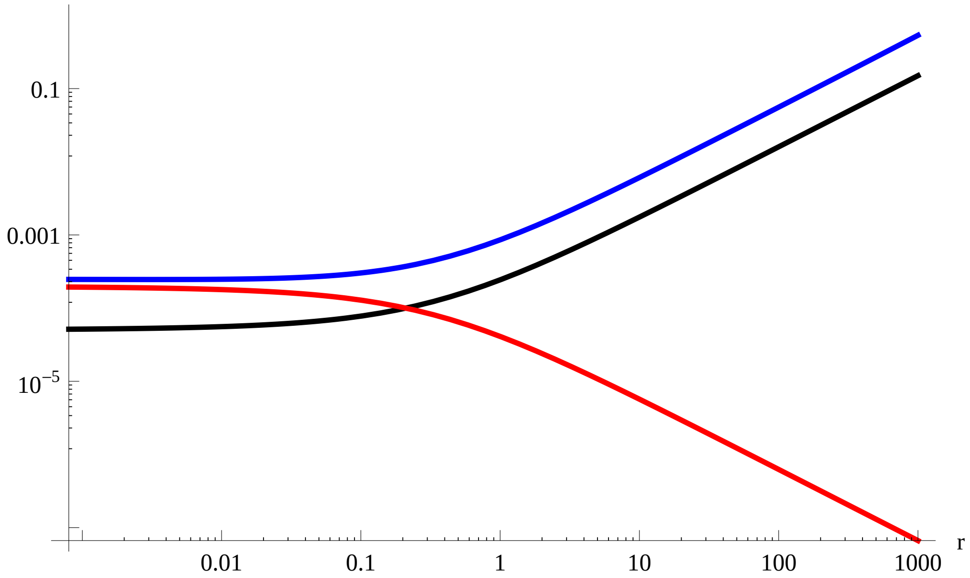

Figure B.1: Different contributions to V_{eff} in Log-Log plot. Blue→ Scalar Potential $b^4(r)\frac{e^{2\delta\phi}}{2}$, Black→ $Q_e^2 e^{-2\alpha\phi}$ term, Red→ $Q_m^2 e^{2\alpha\phi}$ term.

big in the $AdS_2 \times R^2$ geometry once the effects of the magnetic field are incorporated. We will modify the potential to be

$$V(\phi) = -2|V_0|\cosh(2\delta\phi) \tag{B.12}$$

instead of eq.(3.4). For $\phi \to \infty$ we see that this makes a small change, thus our analysis in the previous subsection showing that the solution evolves from the $AdS_2 \times R^2$ geometry to the electric scaling solution will be essentially unchanged. However, going to larger values of r the modification in the potential will become important. This modified potential has a maximum for the dilaton at $\phi = 0$ and a corresponding AdS_4 solution with [4] $R^2_{AdS} = -\frac{3}{V_0}$. We find by numerically integrating from the IR that the solution evolves to this AdS_4 geometry in the UV.

To see this first consider a plot of the three different contributions to V_{eff} proportional to $e^{-2\alpha\phi}Q_e^2, e^{2\alpha\phi}Q_m^2$ and $b^4(r)\cosh(2\delta\phi)$ shown in Fig.(B.4). We see that there are three distinct regions. In the far IR $AdS_2 \times R^2$ region, the three contributions are comparable. At intermediate r where we expect an electric scaling solution on the basis of the discussion of the previous subsection the magnetic field makes a subdominant contribution and the other two ontributions indeed scale in the same way. Finally at very large r, in the far UV, the cosmological constant is dominant as expected for an AdS_4 solution.

We also show the metric components $a(r), b(r)$ in a Log-Log plot in Fig(B.5) and (B.6). Once again, we can see three distinct slopes for a, b, corresponding to three different regions

[4]This example was analysed in [61]. The dilaton lies above the BF bound of the resulting AdS_4 theory for our choice of parameters.

in the solution. In the AdS_4 region, as $r \to \infty$, numerically fitting the behaviour gives $a(r), b(r) \sim r^{0.99}$ which is in good agreement[5] with the expected linear behaviour. Finally, Fig(B.6) shows the scalar function $\phi(r)$ settling to zero with the expected fall-off as $r \to \infty$. These results confirm that the system evolves to AdS_4 in the far UV.

[5]The fit was done for $r \sim 10^7$.

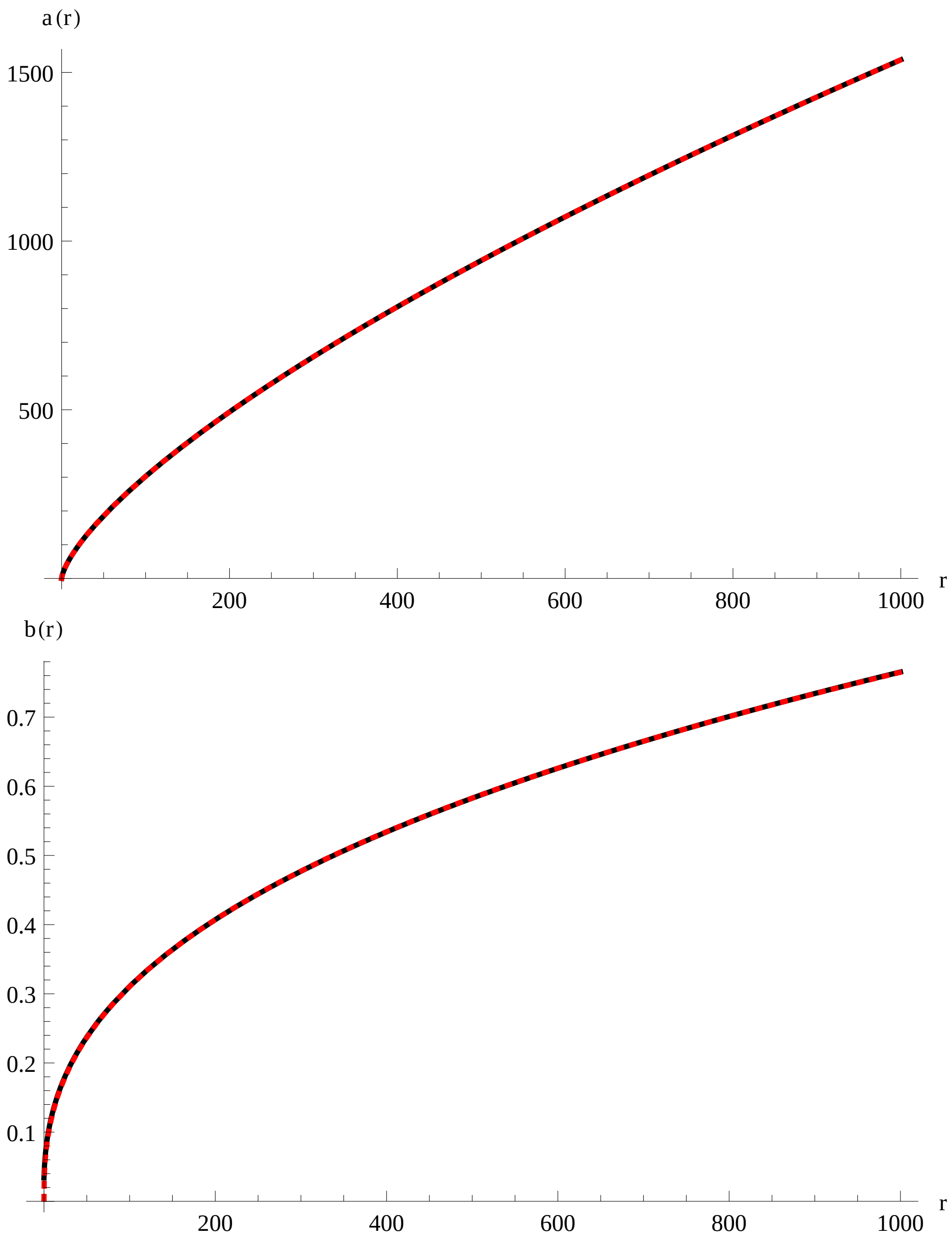

Figure B.2: In the top plot, $a(r) \sim r^{\gamma}$ with $\gamma_{Fit} = 0.706$ whereas $\gamma_{Analytical} = 0.707$. In the bottom plot, $b(r) \sim r^{\beta}$ with $\beta_{Fit} = 0.391$ whereas $\beta_{Analytical} = 0.390$.

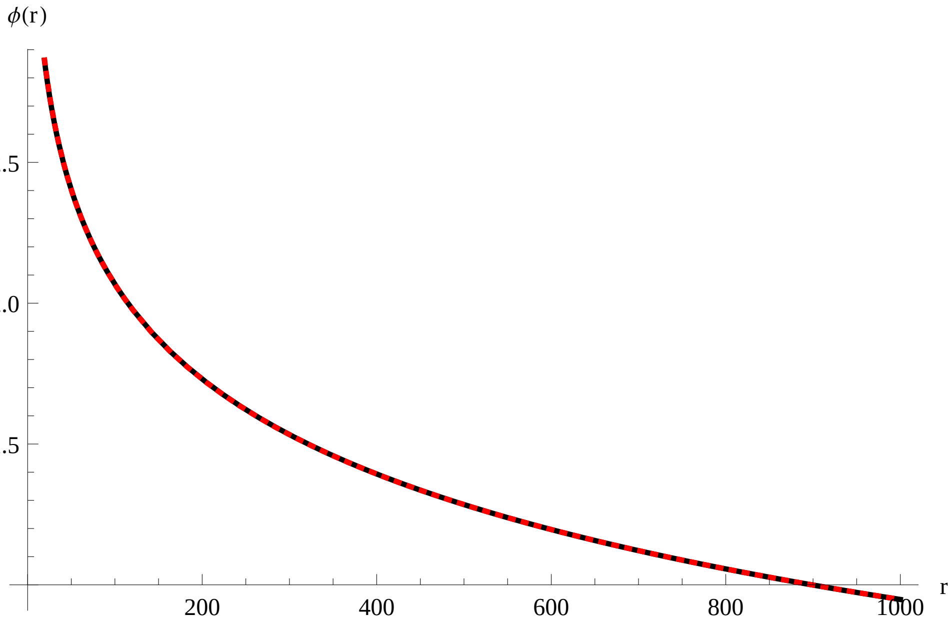

Figure B.3: $\phi = k\ log[r]$. $k_{Fit} = -0.4858$ as compared to $k_{Analytical} = -0.4878$.

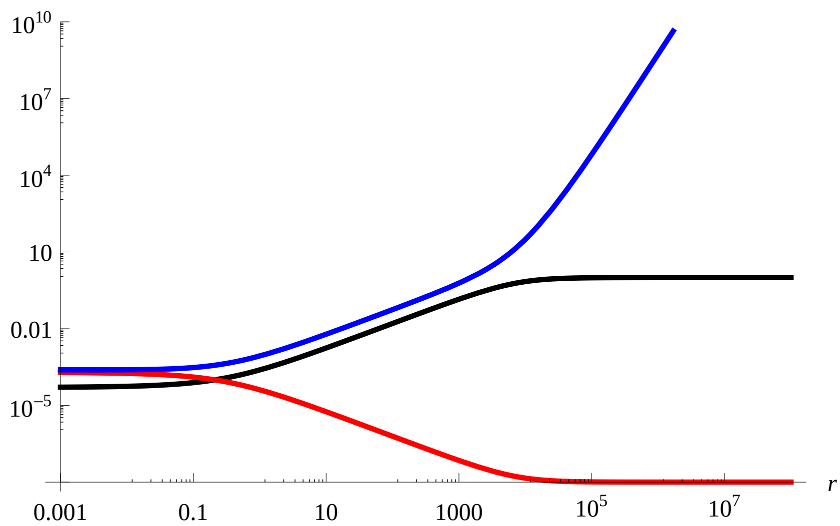

Figure B.4: Different contributions to V_{eff} in Log-Log plot. Blue→ Scalar Potential $b^4(r)\cosh(2\delta\phi)$, Black→ $Q_e^2 e^{-2\alpha\phi}$ term, Red→ $Q_m^2 e^{2\alpha\phi}$ term.

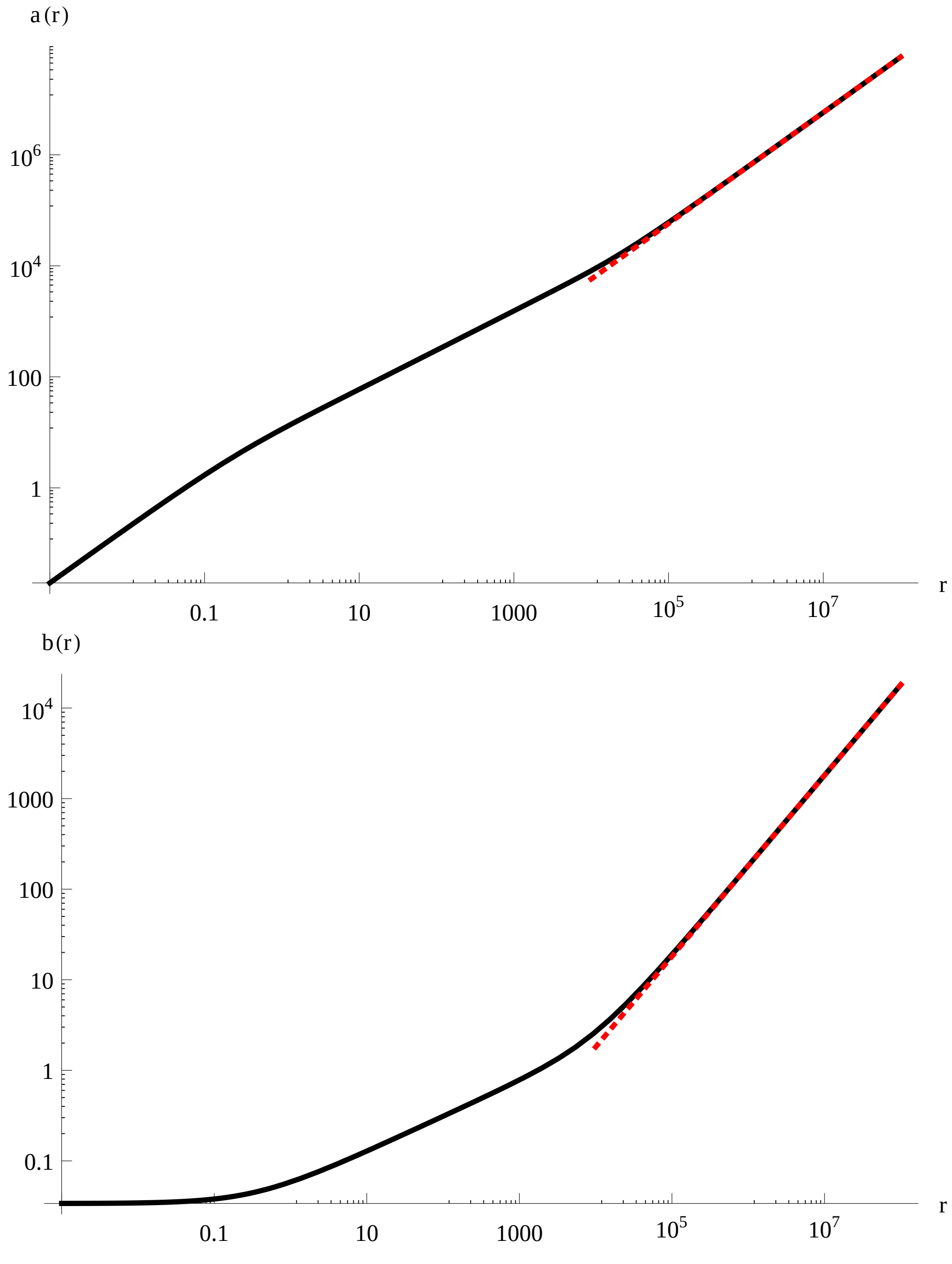

Figure B.5: In the Log-Log plot both curves show three different slopes for the metric components, which correspond to the three regions $AdS_2 \times R^2$, Electric Scaling Region and AdS_4 respectively.

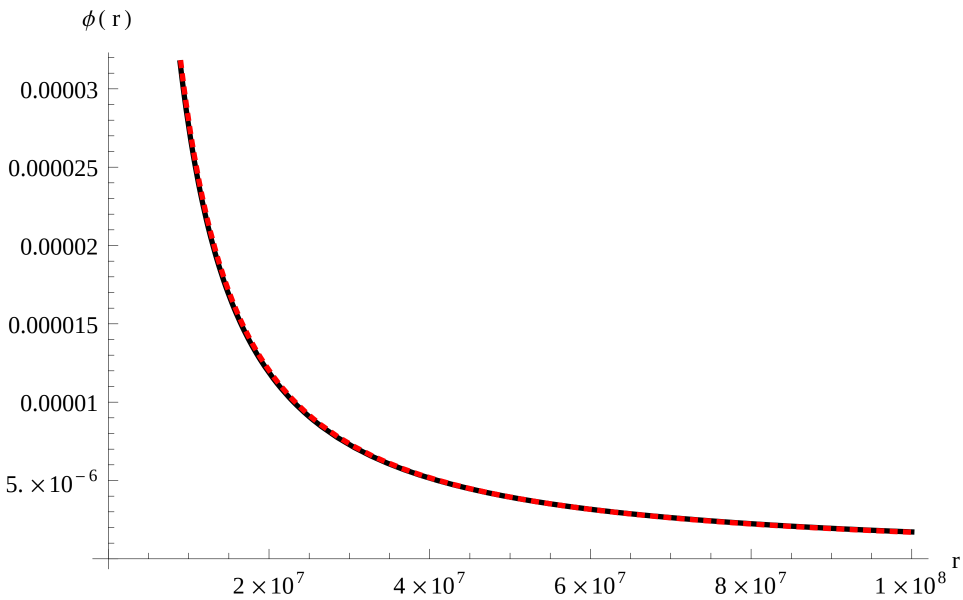

Figure B.6: $\phi(r)$ approaches zero like $r^{-1.22}$ as $r \to \infty$. This agrees with the fall off of non-normalizable component of dilaton in AdS_4.

Appendix C

Appendices for Chapter 4: *Conformal Invariance and the Four Point Scalar Correlator in Slow-Roll Inflation*

C.1 Two and Three Point Functions and Normalizations

In this appendix we will summarize the two point functions of scalar and tensor perturbations and the scalar-scalar-tensor three point function and issues related to their normalizations. The wave function in momentum space, written in eq.(4.37) contains the relevant coefficient functions for our discussion. The label s, s' corresponds to the polarizations of the graviton as shown in eq.(4.39). The polarization tensors $\epsilon^s_{ij}(\boldsymbol{k})$, in eq.(4.39) are transverse and traceless as already mentioned and are normalized according to,

$$\epsilon^{s,ij}\epsilon^{s'}_{ij} = 2\delta^{s,s'}. \tag{C.1}$$

Similarly, we define for the stress tensor

$$T^s(\boldsymbol{k}) = T_{ij}(\boldsymbol{k})\epsilon^{s,ij}(-\boldsymbol{k}). \tag{C.2}$$

In momentum space the coefficient functions are related to position spaces ones in eq.(4.36) and can be written as,

$$\langle O(\boldsymbol{k_1})O(\boldsymbol{k_2})\rangle = \int d^3\boldsymbol{x}d^3\boldsymbol{y}e^{-i\boldsymbol{k_1}\cdot\boldsymbol{x}}e^{-i\boldsymbol{k_2}\cdot\boldsymbol{y}}\langle O(\boldsymbol{x})O(\boldsymbol{y})\rangle. \tag{C.3}$$

With this convention all the other coefficient functions, $\langle T_{ij}(\boldsymbol{x})T_{kl}(\boldsymbol{y})\rangle$, $\langle O(\boldsymbol{x})O(\boldsymbol{y})T_{ij}(\boldsymbol{z})\rangle$ and $\langle O(\boldsymbol{x})O(\boldsymbol{y})O(\boldsymbol{z})O(\boldsymbol{w})\rangle$, will be related to their values in momentum space accordingly.

The coefficient functions, $\langle O(\boldsymbol{k_1})O(\boldsymbol{k_2})\rangle$, $\langle T^s(\boldsymbol{k_1})T^{s'}(\boldsymbol{k_2})\rangle$ are well known, in the literature. We write them here,

$$\langle O(\boldsymbol{k_1})O(\boldsymbol{k_2})\rangle = (2\pi)^3\delta^3(\boldsymbol{k_1}+\boldsymbol{k_2})k_1^3 \tag{C.4}$$

and

$$\langle T^s(\boldsymbol{k_1})T^{s'}(\boldsymbol{k_2})\rangle = (2\pi)^3\delta^3(\boldsymbol{k_1}+\boldsymbol{k_2})k_1^3\frac{\delta^{ss'}}{2}. \tag{C.5}$$

From eq.(C.4) and the wave function eq.(4.37) we get

$$\langle\zeta(\boldsymbol{k_1})\zeta(\boldsymbol{k_2})\langle= (2\pi)^3\delta(k_1+k_2)P_\zeta(\boldsymbol{k_1}) \tag{C.6}$$

where

$$P_\zeta(\boldsymbol{k_1}) = \frac{H^2}{M_{pl}^2}\frac{1}{\epsilon}\frac{1}{4k_1^3}. \tag{C.7}$$

For the slow-roll model of inflation being considered here the three point coefficient function $\langle O(\boldsymbol{k_1})O(\boldsymbol{k_2})T^s(\boldsymbol{k_3})\rangle$ was computed in [117]. It was also obtained in [131] from more general considerations, which is

$$\begin{aligned}\langle O(\boldsymbol{k_1})O(\boldsymbol{k_2})T_{ij}(\boldsymbol{k_3})\rangle e^{s,ij} =& -2(2\pi)^3\delta(\sum_{J=1}^{4}\boldsymbol{k}_J)e^{s,ij}k_{1i}k_{2j}S(k_1,k_2,k_3).\\ \text{with}\quad S(k_1,k_2,k_3) =&(k_1+k_2+k_3) - \frac{\sum_{i>j}k_ik_j}{(k_1+k_2+k_3)} - \frac{k_1k_2k_3}{(k_1+k_2+k_3)^2}.\end{aligned} \tag{C.8}$$

C.2 Ward Identities under Spatial and Time Reparameterization

In this appendix we will derive the Ward identities obeyed by the coefficient functions due to both spatial and time reparameterizations. They are also called the momentum and Hamiltonian constraints respectively. We will also discuss the transformation of the scalar and tensor perturbations under special conformal transformation (SCT) following invariance of wave function under SCT.

C.2.1 Ward Identities under Spatial and Time Reparameterization

We will consider the specific coefficient function $\langle T_{ij}(\boldsymbol{x})O(\boldsymbol{y_1})O(\boldsymbol{y_2})\rangle$ and derive the Ward identities under spatial and time parameterization. For that we need to consider only two out of the four terms in the exponent, the first and the third term, on RHS of the wave function in eq.(4.36),

$$\psi[\delta\phi,\gamma_{ij}] = \exp\left[\frac{M_{Pl}^2}{H^2}\Bigg(-\frac{1}{2}\int d^3x\sqrt{g(\boldsymbol{x})}\; d^3y\sqrt{g(\boldsymbol{y})}\;\delta\phi(\boldsymbol{x})\delta\phi(\boldsymbol{y})\langle O(\boldsymbol{x})O(\boldsymbol{y})\rangle \right.$$
$$-\frac{1}{4}\int d^3x\sqrt{g(\boldsymbol{x})}\; d^3y\sqrt{g(\boldsymbol{y})}\; d^3z\sqrt{g(\boldsymbol{z})} \tag{C.9}$$
$$\left.\delta\phi(\boldsymbol{x})\delta\phi(\boldsymbol{y})\gamma_{ij}(\boldsymbol{z})\langle O(\boldsymbol{x})O(\boldsymbol{y})T^{ij}(\boldsymbol{z})\rangle\Bigg)\right].$$

In the leading order to the perturbations, relevant to our calculation, $\sqrt{g(\boldsymbol{x})}$, defined in eq.(4.20), can be expanded as

$$\sqrt{g(\boldsymbol{x})} = 1 + \frac{1}{2}\gamma_{ii}(\boldsymbol{x}). \tag{C.10}$$

Under the spatial reparameterizations given in eq.(4.24) the scalar and tensor perturbations, $\delta\phi$ and γ_{ij}, transform as given in eq.(4.64) and eq.(4.65) respectively. Following them we can obtain the change in $\sqrt{g(\boldsymbol{x})}$ under the spatial reparameterizations

$$\sqrt{g(\boldsymbol{x})} \to \sqrt{g(\boldsymbol{x})} - \partial_i v_i(\boldsymbol{x}). \tag{C.11}$$

Using eq.(4.64), eq.(4.65) and eq.(C.11) we can obtain the change in the two terms on the RHS of eq.(C.9). They are, for the first term,

$$\begin{aligned}&\delta^S\left[-\frac{1}{2}\int d^3x\sqrt{g(\boldsymbol{x})}\; d^3y\sqrt{g(\boldsymbol{y})}\;\delta\phi(\boldsymbol{x})\delta\phi(\boldsymbol{y})\langle O(\boldsymbol{x})O(\boldsymbol{y})\rangle\right] = \\ &\frac{1}{2}\int d^3xd^3y\left[\frac{\partial}{\partial x^i}\Big\{v^i(\boldsymbol{x})\delta\phi(\boldsymbol{x})\Big\}\delta\phi(\boldsymbol{y}) + \delta\phi(\boldsymbol{x})\frac{\partial}{\partial y^i}\Big\{v^i(\boldsymbol{y})\delta\phi(\boldsymbol{y})\Big\}\right]\langle O(\boldsymbol{x})O(\boldsymbol{y})\rangle\end{aligned} \tag{C.12}$$

and similarly for the second term

$$\begin{aligned}&\delta^S\left[-\frac{1}{4}\int d^3x\sqrt{g(\boldsymbol{x})}\; d^3y\sqrt{g(\boldsymbol{y})}\; d^3z\sqrt{g(\boldsymbol{z})}\delta\phi(\boldsymbol{x})\delta\phi(\boldsymbol{y})\gamma_{ij}(\boldsymbol{z})\langle O(\boldsymbol{x})O(\boldsymbol{y})T^{ij}(\boldsymbol{z})\rangle\right] \\ &= \frac{1}{2}\int d^3x\; d^3y\; d^3z\frac{\partial v^i(\boldsymbol{z})}{\partial z^j}\delta\phi(\boldsymbol{x})\delta\phi(\boldsymbol{y})\langle O(\boldsymbol{x})O(\boldsymbol{y})T^{ij}(\boldsymbol{z})\rangle.\end{aligned} \tag{C.13}$$

The invariance of the wave function under spatial reparameterizations as stated in eq.(4.66), translates to the requirement that the total change of the RHS of eq.(C.9) vanishes. Which in turn implies the sum of eq.(C.12) and eq.(C.13) vanishes. This requirement, after performing an integration by parts to move the derivatives in the RHS. of eq.(C.12) and eq.(C.13) to the coefficient functions, leads us to the desired Ward identity given in eq.(4.67), which is the momentum constraint.

Under the time reparameterization in eq.(4.26), at late times when $e^{-Ht} \to 0$, the scalar perturbation, $\delta\phi$, does not change and the tensor perturbation, γ_{ij}, changes as given in eq.(4.68). Also $\sqrt{g(\boldsymbol{x})}$, in eq.(C.10), changes by,

$$\sqrt{g(\boldsymbol{x})} \to \sqrt{g(\boldsymbol{x})} + 3H\epsilon(\boldsymbol{x}). \tag{C.14}$$

Using these we can obtain the change in the two terms on the RHS of eq.(C.9) under time reparameterization, similarly as we did for the spatial reparameterization. They are, for the first term,

$$\begin{aligned} \delta^T\bigg[-\frac{1}{2}\int d^3x\sqrt{g(\boldsymbol{x})}\; d^3y\sqrt{g(\boldsymbol{y})}\; \delta\phi(\boldsymbol{x})\delta\phi(\boldsymbol{y})\langle O(\boldsymbol{x})O(\boldsymbol{y})\rangle\bigg] = -\frac{1}{2}\int d^3x\; d^3y\; d^3z \\ \delta\phi(\boldsymbol{x})\delta\phi(\boldsymbol{y})H\epsilon(\boldsymbol{z})\Big[3\delta^3(z-x)\langle O(\boldsymbol{x})O(\boldsymbol{y})\rangle + 3\delta^3(z-y)\langle O(\boldsymbol{x})O(\boldsymbol{y})\rangle\Big] \end{aligned} \tag{C.15}$$

and similarly for the second term,

$$\begin{aligned} &\delta^T\bigg[-\frac{1}{4}\int d^3x\sqrt{g(\boldsymbol{x})}\; d^3y\sqrt{g(\boldsymbol{y})}\; d^3z\sqrt{g(\boldsymbol{z})}\delta\phi(\boldsymbol{x})\delta\phi(\boldsymbol{y})\gamma_{ij}(\boldsymbol{z})\langle O(\boldsymbol{x})O(\boldsymbol{y})T^{ij}(\boldsymbol{z})\rangle\bigg] \\ &= -\frac{1}{2}\int d^3x\; d^3y\; d^3zH\epsilon(\boldsymbol{z})\delta\phi(\boldsymbol{x})\delta\phi(\boldsymbol{y})\langle O(\boldsymbol{x})O(\boldsymbol{y})T^{ii}(\boldsymbol{z})\rangle. \end{aligned} \tag{C.16}$$

The invariance of the wave function under the time reparameterization as mentioned in eq.(4.69) then implies that the sum of eq.(C.15) and eq.(C.16) vanishes. Which leads us to the constraint on the coefficient function under time reparameterization as written in eq.(4.70), also called the Hamiltonian constraint.

C.2.2 Transformations of the Scalar and Tensor Perturbations under SCT

At late times, $e^{-Ht} \to 0$, the special conformal transformation (SCT) takes the form as given in eq.(4.71) and eq.(4.72). Under SCT the scalar perturbation, $\delta\phi(\boldsymbol{x})$, transforms like a scalar,

$$\delta\phi(\boldsymbol{x}) \to \delta\phi'(\boldsymbol{x}) = \delta\phi(x^i - \delta x^i). \tag{C.17}$$

Therefore under SCT the change in scalar perturbation is,

$$\delta(\delta\phi) = \delta\phi'(\boldsymbol{x}) - \delta\phi(\boldsymbol{x}) = -(x^2b^i - 2x^i(\boldsymbol{x}\cdot\boldsymbol{b}))\frac{\partial}{\partial x^i}\delta\phi. \tag{C.18}$$

Since $e^{2Ht}g_{mn}$ appears as metric component in eq.(4.14), eq.(4.19), it should transform as a tensor under coordinate transformation

$$e^{2Ht'}g'_{ij}(\boldsymbol{x'}) = e^{2Ht}g_{mn}(\boldsymbol{x})\frac{\partial x^m}{\partial x'^i}\frac{\partial x^n}{\partial x'^j}. \tag{C.19}$$

From here one obtains the change in the tensor perturbation due to SCT,

$$\begin{aligned}
&\gamma_{ij}(\boldsymbol{x}) \to \gamma'_{ij}(\boldsymbol{x}) = \gamma_{ij}(\boldsymbol{x}) + \delta\gamma_{ij}(\boldsymbol{x}),\\
&\delta\gamma_{ij}(\boldsymbol{x}) = 2M^m{}_j\gamma_{im} + 2M^m{}_i\gamma_{mj} - (x^2b^m - 2x^m(\boldsymbol{x}\cdot\boldsymbol{b}))\frac{\partial\gamma_{ij}(\boldsymbol{x})}{\partial x^m},\\
&M^m{}_j = x^m b^j - x^j b^m.
\end{aligned} \tag{C.20}$$

The invariance of wave function under SCT implies that,

$$\psi[\gamma_{ij}(\boldsymbol{x})] = \psi[\gamma'_{ij}(\boldsymbol{x})] = \psi[\gamma_{ij}(\boldsymbol{x}) + \delta\gamma_{ij}(\boldsymbol{x})]. \tag{C.21}$$

Ignoring scalar perturbations one obtains,

$$\int d^3x\gamma_{ij}(\boldsymbol{x})T_{ij}(\boldsymbol{x}) = \int d^3x\,(\gamma_{ij}(\boldsymbol{x}) + \delta\gamma_{ij}(\boldsymbol{x}))\,T_{ij}(\boldsymbol{x}). \tag{C.22}$$

After doing integration by parts one can move the derivatives acting on γ_{ij} to T_{ij} to obtain,

$$\int d^3x\gamma_{ij}(\boldsymbol{x})T_{ij}(\boldsymbol{x}) = -\int d^3x\gamma_{ij}(\boldsymbol{x})\,(T_{ij}(\boldsymbol{x}) + \delta T_{ij}(\boldsymbol{x}))\,. \tag{C.23}$$

From eq.(C.23) one can obtain the change in $T_{ij}(\boldsymbol{x})$ under SCT. Similar arguments based on invariance of the wave function, can lead us from eq.(C.18) to the change in $O(\boldsymbol{x})$ under SCT. The position space expression for them are given in eq.(4.73) and eq.(4.74). We can obtain the changes in $O(\boldsymbol{x})$ and $T_{ij}(\boldsymbol{x})$ under SCT in momentum space in a straight forward manner as given below

$$\delta\phi(\boldsymbol{k}) \to \delta\phi'(\boldsymbol{k}) = \delta\phi(\boldsymbol{k}) + \delta\big(\delta\phi(\boldsymbol{k})\big), \tag{C.24}$$

$$O(\boldsymbol{k}) \to O'(\boldsymbol{k}) = O(\boldsymbol{k}) + \delta O(\boldsymbol{k}), \tag{C.25}$$

$$\gamma_{ij}(\boldsymbol{k}) \to \gamma'_{ij}(\boldsymbol{k}) = \gamma_{ij}(\boldsymbol{k}) + \delta\gamma_{ij}(\boldsymbol{k}), \tag{C.26}$$

$$T_{ij}(\boldsymbol{k}) \to T'_{ij}(\boldsymbol{k}) = T_{ij}(\boldsymbol{k}) + \delta T_{ij}(\boldsymbol{k}) \tag{C.27}$$

where

$$\delta\big(\delta\phi(\boldsymbol{k})\big) = 6(\boldsymbol{b}.\partial)\delta\phi(\boldsymbol{k}) + 2k_j\partial_{k_j}(\boldsymbol{b}\cdot\boldsymbol{\partial_k})\delta\phi(\boldsymbol{k}) - (\boldsymbol{b}\cdot\boldsymbol{k})\partial_{k^i}\partial_{k^i}\delta\phi(\boldsymbol{k}), \tag{C.28}$$

$$\delta O(\boldsymbol{k}) = 2k_j\partial_{k_j}(\boldsymbol{b}\cdot\boldsymbol{\partial_k})O(\boldsymbol{k}) - (\boldsymbol{b}\cdot\boldsymbol{k})\partial_{k^i}\partial_{k^i}O(\boldsymbol{k}), \tag{C.29}$$

$$\delta\gamma_{ij}(\boldsymbol{k}) = 6(\boldsymbol{b}.\partial)\gamma_{ij} + 2\tilde{M}^l_i\gamma_{lj} + 2\tilde{M}^l_j\gamma_{il} + 2k_l\partial_{k_l}(\boldsymbol{b}\cdot\boldsymbol{\partial_k})\gamma_{ij} - (\boldsymbol{b}\cdot\boldsymbol{k})\partial_{k^l}\partial_{k^l}\gamma_{ij}, \tag{C.30}$$

$$\delta T_{ij}(\boldsymbol{k}) = 2\tilde{M}^l_iT_{lj} + 2\tilde{M}^l_jT_{il} + 2k_l\partial_{k_l}(\boldsymbol{b}\cdot\boldsymbol{\partial_k})T_{ij} - (\boldsymbol{b}\cdot\boldsymbol{k})\partial_{k^l}\partial_{k^l}T_{ij}, \tag{C.31}$$

$$\tilde{M}^l_i \equiv b^l\partial_{k^i} - b^i\partial_{k^l}. \tag{C.32}$$

C.3 More Details on Calculating the AdS Correlator

In this appendix we will discuss in some more detail the algebra leading us to the four point scalar correlator in AdS, written in eq.(4.121), which is the unknown coefficient in on-shell action in AdS space, $S^{\text{AdS}}_{\text{on-shell}}$.

The basic technique to compute this correlator is simply to consider the Feynman-Witten diagrams in AdS that are shown in 4.1. These diagrams are just like flat space Feynman diagrams, except that the propagators between bulk points are replaced by AdS Green functions, and the lines between the bulk and the boundary are contracted with regular solutions to the wave equation in AdS, which are called bulk to boundary propagators.

We start with our action in eq.(4.91) for a canonically coupled massless scalar field, $\delta\phi$, in AdS_4 space-time. The stress tensor for the scalar field, $T_{\mu\nu}$, acts as a source coupled to the metric perturbation $\delta g_{\mu\nu}$. In the gauge given in eq.(4.103), the evaluation of the Witten diagram simplifies to the expression given in (4.104), which we copy here for the reader's convenience

$$\int dz_1 dz_2 \sqrt{-g_1}\sqrt{-g_2} T_{i_1 j_1}(z_1) g^{i_1 i_2} g^{j_1 j_2} G^{\text{grav}}_{i_2 j_2, k_2 l_2}(\boldsymbol{k}, z_1, z_2) g^{k_1 k_2} g^{l_1 l_2} T_{k_1 l_1}(z_2)$$
$$G^{\text{grav}}_{ij,kl}(\boldsymbol{k}, z_1, z_2) = \int \left[\frac{(z_1)^{\frac{-1}{2}} J_{\frac{3}{2}}(pz_1) J_{\frac{3}{2}}(pz_2)(z_2)^{\frac{-1}{2}}}{\left(\boldsymbol{k}^2 + p^2 - i\epsilon\right)} \frac{1}{2}\left(\mathcal{T}_{ik}\mathcal{T}_{jl} + \mathcal{T}_{il}\mathcal{T}_{jk} - \frac{2\mathcal{T}_{ij}\mathcal{T}_{kl}}{d-1}\right)\right] \frac{-dp^2}{2}, \tag{C.33}$$

Note that here, as opposed to (4.104), we have suppressed all except for the radial coordinates.

In fact the Bessel functions, which appear above simplify greatly in $d = 3$, so that we have $J_{3/2}(z)$ which appears in eq.(4.109) refers to the Bessel function with index 3/2. It has the form,

$$J_{3/2}(z) = \sqrt{\frac{2}{\pi}} \frac{1}{\sqrt{z}} \left(-\cos z + \frac{\sin z}{z}\right) = \sqrt{\frac{2}{\pi}} \frac{(1-iz)e^{iz} - (1+iz)e^{-iz}}{2iz\sqrt{z}}. \tag{C.34}$$

As we will see below, this makes the z-integrals involved in the evaluation of (C.33) very simple. The integral over p can also be done by residues. However, from an algebraic viewpoint, it is simply to replace $\mathcal{T}_{ij} = \delta_{ij} + k_i k_j/p^2$ with $\tilde{\mathcal{T}}_{ij} = \delta_{ij} - k_i k_j/k^2$, which is the transverse traceless projector onto the exchanged momentum.

This replacement leads to an additional "remainder" term, which accounts for the contribution of the longitudinal modes of the graviton. It also reduces our propagator to the form given in eq.(4.14) of [162], for $d = 3$ which reduces to,

$$\begin{aligned} I =& \frac{1}{4}\frac{M_{Pl}^2}{2}\Big[\int d^4x_1 d^4x_2 \sqrt{g(z_1)}\sqrt{g(z_2)}(z_1z_2)^2 t_{ij}(x_1)G(x_1,x_2)t_{ij}(x_2) \\ & - 2\int d^4x_1\sqrt{g(z_1)}z_1^2 T_{zj}\frac{1}{\partial^2}T_{zj} - \int d^4x_1\sqrt{g(z_1)}z_1^3\partial_j T_{zj}\frac{1}{\partial^2}T_{zz} \\ & - \frac{1}{2}\int d^4x_1\sqrt{g(z_1)}z_1^2\partial_j T_{zj}\left(\frac{1}{\partial^2}\right)^2\partial_i T_{zi}\Big]. \end{aligned} \tag{C.35}$$

Note that in writing the above equation we have corrected two typographical errors in eq.(4.14) of [162]. First, an overall factor of $\frac{1}{4}$ and second, z_1^3 in place of z_1^2 in the third term on the RHS of eq.(C.35). In the first term on the RHS of eq.(C.35), $t_{ij} = \widehat{P}_{ijkl}T_{kl}$, such that $\widehat{P}_{ijkl}$ is the transverse traceless projector in flat space, eq.(4.125), and $G(x_1, x_2)$ is the Green's function for a free massless scalar field in Euclidean AdS_4, obtained in appendix A, see eq.(A.3), of [162].

It is straightforward to see that the first term on the RHS of eq.(C.35) becomes the contribution from the transverse graviton, $\widetilde{W}$ in eq.(4.108), and also the three other terms on the RHS of eq.(C.35) which are the contributions from the longitudinal graviton become R_1, R_2 and R_3 in eq.(4.112) respectively.

Next we proceed to perform the integrations in eq.(4.108) and eq.(4.112). We start with $\widetilde{W}$ in eq.(4.108).

After being fourier transformed to momentum space the stress tensor, appearing in eq.(4.108), becomes

$$T_{ij}(\boldsymbol{k}, z) = \int d^3\boldsymbol{x}\ T_{ij}(\boldsymbol{x}, z)\ e^{-i\ \boldsymbol{k}\cdot\boldsymbol{x}}. \tag{C.36}$$

Using eq.(C.36), $\widetilde{W}$, as in eq.(4.108), takes the form

$$\widetilde{W} = \int dz_1 dz_2 \frac{d^3\boldsymbol{k}}{(2\pi)^3} T_{i_1j_1}(-\boldsymbol{k}, z_1)\delta^{i_1i_2}\delta^{j_1j_2}\widetilde{G}_{i_2j_2,k_2l_2}(\boldsymbol{k}, z_1, z_2)\delta^{k_1k_2}\delta^{l_1l_2}T_{k_1l_1}(\boldsymbol{k}, z_2) \tag{C.37}$$

in momentum space with

$$\widetilde{G}_{ij,kl}(\boldsymbol{k}, z_1, z_2) = \int_0^\infty \frac{dp^2}{2}\left[\frac{J_{\frac{3}{2}}(pz_1)J_{\frac{3}{2}}(pz_2)}{\sqrt{z_1z_2}\left(\boldsymbol{k}^2+p^2\right)}\frac{1}{2}\left(\widetilde{\mathcal{T}}_{ik}\widetilde{\mathcal{T}}_{jl} + \widetilde{\mathcal{T}}_{il}\widetilde{\mathcal{T}}_{jk} - \widetilde{\mathcal{T}}_{ij}\widetilde{\mathcal{T}}_{kl}\right)\right]. \tag{C.38}$$

The indices i_1, j_1 etc which appear in eq.(C.37) take values along the $x^i, i = 1, 2, 3$ directions eq.(4.93). The z components of the stress tensor do not appear because of our choice of gauge, eq.(4.103).

In eq.(C.37) the graviton propagator $\widetilde{G}_{ijkl}(\boldsymbol{k}, z_1, z_2)$ is contracted against two factors of the stress tensors $T_{ij}(\boldsymbol{k}, z)$. The stress tensor for the scalar perturbation $\delta\phi$, acts like a source term for the metric perturbation $\delta g_{\mu\nu}$ as evident from the interaction vertex in eq.(4.97).

From the expression of stress tensor in eq.(4.98) one can obtain,

$$T_{ij}(z,\boldsymbol{x}) = 2(\partial_i\delta\phi)(\partial_j\delta\phi) - \delta_{ij}\left[(\partial_z\delta\phi)^2 + \eta^{mn}(\partial_m\delta\phi)(\partial_n\delta\phi)\right]. \tag{C.39}$$

The two insertions of the stress tensor in eq.(C.37) correspond to two different values of the radial variable $z = z_1$ and $z = z_2$, which are integrated over. For the S-channel contribution one should substitute for $\delta\phi$ from eq.(4.101) in eq.(C.39) and keep only the bilinears of the form $\phi(\boldsymbol{k_1})\phi(\boldsymbol{k_2})$ at $z = z_1$ and similarly $\phi(\boldsymbol{k_3})\phi(\boldsymbol{k_4})$ at $z = z_2$. For the T- channel and U- channel contributions one just needs to exchange two of the external momenta in the S-channel answer like $\boldsymbol{k_2} \leftrightarrow \boldsymbol{k_3}$ and $\boldsymbol{k_2} \leftrightarrow \boldsymbol{k_4}$ respectively.

In momentum space, the stress tensors, to be substituted for in eq.(C.37), becomes

$$\begin{aligned} T_{ij}[\phi_1(z_1),\phi_2(z_1)] &= -4\left\{k_{1i}k_{2j}\phi_1\phi_2 + \frac{1}{2}\eta_{ij}\left[(\partial_{z_1}\phi_1)(\partial_{z_1}\phi_2) - \boldsymbol{k_1}\cdot\boldsymbol{k_2}\,\phi_1\phi_2\right]\right\}, \\ T_{kl}[\phi_3(z_2),\phi_4(z_2)] &= -4\left\{k_{3k}k_{4l}\phi_3\phi_4 + \frac{1}{2}\eta_{kl}\left[(\partial_{z_2}\phi_3)(\partial_{z_2}\phi_4) - \boldsymbol{k_3}\cdot\boldsymbol{k_4}\,\phi_3\phi_4\right]\right\}. \end{aligned} \tag{C.40}$$

We have used $\partial_m\phi = -ik_m\phi$ and $g^{ij} = z^2\eta^{ij}$ and also the abbreviations

$$\begin{aligned} \phi_1 &\equiv \phi(\boldsymbol{k_1})(1+k_1z_1)e^{-k_1z_1}, &\quad \phi_2 &\equiv \phi(\boldsymbol{k_2})(1+k_2z_1)e^{-k_2z_1}, \\ \phi_3 &\equiv \phi(\boldsymbol{k_3})(1+k_3z_2)e^{-k_3z_1}, &\quad \phi_4 &\equiv \phi(\boldsymbol{k_4})(1+k_4z_2)e^{-k_4z_2}. \end{aligned} \tag{C.41}$$

It is important to note that only the first term on the RHS of eq.(C.40) in both T_{ij} and T_{kl} contribute to $\widetilde{W}$ in eq.(C.37). This is because the second term in T_{ij} on the RHS of eq.(C.40) carries η_{ij} which when contracted with the transverse projector $\left(\widetilde{\mathcal{T}}_{ik}\widetilde{\mathcal{T}}_{jl} + \widetilde{\mathcal{T}}_{il}\widetilde{\mathcal{T}}_{jk} - \widetilde{\mathcal{T}}_{ij}\widetilde{\mathcal{T}}_{kl}\right)$ of the graviton propagator $\widetilde{G}_{i_2j_2,k_2l_2}(\boldsymbol{k},z_1,z_2)$ in eq.(C.38), gives zero.

$$\eta_{ij}\left(\widetilde{\mathcal{T}}_{ik}\widetilde{\mathcal{T}}_{jl} + \widetilde{\mathcal{T}}_{il}\widetilde{\mathcal{T}}_{jk} - \widetilde{\mathcal{T}}_{ij}\widetilde{\mathcal{T}}_{kl}\right) = 0. \tag{C.42}$$

Therefore, the relevant terms in the stress tensors are,

$$\begin{aligned} T_{ij}(z_1) &= -4k_{1i}k_{2j}\phi_1\phi_2, \\ T_{kl}(z_2) &= -4k_{3k}k_{4l}\phi_3\phi_4. \end{aligned} \tag{C.43}$$

Finally substituting in eq.(C.37) for T_{ij} from eq.(C.43) with the ϕ_i's in eq.(C.41) and the graviton propagator in eq.(C.38) we obtain $\widetilde{W}^S(\boldsymbol{k_1},\boldsymbol{k_2},\boldsymbol{k_3},\boldsymbol{k_4})$ as,

$$\begin{aligned} \widetilde{W}^S(\boldsymbol{k_1},\boldsymbol{k_2},\boldsymbol{k_3},\boldsymbol{k_4}) =& 16(2\pi)^3\delta^3(\sum_i \boldsymbol{k}_i)\phi(\boldsymbol{k_1})\phi(\boldsymbol{k_2})\phi(\boldsymbol{k_3})\phi(\boldsymbol{k_4}) \\ & k_1^ik_2^jk_3^kk_4^l\left(\widetilde{\mathcal{T}}_{ik}\widetilde{\mathcal{T}}_{jl} + \widetilde{\mathcal{T}}_{il}\widetilde{\mathcal{T}}_{jk} - \widetilde{\mathcal{T}}_{ij}\widetilde{\mathcal{T}}_{kl}\right)S(k_1,k_2,k_3,k_4) \end{aligned} \tag{C.44}$$

where

$$S(k_1,k_2,k_3,k_4) = \int_0^\infty \frac{dp^2}{2(p^2+K_s^2)} \int_0^\infty \frac{dz_1}{z_1^2}(1+k_1z_1)(1+k_2z_1)(z_1)^{\frac{3}{2}} J_{\frac{3}{2}}(pz_1) e^{-(k_1+k_2)z_1} \int_0^\infty \frac{dz_2}{z_2^2}(1+k_3z_2)(1+k_4z_2)(z_2)^{\frac{3}{2}} J_{\frac{3}{2}}(pz_2) e^{-(k_3+k_4)z_1}, \tag{C.45}$$

and K_s which is the norm of the momentum of the graviton exchanged in the S channel, is

$$\boldsymbol{k}_s = \boldsymbol{k_1} + \boldsymbol{k_2} = -(\boldsymbol{k_3} + \boldsymbol{k_4}) \tag{C.46}$$

$S(k_1, k_2k_3, k_4)$ can be evaluated by explicitly carrying out the integrals. We first do the z_1, z_2 integrals by noting that,

$$\int_0^\infty \frac{dz_1}{z_1^2}(1+k_1z_1)(1+k_2z_1)(z_1)^{\frac{3}{2}} J_{\frac{3}{2}}(pz_1) e^{-(k_1+k_2)z_1} = \sqrt{\frac{2}{\pi}} \frac{p^{3/2}\left(k_1^2+4k_2k_1+k_2^2+p^2\right)}{\left((k_1+k_2)^2+p^2\right)^2} \tag{C.47}$$

This gives,

$$S(k_1,k_2,k_3,k_4) = \int_0^\infty dp \frac{2}{\pi} \frac{p^4\left(k_1^2+4k_2k_1+k_2^2+p^2\right)\left(k_3^2+4k_4k_3+k_4^2+p^2\right)}{\left((k_1+k_2)^2+p^2\right)^2\left((k_3+k_4)^2+p^2\right)^2\left(K_s^2+p^2\right)}, \tag{C.48}$$

The p integral is now easy to do, by noting that the integrand is an even function of p, and then doing the integral by the method of residues. This is a significant advantage of massless fields in momentum space in AdS$_{d+1}$, where d is odd: exchange interactions can be evaluated algebraically! This leads to

$$\begin{aligned} S = -2\Bigg[& \frac{k_1k_2(k_1+k_2)^2\left((k_1+k_2)^2-k_3^2-k_4^2-4k_3k_4\right)}{(k_1+k_2-k_3-k_4)^2(k_1+k_2+k_3+k_4)^2(k_1+k_2-K_s)(k_1+k_2+K_s)} \\ & \Big(-\frac{k_1+k_2}{2k_1k_2} - \frac{k_1+k_2}{-(k_1+k_2)^2+k_3^2+k_4^2+4k_3k_4} + \frac{k_1+k_2}{K_s^2-(k_1+k_2)^2} \\ & + \frac{1}{-k_1-k_2+k_3+k_4} - \frac{1}{k_1+k_2+k_3+k_4} + \frac{3}{2(k_1+k_2)}\Big) + (1,2 \leftrightarrow 3,4) \\ & - \frac{K_s^3\left(-k_1^2-4k_2k_1-k_2^2+K_s^2\right)\left(-k_3^2-4k_4k_3-k_4^2+K_s^2\right)}{2\left(-k_1^2-2k_2k_1-k_2^2+K_s^2\right)^2\left(-k_3^2-2k_4k_3-k_4^2+K_s^2\right)^2}\Bigg]. \end{aligned} \tag{C.49}$$

This value of S from eq.(C.49) along with the index contraction

$$\begin{aligned}
&k_1^i k_2^j k_3^k k_4^l(\widetilde{\mathcal{T}}_{ik}\widetilde{\mathcal{T}}_{jl}+\widetilde{\mathcal{T}}_{il}\widetilde{\mathcal{T}}_{jk}-\widetilde{\mathcal{T}}_{ij}\widetilde{\mathcal{T}}_{kl}) = \left\{\boldsymbol{k_1}.\boldsymbol{k_3}+\frac{\{(\boldsymbol{k_2}+\boldsymbol{k_1}).\boldsymbol{k_1}\}\{(\boldsymbol{k_4}+\boldsymbol{k_3}).\boldsymbol{k_3}\}}{|\boldsymbol{k_1}+\boldsymbol{k_2}|^2}\right\}\\
&\left\{\boldsymbol{k_2}.\boldsymbol{k_4}+\frac{\{(\boldsymbol{k_1}+\boldsymbol{k_2}).\boldsymbol{k_2}\}\{(\boldsymbol{k_3}+\boldsymbol{k_4}).\boldsymbol{k_4}\}}{|\boldsymbol{k_1}+\boldsymbol{k_2}|^2}\right\}+\left\{\boldsymbol{k_1}.\boldsymbol{k_4}+\frac{\{(\boldsymbol{k_2}+\boldsymbol{k_1}).\boldsymbol{k_1}\}\{(\boldsymbol{k_4}+\boldsymbol{k_3}).\boldsymbol{k_4}\}}{|\boldsymbol{k_1}+\boldsymbol{k_2}|^2}\right\}\\
&\left\{\boldsymbol{k_2}.\boldsymbol{k_3}+\frac{\{(\boldsymbol{k_2}+\boldsymbol{k_1}).\boldsymbol{k_2}\}\{(\boldsymbol{k_4}+\boldsymbol{k_3}).\boldsymbol{k_3}\}}{|\boldsymbol{k_1}+\boldsymbol{k_2}|^2}\right\}-\left\{\boldsymbol{k_1}.\boldsymbol{k_2}-\frac{\{(\boldsymbol{k_2}+\boldsymbol{k_1}).\boldsymbol{k_1}\}\{(\boldsymbol{k_1}+\boldsymbol{k_2}).\boldsymbol{k_2}\}}{|\boldsymbol{k_1}+\boldsymbol{k_2}|^2}\right\}\\
&\left\{\boldsymbol{k_3}.\boldsymbol{k_4}-\frac{\{(\boldsymbol{k_3}+\boldsymbol{k_4}).\boldsymbol{k_4}\}\{(\boldsymbol{k_4}+\boldsymbol{k_3}).\boldsymbol{k_3}\}}{|\boldsymbol{k_1}+\boldsymbol{k_2}|^2}\right\},
\end{aligned} \tag{C.50}$$

can now be substituted in eq.(C.44) to obtain eq.(4.115).

Once the transverse graviton contribution, $\widetilde{W}$, is calculated, we are left with the longitudinal contributions for the graviton eq.(4.111). The momentum space expressions for eq.(4.112) becomes

$$\begin{aligned}
R_1 &= \int \frac{dz_1}{z_1^2}\frac{d^3\boldsymbol{k}}{(2\pi)^3}T_{zj}(\boldsymbol{k},z_1)\frac{1}{k^2}T_{zj}(-\boldsymbol{k},z_1),\\
R_2 &= \frac{1}{2}i\int \frac{dz_1}{z_1}\frac{d^3\boldsymbol{k}}{(2\pi)^3}k_jT_{zj}(\boldsymbol{k},z_1)\frac{1}{k^2}T_{zz}(-\boldsymbol{k},z_1),\\
R_3 &= -\frac{1}{4}\int \frac{dz_1}{z_1^2}\frac{d^3\boldsymbol{k}}{(2\pi)^3}k_jT_{zj}(\boldsymbol{k},z_1)\frac{1}{k^4}k_iT_{zi}(-\boldsymbol{k},z_1).
\end{aligned} \tag{C.51}$$

Using the relevant components of the stress tensors obtained from eq.(4.98), as given below,

$$T_{zj}(\phi_1,\phi_2) = iz_1e^{-(k_1+k_2)z_1}\Big[k_1^2k_{2j}(1+k_2z_1)+k_2^2k_{1j}(1+k_1z_1)\Big], \tag{C.52}$$

$$\begin{aligned}
T_{zz}(\phi_1,\phi_2) &= e^{-(k_1+k_2)z_1}\Big[\boldsymbol{k_1}.\boldsymbol{k_2}+(\boldsymbol{k_1}.\boldsymbol{k_2})(k_1+k_2)z_1\\
&\quad +k_1k_2(k_1k_2+\boldsymbol{k_1}.\boldsymbol{k_2})z_1^2\Big],
\end{aligned} \tag{C.53}$$

$$\begin{aligned}
k_jT_{zj}(\phi_1,\phi_2) &= z_1e^{-(k_1+k_2)z_1}\Big[2k_1^2k_2^2+(\boldsymbol{k_1}.\boldsymbol{k_2})(k_1^2+k_2^2)\\
&\quad +k_1k_2(k_1+k_2)(k_1k_2+\boldsymbol{k_1}.\boldsymbol{k_2})z_1\Big]
\end{aligned} \tag{C.54}$$

in eq.(C.51) one obtains eq.(4.116). Adding eq.(4.115) and eq.(4.116) one finally obtains $S^{\rm AdS}_{\rm on\text{-}shell}$ as given in eq.(4.121).

C.4 Possibility of Additional Contributions in Changing Gauge

Once we obtained the four point function $\langle\delta\phi(\boldsymbol{k_1})\delta\phi(\boldsymbol{k_2})\delta\phi(\boldsymbol{k_3})\delta\phi(\boldsymbol{k_4})\rangle$, eq.(4.132), in gauge 2, we finally moved to gauge 1 using the relation eq.(4.34). It was mentioned in subsection 4.5.1, in the footnote, that there will be additional higher order terms in ζ on RHS of eq.(4.34) which might lead to additional contribution in $\langle\zeta(\boldsymbol{k_1})\zeta(\boldsymbol{k_2})\zeta(\boldsymbol{k_3})\zeta(\boldsymbol{k_4})\rangle$ coming from the two point function $\langle\delta\phi(\boldsymbol{k_1})\delta\phi(\boldsymbol{k_2})\rangle$. In this appendix we will first compute the additional higher order terms in eq.(4.34) and then argue that the possible additional contributions to eq(4.34) are further suppressed in the slow-roll parameters.

For the discussion of contribution due to higher order terms in ζ, we will not consider any tensor perturbations and define the scalar perturbation, ζ, in the metric in the following way, from eq.(4.17),

$$h_{ij} = e^{2(\rho(t)+\zeta)}\delta_{ij}. \tag{C.55}$$

The scalar perturbation in the inflaton is defined in eq.(4.23). As was discussed in subsection 4.2.1, to go from gauge 2 to gauge 1 one needs to do a time reparameterization, which to leading order in ζ was given in eq.(4.31). Considering the time coordinate in gauge 2 being $\tilde{t}$ and that in gauge 1 being t, we write this infinitesimal time reparameterization as,

$$\tilde{t} = t + T. \tag{C.56}$$

The scalar perturbation in the inflaton in gauge 2 is given eq.(4.23), the scalar perturbation in the metric, ζ, is zero in this gauge and the metric takes the form,

$$ds^2 = -d\tilde{t}^2 + e^{2\rho(\tilde{t})}\delta_{ij}dx^i dx^j. \tag{C.57}$$

Notice that for $\rho(\tilde{t}) = H\tilde{t}$ we get eq.(4.18), here we allow for a more general time dependence.

In gauge 1 there is no scalar perturbation in the inflaton, $\delta\phi = 0$ and the metric, now containing a scalar perturbation, becomes,

$$ds^2 = -dt^2 + e^{2(\rho(t)+\zeta)}\delta_{ij}dx^i dx^j. \tag{C.58}$$

Using the time reparameterization, eq.(C.56), in eq.(4.23) and demanding that $\delta\phi$ vanishes as we go to gauge 1 yields the relation, upto cubic order in T [1],

$$\delta\phi = -T\partial_t\bar{\phi}(t) - \frac{T^2}{2}\partial_t^2\bar{\phi}(t) - \frac{T^3}{6}\partial_t^3\bar{\phi}(t). \tag{C.59}$$

Using the time parameterization, eq.(C.56), in the metric of gauge 2, eq.(C.57), and then comparing with the metric in gauge 1, eq.((C.58)), we obtain ζ, upto cubic order in T ,

$$\zeta = T\partial_t\rho + \frac{T^2}{2}\partial_t^2\rho + \frac{T^3}{6}\partial_t^3\rho. \tag{C.60}$$

Inverting this equation we obtain T in terms of ζ,

$$T = \frac{\zeta}{\partial_t\rho} - \frac{\zeta^2}{2(\partial_t\rho)^3}\partial_t^2\rho - \frac{\zeta^3}{6(\partial_t\rho)^4}\partial_t^3\rho. \tag{C.61}$$

[1] Here we neglected a term like $\partial_t\delta\phi$, because at late times, upon horizon crossing $\delta\phi$ becomes constant.

Substituting for T from eq.C.61 in eq.C.59, we obtain the correction to eq.(4.34) due to higher order terms in ζ,

$$\begin{aligned}\delta\phi = &-\frac{\zeta}{\partial_t\rho}\partial_t\bar{\phi} + \frac{1}{2}\frac{\zeta^2}{(\partial_t\rho)^2}(\partial_t\bar{\phi})^2\left(\frac{\partial_t^2\rho}{\partial_t\rho\;\partial_t\bar{\phi}} - \frac{\partial_t^2\bar{\phi}}{(\partial_t\bar{\phi})^2}\right)\\ &-\frac{1}{2}\frac{\zeta^3}{(\partial_t\rho)^3}(\partial_t\bar{\phi})^3\left(-\frac{1}{3}\frac{\partial_t^3\rho}{\partial_t\rho\;(\partial_t\bar{\phi})^2} - \frac{\partial_t^2\rho}{\partial_t\rho}\frac{\partial_t^2\bar{\phi}}{(\partial_t\bar{\phi})^3} + \frac{1}{3}\frac{\partial_t^3\bar{\phi}}{(\partial_t\bar{\phi})^3}\right).\end{aligned} \tag{C.62}$$

The linear term in ζ on the RHS of eq.(C.62) gives the leading contribution to the four point correlator of curvature perturbations $\langle\zeta(\boldsymbol{k_1})\zeta(\boldsymbol{k_2})\zeta(\boldsymbol{k_3})\zeta(\boldsymbol{k_4})\rangle$ as obtained in eq.(4.133). This arises due to the quartic coefficient term $\langle O(\boldsymbol{k_1})O(\boldsymbol{k_2})O(\boldsymbol{k_3})O(\boldsymbol{k_4})\rangle$ in eq.(4.37). Additional contributions to the $\langle\zeta(\boldsymbol{k_1})\zeta(\boldsymbol{k_2})\zeta(\boldsymbol{k_3})\zeta(\boldsymbol{k_4})\rangle$ correlator arise from the higher terms on the RHS of eq.(C.62). For example the term going like ζ^2 on the RHS of eq.(C.62) when inserted twice in the quadratic term of the wave function, which goes like $\frac{M_{Pl}^2}{H^2}\int -\delta\phi\delta\phi\langle OO\rangle$, eq.(4.37), can give a contribution of this type. However, due to the extra factor $\left(\frac{\partial_t^2\rho}{\partial_t\rho\;\partial_t\bar{\phi}} - \frac{\partial_t^2\bar{\phi}}{(\partial_t\bar{\phi})^2}\right)$ that multiples the ζ^2 term on the RHS of eq.(C.62) such a contribution will be of order ϵ and therefore will be suppressed in the slow-roll parameters.

Similarly, it is easy to see that the other terms in the expansion in eq.(C.62) also give subleading contributions to the four-point correlator.

C.5 Conformal Transformations and Compensating Reparameterizations

Following our discussion in section 4.6.1, in this Appendix we will show that the probability distribution $P[\delta\phi]$, defined in eq.(4.88), is invariant under the combined conformal transformation, eq.(4.71), eq.(4.72), and the compensating coordinate reparameterization, eq.(4.77) upto quartic order in $\delta\phi$. This will, in turn, prove the invariance of the scalalr four point function under the combined transformations mentioned above.

The probability distribution was calculated upto quartic order in $\delta\phi$ in eq.(4.126). Let us begin by writing the different terms in $P[\delta\phi]$ schematically as,

$$\begin{aligned}P[\delta\phi] = \exp\Bigg[&-\int\delta\phi\delta\phi\langle OO\rangle + \frac{1}{8}\int\delta\phi\delta\phi\delta\phi\delta\phi\frac{\widehat{P}_{ijkl}(\boldsymbol{k}_{12})}{k_{12}^3}\langle OOT_{ij}\rangle\langle OOT_{kl}\rangle\\ &+\frac{1}{12}\int\delta\phi\delta\phi\delta\phi\delta\phi\langle OOOO\rangle\Bigg]\end{aligned} \tag{C.63}$$

with, $k_{12} = |\boldsymbol{k_1} + \boldsymbol{k_2}|$. In particular the second term in the RHS of eq.(C.63) is responsible for the ET contribution and we will refer to it loosely as the ET term below.

The invariance of $P[\delta\phi]$ under the combined transformations works out in a rather non-trivial way as follows. The first and third terms in the RHS of eq.(C.63) which are quadratic and proportional to $\langle OOOO\rangle$ respectively, are both invariant under a conformal transformation. But the ET term in the RHS of eq.(C.63) is not. However, its transformation under a conformal transformation is exactly canceled by the transformation of the first term in the RHS of eq.(C.63) under the compensating reparameterization. Under a conformal transformation $\delta\phi$ transforms linearly, therefore the resulting change of the ET term under a conformal transformation is quartic in $\delta\phi$. Now as we see from eq.(4.137) under the compensation reparameterization $\delta\phi$ transforms by a term which is cubic in $\delta\phi$. As a result the change under the compensating reparameterization of the first term in the RHS of eq.(C.63), which is quadratic in $\delta\phi$ to begin with, is also quartic in $\delta\phi$. We will show in this appendix that these two terms exactly cancel. Additional contributions under the compensating reparameterization arise from the second and third terms in eq.(C.63) but these are of order $(\delta\phi)^6$ and not directly of concern for us, since we are only keeping terms upto quartic order in $\delta\phi$. We expect that once all terms of the required order are kept $P[\delta\phi]$ should be invariant to all orders in $\delta\phi$.

We turn now to establishing this argument in more detail. First, we will calculate the change in the first term in the RHS of eq.(C.63) under the compensating reparameterization. Next, we will calculate the change in the ET term in eq.(C.63) under a conformal transformation and show that they cancel each other.

C.5.1 Change in $\int \delta\phi\delta\phi\langle OO\rangle$ under the Compensating Reparameterization

The change of $\int \delta\phi\delta\phi\langle OO\rangle$ under the coordinate reparameterization $x^i \to x^i + v^i(x)$ with $v^i(\boldsymbol{x}) = -\frac{6b^k\gamma_{kj}(\boldsymbol{x})}{\partial^2}$ can be written in momentum space as,

$$\delta^R\Big[-\int \delta\phi\delta\phi\langle OO\rangle\Big] = I_1 + I_2, \tag{C.64}$$

$$I_1 = -\int \frac{d^3\boldsymbol{k_1}}{(2\pi)^3}\frac{d^3\boldsymbol{k_2}}{(2\pi)^3}\delta^R\big(\delta\phi(\boldsymbol{k_1})\big)\delta\phi(\boldsymbol{k_2})\langle O(-\boldsymbol{k_1})O(-\boldsymbol{k_2})\rangle, \tag{C.65}$$

$$I_2 = -\int \frac{d^3\boldsymbol{k_1}}{(2\pi)^3}\frac{d^3\boldsymbol{k_2}}{(2\pi)^3}\delta\phi(\boldsymbol{k_1})\delta^R\big(\delta\phi(\boldsymbol{k_2})\big)\langle O(-\boldsymbol{k_1})O(-\boldsymbol{k_2})\rangle. \tag{C.66}$$

Using $\delta^R\big(\delta\phi(\boldsymbol{k})\big)$ from eq.(4.137), one gets

$$\begin{aligned} I_1 = 3b^m \int \frac{d^3k_1}{(2\pi)^3}\frac{d^3k_2}{(2\pi)^3}\frac{d^3k_3}{(2\pi)^3}\frac{d^3k_4}{(2\pi)^3}\frac{d^3k_5}{(2\pi)^3}\delta\phi(\boldsymbol{k_1}-\boldsymbol{k}_5)\delta\phi(\boldsymbol{k_2})\delta\phi(\boldsymbol{k_3})\delta\phi(\boldsymbol{k_4}) \\ k_1^i\,\frac{\widehat{P}_{imkl}(\boldsymbol{k}_5)}{k_5^8}\langle O(-\boldsymbol{k_1})O(-\boldsymbol{k_2})\rangle\ \langle O(-\boldsymbol{k_3})O(-\boldsymbol{k_4})T_{kl}(-\boldsymbol{k}_5)\rangle. \end{aligned} \tag{C.67}$$

With the change of variable

$$\boldsymbol{k_1} = \mathbf{q}_1 + \boldsymbol{k}_5 \tag{C.68}$$

and then again relabeling $\mathbf{q}_1 \to \boldsymbol{k_1}$ one arrives at,

$$\begin{aligned} I_1 =& 3b^m \int \frac{d^3k_1}{(2\pi)^3}\frac{d^3k_2}{(2\pi)^3}\frac{d^3k_3}{(2\pi)^3}\frac{d^3k_4}{(2\pi)^3}\frac{d^3k_5}{(2\pi)^3}\delta\phi(\boldsymbol{k_1})\delta\phi(\boldsymbol{k_2})\delta\phi(\boldsymbol{k_3})\delta\phi(\boldsymbol{k_4}) \\ & \frac{\widehat{P}_{imkl}(\boldsymbol{k}_5)}{k_5^8}(k_1^i + k_5^i)\ \langle O(-\boldsymbol{k_1} - \boldsymbol{k}_5)O(-\boldsymbol{k_2})\rangle\langle O(-\boldsymbol{k_3})O(-\boldsymbol{k_4})T_{kl}(-\boldsymbol{k}_5)\rangle. \end{aligned} \tag{C.69}$$

Similar procedure for I_2 gives,

$$\begin{aligned} I_2 =& 3b^m \int \frac{d^3k_1}{(2\pi)^3}\frac{d^3k_2}{(2\pi)^3}\frac{d^3k_3}{(2\pi)^3}\frac{d^3k_4}{(2\pi)^3}\frac{d^3k_5}{(2\pi)^3}\delta\phi(\boldsymbol{k_1})\delta\phi(\boldsymbol{k_2})\delta\phi(\boldsymbol{k_3})\delta\phi(\boldsymbol{k_4}) \\ & \frac{\widehat{P}_{imkl}(\boldsymbol{k}_5)}{k_5^8}(k_2^i + k_5^i)\ \langle O(-\boldsymbol{k_1})O(-\boldsymbol{k_2} - \boldsymbol{k}_5)\rangle\langle O(-\boldsymbol{k_3})O(-\boldsymbol{k_4})T_{kl}(-\boldsymbol{k}_5)\rangle. \end{aligned} \tag{C.70}$$

Substituting for I_1 and I_2 in eq.(C.64) one obtains,

$$\begin{aligned} \delta^R\Big[-\int \delta\phi\delta\phi\langle OO\rangle\Big] = 3b^m \int \prod_{i=1}^{4}\left(\frac{d^3k_i}{(2\pi)^3}\delta\phi(\boldsymbol{k}_i)\right)\frac{d^3k_5}{(2\pi)^3}\frac{\widehat{P}_{imkl}(\boldsymbol{k}_5)}{k_5^8} \\ \big\{(k_1^i + k_5^i)\ \langle O(-\boldsymbol{k_1} - \boldsymbol{k}_5)O(-\boldsymbol{k_2})\rangle + (k_2^i + k_5^i)\ \langle O(-\boldsymbol{k_1})O(-\boldsymbol{k_2} - \boldsymbol{k}_5)\rangle\big\} \\ \langle O(-\boldsymbol{k_3})O(-\boldsymbol{k_4})T_{kl}(-\boldsymbol{k}_5)\rangle. \end{aligned} \tag{C.71}$$

We further use the Ward identity for the conservation of stress tensor,

$$\begin{aligned} \partial_{x_3^j}\langle O(\boldsymbol{x}_1)O(\boldsymbol{x}_2)T_{ij}(\boldsymbol{x}_3)\rangle =& \delta^3(\boldsymbol{x}_3 - \boldsymbol{x}_1)\langle\partial_{x_1^j}O(\boldsymbol{x}_1)O(\boldsymbol{x}_2)\rangle \\ &+ \delta^3(\boldsymbol{x}_3 - \boldsymbol{x}_2)\langle O(\boldsymbol{x}_1)\partial_{x_2^j}O(\boldsymbol{x}_2)\rangle \end{aligned} \tag{C.72}$$

which in momentum space is of the form,

$$\begin{aligned} (k_3^i + k_1^i)\ \langle O(\boldsymbol{k_1} + \boldsymbol{k_3})O(\boldsymbol{k_2})\rangle + (k_3^i + k_2^i)\ \langle O(\boldsymbol{k_1})O(\boldsymbol{k_2} + \boldsymbol{k_3})\rangle \\ = k_3^j\langle O(\boldsymbol{k_1})O(\boldsymbol{k_2})T_{ij}(\boldsymbol{k_3})\rangle. \end{aligned} \tag{C.73}$$

Using eq.(C.73), one can simplify eq.(C.71) further to obtain,

$$\begin{aligned} \delta^R\Big[-\int \delta\phi\delta\phi\langle OO\rangle\Big] = 3b^m \int \prod_{i=1}^{4}\left[\frac{d^3k_i}{(2\pi)^3}\delta\phi(\boldsymbol{k}_i)\right]\frac{d^3k_5}{(2\pi)^3}\frac{\widehat{P}_{imkl}(\boldsymbol{k}_5)}{k_5^8} \\ k_5^j\ \langle O(-\boldsymbol{k_1})O(-\boldsymbol{k_2})T_{ij}(-\boldsymbol{k}_5)\rangle\ \langle O(-\boldsymbol{k_3})O(-\boldsymbol{k_4})T_{kl}(-\boldsymbol{k}_5)\rangle. \end{aligned} \tag{C.74}$$

C.5.2 Change in ET Contribution Term under Conformal Transformation

The ET term in the RHS of eq.(C.63) in more detail is given by

$$\begin{aligned} P[\delta\phi]_{ET} &= \exp\left[\int \prod_{J=1}^{4}\left\{\frac{d^3k_J}{(2\pi)^3}\delta\phi(\boldsymbol{k}_J)\right\} I\right], \text{ with} \\ I &= \int \frac{d^3k_5}{(2\pi)^3}\frac{d^3k_6}{(2\pi)^3}\frac{\langle T_{ij}(\boldsymbol{k}_5)T_{kl}(\boldsymbol{k}_6)\rangle}{k_5^3\ k_6^3}\langle O(\boldsymbol{k_1})O(\boldsymbol{k_2})T_{ij}(\boldsymbol{k}_5)\rangle\ \langle O(\boldsymbol{k_3})O(\boldsymbol{k_4})T_{kl}(\boldsymbol{k}_6)\rangle. \end{aligned} \tag{C.75}$$

Where we have used the relation,

$$\widehat{P}_{ijkl} = \frac{8\langle T_{ij}(\boldsymbol{k}_5)T_{kl}(-\boldsymbol{k}_5)\rangle'}{k_5^3} \tag{C.76}$$

to write $\widehat{P}_{ijkl}$ appearing in eq.(4.126) in terms of $\langle T_{ij}(\boldsymbol{k}_5)T_{kl}(-\boldsymbol{k}_5)\rangle'$. In the above expression one can integrate over k_5 and k_6 using the momentum conserving delta function in $\langle T_{ij}(\boldsymbol{k}_5)T_{kl}(\boldsymbol{k}_6)\rangle$ and also in the coefficient functions $\langle O(\boldsymbol{k_1})O(\boldsymbol{k_2})T_{ij}(\boldsymbol{k}_5)\rangle$ and $\langle O(\boldsymbol{k_2})O(\boldsymbol{k_3})T_{ij}(\boldsymbol{k}_6)\rangle$ to get the ET term in eq.(4.126). Under a conformal transformation $\delta\phi$ transforms as given in eq.(C.28). After integrating by parts we obtain,

$$\delta^C\left[\int \prod_{J=1}^{4}\left\{\frac{d^3k_J}{(2\pi)^3}\delta\phi(\boldsymbol{k}_J)\right\} I\right] = -\int \prod_{J=1}^{4}\left\{\frac{d^3k_J}{(2\pi)^3}\delta\phi(\boldsymbol{k}_J)\right\} \delta^C(I). \tag{C.77}$$

Where the resulting change in I is given by

$$\begin{aligned} \delta^C(I) = \int &\frac{d^3k_5}{(2\pi)^3}\frac{d^3k_6}{(2\pi)^3}\frac{\langle T_{ij}(\boldsymbol{k}_5)T_{kl}(\boldsymbol{k}_6)\rangle}{k_5^3\ k_6^3} \\ &\Big[\langle \delta O(\boldsymbol{k_1})O(\boldsymbol{k_2})T_{ij}(\boldsymbol{k}_5)\rangle\ \langle O(\boldsymbol{k_3})O(\boldsymbol{k_4})T_{kl}(\boldsymbol{k}_6)\rangle \\ &+ \langle O(\boldsymbol{k_1})\delta O(\boldsymbol{k_2})T_{ij}(\boldsymbol{k}_5)\rangle\ \langle O(\boldsymbol{k_3})O(\boldsymbol{k_4})T_{kl}(\boldsymbol{k}_6)\rangle \\ &+ \langle O(\boldsymbol{k_1})O(\boldsymbol{k_2})T_{ij}(\boldsymbol{k}_5)\rangle\ \langle \delta O(\boldsymbol{k_3})O(\boldsymbol{k_4})T_{kl}(\boldsymbol{k}_6)\rangle \\ &+ \langle O(\boldsymbol{k_1})O(\boldsymbol{k_2})T_{ij}(\boldsymbol{k}_5)\rangle\ \langle O(\boldsymbol{k_3})\delta O(\boldsymbol{k_4})T_{kl}(\boldsymbol{k}_6)\rangle\Big] \end{aligned} \tag{C.78}$$

and $\delta O(\boldsymbol{k})$ is given in eq.(C.29).

Now we will use the fact that $\langle O(\boldsymbol{k_3})O(\boldsymbol{k_4})T_{kl}(\boldsymbol{k}_6)\rangle$ is invariant under special conformal transformation, which will allow us to write,

$$\langle \delta O(\boldsymbol{k_1})O(\boldsymbol{k_2})T_{ij}(\boldsymbol{k}_5)\rangle + \langle O(\boldsymbol{k_1})\delta O(\boldsymbol{k_2})T_{ij}(\boldsymbol{k}_5)\rangle = -\langle O(\boldsymbol{k_1})O(\boldsymbol{k_2})\delta T_{ij}(\boldsymbol{k}_5)\rangle. \tag{C.79}$$

Using eq.(C.79) back in eq.(C.78),

$$\delta^C(I) = -\int \frac{d^3k_5}{(2\pi)^3}\frac{d^3k_6}{(2\pi)^3}\frac{\langle T_{ij}(\boldsymbol{k}_5)T_{kl}(\boldsymbol{k}_6)\rangle}{k_5^3\ k_6^3}\Big[\langle O(\boldsymbol{k_1})O(\boldsymbol{k_2})\delta T_{ij}(\boldsymbol{k}_5)\rangle \\ \langle O(\boldsymbol{k_3})O(\boldsymbol{k_4})T_{kl}(\boldsymbol{k}_6)\rangle + \langle O(\boldsymbol{k_1})O(\boldsymbol{k_2})T_{ij}(\boldsymbol{k}_5)\rangle\ \langle O(\boldsymbol{k_3})O(\boldsymbol{k_4})\delta T_{kl}(\boldsymbol{k}_6)\rangle\Big]. \tag{C.80}$$

Next we use the expression for the change of $T_{ij}(\boldsymbol{k})$ as given in eq.(C.31) in the above expression and integrate by parts to move the derivatives acting on $T_{ij}(\boldsymbol{k})$ to other terms. After using the fact that $\langle T_{ij}(\boldsymbol{k}_5)T_{kl}(\boldsymbol{k}_6)\rangle$ is also invariant under conformal transformation, we are left with the terms which arise when the differential operators acts on the factors of $1/k_5^3$ and $1/k_6^3$. This gives,

$$\delta^C(I) = \int \frac{d^3k_5}{(2\pi)^3}\frac{d^3k_6}{(2\pi)^3}\frac{12}{k_5^3\ k_6^3}\Big[\frac{1}{k_5^2}(b_m k_{5i} - b_i k_{5m})\langle T_{mj}(\boldsymbol{k}_5)T_{kl}(\boldsymbol{k}_6)\rangle \\ + \frac{1}{k_6^2}(b_m k_{6k} - b_k k_{6m})\langle T_{ij}(\boldsymbol{k}_5)T_{ml}(\boldsymbol{k}_6)\rangle\Big] \\ \langle O(\boldsymbol{k_1})O(\boldsymbol{k_2})T_{ij}(\boldsymbol{k}_5)\rangle\ \langle O(\boldsymbol{k_3})O(\boldsymbol{k_4})T_{kl}(\boldsymbol{k}_6)\rangle. \tag{C.81}$$

Further we can use the fact that $\langle T_{ij}(\boldsymbol{k}_5)T_{ml}(\boldsymbol{k}_6)\rangle$ satisfies the relation

$$k_{5m}\langle T_{mj}(\boldsymbol{k}_5)T_{kl}(\boldsymbol{k}_6)\rangle = 0 \tag{C.82}$$

which follows for example from eq.(C.76) and the fact that $\widehat{P}_{ijkl}$ is transverse and traceless. This yields,

$$\delta^C(I) = \int \frac{d^3k_5}{(2\pi)^3}\frac{d^3k_6}{(2\pi)^3}\frac{24}{k_5^3\ k_6^3}\frac{b_m k_{5i}}{k_5^2}\langle T_{mj}(\boldsymbol{k}_5)T_{kl}(\boldsymbol{k}_6)\rangle \\ \langle O(\boldsymbol{k_1})O(\boldsymbol{k_2})T_{ij}(\boldsymbol{k}_5)\rangle\ \langle O(\boldsymbol{k_3})O(\boldsymbol{k_4})T_{kl}(\boldsymbol{k}_6)\rangle. \tag{C.83}$$

In obtaining the above equation we have also used the fact that I is symmetric under the exchange

$$\text{the external momenta } \boldsymbol{k_1} \Leftrightarrow \boldsymbol{k_3},\ \boldsymbol{k_2} \Leftrightarrow \boldsymbol{k_4},\ \boldsymbol{k}_5 \Leftrightarrow \boldsymbol{k}_6 \\ \text{and for the indices } \{i,j\} \Leftrightarrow \{k,l\}. \tag{C.84}$$

Finally, using eq(C.76) gives,

$$\delta^C(I) = 3b_m \int \frac{d^3k_5}{(2\pi)^3}\frac{\widehat{P}_{imkl}(\boldsymbol{k}_5)}{k_5^8}k_{5j}\langle O(\boldsymbol{k_1})O(\boldsymbol{k_2})T_{ij}(\boldsymbol{k}_5)\rangle\langle O(\boldsymbol{k_3})O(\boldsymbol{k_4})T_{kl}(-\boldsymbol{k}_5)\rangle. \tag{C.85}$$

Using $\delta^C(I)$ from eq.(C.85) in eq.(C.77) and comparing with eq.(C.74), we see that they exactly cancel each other so that their sum vanishes. This proves that $P[\delta\phi]$ is invariant upto quartic order in $\delta\phi$.

C.6 More Details on Different Limits of the Final Result

As was mentioned in subsection 4.6.3, in this appendix we will provide more details on the discussion of different limits of our final result in the following subsections.

C.6.1 Details on Deriving eq.(4.169) for Limit II in Subsection 4.6.3

Let us start examining the behavior of $\langle O(\boldsymbol{k_1})O(\boldsymbol{k_2})O(\boldsymbol{k_3})O(\boldsymbol{k_4})\rangle'$ in the limit $\boldsymbol{k_2} \to \infty$. We do so by parameterizing $\boldsymbol{k_2} = \boldsymbol{a}/\epsilon$ and then take the limit $\epsilon \to 0$, with $\boldsymbol{k_3}, \boldsymbol{k_4}$ held fixed and $\boldsymbol{k_1} = -(\boldsymbol{k_2} + \boldsymbol{k_3} + \boldsymbol{k_4})$. One then obtains,

$$\lim_{\epsilon\to 0}\langle O(\boldsymbol{k_1})O(\boldsymbol{k_2})O(\boldsymbol{k_3})O(\boldsymbol{k_4})\rangle' = \frac{1}{\epsilon}W^{div.} + W^{const.} + \mathcal{O}(\epsilon)\,. \tag{C.86}$$

Here $W^{div.}$ is the coefficient of a term which is divergent as $\epsilon \to 0$, and $W^{\text{const.}}$ is a term which is ϵ independent. The presence of a divergent term might at first seem to contradict eq.(4.169). However it turns out that the divergent piece is entirely a contact term analytic in the momenta.

$$W^{div.} = W^{div.}_s + W^{div.}_t + W^{div.}_u \tag{C.87}$$

where the contributions from the individual channels are

$$\frac{1}{\epsilon}W^{div.}_s = -\frac{5}{8k_2}(\boldsymbol{k_2}\cdot\boldsymbol{k_3})(\boldsymbol{k_2}\cdot\boldsymbol{k_4}) + \frac{k_2}{4}\boldsymbol{k_3}\cdot\boldsymbol{k_4}, \tag{C.88}$$

$$\frac{1}{\epsilon}W^{div.}_t = \frac{1}{\epsilon}W^{div.}_u = -\frac{1}{8k_2}(\boldsymbol{k_2}\cdot\boldsymbol{k_3})(\boldsymbol{k_2}\cdot\boldsymbol{k_4}) - \frac{k_2}{4}\boldsymbol{k_3}\cdot\boldsymbol{k_4}\,. \tag{C.89}$$

These terms are clearly analytic functions of $\boldsymbol{k_3}, \boldsymbol{k_4}$. Such analytic terms in position space give rise to contact terms, which are proportional to delta functions or their derivatives for one or more of the arguments. We had mentioned in our discussion after eq.(4.161) that we are neglecting such contact terms in the OPE, it is therefore no contradiction that they are appearing in an expansion of the full answer in eq.(C.86) above, but did not appear in our discussion based on the OPE in eq.(4.169).

Neglecting these divergent pieces we get in the limit $\epsilon \to 0$ that

$$\lim_{\epsilon\to 0}\langle O(\boldsymbol{k_1})O(\boldsymbol{k_2})O(\boldsymbol{k_3})O(\boldsymbol{k_4})\rangle' = W^{const}. \tag{C.90}$$

We get contributions to W^{const} from all the three channels,

$$W^{const} = W^{const}_S + W^{const}_T + W^{const}_U \tag{C.91}$$

where,

$$W^{const}_T + W^{const}_U = \frac{(\boldsymbol{k_2}\cdot\boldsymbol{k_3})(k_3^2 - k_4^2)}{8k_2}. \tag{C.92}$$

It is obvious from RHS of eq.(C.92) that the contribution to W^{const} from T and U channels are analytic functions of $\boldsymbol{k_3}, \boldsymbol{k_4}$. Therefore, effectively they don't contribute to W^{const} for the same reason described earlier, and the contribution to $W^{const.}$ comes only from the S-channel, which is

$$W_S^{const} = W_{S(1)}^{const.} + W_{S(2)}^{const.}, \tag{C.93}$$

with

$$\begin{aligned} W_{S(1)}^{const} &= \frac{3}{8}\frac{(\boldsymbol{k_2}\cdot\boldsymbol{k_3})(\boldsymbol{k_2}\cdot\boldsymbol{k_4})}{k_2^2}\left((\tilde{k}+k_3+k_4) - \frac{\tilde{k}k_3 + k_3k_4 + k_4\tilde{k}}{(\tilde{k}+k_3+k_4)} - \frac{\tilde{k}k_3k_4}{(\tilde{k}+k_3+k_4)^2}\right), \\ W_{S(2)}^{const.} &= \frac{3}{64}\tilde{k}\left(-\tilde{k}^2 + k_3^2 + k_4^2\right) + \frac{3k_3^2k_4^2}{8(\tilde{k}+k_3+k_4)} + \frac{5(\boldsymbol{k_2}\cdot\boldsymbol{k_3})(k_3^2-k_4^2)}{16k_2}. \end{aligned} \tag{C.94}$$

It is obvious from eq.(C.94) that the term $W_{S(2)}^{const.}$ does not contribute to eq.(C.90), because the first two terms on LHS of $W_{S(2)}^{const.}$ does not depend on $\boldsymbol{k_2}$ and the last term is analytic in the momenta $\boldsymbol{k_3}, \boldsymbol{k_4}$, therefore when fourier transformed back to position space they produce delta functions or derivatives of them.

Finally we get,

$$\begin{aligned} \lim_{\epsilon\to 0}\langle O(\boldsymbol{k_1})O(\boldsymbol{k_2})O(\boldsymbol{k_3})O(\boldsymbol{k_4})\rangle' \sim & \frac{(\boldsymbol{k_2}\cdot\boldsymbol{k_3})(\boldsymbol{k_2}\cdot\boldsymbol{k_4})}{k_2^2}\Bigg((\tilde{k}+k_3+k_4) \\ & - \frac{\tilde{k}k_3 + k_3k_4 + k_4\tilde{k}}{(\tilde{k}+k_3+k_4)} - \frac{\tilde{k}k_3k_4}{(\tilde{k}+k_3+k_4)^2}\Bigg). \end{aligned} \tag{C.95}$$

Therefore we have confirmed eq(4.169).

C.6.2 More Details on Obtaining eq.(4.173)

In this subsection we will explain in more detail the contribution of the ET contribution term to the scalar four point correlator $\langle\delta\phi(\boldsymbol{k_1})\delta\phi(\boldsymbol{k_2})\delta\phi(\boldsymbol{k_3})\delta\phi(\boldsymbol{k_4})\rangle_{ET}$ in counter-collinear limit eq.(4.172). It is obvious from eq.(4.129) and eq.(4.130) that in this limit the dominant contribution in $\langle\delta\phi(\boldsymbol{k_1})\delta\phi(\boldsymbol{k_2})\delta\phi(\boldsymbol{k_3})\delta\phi(\boldsymbol{k_4})\rangle_{ET}$ comes from the S-channel term, $\widehat{G}^S(\boldsymbol{k_1},\boldsymbol{k_2},\boldsymbol{k_3},\boldsymbol{k_4})$. This term diverges as $1/k_{12}^3$ in the counter-collinear limit. In the RHS of eq.(4.130) the term within the parenthesis is due to the four external momenta corresponding to the four perturbations being contracted with the transverse traceless projector $\widehat{P}_{ijkl}$, eq.(4.125), as follows,

$$
\begin{aligned}
&k_1^i k_2^j k_3^k k_4^l \widehat{P}_{ijkl}(\boldsymbol{k_1}+\boldsymbol{k_2}) = \\
&\Bigg[\Big\{\boldsymbol{k_1}.\boldsymbol{k_3} + \frac{\{(\boldsymbol{k_2}+\boldsymbol{k_1}).\boldsymbol{k_1}\}\{(\boldsymbol{k_4}+\boldsymbol{k_3}).\boldsymbol{k_3}\}}{|\boldsymbol{k_1}+\boldsymbol{k_2}|^2}\Big\}\Big\{\boldsymbol{k_2}.\boldsymbol{k_4} + \frac{\{(\boldsymbol{k_1}+\boldsymbol{k_2}).\boldsymbol{k_2}\}\{(\boldsymbol{k_3}+\boldsymbol{k_4}).\boldsymbol{k_4}\}}{|\boldsymbol{k_1}+\boldsymbol{k_2}|^2}\Big\} \\
&+\Big\{\boldsymbol{k_1}.\boldsymbol{k_4} + \frac{\{(\boldsymbol{k_2}+\boldsymbol{k_1}).\boldsymbol{k_1}\}\{(\boldsymbol{k_4}+\boldsymbol{k_3}).\boldsymbol{k_4}\}}{|\boldsymbol{k_1}+\boldsymbol{k_2}|^2}\Big\}\Big\{\boldsymbol{k_2}.\boldsymbol{k_3} + \frac{\{(\boldsymbol{k_2}+\boldsymbol{k_1}).\boldsymbol{k_2}\}\{(\boldsymbol{k_4}+\boldsymbol{k_3}).\boldsymbol{k_3}\}}{|\boldsymbol{k_1}+\boldsymbol{k_2}|^2}\Big\} \\
&-\Big\{\boldsymbol{k_1}.\boldsymbol{k_2} - \frac{\{(\boldsymbol{k_2}+\boldsymbol{k_1}).\boldsymbol{k_1}\}\{(\boldsymbol{k_1}+\boldsymbol{k_2}).\boldsymbol{k_2}\}}{|\boldsymbol{k_1}+\boldsymbol{k_2}|^2}\Big\}\Big\{\boldsymbol{k_3}.\boldsymbol{k_4} - \frac{\{(\boldsymbol{k_3}+\boldsymbol{k_4}).\boldsymbol{k_4}\}\{(\boldsymbol{k_4}+\boldsymbol{k_3}).\boldsymbol{k_3}\}}{|\boldsymbol{k_1}+\boldsymbol{k_2}|^2}\Big\}\Bigg].
\end{aligned}
\tag{C.96}
$$

One can also use the polarization tensors ϵ^s_{ij}, defined in eq.(4.39), to write the RHS of eq.(C.96) in an alternate way. In a spherical coordinate system having $\{\boldsymbol{e}, \bar{\boldsymbol{e}}, \widehat{\boldsymbol{k}}_{12}\}$ as basis (denoting $\widehat{\boldsymbol{k}} = \frac{\boldsymbol{k}}{k}$) one can obtain the relation

$$
\sum_s \epsilon^s_{ij}\epsilon^s_{kl} = \widehat{P}_{ijkl}. \tag{C.97}
$$

Let us define θ_i being the angle between $\boldsymbol{k}_i$ and $\boldsymbol{k}_{12}$, whereas ϕ_i being the angle between $\boldsymbol{k}_i$ and $\boldsymbol{e}$. As was shown in [107], see eq.(2.32), using eq.(C.97), one can then get,

$$
k_1^i k_2^j k_3^k k_4^l \widehat{P}_{ijkl}(\boldsymbol{k_1}+\boldsymbol{k_2}) = k_1^2 k_3^2 \sin^2(\theta_1)\sin^2(\theta_3)\cos(2\chi_{12,34}). \tag{C.98}
$$

Using eq.(C.96), eq.(C.98) and eq.(4.131) in eq.(4.130), one obtains the form of the ET contribution term $\langle \delta\phi(\boldsymbol{k_1})\delta\phi(\boldsymbol{k_2})\delta\phi(\boldsymbol{k_3})\delta\phi(\boldsymbol{k_4})\rangle_{ET}$ in the counter-collinear limit as in eq.(4.173) in a straight forward way.

C.6.3 More Details on the Check of the Relative Coefficient between CF and ET Terms

In subsection 4.6.3 towards the end we discussed the counter-collinear limit in an alternative but equivalent way compared to what already exists in literature. We took all the individual momenta i.e. $\boldsymbol{k}_i,\ i = 1,2,3,4$ to diverge keeping $\boldsymbol{k_1}+\boldsymbol{k_2} = -(\boldsymbol{k_3}+\boldsymbol{k_4})$ fixed. This way of interpreting the counter-collinear limit provides us a further check to fix the relative coefficient between the CF term in eq.(4.128) and the ET term in eq.(4.129). Here we will discuss in some detail.

We implement this alternate way of counter-collinear limit in two steps. First we take $\boldsymbol{k_1}, \boldsymbol{k_1} \to \infty$ keeping $\boldsymbol{k}_{12}$ fixed and then we take $\boldsymbol{k_3}, \boldsymbol{k_4} \to \infty$ keeping $\boldsymbol{k_3}+\boldsymbol{k_3}$ fixed. After the first limit the $\langle O(\boldsymbol{k_1})O(\boldsymbol{k_2})O(\boldsymbol{k_3})O(\boldsymbol{k_4})\rangle$, given in eq.(4.123), becomes,

$$
\langle O(\boldsymbol{k_1})O(\boldsymbol{k_2})O(\boldsymbol{k_3})O(\boldsymbol{k_4})\rangle \to 4(2\pi)^3\delta^3\Big(\sum_J \boldsymbol{k}_J\Big)\frac{3}{8}\frac{(\boldsymbol{k_2}.\boldsymbol{k_3})(\boldsymbol{k_2}.\boldsymbol{k_4})}{k_2^2}S(k_3,k_4) \tag{C.99}
$$

with $S(k_3, k_4)$ being given in eq.(4.131). Next we take the limit, i.e. $\boldsymbol{k_3}, \boldsymbol{k_4} \to \infty$ keeping

$\boldsymbol{k_3} + \boldsymbol{k_3}$ fixed and in this limit the leading non-analytic behavior of $S(k_3, k_4)$ goes as,

$$S(k_3, k_4) \sim -\frac{3}{8}\frac{k_{34}^3}{k_3^2}. \tag{C.100}$$

Using eq.(C.100), one obtains the limiting behavior of the CF term contribution to scalar 4 point correlator, eq.(4.128) in the counter-collinear limit as,

$$\langle\delta\phi(\boldsymbol{k_1})\delta\phi(\boldsymbol{k_2})\delta\phi(\boldsymbol{k_3})\delta\phi(\boldsymbol{k_4})\rangle_{CF} = -8(2\pi)^3\delta^3\big(\sum_J \boldsymbol{k}_J\big)\left(\frac{3}{8}\right)^2\frac{(\boldsymbol{k_2}.\boldsymbol{k_3})(\boldsymbol{k_2}.\boldsymbol{k_4})}{k_2^2}\frac{k_{34}^3}{k_3^2}. \tag{C.101}$$

For the ET contribution to the scalar four point correlator, eq.(4.129), we have two factors of S, and as it was mentioned in the previous subsection, the term within the parenthesis in the RHS of eq.(4.130) is $k_1^i k_2^j k_3^k k_4^l \widehat{P}_{ijkl}(\boldsymbol{k_1} + \boldsymbol{k_2})$, eq.(C.96). In the sequence of steps for the counter-collinear limit we are concerned with, this term goes as,

$$k_1^i k_2^j k_3^k k_4^l \widehat{P}_{ijkl}(\boldsymbol{k_1} + \boldsymbol{k_2}) \sim -2(\boldsymbol{k_2}.\boldsymbol{k_3})(\boldsymbol{k_2}.\boldsymbol{k_4}). \tag{C.102}$$

Using eq.(C.100) and eq.(C.102) in eq.(4.129), we obtain the form of the contribution of the ET term in 4 point scalar correlator as,

$$\langle\delta\phi(\boldsymbol{k_1})\delta\phi(\boldsymbol{k_2})\delta\phi(\boldsymbol{k_3})\delta\phi(\boldsymbol{k_4})\rangle_{ET} = -8(2\pi)^3\delta^3\big(\sum_J \boldsymbol{k}_J\big)\left(\frac{3}{8}\right)^2\frac{(\boldsymbol{k_2}.\boldsymbol{k_3})(\boldsymbol{k_2}.\boldsymbol{k_4})}{k_2^2}\frac{k_{34}^3}{k_3^2}. \tag{C.103}$$

Now comparing eq.(C.101)and eq.(C.103) we conclude that, once we take the counter-collinear limit in the sequential order prescribed above, the leading behavior of both the CF and ET term matches perfectly including coefficients and thus provides a further check on the relative coefficient of these two contributions.

Bibliography

[1] J. Polchinski. *String theory. Vol. 2: Superstring theory and beyond*. Cambridge, New York, (2003). 2

[2] R. Bousso and J. Polchinski, "Quantization of four form fluxes and dynamical neutralization of the cosmological constant.", *JHEP*, **0006**, (2000), 006, [hep-th/0004134]. 2

[3] O. Aharony, S. S. Gubser, J. M. Maldacena, H. Ooguri, and Y. Oz, "Large N field theories, string theory and gravity.", *Phys.Rept.*, **323**, (2000), 183–386, [hep-th/9905111]. 3

[4] S. A. Hartnoll, "Lectures on holographic methods for condensed matter physics.", *Class.Quant.Grav.*, **26**, (2009), 224002, [arXiv:0903.3246]. 8

[5] C. P. Herzog, "Lectures on Holographic Superfluidity and Superconductivity.", *J.Phys.*, **A42**, (2009), 343001, [arXiv:0904.1975]. 8

[6] J. McGreevy, "Holographic duality with a view toward many-body physics.", *Adv.High Energy Phys.*, **2010**, (2010), 723105, [arXiv:0909.0518]. 8

[7] S. Sachdev, "What can gauge-gravity duality teach us about condensed matter physics?.", *Ann.Rev.Condensed Matter Phys.*, **3**, (2012), 9–33, [arXiv:1108.1197]. 8, 9

[8] J. Casalderrey-Solana, H. Liu, D. Mateos, K. Rajagopal, and U. A. Wiedemann, "Gauge/String Duality, Hot QCD and Heavy Ion Collisions.", arXiv:1101.0618, [arXiv:1101.0618]. 8

[9] C. P. Herzog, P. Kovtun, S. Sachdev, and D. T. Son, "Quantum critical transport, duality, and M-theory.", *Phys.Rev.*, **D75**, (2007), 085020, [hep-th/0701036]. 8

[10] S. Sachdev, "Strange metals and the AdS/CFT correspondence.", *Journal of Statistical Mechanics: Theory and Experiment*, **11**, (November, 2010), 22, [arXiv:1010.0682]. 8

[11] F. D. M. Haldane, "Effective harmonic-fluid approach to low-energy properties of one-dimensional quantum fluids.", *Phys. Rev. Lett.*, **47**, (Dec, 1981), 1840–1843. 8

[12] D. Baumann, "TASI Lectures on Inflation.", arXiv:0907.5424, [arXiv:0907.5424]. 12, 13

[13] P. Ade et al., "Detection of B-Mode Polarization at Degree Angular Scales by BICEP2.", *Phys.Rev.Lett.*, **112**, (2014), 241101, [arXiv:1403.3985]. 11

[14] N. Iizuka, S. Kachru, N. Kundu, P. Narayan, N. Sircar, et al., "Bianchi Attractors: A Classification of Extremal Black Brane Geometries.", *JHEP*, **1207**, (2012), 193, [arXiv:1201.4861]. 12

[15] N. Kundu, P. Narayan, N. Sircar, and S. P. Trivedi, "Entangled Dilaton Dyons.", *JHEP*, **JHEP03**, (2013), 155, [arXiv:1208.2008]. 13

[16] A. Ghosh, N. Kundu, S. Raju, and S. P. Trivedi, "Conformal Invariance and the Four Point Scalar Correlator in Slow-Roll Inflation.", *JHEP*, **1407**, (2014), 011, [arXiv:1401.1426]. 13, 108

[17] L. D. Landau and E. M. Lifshitz. *The Classical Theory of Fields.* Butterworth-Heinemann, 4 edition, January (1980). 16, 19, 127, 131

[18] M. P. Ryan and L. C. Shepley. *Homogeneous relativistic cosmologies.* Princeton, N.J. : Princeton University Press, (1975). 16, 19, 20, 21, 22, 127, 128, 129

[19] M. Kataoka and O. Nakanishi, "Helical spin density wave due to antisymmetric exchange interaction.", *Journal of the Physical Society of Japan*, **50**, (1981), no. 12, 3888–3896, [http://dx.doi.org/10.1143/JPSJ.50.3888]. 17, 19, 32

[20] M. L. Plumer and M. B. Walker, "Wavevector and spin reorientation in mnsi.", *Journal of Physics C: Solid State Physics*, **14**, (1981), no. 31, 4689. 17, 19, 32

[21] P. Fulde and R. A. Ferrell, "Superconductivity in a strong spin-exchange field.", *Phys. Rev.*, **135**, (Aug, 1964), A550–A563. 17

[22] A. I. Larkin and Y. Ovchinnikov, "Inhomogeneous state of superconductors.", *Sov. Phys. JETP*, **20: 762**, (1965). 17

[23] D. Deryagin, D. Y. Grigoriev, and V. Rubakov, "Standing wave ground state in high density, zero temperature QCD at large N(c).", *Int.J.Mod.Phys.*, **A7**, (1992), 659–681. 17

[24] S. Brazovskii, "Phase transition of an isotropic system to a nonuniform state.", *Sov. Phys. JETP*, **41: 85**, (1975). 17

[25] S. K. Domokos and J. A. Harvey, "Baryon number-induced Chern-Simons couplings of vector and axial-vector mesons in holographic QCD.", *Phys.Rev.Lett.*, **99**, (2007), 141602, [arXiv:0704.1604]. 17, 32

[26] S. Nakamura, H. Ooguri, and C.-S. Park, "Gravity Dual of Spatially Modulated Phase.", *Phys.Rev.*, **D81**, (2010), 044018, [arXiv:0911.0679]. 17, 32, 47

[27] H. Ooguri and C.-S. Park, "Holographic End-Point of Spatially Modulated Phase Transition.", *Phys.Rev.*, **D82**, (2010), 126001, [arXiv:1007.3737]. 17, 32, 47

[28] H. Ooguri and C.-S. Park, "Spatially Modulated Phase in Holographic Quark-Gluon Plasma.", *Phys.Rev.Lett.*, **106**, (2011), 061601, [arXiv:1011.4144]. 17, 32, 47

[29] A. Donos and J. P. Gauntlett, "Holographic helical superconductors.", *JHEP*, **1112**, (2011), 091, [arXiv:1109.3866]. 17, 32, 47

[30] A. Donos, J. P. Gauntlett, and C. Pantelidou, "Spatially modulated instabilities of magnetic black branes.", *JHEP*, **1201**, (2012), 061, [arXiv:1109.0471]. 17, 32, 47, 124

[31] A. Donos and J. P. Gauntlett, "Holographic striped phases.", *JHEP*, **1108**, (2011), 140, [arXiv:1106.2004]. 17, 32, 47

[32] D. Marolf, "Black holes and branes in supergravity.", arXiv:1107.1022, [arXiv:1107.1022]. 17

[33] H. K. Kunduri, J. Lucietti, and H. S. Reall, "Near-horizon symmetries of extremal black holes.", *Class.Quant.Grav.*, **24**, (2007), 4169–4190, [arXiv:0705.4214]. 17

[34] S. S. Gubser, "Breaking an Abelian gauge symmetry near a black hole horizon.", *Phys.Rev.*, **D78**, (2008), 065034, [arXiv:0801.2977]. 17

[35] G. T. Horowitz, "Introduction to Holographic Superconductors.", *Lect.Notes Phys.*, **828**, (2011), 313–347, [arXiv:1002.1722]. 17

[36] R. Gregory and R. Laflamme, "Black strings and p-branes are unstable.", *Phys.Rev.Lett.*, **70**, (1993), 2837–2840, [hep-th/9301052]. 17

[37] R. Gregory and R. Laflamme, "The Instability of charged black strings and p-branes.", *Nucl.Phys.*, **B428**, (1994), 399–434, [hep-th/9404071]. 17

[38] L. Lehner and F. Pretorius, "Final State of Gregory-Laflamme Instability.", arXiv:1106.5184, [arXiv:1106.5184]. 17

[39] S. Kachru, X. Liu, and M. Mulligan, "Gravity duals of Lifshitz-like fixed points.", *Phys.Rev.*, **D78**, (2008), 106005, [arXiv:0808.1725]. 17, 21, 25

[40] M. Taylor, "Non-relativistic holography.", arXiv:0812.0530, [arXiv:0812.0530]. 17, 21, 25

[41] S. A. Hartnoll, J. Polchinski, E. Silverstein, and D. Tong, "Towards strange metallic holography.", *JHEP*, **1004**, (2010), 120, [arXiv:0912.1061]. 17, 51

[42] K. Balasubramanian and K. Narayan, "Lifshitz spacetimes from AdS null and cosmological solutions.", *JHEP*, **1008**, (2010), 014, [arXiv:1005.3291]. 17

[43] A. Donos and J. P. Gauntlett, "Lifshitz Solutions of D=10 and D=11 supergravity.", *JHEP*, **1012**, (2010), 002, [arXiv:1008.2062]. 17

[44] R. Gregory, S. L. Parameswaran, G. Tasinato, and I. Zavala, "Lifshitz solutions in supergravity and string theory.", *JHEP*, **1012**, (2010), 047, [arXiv:1009.3445]. 17

[45] A. Donos, J. P. Gauntlett, N. Kim, and O. Varela, "Wrapped M5-branes, consistent truncations and AdS/CMT.", *JHEP*, **1012**, (2010), 003, [arXiv:1009.3805]. 17

[46] D. Cassani and A. F. Faedo, "Constructing Lifshitz solutions from AdS.", *JHEP*, **1105**, (2011), 013, [arXiv:1102.5344]. 17

[47] N. Halmagyi, M. Petrini, and A. Zaffaroni, "Non-Relativistic Solutions of N=2 Gauged Supergravity.", *JHEP*, **1108**, (2011), 041, [arXiv:1102.5740]. 17

[48] S. Ferrara, R. Kallosh, and A. Strominger, "N=2 extremal black holes.", *Phys.Rev.*, **D52**, (1995), 5412–5416, [hep-th/9508072]. 17

[49] S. Bellucci, S. Ferrara, R. Kallosh, and A. Marrani, "Extremal Black Hole and Flux Vacua Attractors.", *Lect.Notes Phys.*, **755**, (2008), 115–191, [arXiv:0711.4547]. 17

[50] S. Ferrara, G. W. Gibbons, and R. Kallosh, "Black holes and critical points in moduli space.", *Nucl.Phys.*, **B500**, (1997), 75–93, [hep-th/9702103]. 17

[51] G. W. Gibbons, R. Kallosh, and B. Kol, "Moduli, scalar charges, and the first law of black hole thermodynamics.", *Phys.Rev.Lett.*, **77**, (1996), 4992–4995, [hep-th/9607108]. 17

[52] A. Sen, "Black hole entropy function and the attractor mechanism in higher derivative gravity.", *JHEP*, **0509**, (2005), 038, [hep-th/0506177]. 17

[53] K. Goldstein, N. Iizuka, R. P. Jena, and S. P. Trivedi, "Non-supersymmetric attractors.", *Phys.Rev.*, **D72**, (2005), 124021, [hep-th/0507096]. 17, 52

[54] R. Kallosh, N. Sivanandam, and M. Soroush, "The Non-BPS black hole attractor equation.", *JHEP*, **0603**, (2006), 060, [hep-th/0602005]. 17

[55] S. Kachru, R. Kallosh, and M. Shmakova, "Generalized Attractor Points in Gauged Supergravity.", *Phys.Rev.*, **D84**, (2011), 046003, [arXiv:1104.2884]. 17

[56] G. T. Horowitz and B. Way, "Lifshitz Singularities.", *Phys.Rev.*, **D85**, (2012), 046008, [arXiv:1111.1243]. 24, 47, 55

[57] C. M. Brown and O. DeWolfe, "The Godel-Schrodinger Spacetime and Stringy Chronology Protection.", *JHEP*, **1201**, (2012), 032, [arXiv:1110.3840]. 45

[58] S. Kachru, N. Kundu, A. Saha, R. Samanta, and S. P. Trivedi, "Interpolating from Bianchi Attractors to Lifshitz and AdS Spacetimes.", *JHEP*, **1403**, (2014), 074, [arXiv:1310.5740]. 46, 124

[59] C. Charmousis, B. Gouteraux, B. S. Kim, E. Kiritsis, and R. Meyer, "Effective Holographic Theories for low-temperature condensed matter systems.", *JHEP*, **1011**, (2010), 151, [arXiv:1005.4690]. 47, 49, 51, 52, 61

[60] E. Perlmutter, "Domain Wall Holography for Finite Temperature Scaling Solutions.", *JHEP*, **1102**, (2011), 013, [arXiv:1006.2124]. 47, 51

[61] N. Iizuka, N. Kundu, P. Narayan, and S. P. Trivedi, "Holographic Fermi and Non-Fermi Liquids with Transitions in Dilaton Gravity.", *JHEP*, **1201**, (2012), 094, [arXiv:1105.1162]. 47, 51, 52, 55, 61, 66, 72, 140

[62] B. Gouteraux and E. Kiritsis, "Generalized Holographic Quantum Criticality at Finite Density.", *JHEP*, **1112**, (2011), 036, [arXiv:1107.2116]. 47, 51

[63] N. Ogawa, T. Takayanagi, and T. Ugajin, "Holographic Fermi Surfaces and Entanglement Entropy.", *JHEP*, **1201**, (2012), 125, [arXiv:1111.1023]. 47, 50, 65, 68

[64] L. Huijse, S. Sachdev, and B. Swingle, "Hidden Fermi surfaces in compressible states of gauge-gravity duality.", *Phys.Rev.*, **B85**, (2012), 035121, [arXiv:1112.0573]. 47, 50, 53, 54, 65

[65] X. Dong, S. Harrison, S. Kachru, G. Torroba, and H. Wang, "Aspects of holography for theories with hyperscaling violation.", *JHEP*, **1206**, (2012), 041, [arXiv:1201.1905]. 47, 73

[66] N. Iizuka, S. Kachru, N. Kundu, P. Narayan, N. Sircar, et al., "Extremal Horizons with Reduced Symmetry: Hyperscaling Violation, Stripes, and a Classification for the Homogeneous Case.", *JHEP*, **1303**, (2013), 126, [arXiv:1212.1948]. 47, 124

[67] S. S. Gubser and F. D. Rocha, "Peculiar properties of a charged dilatonic black hole in AdS_5.", *Phys.Rev.*, **D81**, (2010), 046001, [arXiv:0911.2898]. 49, 51

[68] K. Goldstein, S. Kachru, S. Prakash, and S. P. Trivedi, "Holography of Charged Dilaton Black Holes.", *JHEP*, **1008**, (2010), 078, [arXiv:0911.3586]. 49, 51, 55

[69] L. Huijse and S. Sachdev, "Fermi surfaces and gauge-gravity duality.", *Phys.Rev.*, **D84**, (2011), 026001, [arXiv:1104.5022]. 49

[70] M. M. Wolf, "Violation of the entropic area law for Fermions.", *Phys.Rev.Lett.*, **96**, (2006), 010404, [quant-ph/0503219]. 50

[71] D. Gioev and I. Klich, "Entanglement Entropy of Fermions in Any Dimension and the Widom Conjecture.", *Physical Review Letters*, **96**, (March, 2006), 100503, [quant-ph/0504151]. 50

[72] B. Swingle, "Entanglement Entropy and the Fermi Surface.", *Phys.Rev.Lett.*, **105**, (2010), 050502, [arXiv:0908.1724]. 50

[73] B. Swingle, "Conformal Field Theory on the Fermi Surface.", *Phys.Rev.*, **B86**, (2012), 035116, [arXiv:1002.4635]. 50

[74] Y. Zhang, T. Grover, and A. Vishwanath, "Entanglement entropy of critical spin liquids.", *Phys.Rev.Lett.*, **107**, (2011), 067202, [arXiv:1102.0350]. 50

[75] F. Denef, S. A. Hartnoll, and S. Sachdev, "Quantum oscillations and black hole ringing.", *Phys.Rev.*, **D80**, (2009), 126016, [arXiv:0908.1788]. 50

[76] T. Faulkner and N. Iqbal, "Friedel oscillations and horizon charge in 1D holographic liquids.", *JHEP*, **1307**, (2013), 060, [arXiv:1207.4208]. 50

[77] S. A. Hartnoll and E. Shaghoulian, "Spectral weight in holographic scaling geometries.", *JHEP*, **1207**, (2012), 078, [arXiv:1203.4236]. 50

[78] S.-S. Lee, "A Non-Fermi Liquid from a Charged Black Hole: A Critical Fermi Ball.", *Phys.Rev.*, **D79**, (2009), 086006, [arXiv:0809.3402]. 51

[79] H. Liu, J. McGreevy, and D. Vegh, "Non-Fermi liquids from holography.", *Phys.Rev.*, **D83**, (2011), 065029, [arXiv:0903.2477]. 51

[80] M. Cubrovic, J. Zaanen, and K. Schalm, "String Theory, Quantum Phase Transitions and the Emergent Fermi-Liquid.", *Science*, **325**, (2009), 439–444, [arXiv:0904.1993]. 51

[81] T. Faulkner, H. Liu, J. McGreevy, and D. Vegh, "Emergent quantum criticality, Fermi surfaces, and AdS(2).", *Phys.Rev.*, **D83**, (2011), 125002, [arXiv:0907.2694]. 51

[82] T. Faulkner and J. Polchinski, "Semi-Holographic Fermi Liquids.", *JHEP*, **1106**, (2011), 012, [arXiv:1001.5049]. 51

[83] K. Goldstein, N. Iizuka, S. Kachru, S. Prakash, S. P. Trivedi, et al., "Holography of Dyonic Dilaton Black Branes.", *JHEP*, **1010**, (2010), 027, [arXiv:1007.2490]. 51, 73

[84] R. Meyer, B. Gouteraux, and B. S. Kim, "Strange Metallic Behaviour and the Thermodynamics of Charged Dilatonic Black Holes.", *Fortsch.Phys.*, **59**, (2011), 741–748, [arXiv:1102.4433]. 51

[85] B. Gouteraux, B. S. Kim, and R. Meyer, "Charged Dilatonic Black Holes and their Transport Properties.", *Fortsch.Phys.*, **59**, (2011), 723–729, [arXiv:1102.4440]. 51

[86] B. Gouteraux, J. Smolic, M. Smolic, K. Skenderis, and M. Taylor, "Holography for Einstein-Maxwell-dilaton theories from generalized dimensional reduction.", *JHEP*, **1201**, (2012), 089, [arXiv:1110.2320]. 51

[87] L. Bombelli, R. K. Koul, J. Lee, and R. D. Sorkin, "A Quantum Source of Entropy for Black Holes.", *Phys.Rev.*, **D34**, (1986), 373–383. 51

[88] M. Srednicki, "Entropy and area.", *Phys.Rev.Lett.*, **71**, (1993), 666–669, [hep-th/9303048]. 51

[89] C. Holzhey, F. Larsen, and F. Wilczek, "Geometric and renormalized entropy in conformal field theory.", *Nucl.Phys.*, **B424**, (1994), 443–467, [hep-th/9403108]. 51

[90] P. Calabrese and J. L. Cardy, "Entanglement entropy and quantum field theory.", *J.Stat.Mech.*, **0406**, (2004), P06002, [hep-th/0405152]. 51

[91] P. Calabrese and J. L. Cardy, "Entanglement entropy and quantum field theory: A Non-technical introduction.", *Int.J.Quant.Inf.*, **4**, (2006), 429, [quant-ph/0505193]. 51

[92] S. Ryu and T. Takayanagi, "Holographic derivation of entanglement entropy from AdS/CFT.", *Phys.Rev.Lett.*, **96**, (2006), 181602, [hep-th/0603001]. 51, 65

[93] S. Ryu and T. Takayanagi, "Aspects of Holographic Entanglement Entropy.", *JHEP*, **0608**, (2006), 045, [hep-th/0605073]. 51, 65

[94] S. Harrison, S. Kachru, and H. Wang, "Resolving Lifshitz Horizons.", *JHEP*, **1402**, (2014), 085, [arXiv:1202.6635]. 51, 124

[95] J. Bhattacharya, S. Cremonini, and A. Sinkovics, "On the IR completion of geometries with hyperscaling violation.", *JHEP*, **1302**, (2013), 147, [arXiv:1208.1752]. 51, 124

[96] E. Shaghoulian, "Holographic Entanglement Entropy and Fermi Surfaces.", *JHEP*, **1205**, (2012), 065, [arXiv:1112.2702]. 55

[97] H. Liu and M. Mezei, "A Refinement of entanglement entropy and the number of degrees of freedom.", *JHEP*, **1304**, (2013), 162, [arXiv:1202.2070]. 72

[98] E. Witten, "SL(2,Z) action on three-dimensional conformal field theories with Abelian symmetry.", hep-th/0307041, [hep-th/0307041]. 73

[99] S. A. Hartnoll, P. K. Kovtun, M. Muller, and S. Sachdev, "Theory of the Nernst effect near quantum phase transitions in condensed matter, and in dyonic black holes.", *Phys.Rev.*, **B76**, (2007), 144502, [arXiv:0706.3215]. 73

[100] K. Narayan, "On Lifshitz scaling and hyperscaling violation in string theory.", *Phys.Rev.*, **D85**, (2012), 106006, [arXiv:1202.5935]. 73

[101] H. Singh, "Lifshitz/Schródinger Dp-branes and dynamical exponents.", *JHEP*, **1207**, (2012), 082, [arXiv:1202.6533]. 73

[102] P. Dey and S. Roy, "Lifshitz-like space-time from intersecting branes in string/M theory.", *JHEP*, **1206**, (2012), 129, [arXiv:1203.5381]. 73

[103] P. Dey and S. Roy, "Intersecting D-branes and Lifshitz-like space-time.", *Phys.Rev.*, **D86**, (2012), 066009, [arXiv:1204.4858]. 73

[104] E. Perlmutter, "Hyperscaling violation from supergravity.", *JHEP*, **1206**, (2012), 165, [arXiv:1205.0242]. 73

[105] P. Ade et al., "Planck 2013 results. XXII. Constraints on inflation.", arXiv:1303.5082, [arXiv:1303.5082]. 76

[106] P. Ade et al., "Planck 2013 Results. XXIV. Constraints on primordial non-Gaussianity.", arXiv:1303.5084, [arXiv:1303.5084]. 76, 120

[107] D. Seery, M. S. Sloth, and F. Vernizzi, "Inflationary trispectrum from graviton exchange.", *JCAP*, **0903**, (2009), 018, [arXiv:0811.3934]. 77, 78, 108, 113, 120, 165

[108] T. Banks, M. R. Douglas, G. T. Horowitz, and E. J. Martinec, "AdS dynamics from conformal field theory.", hep-th/9808016, [hep-th/9808016]. 78

[109] D. Harlow and D. Stanford, "Operator Dictionaries and Wave Functions in AdS/CFT and dS/CFT.", arXiv:1104.2621, [arXiv:1104.2621]. 78

[110] K. Abazajian, K. Arnold, J. Austermann, B. Benson, C. Bischoff, et al., "Inflation Physics from the Cosmic Microwave Background and Large Scale Structure.", arXiv:1309.5381, [arXiv:1309.5381]. 78

[111] E. Komatsu, "Hunting for Primordial Non-Gaussianity in the Cosmic Microwave Background.", *Class.Quant.Grav.*, **27**, (2010), 124010, [arXiv:1003.6097]. 78

[112] V. Desjacques and U. Seljak, "Primordial non-Gaussianity from the large scale structure.", *Class.Quant.Grav.*, **27**, (2010), 124011, [arXiv:1003.5020]. 78

[113] D. Seery, J. E. Lidsey, and M. S. Sloth, "The inflationary trispectrum.", *JCAP*, **0701**, (2007), 027, [astro-ph/0610210]. 78

[114] F. Arroja and K. Koyama, "Non-gaussianity from the trispectrum in general single field inflation.", *Phys. Rev. D*, **77**, (Apr, 2008), 083517. 78

[115] F. Arroja, S. Mizuno, K. Koyama, and T. Tanaka, "Full trispectrum in single field dbi inflation.", *Phys. Rev. D*, **80**, (Aug, 2009), 043527. 78

[116] X. Chen, B. Hu, M. xin Huang, G. Shiu, and Y. Wang, "Large primordial trispectra in general single field inflation.", *Journal of Cosmology and Astroparticle Physics*, **2009**, (2009), no. 08, 008. 78

[117] J. M. Maldacena, "Non-Gaussian features of primordial fluctuations in single field inflationary models.", *JHEP*, **0305**, (2003), 013, [astro-ph/0210603]. 78, 81, 84, 86, 109, 113, 114, 117, 148

[118] J. M. Maldacena and G. L. Pimentel, "On graviton non-Gaussianities during inflation.", *JHEP*, **1109**, (2011), 045, [arXiv:1104.2846]. 78, 79, 109

[119] I. Antoniadis, P. O. Mazur, and E. Mottola, "Conformal invariance and cosmic background radiation.", *Phys.Rev.Lett.*, **79**, (1997), 14–17, [astro-ph/9611208]. 78

[120] F. Larsen, J. P. van der Schaar, and R. G. Leigh, "De Sitter holography and the cosmic microwave background.", *JHEP*, **0204**, (2002), 047, [hep-th/0202127]. 78

[121] F. Larsen and R. McNees, "Inflation and de Sitter holography.", *JHEP*, **0307**, (2003), 051, [hep-th/0307026]. 78

[122] P. McFadden and K. Skenderis, "Holographic Non-Gaussianity.", *JCAP*, **1105**, (2011), 013, [arXiv:1011.0452]. 78

[123] I. Antoniadis, P. O. Mazur, and E. Mottola, "Conformal Invariance, Dark Energy, and CMB Non-Gaussianity.", *JCAP*, **1209**, (2012), 024, [arXiv:1103.4164]. 78

[124] P. Creminelli, "Conformal invariance of scalar perturbations in inflation.", *Phys.Rev.*, **D85**, (2012), 041302, [arXiv:1108.0874]. 78

[125] A. Bzowski, P. McFadden, and K. Skenderis, "Holographic predictions for cosmological 3-point functions.", *JHEP*, **1203**, (2012), 091, [arXiv:1112.1967]. 78, 86, 94, 117

[126] P. McFadden and K. Skenderis, "Cosmological 3-point correlators from holography.", *JCAP*, **1106**, (2011), 030, [arXiv:1104.3894]. 78

[127] A. Kehagias and A. Riotto, "Operator Product Expansion of Inflationary Correlators and Conformal Symmetry of de Sitter.", *Nucl.Phys.*, **B864**, (2012), 492–529, [arXiv:1205.1523]. 78

[128] A. Kehagias and A. Riotto, "The Four-point Correlator in Multifield Inflation, the Operator Product Expansion and the Symmetries of de Sitter.", *Nucl.Phys.*, **B868**, (2013), 577–595, [arXiv:1210.1918]. 78

[129] K. Schalm, G. Shiu, and T. van der Aalst, "Consistency condition for inflation from (broken) conformal symmetry.", *JCAP*, **1303**, (2013), 005, [arXiv:1211.2157]. 78

[130] A. Bzowski, P. McFadden, and K. Skenderis, "Holography for inflation using conformal perturbation theory.", *JHEP*, **1304**, (2013), 047, [arXiv:1211.4550]. 78, 117

[131] I. Mata, S. Raju, and S. Trivedi, "CMB from CFT.", *JHEP*, **1307**, (2013), 015, [arXiv:1211.5482]. 78, 86, 94, 107, 109, 117, 118, 119, 122, 148

[132] J. Garriga and Y. Urakawa, "Inflation and deformation of conformal field theory.", *JCAP*, **1307**, (2013), 033, [arXiv:1303.5997]. 78

[133] P. Creminelli and M. Zaldarriaga, "Single field consistency relation for the 3-point function.", *JCAP*, **0410**, (2004), 006, [astro-ph/0407059]. 79

[134] C. Cheung, A. L. Fitzpatrick, J. Kaplan, and L. Senatore, "On the consistency relation of the 3-point function in single field inflation.", *JCAP*, **0802**, (2008), 021, [arXiv:0709.0295]. 79

[135] L. Senatore and M. Zaldarriaga, "A Note on the Consistency Condition of Primordial Fluctuations.", *JCAP*, **1208**, (2012), 001, [arXiv:1203.6884]. 79

[136] P. Creminelli, C. Pitrou, and F. Vernizzi, "The CMB bispectrum in the squeezed limit.", *JCAP*, **1111**, (2011), 025, [arXiv:1109.1822]. 79

[137] N. Bartolo, S. Matarrese, and A. Riotto, "Non-Gaussianity in the Cosmic Microwave Background Anisotropies at Recombination in the Squeezed limit.", *JCAP*, **1202**, (2012), 017, [arXiv:1109.2043]. 79

[138] P. Creminelli, J. Norena, and M. Simonovic, "Conformal consistency relations for single-field inflation.", *JCAP*, **1207**, (2012), 052, [arXiv:1203.4595]. 79

[139] P. Creminelli, A. Joyce, J. Khoury, and M. Simonovic, "Consistency Relations for the Conformal Mechanism.", *JCAP*, **1304**, (2013), 020, [arXiv:1212.3329]. 79

[140] K. Hinterbichler, L. Hui, and J. Khoury, "Conformal Symmetries of Adiabatic Modes in Cosmology.", *JCAP*, **1208**, (2012), 017, [arXiv:1203.6351]. 79

[141] V. Assassi, D. Baumann, and D. Green, "On Soft Limits of Inflationary Correlation Functions.", *JCAP*, **1211**, (2012), 047, [arXiv:1204.4207]. 79

[142] W. D. Goldberger, L. Hui, and A. Nicolis, "One-particle-irreducible consistency relations for cosmological perturbations.", *Phys.Rev.*, **D87**, (2013), 103520, [arXiv:1303.1193]. 79

[143] K. Hinterbichler, L. Hui, and J. Khoury, "An Infinite Set of Ward Identities for Adiabatic Modes in Cosmology.", *JCAP*, **1401**, (2014), 039, [arXiv:1304.5527]. 79

[144] P. Creminelli, A. Perko, L. Senatore, M. Simonovi, and G. Trevisan, "The Physical Squeezed Limit: Consistency Relations at Order q^2.", *JCAP*, **1311**, (2013), 015, [arXiv:1307.0503]. 79

[145] L. Berezhiani and J. Khoury, "Slavnov-Taylor Identities for Primordial Perturbations.", *JCAP*, **1402**, (2014), 003, [arXiv:1309.4461]. 79

[146] T. Banks and W. Fischler, “Holographic Theories of Inflation and Fluctuations.”, ., ., (2011), ., [arXiv:1111.4948]. 79

[147] T. Banks, W. Fischler, T. Torres, and C. L. Wainwright, “Holographic Fluctuations from Unitary de Sitter Invariant Field Theory.”, ., ., (2013), ., [arXiv:1306.3999]. 79

[148] J. M. Bardeen, “Gauge Invariant Cosmological Perturbations.”, *Phys.Rev.*, **D22**, (1980), 1882–1905. 84

[149] J. M. Bardeen, P. J. Steinhardt, and M. S. Turner, “Spontaneous Creation of Almost Scale - Free Density Perturbations in an Inflationary Universe.”, *Phys.Rev.*, **D28**, (1983), 679. 84

[150] D. Lyth, “Large Scale Energy Density Perturbations and Inflation.”, *Phys.Rev.*, **D31**, (1985), 1792–1798. 84

[151] D. Salopek and J. Bond, “Nonlinear evolution of long wavelength metric fluctuations in inflationary models.”, *Phys.Rev.*, **D42**, (1990), 3936–3962. 84

[152] S. Weinberg, “Adiabatic modes in cosmology.”, *Phys.Rev.*, **D67**, (2003), 123504, [astro-ph/0302326]. 84

[153] S. Weinberg, “Damping of tensor modes in cosmology.”, *Phys.Rev.*, **D69**, (2004), 023503, [astro-ph/0306304]. 84

[154] S. Weinberg. *Cosmology.* Oxford University Press, (2008). 84

[155] E. D’Hoker, D. Z. Freedman, S. D. Mathur, A. Matusis, and L. Rastelli, “Graviton exchange and complete four point functions in the AdS / CFT correspondence.”, *Nucl.Phys.*, **B562**, (1999), 353–394, [hep-th/9903196]. 91

[156] G. Arutyunov and S. Frolov, “Four point functions of lowest weight CPOs in N=4 SYM(4) in supergravity approximation.”, *Phys.Rev.*, **D62**, (2000), 064016, [hep-th/0002170]. 91

[157] J. B. Hartle. *TASI Lectures On Quantum Cosmology.* High Energy Physics 1985-Vol 2; Editors : Mark J Bowick and Feza Gursey; World Scientific., (1985). 92

[158] S. M. Christensen and M. J. Duff, “Quantizing Gravity with a Cosmological Constant.”, *Nucl. Phys.*, **B170**, (1980), 480. 98

[159] M. J. G. Veltman. *Lectures on Quantum Theory Of Gravitation in Les Houches 1975 : Session XXVIII : Methods in Field Theory; Editors : R Balian and J Zinn-Justin.* North-Holland/World Scientific, (1975). 98, 99

[160] S. Raju, “Recursion Relations for AdS/CFT Correlators.”, *Phys.Rev.*, **D83**, (2011), 126002, [arXiv:1102.4724]. 98, 100

[161] S. Raju, "BCFW for Witten Diagrams.", *Phys. Rev. Lett.*, **106**, (2011), 091601, [arXiv:1011.0780]. 100

[162] H. Liu and A. A. Tseytlin, "On four point functions in the CFT / AdS correspondence.", *Phys.Rev.*, **D59**, (1999), 086002, [hep-th/9807097]. 100, 153

[163] See supplemental Mathematica program allchecks.nb available with the arXiv source of the paper: *Conformal Invariance and the Four Point Scalar Correlator in Slow-Roll Inflation* - arXiv:1401.1426 - http://arxiv.org/abs/1401.1426. 109, 113

[164] S. Raju, "New Recursion Relations and a Flat Space Limit for AdS/CFT Correlators.", *Phys.Rev.*, **D85**, (2012), 126009, [arXiv:1201.6449]. 110

[165] S. Raju, "Four Point Functions of the Stress Tensor and Conserved Currents in AdS_4/CFT_3.", *Phys.Rev.*, **D85**, (2012), 126008, [arXiv:1201.6452]. 110

[166] J. Smidt, A. Amblard, A. Cooray, A. Heavens, D. Munshi, et al., "A Measurement of Cubic-Order Primordial Non-Gaussianity With WMAP 5-Year Data.", arXiv:1001.5026, [arXiv:1001.5026]. 120